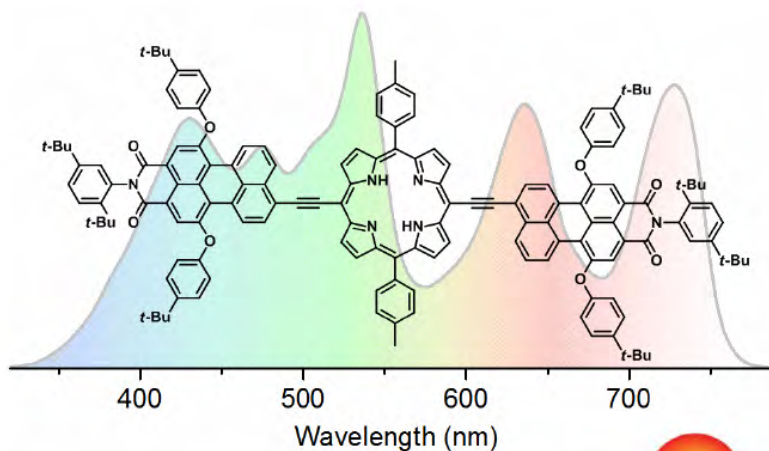
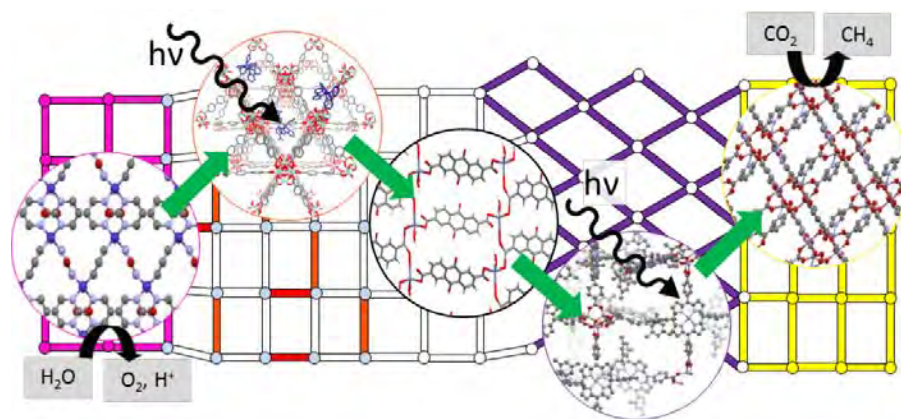
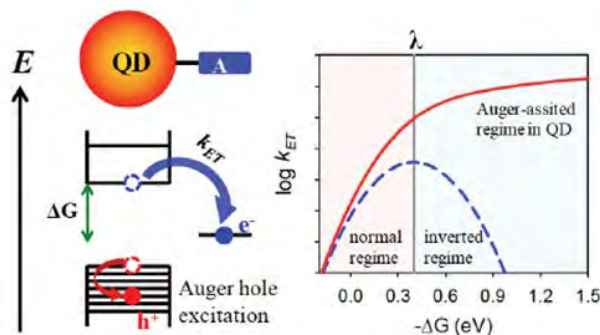


Proceedings of the  
**Thirty-Seventh  
DOE Solar Photochemistry  
P. I. Meeting**



**Marriott Washingtonian Center  
Gaithersburg, Maryland  
May 31 - June 3, 2015**



**Sponsored by:  
Chemical Sciences, Geosciences, and Biosciences Division  
U.S. Department of Energy**



# Program and Abstracts

## 37<sup>th</sup> Solar Photochemistry Principal Investigators Meeting

Marriott Washingtonian Center  
Gaithersburg, Maryland  
May 31 - June 3, 2015

Chemical Sciences, Geosciences, and Biosciences Division  
Office of Basic Energy Sciences  
Office of Science  
U.S. Department of Energy

**Cover Graphics:**

The cover figures are drawn from the abstracts of this meeting. One represents the Auger assisted electron transfer in quantum dots (Lian *et al.*, p. 68). Another depicts the absorption spectrum of panchromatic perylen-porphyrin dyes (Bocian *et al.*, p. 104). A third shows a metal organic framework assembly for photo-induced fuel formation (Morris *et al.*, p. 93).

## ***Supra Photosynthesis***

At the first Solar Photochemistry meeting for the P.I.s in May 1977, Dr. Richard Kandel, the Director of the Program set forth the mission of the Program with the following statement:

“The term solar photochemistry as used here is meant to include all research carried out with the long term goal of developing methods for capturing solar energy photochemically as a fuel (such as hydrogen from the decomposition of water), as electricity (in a photogalvanic cell) or in chemical bonds for subsequent release as heat. . . . I have use the term artificial photosynthesis and defined it as the generation of fuel or electricity using model systems which mimic natural photosynthetic systems in light gathering and charge separation.”

Almost forty years have passed since that first meeting and we have learned much that has advanced the goals set forth in that mission statement. At that time, the structure and composition of the photosynthetic reactions centers and the thylakoid membrane were only crudely known. A matter of heated discussion was the identity of the “primary acceptor” for the electron in the excited state of the reaction center chlorophylls. It was clear that several manganese atoms were present in the oxygen evolving complex, but how many and in what position they were to be found was a mystery. A new tool to study this structure, X-ray absorption and fluorescence from Synchrotron Radiation had just come on line.

In research on emulation of photosynthesis, the hottest topic was the attempt to confirm Marcus theory as a valid description for electron transfer. The question was posed as to whether it were possible to separate charges through electron transfer from a donor to an acceptor for as long as a microsecond, and the suggestion was made that ruthenium complexes might be a good place to start. Three years after the publication by Fujishima and Honda on photo-induced water splitting at  $\text{TiO}_2$ , a furious race was being run to discover a semiconductor electrode that would split water with visible light without itself decomposing. Dye sensitization was an odd area of study where dyes adsorbed in a monolayer from an aqueous electrolyte onto planar electrodes absorbed a per cent of the incident light and produced electrons in the electrode with a yield of a few per cent.

One need only examine the contents of the 2015 book of abstracts from the Program to see how far we have come in this field. A simple overview of the Program history will confirm this as well. The thermal storage of solar energy in photo-isomerized compounds was taken to the scale-up stage in industry before being determined to be unsuitable for manufacture owing to thermal instabilities. Photoelectrochemical solar cells where Si microelectrodes in HBr produced electricity were brought to the manufacturing stage in the late eighties, but could not compete with cheap oil. Photogalvanic cells were shown to be inefficient, but dye sensitization solved its problem of low yields for electron transfer and low absorption to become the highly researched dye sensitized solar cells of today. The ability and stability of homogeneous catalysts in water splitting have improved by many orders of magnitude; the problem of solar fuels evolution at semiconductor electrodes was taken over into the DOE Applied Technology Offices early in the nineties for  $\text{H}_2$  production and has recently formed the basis of the Energy Innovation Hub, the Joint Center for Artificial Photosynthesis.

With this progress in the Program mission, it is perhaps time to appreciate the research in the Solar Photochemistry Program as **Supra Photosynthesis**, as above and more advanced than the original photosynthetic model systems that motivated the Program's creation in 1977. It is evident that the demands of the modern economy impose more demanding figures of merit upon the human systems for chemically-based energy conversion than Nature does upon its photosynthetic systems. The photosynthetic system shuts down above AM 0.1, but a man-made system for energy conversion must function as if it were light starved at AM 1.0. The need for durability is also far greater than in Nature.

The photosynthetic system evolved with organic structures, most likely because organic media can be changed by Nature on a much quicker time frame than solid inorganic matter. Chemists can also emulate the end result organic matter in photosynthesis, and can synthesize new variants much faster than Nature. However, they can also readily make structures of solid inorganic composition that Nature rarely produces – new photoelectrodes and nanostructures of metals and semiconductors of an immense variety.

The models presently under study for light absorption, energy transfer, electron transfer and harvesting of light energy as electricity or fuels are of a greater dimension than those found in the photosynthetic reaction centers. It is now possible to control light absorption through quantum effects in inorganic nanoparticles through size variation and the models of electron transfer from these particles differ from those occurring in the components of a photo-activated thylakoid membrane. The primary photo-induced charge separation and dark recombination in organic molecular solar cells, where nano-crystalline domains of organic chromophores and unique fullerene compounds exchange charge, operate with poorly-understood and complex models for charge transfer. The oxygen evolving reaction in photosynthesis has a designed and deterministic reaction pathway for handling electron and proton transfer and today we probe the feasibility of less controlled pathways in a number of systems.

If we are moving away from the photosynthetic reaction center as the guiding model for systems research in this Program, then where are we headed? Certainly Grand Challenge research in the area of light, energy, and matter has been and will always be of interest in this Program, as will be fundamental studies of light absorption, energy transfer, electron transfer and small molecule activation for fuels generation. However, as we build upon these concepts to make sub-systems and systems for solar energy conversion, where we are headed is a research regime where we are using and discovering a number of model systems to emulate and explore. The photosynthetic system still serves as a good reference point, but there are many other aspects of biological reaction pathways and structures that could be of great use in non-biological systems. The solid state p-n junction solar cell made of electronic grade materials for use in extra-terrestrial applications is one such model, but it needs to be brought down to earth, to be made terrestrial. The Grätzel formulation of the dye-sensitized solar cell is another example and differs from both of these, but Nature is telling us that there are limits to this formulation and we seek a design for a Next Generation Dye Sensitized Solar Cell.

For those scientists who seek to step outside Grand Challenge and fundamental research problems and into basic research in the world of systems and sub-systems for energy transduction, there is the new challenge of learning how to envision and design these new systems and how to extrapolate from them to the basic research problems which will enable their assembly and operation. The converse also holds. How can one go from fundamentals and sub-systems in photochemistry research to design a system? How does

one go from regimes where reactions are studied at low concentration and are linear in behavior to systems where the reactive components are highly concentrated and have nonlinearities and feedback loops in their behavior? Systems research will never be the major part of the research effort of this Program since few systems will be worthy of such detailed inspection. However, the mastery of this conceptual process, of transition from fundamental to system research, is a discipline in itself, with rules that must be learned, being guided by the physics and chemistry of species and assemblies reactive to light.

Mark T. Spitler

May 2015



## FOREWORD

The 37th Department of Energy Solar Photochemistry P.I. Meeting, sponsored by the Chemical Sciences, Geosciences, and Biosciences Division of the Office of Basic Energy Sciences, is being held May 31 - June 3, 2015 at the Marriott Washingtonian Center in Gaithersburg, Maryland. These proceedings include the meeting agenda, abstracts of the formal presentations and posters of the conference, and an address list for the participants.

This Conference is the annual meeting of the grantees who perform research in solar photochemical energy conversion with the support of the Chemical Sciences, Geosciences, and Biosciences Division. This gathering is intended to enable the exchange of new ideas and research concepts between attendees and to further the collaboration and cooperation required for progress in such a difficult field.

This year, the Meeting will be attended by all of the P.I.s of the Solar Photochemistry Program, the first complete meeting of the P.I.s in three years. It is appropriate therefore that there will be guest lecturers to span the entire interests of the Program in our opening sessions on Monday and Tuesday mornings, with Monday featuring a presentation by Professor Marc Baldo of M.I.T. , Director of the EFRC Center for Excitonics and with Tuesday one from Professor Roel van de Krol, Head of the Institute for Solar Fuels at the Helmholtz Center, Berlin. In addition, the meeting is also structured during its daily oral presentation sessions to feature opportunities for discussion of the critical research problems in this topic. A dynamic and instructive exchange is expected.

We would like to express our appreciation to Nada Dimitrijevic for her help in the assembly of this abstract book, to Diane Marceau of the Division of Chemical Sciences, Geosciences, and Biosciences, and to Connie Lansdon of the Oak Ridge Institute of Science and Education for their assistance with the coordination of the logistics of this meeting. We must also thank all of the researchers whose energy and dedication have made the advances in solar photoconversion of this meeting possible.

Mark T. Spitler  
Christopher Fecko  
Chemical Sciences, Geosciences,  
and Biosciences Division  
Office of Basic Energy Sciences

Solar Photochemistry P. I. Meeting Overview					
Time	Sunday, May 31	Monday, June 1	Tuesday, June 2	Wednesday, June 3	
7:00					7:00
7:15		Breakfast	Breakfast	Breakfast	7:15
8:00		7:00-8:30	7:00-8:15	7:00-8:15	8:00
8:15					8:15
8:30		Opening Remarks	Session IV <i>Solar Fuels</i>	Session VII <i>Catalysis of Water Splitting</i>	8:30
8:45					8:45
9:00		Session I <i>Control of Energy Transfer</i>			9:00
9:15					9:15
9:30					Break
9:45			9:30-10:00	9:45	
10:00		Break	Break		10:00
10:15		10:00-10:30	10:00-10:30		10:15
10:30				Session VIII <i>Fundamentals of Charge Separation and Transport</i>	10:30
10:45			Session V <i>Photoevents in Nanoparticles</i>		10:45
11:00		Session I Continued			11:00
11:15					11:15
11:30					11:30
11:45				11:45	
12:00					12:00
12:15		Lunch	Lunch	Lunch	12:15
12:30		11:50-1:00	12:00-1:00	11:50-1:00	12:30
12:45					12:45
1:00				Session IX <i>Photochemistry of Complex Systems</i>	1:00
1:15					1:15
1:30		Individual Time			1:30
1:45					1:45
2:00			Individual Time		2:00
2:15				2:15	
2:30				2:30	
2:45				2:45	
3:00	Registration			Closing Remarks	3:00
3:15	3:00-6:00	Session II <i>Model Systems for Spectral Sensitization</i>			3:15
3:30					3:30
3:45			Session VI <i>Photophysics on the Nanoscale</i>		3:45
4:00	No Host Reception				4:00
4:15	5:00-6:00				4:15
4:30	at the bar	Session III <i>New Surfaces for Dyes</i>			4:30
4:45					4:45
5:00				5:00	
5:15				5:15	
5:30			Individual Time	5:30	
5:45				5:45	
6:00				6:00	
6:15		Dinner		6:15	
6:30	Dinner	5:30-8:00		6:30	
6:45	6:00-7:15	on the town	Dinner	6:45	
7:00			6:00-7:15	7:00	
7:15				7:15	
7:30	Welcome			7:30	
7:45				7:45	
8:00	After Dinner Session	Posters	Posters	8:00	
8:15				8:15	
8:30		Odd numbers	Even Numbers	8:30	
8:45	Reception Continues			8:45	
9:00	8:45-10:00			9:00	
9:30	at the bar	8:00-10:00	8:00-10:00	9:30	
10:00				10:00	

# *Table of Contents*



# TABLE OF CONTENTS

<b>Foreword</b> .....	vii
<b>Overview</b> .....	viii
<b>Program</b> .....	xxiii

## Abstracts of Oral Presentations

### Sunday Evening – After Dinner Session

Revealing the Excited State Intricacies of Methyl Ammonium Lead Halide Perovskites Jeffrey A. Christians, Joseph S. Manser, Yong-Siou Chen, Kevin Stamplecoskie, and <b>Prashant V. Kamat</b> , University of Notre Dame .....	3
Enhanced Molecular Photophysics and Photochemistry in Cu(I) and Ir(III) MLCT Chromophores Catherine E. McCusker, Michelle M. McGoorty, and <b>Felix N. Castellano</b> , North Carolina State University.....	8

### Session I – Control of Energy Transfer

Sensitization of Molecular Triplet Excitonic Processes with Colloidal Semiconductor Nanocrystals Nick Thompson, Dan Congreve, Mengfei Wu, Mounqi Bawendi, Vladimir Bulović, Troy Van Voorhis, and <b>Marc Baldo</b> , Massachusetts Institute of Technology.....	13
Singlet Fission <b>Josef Michl</b> , Paul I. Dron, Teruo Umemoto, Yves-Marie Hervault, Millicent B. Smith, Cyprien Lemouchi, Alexandre G. L. Olive, Cecile Givélet, Matibur Zamadar, Zdenek Havlas, Farhad Tamadon, Lance F. Culnane, Dean Antic, Eric A. Buchanan, Andrew J. Chomas, Jonathan B. Bair, Matthew R. Schreiber, and Jin Wen, University of Colorado at Boulder.....	16
Self-ordering Molecular Assemblies for Photochemical Charge Separation and Transport <b>Michael R. Wasielewski</b> , Yi-Lin Wu, Patrick E. Hartnett, Kristen E. Brown, Leah E. Shoer, Daniel M. Gardner, Scott M. Dyar, Eric A. Margulies, Samuel W. Eaton, and Tobin J. Marks, Northwestern University.....	19
Organic Macromolecular Materials for Long-Range and Efficient Transport Properties in Light Energy Conversion Applications <b>Theodore Goodson III</b> , University of Michigan at Ann Arbor.....	25

## **Session II – Model Systems for Spectral Sensitization**

- Fundamental Studies of Illuminated Semiconductor/Electrolyte Interfaces  
Meghan Kern, Laurie King, Theodore Kraus, Katarzyna Skoruspka, Kevin Watkins,  
Mark Spitler, and **Bruce Parkinson**, University of Wyoming..... 31
- Synthesis and Spectroscopy of Transition Metal-based Chromophores: Tailoring First-  
row Photophysics for Applications in Solar Energy Conversion  
**James K. McCusker**, Michigan State University..... 35
- Electron Transfer Dynamics in Efficient Molecular Solar Cells  
Ke Hu, William Ward, Byron H. Farnum, Patrik Johansson, and **Gerald J. Meyer**,  
University of North Carolina at Chapel Hill..... 38

## **Session III – New Surfaces for Dyes**

- The Relation between Structure and Photochemical Properties of Polyoxotitanate and  
Polysulfurcadmate Nanoparticles  
**Philip Coppens**, University at Buffalo SUNY..... 45
- Controlled Electro-Photonic Structure for Effective Solar Energy Harvesting in Dye  
Sensitized and Quantum Dot Solar Cells  
Yukihiro Hara, Timothy Garvey, Yulan Fu, Byron Farnum, Abay Gadisa, Leila Alibabai,  
Rudresh Ghosh, and **Rene Lopez**, University of North Carolina at Chapel Hill..... 48

## **Session IV – Solar Fuels**

- Towards Highly Efficient Metal Oxide Photoelectrodes for Water Splitting  
**Roel van de Krol**, Fatwa F. Abdi, Carolin Zachäus, and Sean P. Berglund, Helmholtz-  
Zentrum Berlin für Materialien und Energie GmbH..... 53
- Interfacial Photochemistry of Nanostructured Metal Oxide and Silicon Photoelectrodes  
**Nathan R. Neale**, National Renewable Energy Laboratory..... 56
- Establishing the Role of the Electrode Surface in Solar-Driven Pyridine-Catalyzed CO<sub>2</sub>  
Reduction  
Coleman X. Kronawitter, Peng Zhao, and **Bruce E. Koel**, Princeton University..... 59

## **Session V – Photoevents in Nanoparticles**

- Model Asymmetric Semiconductor Nanorod/Oxide Nanoparticle Hybrid Constructs  
**Jeffrey Pyun**, **S. Scott Saavedra**, and **Neal R. Armstrong**, University of Arizona..... 65
- 1D Exciton Transport and Dissociation in Semiconductor Nanorod Heterostructures  
Kaifeng Wu, Haiming Zhu, Ye Yang, Zheyuan Chen, Jinquan Chen, and **Tianquan  
Lian**, Emory University..... 68

Controlled Exciton/Plasmon Interaction between Individual Colloidal Quantum Dots and Plasmonic Particles in a Liquid Crystal Matrix Paul J. Ackerman, Haridas Mundoor, Ivan I. Smalyukh, and <b>Jaou van de Lagemaat</b> , National Renewable Energy Laboratory.....	71
--	----

**Session VI – Photophysics on the Nanoscale**

The Role of Lattice Strain in the Photophysics of Core/Shell Quantum Dots Ke Gong, Youhong Zeng, Zhong-Jie Jiang, Gary Beane, and <b>David F. Kelley</b> , University of California, Merced.....	77
Two-Dimensional Spectroscopy of Low Bandgap Quantum Dots Samuel D. Park, Dmitry Baranov, Jisu Ryu, and <b>David M. Jonas</b> , University of Colorado at Boulder.....	80
How Light is Absorbed in a Solid State Material <b>Hrvoje Petek</b> , University of Pittsburgh.....	83

**Session VII – Catalysis of Water Splitting**

Water Splitting by Thin Film Metal-Oxo Catalysts D. Kwabena Bediako, Michael X. Huynh, and <b>Daniel G. Nocera</b> , Harvard University..	89
Photocatalysts for H <sub>2</sub> Evolution: Combination of the Light Absorbing Unit and Catalytic Center in a Single Molecule Travis White, Suzanne Witt, Nicholas Leed, Zhanyong, Li, <b>Kim R. Dunbar</b> , and <b>Claudia Turro</b> , The Ohio State University and Texas A&M University.....	91
Electron Transport at Metal Organic Framework Donor-Acceptor Interfaces - Toward High Surface Area Photochemical Water Oxidation Catalysis William A. Maza, Spencer R. Ahrenholtz, and <b>Amanda J. Morris</b> , Virginia Polytechnic Institute.....	93

**Session VIII – Fundamentals of Charge Separation and Transport**

Physical Chemistry of Reaction Dynamics in Ionic Liquids <b>David A. Blank</b> , <b>Edward W. Castner, Jr.</b> , <b>Claudio J. Margulis</b> , Mark Maroncelli, and James F. Wishart, University of Minnesota, Rutgers University, University of Iowa, The Pennsylvania State University and Brookhaven National Laboratory.....	97
Mechanism and Dynamics of Photoinduced Charge Separation in DNA <b>Frederick D. Lewis</b> , Northwestern University.....	101

Fundamental Studies of the Interplay of Molecular Composition, Electronic/Vibrational Characteristics, and Functional Properties of Tetrapyrrolic Chromophores and Arrays <b>David F. Bocian, Dewey Holten</b> , Christine Kirmaier, and <b>Jonathan S. Lindsey</b> , University of California, Riverside, Washington University and North Carolina State University.....	104
---	-----

**Session IX – Photochemistry of Complex Systems**

Fundamental Studies of Light-induced Charge Transfer, Energy Transfer, and Energy Conversion with Supramolecular Systems <b>Joseph T. Hupp</b> , Northwestern University.....	111
Organic, Nanoscale, and Self-Assembled Structures Relevant to Solar Energy Conversion <b>Michael J. Therien</b> , Duke University.....	115
Photoinduced Charge Separation Processes: from Natural Photosynthetic Proteins to Artificial Polymer-Fullerene Interfaces <b>Oleg G. Poluektov</b> , Jens Niklas, Karen L. Mulfort, Lisa M. Utschig, David M. Tiede, and Kristy L. Mardis, Argonne National Laboratory.....	119
Photoinduced Electron Transfer Processes in Doped Conjugated Polymer Films <b>Garry Rumbles</b> , Jessica Ramirez, Hilary Marsh, Jaehong Park, and Obadiah Reid, National Renewable Energy Laboratory.....	123

## **Poster Abstracts** (by poster number)

1. Molecular Origins of Electronic Structure in Inorganic Systems for Solar Photoconversion  
Robert J. Stewart, Christopher Grieco, Adam Rimshaw, and John B. Asbury..... 129
2. Photodetachment and Electron Dynamics in Aliphatic Ionic Liquids  
Francesc Molins i Domenech, Andrew T. Healy, and David A. Blank..... 130
3. Linker Rectifiers for Covalent Attachment of Catalysts to Semiconductor Surfaces  
W. Ding, M. Koepf, C. Koenigsmann, A. Batra, L. Venkataraman, C. F. A. Negre, G. W. Brudvig, R. H. Crabtree, C. A. Schmuttenmaer, and V. S. Batista..... 131
4. Intramolecular Photo-Induced Electron Transfer in Ionic Liquids  
Jessalyn A. Devine, Marissa Saladin, Mark Maroncelli, Gary A. Baker, James F. Wishart, and Edward W. Castner, Jr. ..... 132
5. Hot Carriers in Lead Iodide Perovskites and Si Nanostructures  
Ye Yang, Matthew R. Bergren, Jao van de Lagemaat, Kai Zhu, Nathan R. Neale, and Matthew C. Beard..... 133
6. Dynamics of Charged and Neutral Species in Ionic Liquids: From Molecules to Electrons  
J. C. Araque, C. Xu, S. K. Yadav, M. Shadeck, M. Maroncelli, and C. J. Margulis..... 134
7. CO<sub>2</sub> and H<sub>2</sub>O Reduction in an Aqueous Photoelectrochemical Environment  
Yuan Hu, Yong Yan, Elizabeth L. Zeitler, Jing Gu, Anna Wuttig, and Andrew B. Bocarsly..... 135
8. Solvent and Solute Dynamics in Ionic Liquid + Conventional Solvent Mixtures  
Min Liang, Brian Conway, Xin-Xing Zhang, Edward W. Castner, Jr., and Mark Maroncelli..... 136
9. Semiconductor-Electrocatalyst Contacts: Theory, Experiment, and Applications to Solar Water Photoelectrolysis  
Shannon W. Boettcher, Fuding Lin, Thomas J. Mills, and Benjamin F. Bachman..... 137
10. Nanotechnological and Biological Systems for Light-Driven Hydrogen Evolution  
Kara L. Bren, Richard Eisenberg, and Todd D. Krauss..... 138
11. Lateral Charge Transport Along a Surface Dye Monolayer and Applications for Solar Light-Driven Water Oxidation  
Gary W. Brudvig, Bradley J. Brennan, Alec C. Durrell, Matthieu Koepf, Robert H. Crabtree, Charles A. Schmuttenmaer, and Victor S. Batista..... 139
12. Photoinduced Formation of Transient Ni(I) Porphyrin Captured by X-ray Snapshots and Theoretical Modeling  
M. L. Shelby, M. W. Mara, N. E. Jackson, A. B. Stickrath, L. X. Chen, P. J. LeStrange, and X. Li..... 140

13.	Understanding Roles of Ultrafast and Coherent Electronic and Atomic Motions in Photochemical Reactions <u>L. X. Chen</u> , F. N. Castellano, X. Li, K. L. Mulfort, M. A. Ratner, R. D. Schaller, G. C. Schatz, T. Seideman, D. M. Tiede, and L. Young.....	141
14.	Combined Biomass Valorization and Hydrogen Production in a Photoelectrochemical Cell Hyun Gil Cha, and <u>Kyoung-Shin Choi</u> .....	142
15.	Chromophores and Molecular Catalysts for Oxidation and Reduction Reactions Relevant to Artificial Photosynthesis <u>Javier J. Concepcion</u> , David W. Shaffer, Yan Xie, Gerald Manbeck, and Mehmed Z. Ertem.....	143
16.	Hydroxamate as Water-Stable Anchors for Water-Splitting Solar to Fuel Strategies Gary W. Brudvig, Bradley J. Brennan, Jeffrey Chen, Matthieu Koepf, <u>Robert H. Crabtree</u> , Subhajyoti Chaudhuri, Benjamin Rudsteyn, Charles A. Schmittenmaer, and Victor S. Batista.....	144
17.	Exploring How Symmetry and Vibration Impact Singlet Fission in Molecular Dimers <u>Niels H. Damrauer</u> , Jamie Snyder, Thomas Carey, Jasper Cook, and Tarek Sammakia.....	145
18.	Mono- and Dinuclear Cobalt Complexes with O-Donor Ligands for WOC J. L. Steele, L. Tahsini, M. K. Youmans, Chen S. Sun, and <u>L. H. Doerrer</u> .....	146
19.	Spectroscopic and DFT Studies Related to the Design of Transition Metal Solar Photosensitizers Ryan A. Thomas, Chia Nung Tsai, Shivnath Mazumder, Yuan Jang Chen, H. Bernhard Schlegel, Claudio N. Verani, and <u>John F. Endicott</u> .....	147
20.	Tuning Optoelectronic and Catalytic Properties with Dynamic Strain Drazenka Svedruzic, Eric Benson, Brian A. Gregg, and <u>Sue Ferrere</u> .....	148
21.	Photo-driven Hierarchical Assembly of Inorganic Light Absorber – Nanocluster Catalyst Units for CO <sub>2</sub> Reduction and H <sub>2</sub> O Oxidation Wooyul Kim, and <u>Heinz Frei</u> .....	149
22.	Quantum Chemical Modeling of Transition Metal Containing Systems Andrew Weisman, Louis Brus, Mike Steigerwald, Steve Jerome, and <u>Richard A. Friesner</u> .....	150
23.	Artificial Photosynthesis for the Generation of Fuels using Molecular Catalysts and Metal Carbide-Nitride Composites <u>Etsuko Fujita</u> , James T. Muckerman, and Kotaro Sasaki.....	151
24.	Model Dyes for the Study of Molecule/Metal Oxide Semiconductor Interfaces and Electron Transfer Processes <u>E. Galoppini</u> , R. A. Bartynski, L. Gundlach, A. Batarseh, H. Fan, S. Rangan, J. Nieto-Pescador, and B. Abraham.....	152

25.	Ionic Liquid-Enhanced Electrocatalytic Reduction of CO <sub>2</sub> with a Homogeneous Catalyst <u>David C. Grills</u> .....	153
26.	Complex Photochemistry in a Molecular Artificial Photosynthetic Reaction Center Antaeres Antoniuk-Pablant, Gerdenis Kodis, <u>Ana L. Moore</u> , <u>Thomas A. Moore</u> , and <u>Devens Gust</u> .....	154
27.	Photo-Injection of High Potential Holes into Cu <sub>5</sub> Ta <sub>11</sub> O <sub>30</sub> Nanoparticles by Porphyrin Dyes Ian Sullivan, Chelsea Brown, Manuel J. Llansola-Portoles, Miguel Gervaldo, Gerdenis Kodis, <u>Thomas A. Moore</u> , <u>Devens Gust</u> , <u>Ana Moore</u> , and Paul Maggard.....	155
28.	Molecular and Material Approaches to Overcome Kinetic and Energetic Constraints in Dye-Sensitized Solar Cells Josh Baillargeon, Dhritabrata Mandal, Yuling Xie, and <u>Thomas W. Hamann</u> .....	156
29.	Photochemical Fates of Oxygen on a Mixed Fe+Cr Oxide Surface: Desorption, Dissociation and Stabilization by Coadsorbed Water <u>Michael A. Henderson</u> .....	157
30.	Integrated Synthetic, Computational, Spectroelectrochemical and Spectroscopic Study of Polyoxometalate Water Oxidation Catalyst-Based Photoanodes <u>Craig L. Hill</u> , Tianquan Lian, and Djameladdin G. Musaev.....	158
31.	Using Morphology to Tune Triplet Formation in Films of Singlet Fission Chromophores <u>Justin C. Johnson</u> , Joseph L. Ryerson, Dylan Arias, Paul I. Dron, Josef Michl, and Arthur J. Nozik .....	159
32.	Fundamental Properties of Wurtzite (GaN) <sub>1-x</sub> (ZnO) <sub>x</sub> Semiconductors <u>Peter Khalifah</u> .....	160
33.	Photophysics of Doped Individual Single Walled Carbon Nanotubes Sebastian Schäfer, Nicole M. B. Cogan, and <u>Todd D. Krauss</u> .....	161
34.	Investigation of Performance Losses in p-WSe <sub>2</sub> Layered Photocathodes and Surface Functionalization of Single Layer MoS <sub>2</sub> Jesus M. Velazquez, Joshua D. Wiensch, Jimmy John, and <u>Nathan S. Lewis</u> .....	162
35.	Electron/Hole Selectivity in Organic Semiconductor Contacts for Solar Energy Conversion Chris Weber, Ethan Walker, Colin Bradley, and <u>Mark Lonergan</u> .....	163
36.	Light-Stimulated Hole Injection at Dye-Sensitized Phosphide Photocathodes: Attaching Molecular Sensitizers and Catalysts to p-GaP Photocathodes Elizabeth Brown, and <u>Stephen Maldonado</u> .....	164
37.	Nanostructured Photocatalytic Water Splitting Systems John R. Swierk, Nella M. Vargas-Barbosa, Nicholas S. McCool, Pengtao Xu, Yuguang Li, Megan E. Strayer, <u>Thomas E. Mallouk</u> , Ana L. Moore, Thomas A. Moore, and Devens Gust.....	165

38.	Photoinduced Interfacial Electron Transfer at <i>nano</i> ITO Byron H. Farnum, Animesh Nayak, Akinobu Nakada, M. Kyle Brennaman, Osamu Ishitani, and <u>Thomas J. Meyer</u> .....	166
39.	Exciton and Charge Transport in Conjugated Chains T. Mani, M. J. Bird, A. R. Cook, L. Zaikowski, R. Holroyd, G. Mauro, X. Li., G. Rumbles, J. Blackburn, O. G. Reid, and <u>J. R. Miller</u> .....	167
40.	Photocatalytic Water Oxidation at the Semiconductor-Aqueous Interface: GaN, ZnO and the GaN/ZnO Alloy <u>James T. Muckerman</u> .....	168
41.	Small-Polaron Hopping in W:BiVO <sub>4</sub> and Ni-Doped FeOOH OER Electrocatalyst Alexander J. E. Rettie, William C. Chemelewski, Allen J. Bard, and <u>C. Buddie Mullins</u> .....	169
42.	Extension of Hopfield's Electron Transfer Model to Accommodate Site-Site Correlation <u>Marshall D. Newton</u> .....	170
43.	Pendant Proton Relays and Proton-Coupled Electron Transfer in Electrocatalytic Hydrogen Generation by Ni Hangman Porphyrins D. Kwabena Bediako, Brian H. Solis, Dilek Dogutan, Sharon Hammes-Schiffer, and <u>Daniel G. Nocera</u> .....	171
44.	Z-Scheme Dye Cells for Solar Fuels: Buried Junctions vs. Chromophore-Catalyst Assemblies <u>Arthur J. Nozik</u> .....	172
45.	The Effect of Solvent Coordination on the Mechanism of Formation of a Metal (Co, Ru) Hydride Bond <u>Dmitry E. Polyansky</u> , Etsuko Fujita, and James T. Muckerman.....	173
46.	Excited State Dynamics in Complex Systems for Solar Energy Harvesting: Time-Domain <i>Ab Initio</i> Studies <u>Oleg Prezhdo</u> .....	174
47.	Interfacial Processes between Gas-Phase Molecules and Ga-based Surfaces Probed by Near-Ambient Pressure X-ray Photoelectron Spectroscopy <u>Sylwia Ptasinska</u> , and Xueqiang Zhang.....	175
48.	Ru Complexes under Catalytic Condition of Water Oxidation <u>Yulia Pushkar</u> , Guibo Zhu, Lifen Yan, and Yuliana Smirnova.....	176
49.	Facet-Dependent Photoelectrochemical Performance of TiO <sub>2</sub> Nanostructures: An Experimental and Computational Study <u>Charles A. Schmittenmaer</u> , Christopher Koenigsmann, Chuanhao Li, Wendu Ding, Benjamin Rudshiteyn, Ke R. Yang, Kevin P. Regan, Steven J. Konezny, Gary W. Brudvig, Victor S. Batista, and Jaehong Kim.....	177

50.	Earth Abundant Metal-based Catalysts for Artificial Photosynthesis Lianpeng Tong, Lars Kohler, Ruifa Zong, Rongwei Zhou, Lanka Wickramasinghe, Andrew Kopecky, and <u>Randolph P. Thummel</u> .....	178
51.	High Valence Homogeneous and Amorphous Metal Oxide Clusters as Biomimetic Water-Oxidation Catalysts: Exploring Ligand Dependencies on Domain Structure and Function Using <i>In-Situ</i> X-Ray Structure Characterization Gihan Kwon, Diego Fazi, Jonathan D. Emery, Alex B. F. Martinson, Lin X. Chen, Karen L. Mulfort, and <u>David M. Tiede</u> .....	179
52.	Concerted Experimental and Theoretical Efforts towards the Design of New Cobalt-based Catalysts for Proton/Water Reduction Debashis Basu, Shivnath Mazumder, Habib Baydoun, <u>H. Bernhard Schlegel</u> , and <u>Claudio N. Verani</u> .....	180
53.	Water Oxidation with Langmuir-Blodgett Films of Cobalt [N <sub>2</sub> O <sub>3</sub> ] Amphiphiles Sunalee Gonawala, Habib Baydoun, and <u>Claudio N. Verani</u> .....	181
54.	Water Reduction with Cobalt, Nickel, and Copper Complexes Based on an [N <sub>2</sub> N' <sub>3</sub> ] Ligand Debashis Basu, Pavithra Kankanamalage, Danushka Ekanayake, Shivnath Mazumder, <u>H. Bernhard Schlegel</u> , and <u>Claudio N. Verani</u> .....	182
55.	Design of Efficient Molecular Electrocatalysts for Water and Carbon Dioxide Reduction Using Predictive Models of Thermodynamic Properties Charlene Tsay, Brooke Livesay, Juliet Khosrowabadi Kotyk, Zachary Thammavongsy, and <u>Jenny Y. Yang</u> .....	183
56.	A Molecular Cobalt Catalyst Architected and TiO <sub>2</sub> Modified p-GaInP <sub>2</sub> Photoelectrode for Hydrogen Production Jing Gu, Yong Yan, James Young, Kenneth Steirer, Nathan R. Neale, and <u>John Turner</u> .....	184
57.	Transition Metal Polypyridine Complexes: Studies of Mediation in Dye-Sensitized Solar Cells and Charge Separation <u>Amy L. Prieto</u> .....	185
58.	Transport along Conjugated Polymer Chains <u>M. J. Bird</u> , A. R. Cook, L. Zaikowski, G. Mauro, X. Li., G. Rumbles, J. Blackburn, O. G. Reid, and J. R. Miller .....	186
59.	Do TFSA Anions Slither? Pressure Exposes the Role of Anion Conformational Exchange in Self-Diffusion <u>James F. Wishart</u> , Sophia N. Suarez, David Cuffari, Armando Rua, Kartik Pillar, Jasmine L. Hatcher, Sharon Ramati, and Steven G. Greenbaum .....	187
	<b>List of Participants</b> .....	189
	<b>Author Index</b> .....	199



# *Program*



# 37<sup>th</sup> DOE SOLAR PHOTOCHEMISTRY P. I. MEETING

May 31 - June 3, 2015

Marriott Washingtonian Center  
Gaithersburg, Maryland

## PROGRAM

### Sunday, May 31

- 3:00 – 6:00 p.m.      Registration
- 5:00 – 10:00 p.m.    No Host Reception at Hotel
- 6:00 – 7:15 p.m.      Dinner

### After Dinner Session

Mark T. Spitler, Chair

- 7:30 p.m.      Welcome
- 7:45 p.m.      Revealing the Excited State Intricacies of Methyl Ammonium Lead Halide Perovskites  
Jeffrey A. Christians, Joseph S. Manser, Yong-Siou Chen, Kevin Stamplecoskie, and **Prashant V. Kamat**, University of Notre Dame
- 8:15 p.m.      Enhanced Molecular Photophysics and Photochemistry in Cu(I) and Ir(III) MLCT Chromophores  
Catherine E. McCusker, Michelle M. McGoorty, and **Felix N. Castellano**, North Carolina State University

### Monday Morning, June 1

- 7:00 a.m.      Breakfast

### Session I

### Control of Energy Transfer

Mark T. Spitler, Chair

- 8:30 a.m.      Opening Remarks  
**Tanja Pietraß** and **Mark T. Spitler**, US Department of Energy

- 9:00 a.m. Sensitization of Molecular Triplet Excitonic Processes with Colloidal Semiconductor Nanocrystals  
Nick Thompson, Dan Congreve, Mengfei Wu, Mounqi Bawendi, Vladimir Bulović, Troy Van Voorhis, and **Marc Baldo**, Massachusetts Institute of Technology
- 10:00 a.m. Coffee Break
- 10:30 a.m. Singlet Fission  
**Josef Michl**, Paul I. Dron, Teruo Umemoto, Yves-Marie Hervault, Millicent B. Smith, Cyprien Lemouchi, Alexandre G. L. Olive, Cecile Givélet, Matibur Zamadar, Zdenek Havlas, Farhad Tamadon, Lance F. Culnane, Dean Antic, Eric A. Buchanan, Andrew J. Chomas, Jonathan B. Bair, Matthew R. Schreiber, and Jin Wen, University of Colorado at Boulder
- 11:00 a.m. Self-ordering Molecular Assemblies for Photochemical Charge Separation and Transport  
**Michael R. Wasielewski**, Yi-Lin Wu, Patrick E. Hartnett, Kristen E. Brown, Leah E. Shoer, Daniel M. Gardner, Scott M. Dyar, Eric A. Margulies, Samuel W. Eaton, and Tobin J. Marks, Northwestern University
- 11:30 a.m. Organic Macromolecular Materials for Long-Range and Efficient Transport Properties in Light Energy Conversion Applications  
**Theodore Goodson III**, University of Michigan at Ann Arbor

### **Monday Afternoon, June 1**

- 11:50 p.m. Lunch

### **Session II** **Model Systems for Spectral Sensitization** Elena Galoppini, Chair

- 3:00 p.m. Fundamental Studies of Illuminated Semiconductor/Electrolyte Interfaces  
Meghan Kern, Laurie King, Theodore Kraus, Katarzyna Skoruspka, Kevin Watkins, Mark Spitler, and **Bruce Parkinson**, University of Wyoming
- 3:30 p.m. Synthesis and Spectroscopy of Transition Metal-based Chromophores: Tailoring First-row Photophysics for Applications in Solar Energy Conversion  
**James K. McCusker**, Michigan State University
- 4:00 p.m. Electron Transfer Dynamics in Efficient Molecular Solar Cells  
Ke Hu, William Ward, Byron H. Farnum, Patrik Johansson, and **Gerald J. Meyer**, University of North Carolina at Chapel Hill

**Session III**  
**New Surfaces for Dyes**  
Thomas W. Hamann, Chair

- 4:30 p.m. The Relation between Structure and Photochemical Properties of Polyoxotitanate and Polysulfurcadmate Nanoparticles  
**Philip Coppens**, University at Buffalo SUNY
- 5:00 p.m. Controlled Electro-Photonic Structure for Effective Solar Energy Harvesting in Dye Sensitized and Quantum Dot Solar Cells  
Yukihiro Hara, Timothy Garvey, Yulan Fu, Byron Farnum, Abay Gadisa, Leila Alibabai, Rudresh Ghosh, and **Rene Lopez**, University of North Carolina at Chapel Hill

**Monday Evening, June 1**

5:30 p.m. Dinner on the Town

8:00 - 10:00 p.m. **Posters: Odd numbers**

**Tuesday Morning, June 2**

7:00 a.m. Breakfast

**Session IV**  
**Solar Fuels**  
Arthur J. Nozik, Chair

- 8:15 a.m. Towards Highly Efficient Metal Oxide Photoelectrodes for Water Splitting  
**Roel van de Krol**, Fatwa F. Abdi, Carolin Zachäus, and Sean P. Berglund, Helmholtz-Zentrum Berlin für Materialien und Energie GmbH
- 9:15 a.m. Interfacial Photochemistry of Nanostructured Metal Oxide and Silicon Photoelectrodes  
**Nathan R. Neale**, National Renewable Energy Laboratory
- 9:45 a.m. Establishing the Role of the Electrode Surface in Solar-Driven Pyridine-Catalyzed CO<sub>2</sub> Reduction  
Coleman X. Kronawitter, Peng Zhao, and **Bruce E. Koel**, Princeton University
- 10:00 a.m. Coffee Break

**Session V**  
**Photoevents in Nanoparticles**  
Matthew C. Beard, Chair

- 10:30 a.m. Model Asymmetric Semiconductor Nanorod/Oxide Nanoparticle Hybrid Constructs  
**Jeffrey Pyun, S. Scott Saavedra, and Neal R. Armstrong**, University of Arizona
- 11:00 a.m. 1D Exciton Transport and Dissociation in Semiconductor Nanorod Heterostructures  
Kaifeng Wu, Haiming Zhu, Ye Yang, Zheyuan Chen, Jinqun Chen, and **Tianquan Lian**, Emory University
- 11:30 am. Controlled Exciton/Plasmon Interaction between Individual Colloidal Quantum Dots and Plasmonic Particles in a Liquid Crystal Matrix  
Paul J. Ackerman, Haridas Mundoor, Ivan I. Smalyukh, and **Jao van de Lagemaat**, National Renewable Energy Laboratory

**Tuesday Afternoon, June 2**

12:00 p.m. Lunch

**Session VI**  
**Photophysics on the Nanoscale**  
Todd D. Krauss, Chair

- 3:45 p.m. The Role of Lattice Strain in the Photophysics of Core/Shell Quantum Dots  
Ke Gong, Youhong Zeng, Zhong-Jie Jiang, Gary Beane, and **David F. Kelley**, University of California, Merced
- 4:15 p.m. Two-Dimensional Spectroscopy of Low Bandgap Quantum Dots  
Samuel D. Park, Dmitry Baranov, Jisu Ryu, and **David M. Jonas**, University of Colorado at Boulder
- 4:45 p.m. How Light is Absorbed in a Solid State Material  
**Hrvoje Petek**, University of Pittsburgh

**Tuesday Evening, June 23**

6:00 p.m. Dinner

8:00 – 10:00 p.m. **Posters: Even numbers**

### Wednesday Morning, June 3

7:00 a.m. Breakfast

#### **Session VII** **Catalysis of Water Splitting** Etsuko Fujita, Chair

- 8:15 a.m. Water Splitting by Thin Film Metal-Oxo Catalysts  
D. Kwabena Bediako, Michael X. Huynh, and **Daniel G. Nocera**, Harvard University
- 8:45 a.m. Photocatalysts for H<sub>2</sub> Evolution: Combination of the Light Absorbing Unit and Catalytic Center in a Single Molecule  
Travis White, Suzanne Witt, Nicholas Leed, Zhanyong, Li, **Kim R. Dunbar**, and **Claudia Turro**, The Ohio State University and Texas A&M University
- 9:15 a.m. Electron Transport at Metal Organic Framework Donor-Acceptor Interfaces - Toward High Surface Area Photochemical Water Oxidation Catalysis  
William A. Maza, Spencer R. Ahrenholtz, and **Amanda J. Morris**, Virginia Polytechnic Institute
- 9:30 a.m. Coffee Break

#### **Session VIII** **Fundamentals of Charge Separation and Transport** John R. Miller, Chair

- 10:00 a.m. Physical Chemistry of Reaction Dynamics in Ionic Liquids  
**David A. Blank**, **Edward W. Castner, Jr.**, **Claudio J. Margulis**, Mark Maroncelli, and James F. Wishart, University of Minnesota, Rutgers University, University of Iowa, The Pennsylvania State University and Brookhaven National Laboratory
- 10:40 a.m. Mechanism and Dynamics of Photoinduced Charge Separation in DNA  
**Frederick D. Lewis**, Northwestern University
- 11:10 a.m. Fundamental Studies of the Interplay of Molecular Composition, Electronic/Vibrational Characteristics, and Functional Properties of Tetrapyrrolic Chromophores and Arrays  
**David F. Bocian**, **Dewey Holten**, Christine Kirmaier, and **Jonathan S. Lindsey**, University of California, Riverside, Washington University and North Carolina State University

**Wednesday Afternoon, June 3**

11:50 p.m. Lunch

**Session IX**  
**Photochemistry of Complex Systems**  
Devens Gust, Chair

1:00 p.m. Fundamental Studies of Light-induced Charge Transfer, Energy Transfer, and Energy Conversion with Supramolecular Systems  
**Joseph T. Hupp**, Northwestern University

1:30 p.m. Organic, Nanoscale, and Self-Assembled Structures Relevant to Solar Energy Conversion  
**Michael J. Therien**, Duke University

2:00 p.m. Photoinduced Charge Separation Processes: from Natural Photosynthetic Proteins to Artificial Polymer-Fullerene Interfaces  
**Oleg G. Poluektov**, Jens Niklas, Karen L. Mulfort, Lisa M. Utschig, David M. Tiede, and Kristy L. Mardis, Argonne National Laboratory

2:30 p.m. Photoinduced Electron Transfer Processes in Doped Conjugated Polymer Films  
**Garry Rumbles**, Jessica Ramirez, Hilary Marsh, Jaehong Park, and Obadiah Reid, National Renewable Energy Laboratory

3:00 p.m. Closing Remarks  
**Mark T. Spitler**, U.S. Department of Energy

*Sunday Evening*

*After Dinner Session*



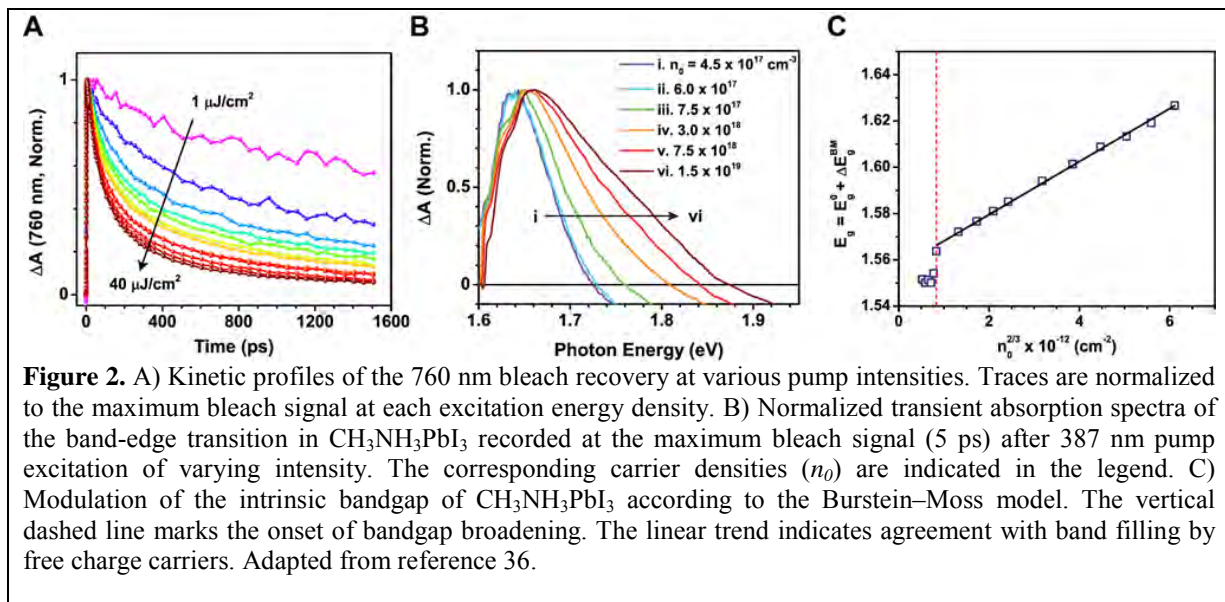
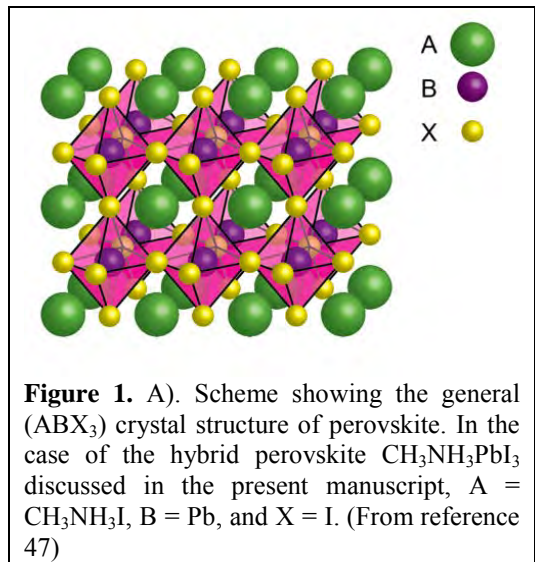
# Revealing the Excited State Intricacies of Methyl Ammonium Lead Halide Perovskites

Jeffrey A. Christians, Joseph S. Manser, Yong-Siou Chen, Kevin Stamplecoskie, and Prashant V. Kamat

Radiation Laboratory, Department of Chemistry and Biochemistry and Department of Chemical and Biomolecular Engineering, University of Notre Dame  
Notre Dame, IN 46556

Organic metal halide perovskites are attractive candidates for designing next generation solar cells. These cells have already delivered solar cell efficiencies greater than 20%. The simple fabrication technique and lower carbon footprint of thin film architecture are additional advantages these materials offer for developing new transformative solar cell technology.

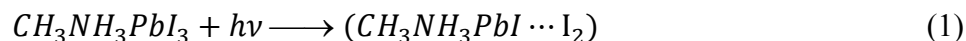
$\text{CH}_3\text{NH}_3\text{I}$  and  $\text{PbI}_2$  crystallize at relatively low temperatures (70-100 °C) to form  $\text{CH}_3\text{NH}_3\text{PbI}_3$  which has a tetragonal perovskite structure of the general form  $\text{ABX}_3$ , where  $\text{A} = \text{CH}_3\text{NH}_3\text{I}$ ,  $\text{B} = \text{Pb}$ , and  $\text{X} = \text{I}$  (Figure 1). Several techniques have been employed to better control  $\text{CH}_3\text{NH}_3\text{PbI}_3$  film crystallinity and morphology. Formation of the crystalline perovskite phase causes a color change from the yellow of the precursor solution to the dark black/brown of the  $\text{CH}_3\text{NH}_3\text{PbI}_3$  with its band gap of approximately 1.6 eV. The major research thrust to date is directed towards the design of solar cells with reproducible and stable performance. A deeper understanding of the photoinduced processes will be a valuable asset to researchers aiming to push the performance of perovskite solar cells nearer the Shockley-



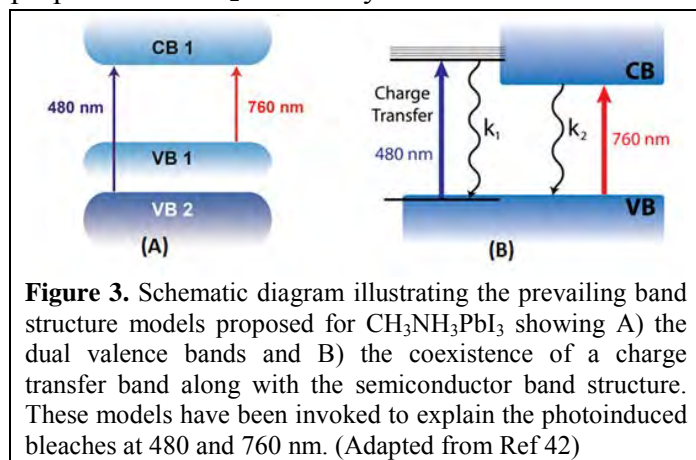
Quessier limit and improve the stability of these devices. Our research group is actively involved in contributing to this growing knowledge base, probing the excited state dynamics of  $\text{CH}_3\text{NH}_3\text{PbI}_3$  and elucidating the ultrafast charge separation and charge recombination processes following short laser pulse excitation.

By using transient absorption spectroscopy we have succeeded in elucidating the excited state behavior of  $\text{CH}_3\text{NH}_3\text{PbI}_3$  as well as the nature of the charge separation responsible photocurrent generation (Figure 2). Accumulation of charges following laser pulse excitation of the perovskite films leads to an increase in the intrinsic bandgap as expected from the Burstein–Moss band filling model. The carrier density dependent bimolecular recombination process and the band-edge shift provide insight into the behavior of photogenerated free charge carriers. Spectrally distinguishable charge separated state and charge transfer complex state of  $\text{CH}_3\text{NH}_3\text{PbI}_3$  have been identified.

The two transitions seen in the absorption spectra at 480 and 780 nm was attributed to the dual valence band structure (Figure 3A). This model predicts the accumulation of charges at a common conduction band minimum, CB1 regardless of the transition excited (*viz.* VB2 to CB1 or VB1 to CB1). Assuming the difference absorbance signal arises predominately due to state filling, we would expect the charge recombination dynamics to be homogeneous at all wavelengths, contrary to what is observed in our experiments. Taken as a whole, we have ascribed the excited state spectral features in  $\text{CH}_3\text{NH}_3\text{PbI}_3$  to a charge transfer band (Reaction 1) which is seen at wavelengths shorter than 680 nm, and a band gap transition (Reaction 2) which is responsible for the 760 nm bleach (Figure 3B).



In order to utilize these cells for solar hydrogen production as well as outdoor application one needs probe the interaction of  $\text{CH}_3\text{NH}_3\text{PbI}_3$  with water. While significant changes are seen in the UV-visible absorbance with water vapor (90% humidity exposure), the presence of the hydrate in the films has no noticeable effect on the charge carrier dynamics at short times ( $< 1.5$  ns). It is proposed that  $\text{H}_2\text{O}$  initially reacts with the surface of the perovskite film, and only slowly permeates through to the center of large domains. The reaction with  $\text{H}_2\text{O}$  at the surface of the perovskite film forms shallow traps in the band structure so that the portion of the  $\text{CH}_3\text{NH}_3\text{PbI}_3$  crystal which is pristine remains largely unaffected. Efforts are underway to evaluate the photovoltaic performance and excited state behavior of  $\text{CH}_3\text{NH}_3\text{PbI}_3$  films during the exposure of variable humidity environments under continuous illumination.



## DOE Sponsored Publications 2012-2015

1. Genovese, M. P.; Lightcap, I. V.; Kamat, P. V., Sun-Believable Solar Paint. A Transformative One-Step Approach for Designing Nanocrystalline Solar Cells. *ACS Nano* **2012**, *6*, 865–872.
2. Santra, P. K.; Kamat, P. V., Mn-Doped Quantum Dot Sensitized Solar Cells. A Strategy to Boost Efficiency Over 5%. *J. Am. Chem. Soc.* **2012**, *134*, 2508–2511.
3. Kamat, P. V., Manipulation of Charge Transfer Across Semiconductor Interface. A Criterion that cannot be Ignored in Photocatalyst Design. *J. Phys. Chem. Lett.* **2012**, *3*, 663-672. (Perspective)
4. Yokomizo, Y.; Krishnamurthy, S.; Kamat, P. V., Photoinduced Electron Charge and Discharge of Graphene-ZnO Nanoparticle Assembly. *Catal. Today* **2013**, *199*, 36-41.
5. Kamat, P. V., Boosting the Efficiency of Quantum Dot Sensitized Solar Cells Through Modulation of Interfacial Charge Transfer. *Acc. Chem. Res.* **2012**, *45*, 1906–1915.
6. Choi, H.; Santra, P. K.; Kamat, P. V., Synchronized Energy and Electron Transfer Processes in Covalently Linked CdSe-Squaraine Dye-TiO<sub>2</sub> Light Harvesting Assembly. *ACS Nano* **2012**, *6*, 5718–5726.
7. Lightcap, I. V.; Kamat, P. V., Fortification of CdSe Quantum Dots with Graphene Oxide. Excited State Interactions and Light Energy Conversion. *J. Am. Chem. Soc.* **2012**, *134*, 7109–7116.
8. Lightcap, I. V.; Murphy, S.; Schumer, T.; Kamat, P. V., Electron Hopping Through Single-to-Few Layer Graphene Oxide Films. Photocatalytically Activated Metal Nanoparticle Deposition. *J. Phys. Chem. Lett.* **2012**, *3*, 1453-1458.
9. Choi, H.; Chena, W. T.; Kamat, P. V., Know Thy Nano Neighbor. Plasmonic *versus* Electron Charging Effects of Gold Nanoparticles in Dye Sensitized Solar Cells. *ACS Nano* **2012**, *6*, 4418–4427.
10. Hines, D. A.; Becker, M. A.; Kamat, P. V., Photoinduced Surface Oxidation and Its Effect on the Exciton Dynamics of CdSe Quantum Dots. *J. Phys. Chem. C* **2012**, *116*, 13452–13457.
11. Chen, W.-T.; Hsu, Y.-J.; Kamat, P. V., Realizing Visible Photoactivity of Metal Nanoparticles. Excited State Behavior and Electron Transfer Properties of Silver (Ag<sub>8</sub>) Clusters *J. Phys. Chem. Lett.* **2012**, *3*, 2493–2499.
12. Lightcap, I. V.; Kamat, P. V., Graphitic Design: Prospects of Graphene-Based Nanocomposites for Solar Energy Conversion, Storage, and Sensing. *Accounts of Chemical Research* **2013**, *46*, 2235–2243. (Review)
13. Santra, P.; Kamat, P. V., Tandem Layered Quantum Dot Solar Cells. Tuning the Photovoltaic Response with Luminescent Ternary Cadmium Chalcogenides. *J. Am. Chem. Soc.* **2013**, *135*, 877–885.
14. Murphy, S.; Huang, L.; Kamat, P. V., Reduced Graphene Oxide-Silver Nanoparticle Composite as an Active SERS Material. *J. Phys. Chem. C* **2013**, *117*, 4740–4747.
15. Choi, H.; Kuno, M.; Hartland, G. V.; Kamat, P. V., CdSe Nanowire Solar Cells using a Carbazole as Surface Modifier. *J. Mater. Chem. A* **2013**, *1*, 5487 - 5491.
16. Kamat, P. V., Quantum Dot Solar Cells. The Next Big Thing in Photovoltaics. *J. Phys. Chem. Lett.* **2013**, *4*, 908–918. (Perspective)
17. Santra, P. K.; Nair, P. V.; Thomas, K. G.; Kamat, P. V., CuInS<sub>2</sub> Sensitized Quantum Dot Solar Cell. Electrophoretic Deposition, Excited State Dynamics and Photovoltaic Performance. *J. Phys. Chem. Lett.* **2013**, *4*, 722-729.

18. Radich, J. G.; Kamat, P. V., Making Graphene Holey. Gold Nanoparticle-Mediated Hydroxyl Radical Attack on Reduced Graphene Oxide. *ACS Nano* **2013**, *7*, 5546-5557.
19. Chen, Y.-S.; Choi, H.; Kamat, P. V., Metal Cluster Sensitized Solar Cells. A New Class of Thiolated Gold Sensitizers Delivering Efficiency Greater Than 2%. *J. Am. Chem. Soc.* **2013**, *135*, 8822–8825.
20. Hines, D. A.; Kamat, P. V., Quantum Dot Surface Chemistry: Ligand Effects and Electron Transfer Reactions. *J. Phys. Chem. C* **2013**, *117*, 14418–14426.
21. Christians, J. A.; Kamat, P. V., Trap and Transfer. Two-Step Hole Injection Across the Sb<sub>2</sub>S<sub>3</sub>/CuSCN Interface in Solid State Solar Cells. *ACS Nano* **2013**, *7*, 7967–7974.
22. Choi, H.; Kamat, P. V., CdS Nanowire Solar Cells. Dual Role of Squaraine Dye as a Sensitizer and a Hole Transporter. *J. Phys. Chem. Lett.* **2013**, *4*, 3983–3991.
23. Choi, H.; Radich, J. G.; Kamat, P. V., Sequentially Layered CdSe/CdS Nanowire Architecture for Improved Nanowire Solar Cell Performance *J. Phys. Chem. C* **2013**, *118*, 206–213.
24. Christians, J. A.; Fung, R.; Kamat, P. V., An Inorganic Hole Conductor for Organo-Lead Halide Perovskite Solar Cells. Improved Hole Conductivity with Copper Iodide. *J. Am. Chem. Soc.* **2014**, *136*, 758–764.
25. Christians, J. A.; Leighton, D. T.; Kamat, P. V., Rate Limiting Interfacial Hole Transfer in Sb<sub>2</sub>S<sub>3</sub> Solid-State Solar Cells. *Energy & Environ. Sci.* **2014**, *7*, 1148 - 1158.
26. Hines, D. A.; Kamat, P. V., Recent Advances in Quantum Dot Surface Chemistry. *ACS Appl Mater. & Interfaces* **2014**, *6*, 3041–3057. (Review)
27. Radich, J. G.; Peeples, N. R.; Santra, P. K.; Kamat, P. V., Charge Transfer Mediation through Cu<sub>x</sub>S. The Hole Story of CdSe in Polysulfide. *J. Phys. Chem. C* **2014**, *118*, 16463–16471.
28. Stamplecoskie, K. G.; Chen, Y.-S.; Kamat, P. V., Excited-State Behavior of Luminescent Glutathione-Protected Gold Clusters. *J. Phys. Chem. C* **2014**, *118*, 1370-1376.
29. Krishnamurthy, S.; Kamat, P. V., CdSe- Graphene Oxide Light Harvesting Assembly. Size Dependent Electron Transfer and Light Energy Conversion Aspects. *ChemPhysChem* **2014**, *15*, 2129-2135.
30. Hines, D. A.; Darz, E. R.; Jasti, R.; Kamat, P. V., Carbon Nanohoops: Excited Singlet and Triplet Behavior of [9]- and [12]-Cycloparaphenylene. *J Phys Chem A* **2014**, *118*, 1595–1600.
31. Chen, Y.-S.; Kamat, P. V., Glutathione Capped Gold Nanoclusters as Photosensitizers. Visible Light Induced Hydrogen Generation in Neutral Water. *J. Am. Chem. Soc.* **2014**, *136*, 6075–6082.
32. An, T.; Gao, Y.; Li, G.; Kamat, P. V.; Peller, J.; Joyce, M. V., Kinetics and Mechanism of •OH Mediated Degradation of Dimethyl Phthalate in Aqueous Solution: Experimental and Theoretical Studies. *Environ. Sci & Technol.* **2014**, *48*, 641-648.
33. Wang, Y.; Liu, K.; Mukherjee, P.; Hines, D. A.; Santra, P.; Shen, H. Y.; Kamat, P.; Waldeck, D. H., Driving charge separation for hybrid solar cells: photo-induced hole transfer in conjugated copolymer and semiconductor nanoparticle assemblies. *Phys. Chem. Chem. Phys.* **2014**, *16*, 5066-5070.
34. Kamat, P. V.; Christians, J. A.; Radich, J. G., Quantum Dot Solar Cells. Hole Transfer as a Limiting Factor in Boosting Photoconversion Efficiency. *Langmuir* **2014**, *30*, 5716–5725. (Review)
35. Kim, J.-P.; Christians, J. A.; Choi, H.; Krishnamurthy, S.; Kamat, P. V., CdSeS Nanowires. Compositionally Controlled Band Gap and Exciton Dynamics. *J. Phys. Chem. Lett.* **2014**, *5*, 1103-1109.
36. Manser, J. S.; Kamat, P. V., Band Filling with Charge Carriers in Organometal Halide Perovskites. *Nature Photonics* **2014**, *8*, 737–743.

37. Becker, M. A.; Radich, J. G.; Bunker, B. A.; Kamat, P. V., How Does a SILAR CdSe Film Grow? Tuning the Deposition Steps to Suppress Interfacial Charge Recombination in Solar Cells. *J Phys Chem Lett.* **2014**, *5*, 1575–1582.
38. Radich, J. G.; Krenselewski, A. L.; Zhu, J.; Kamat, P. V., Is Graphene a Stable Platform for Photocatalysis? Mineralization of Reduced Graphene Oxide with UV-Irradiated TiO<sub>2</sub> Nanoparticles. *Chem. Mater.* **2014**, *26*, 4662–4668.
39. Stamplecoskie, K. G.; Kamat, P. V., Size-Dependent Excited State Behavior of Glutathione-Capped Gold Clusters and Their Light-Harvesting Capacity. *J. Am. Chem. Soc.* **2014**, *136*, 11093–11099.
40. Hoffman, J.; Choi, H.; Kamat, P. V., Size Dependent Energy Transfer Pathways in CdSe Quantum Dot-Squaraine Light Harvesting Assemblies: Förster versus Dexter. *J. Phys. Chem. C* **2014**, *118*, 18453–18461.
41. Jara, D. H.; Yoon, S. J.; Stamplecoskie, K. G.; Kamat, P. V., Size-Dependent Photovoltaic Performance of CuInS<sub>2</sub> Quantum Dot-Sensitized Solar Cells. *Chem. Mater.* **2014**, *26*, 7221–7228.
42. Stamplecoskie, K. G.; Manser, J. S.; Kamat, P. V., Dual Nature of the Excited State in Organic-Inorganic Lead Halide Perovskites. *Energy & Environ. Sci.* **2015**, *8*, 208 - 215.
43. Kirmayer, S.; Edri, E.; Hines, D.; Klein-Kedem, N.; Cohen, H.; Niitsoo, O.; Pinkas, I.; Kamat, P. V.; Hodes, G., Surface Oxidation as a Cause of High Open-Circuit Voltage in CdSe ETA Solar Cells. *Advanced Materials Interfaces* **2015**, *2*, Art No. 1400346 (DOI: 1400310.1401002/admi.201400346).
44. Choi, H.; Chen, Y.-S.; Stamplecoskie, K. G.; Kamat, P. V., Boosting the Photovoltage of Dye-Sensitized Solar Cells with Thiolated Gold Nanoclusters. *J. Phys. Chem. Lett.* **2015**, *6*, 217–223.
45. Hines, D. A.; Forrest, R. P.; Corcelli, S. A.; Kamat, P. V., Predicting the Rate Constant of Electron Tunneling Reactions at the CdSe-Linker-TiO<sub>2</sub> Interface. *J. Phys. Chem. B* **2015**, *119*, in press doi: 10.1021/jp5111295.
46. Chen, Y.-S.; Manser, J. S.; Kamat, P. V., All Solution-Processed Lead Halide Perovskite-BiVO<sub>4</sub> Tandem Assembly for Photolytic Solar Fuels Production. *J. Am. Chem. Soc.* **2015**, *137*, 974-981.
47. Christians, J. A.; Miranda Herrera, P. A.; Kamat, P. V., Transformation of the Excited State and Photovoltaic Efficiency of CH<sub>3</sub>NH<sub>3</sub>PbI<sub>3</sub> Perovskite upon Controlled Exposure to Humidified Air. *J. Am. Chem. Soc.* **2015**, *137*, 1530–1538.
48. Christians, J. A.; Manser, J. S.; Kamat, P. V., Best Practices in Perovskite Solar Cell Efficiency Measurements. Avoiding the Error of Making Bad Cells Look Good. *J. Phys. Chem. Lett.* **2015**, *6*, 852-857. (Viewpoint)
49. Guo, Z.; Manser, J. S.; Wan, Y.; Kamat, P.V.; Huang, L. H. Spatial and temporal Imaging of long-range charge transport in perovskite thin films by ultrafast microscopy. *Nat. Commun.* 2015, in revision.
50. Christians, J. A.; Manser, J. S.; Kamat, P. V. Uncovering the Multifaceted Excited State of CH<sub>3</sub>NH<sub>3</sub>PbI<sub>3</sub>. Charge Separation, Recombination, and Trapping Processes. *J. Phys. Chem. Lett.* 2015 (submitted)

# Enhanced Molecular Photophysics and Photochemistry in Cu(I) and Ir(III) MLCT Chromophores

Catherine E. McCusker, Michelle M. McGoorty, and Felix N. Castellano

Department of Chemistry  
North Carolina State University  
Raleigh, NC 27695-8204

Earth-abundant copper(I) bis-phenanthroline complexes are potential alternatives to the more familiar 2<sup>nd</sup> and 3<sup>rd</sup> row transition metal containing photosensitizers. Copper(I) diimine complexes have metal-to-ligand charge transfer (MLCT) absorptive properties similar to  $[\text{Ru}(\text{bpy})_3]^{2+}$ , without the deactivating ligand field states found in other first row transition metal complexes. However, upon excitation, Cu(I) diimine complexes undergo a significant structural rearrangement, leading to excited states which are highly susceptible to exciplex formation and possess very short lifetimes. These properties limit their usefulness as photosensitizers, especially in donor solvents. Methyl groups in the 3,8- positions of the phenanthroline ligand, combined with bulky *sec*-butyl groups in the 2,9- positions cooperatively restrict the degree of structural distortion in the Cu(I) MLCT excited state thereby extending its lifetime to the microseconds time scale, Figure 1. This long lifetime is maintained in donor solvents such as methanol and acetonitrile, which enabled  $[\text{Cu}(\text{dsbtmp})_2](\text{PF}_6)$  to sensitize solar hydrogen photocatalysis in a water/acetonitrile mixture.

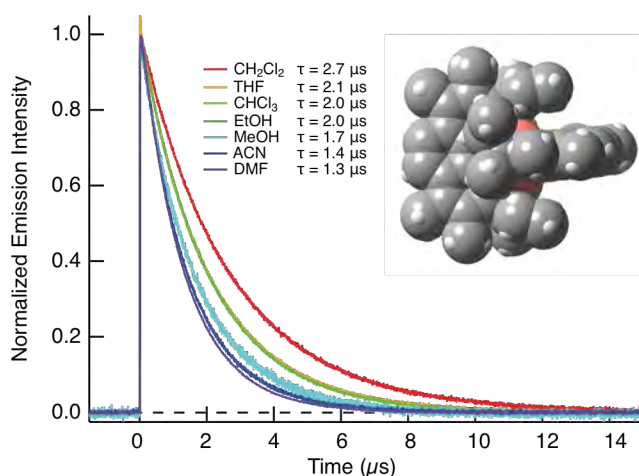


**Figure 1.** Time resolved emission decay kinetics of  $[\text{Cu}(\text{dsbtmp})_2](\text{PF}_6)$  ( $\text{dsbtmp}$  = 2,9-di(*sec*-butyl)-3,4,7,8-tetramethyl-1,10-phenanthroline). Solvents and lifetimes are given in the legend. Inset shows a space filling model of  $[\text{Cu}(\text{dsbtmp})_2](\text{PF}_6)$ .

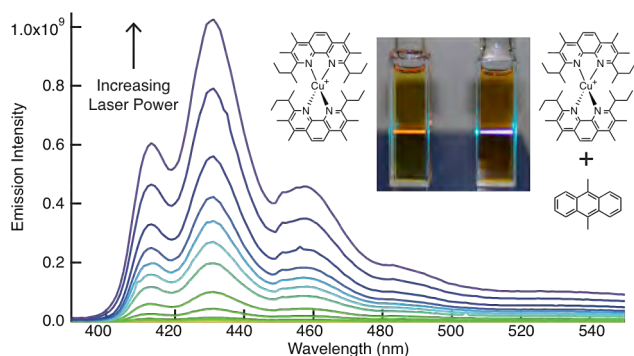
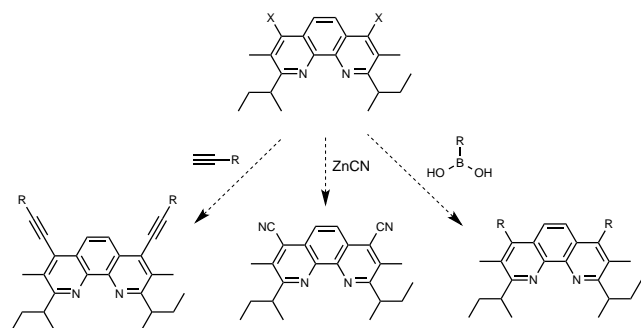


**Figure 2.** Upconverted emission from  $[\text{Cu}(\text{dsbtmp})_2](\text{PF}_6)$  and DMA after 488 nm excitation. Inset shows a digital photograph of emission from  $[\text{Cu}(\text{dsbtmp})_2](\text{PF}_6)$  alone and  $[\text{Cu}(\text{dsbtmp})_2](\text{PF}_6)$  with DMA after 488 nm excitation.

Upconversion photochemistry based on sensitized triplet-triplet annihilation represents a means to generate high-energy emission from low-energy excitation, which has potential applications in a variety of solar energy conversion schemes including solar fuels photochemistry. In these applications it is desirable to replace the traditional 2<sup>nd</sup> and 3<sup>rd</sup> row transition metal photosensitizers with more earth-abundant first row metal complexes. Initially,  $[\text{Cu}(\text{dpp})_2](\text{PF}_6)$  ( $\text{dpp}$  = 2,9-diphenyl-1,10-phenanthroline) was shown to sensitize red-to-green and orange-to-blue photon

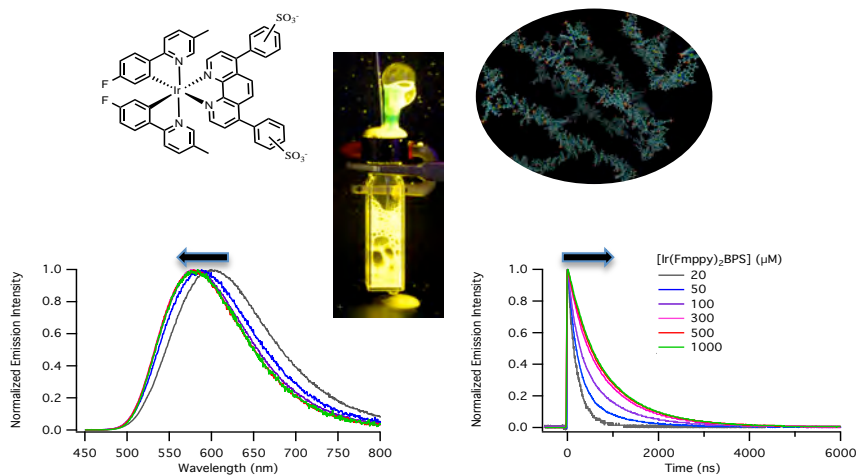
upconversion, but performance was limited by its short excited state lifetime ( $\tau = 250$  ns). Recent work has found that the long-lived  $[\text{Cu}(\text{dsbtmp})_2](\text{PF}_6)$  is able to efficiently sensitize visible-to-near UV upconversion with a series of anthracene derivatives, Figure 2. The upconversion quantum yields of 9,10-diphenylanthracene (DPA) and 9,10-dimethylanthracene (DMA) sensitized by  $[\text{Cu}(\text{dsbtmp})_2](\text{PF}_6)$  (17.8% and 9.2% respectively) represent marked improvements over Ru(II) polypyridyl sensitized upconversion using the same acceptors.

The 2,9-*sec*-butyl groups and the 3,8-methyl groups of the dsbtmp ligand both play an important role in restricting the excited state structural distortion in  $[\text{Cu}(\text{dsbtmp})_2](\text{PF}_6)$ , resulting in a long-



lived excited state. Varying the substituents at the 4,7-positions of the phenanthroline ring will allow for the modification of the photophysical, electrochemical, and solubility properties of the copper *bis* phenanthroline complex, while maintaining the long lifetime of  $[\text{Cu}(\text{dsbtmp})_2](\text{PF}_6)$ . The recently developed synthon shown to the left will allow us to create a library of long-lived Cu(I) photosensitizers moving forward.

The exciting photophysical properties of photoluminescent Ir(III) complexes have been exploited for a variety of applications, including lighting technology, photocatalysis, biological labeling, and analyte sensing. *Bis*-cyclometalated diimine complexes in particular boast long excited state lifetimes, high quantum yields, and chemically tunable emission energies that have been shown to span the visible region of the spectrum. However, the aqueous insolubility of these complexes remains a practical challenge for integration into solar fuels photochemistry schemes. We have designed a series of *bis*-cyclometalated Ir(III) photosensitizers which incorporate a bathophenanthroline disulfonate ancillary ligand to promote aqueous solubility. Surprisingly, compared to organic solvents, these complexes exhibit enhanced aqueous photophysics due to the unexpected formation of aggregates. This photophysical enhancement is observed by increasing the chromophore concentration, resulting in blue-shifted emission energies, as well as



longer excited state lifetimes and higher emission quantum yields. The self-assembly process is clearly evident from simple bubble degassing experiments, which completely removes the chromophores from the aqueous solution in the form of photoluminescent bubbles. Molecular dynamic simulations indicate the formation of

amorphous and dynamic aggregate clusters, which can be further promoted by the addition of

salts such as NaCl. This novel form of aggregation induced emission enhancement offers a unique way to fine tune and improve the photophysical properties of water soluble Ir(III) photosensitizers for a variety of applications.

### DOE Sponsored Publications 2013-2015

1. *Orange-to-Blue and Red-to-Green Photon Upconversion with a Broadband Absorbing Copper(I) MLCT Sensitizer.* McCusker, C.E.; Castellano, F.N. *Chem. Commun.* **2013**, 49, 3537-3539.
2. *Tracking of Tuning Effects in Bis-Cyclometallated Iridium Complexes: A Combined TRIR, Electrochemical, and Computational Study.* Chirdon, D.N.; McCusker, C.E.; Castellano, F.N.; Bernhard, S. *Inorg. Chem.* **2013**, 52, 8795-8804.
3. *Design of a Long-Lifetime, Earth-Abundant, Aqueous Compatible Cu(I) Photosensitizer Using Cooperative Steric Effects.* McCusker, C.E.; Castellano, F.N. *Inorg. Chem.* **2013**, 52, 8114-8120.
4. *Robust Cuprous Phenanthroline Sensitizer for Solar Hydrogen Photocatalysis.* Khnazyer, R.S.; McCusker, C.E.; Olaiya, B.S.; Castellano, F.N. *J. Am. Chem. Soc.* **2013**, 135, 14068-14070.
5. *Excited State Equilibrium Induced Lifetime Extension in a Dinuclear Platinum(II) Complex.* McCusker, C.E.; Chakraborty, A.; Castellano, F.N. *J. Phys. Chem. A* **2014**, 118, 10391-10399.
6. *Triplet State Formation in Homo- and Heterometallic Diketopyrrolopyrrole Chromophores.* McCusker, C.E.; Hablot, D.; Ziessel, R.; Castellano, F.N. *Inorg. Chem.* **2014**, 53, 12564-12571.
7. *Enhancing Molecular Photophysics by Merging Organic and Inorganic Chromophores.* Castellano, F.N. *Acc. Chem. Res.* **2015**, 48, 828-839.
8. *Transient Absorption Dynamics of Sterically Congested Cu(I) MLCT Excited States.* Garakyaraghi, S.; Danilov, E.O.; McCusker, C.E.; Castellano, F.N. *J. Phys. Chem. A* **2015**, 119, 3181-3193.
9. *Efficient Visible to Near-UV Photochemical Upconversion Sensitized by a Long Lifetime Cu(I) MLCT Complex.* McCusker, C.E.; Castellano, F.N. *Inorg. Chem.* **2015**, submitted.

# *Session I*

## *Control of Energy Transfer*



## Sensitization of Molecular Triplet Excitonic Processes with Colloidal Semiconductor Nanocrystals

Nick Thompson, Dan Congreve, Mengfei Wu, Mounqi Bawendi, Vladimir Bulović, Troy Van Voorhis, and Marc Baldo  
Energy Frontier Research Center for Excitonics  
Massachusetts Institute of Technology  
Cambridge, MA, 02139

Triplet excitons can be the dominant excitation in molecular photochemical processes and optoelectronic devices. They exhibit long lifetimes, are often the lowest energy excitation in the system, and comprise three quarters of the excitons formed from free carriers. Triplets are also crucial to exciton fission and fusion processes, where excitons are split or combined allowing wavelength up and down conversion with minimal energetic loss.

Unfortunately, triplet excitons are often an undesirable energy sink – spin-forbidden from emitting light and strongly bound relative to free electron-hole pairs. Harvesting their energy is consequently an important technological challenge. The solution in the visible-spectrum is to employ molecules with strong spin-orbit coupling and efficient phosphorescence from their triplet states. However, phosphorescent molecular acceptors have proved ineffective in the infrared ( $h\nu < \sim 1.5$  eV) because of strong, non-radiative dissipation.

We show that inorganic nanocrystals are an especially effective means of harvesting and sensitizing non-emissive triplets with energies in the infrared. This is in contrast to prior, unsuccessful, attempts to transfer triplets to bulk inorganic semiconductors, as well as reported work with colloidal nanocrystals, which has relied on Förster transfer from emissive molecular donor states such as singlet excitons or spin-mixed triplet excitons of a phosphorescent molecule.

We have demonstrated triplet exciton harvesting by colloidal semiconducting nanocrystals at the conclusion of singlet exciton fission in tetracene; see Fig. 1. We find almost unity triplet energy transfer efficiency from tetracene to PbS nanocrystals when the solvating ligands on the nanocrystals are short, *e.g.* caprylic acid. Because the PbS nanocrystals are efficiently radiative, we believe that this energy transfer process will enable radiative and long range, Förster-type energy transfer to silicon solar cells, thereby linking the exciton fission process to conventional solar cells. Because singlet exciton fission can circumvent the conventional single junction limit of solar cells, triplet energy transfer from molecules to nanocrystals should increase the efficiency of silicon solar cells from 25% to 30% or more.

We have also investigated the reverse process of energy transfer from colloidal semiconductor nanocrystals to molecular triplet excitons. One technological motivation for this work is the sensitization of optical upconversion from the infrared. Traditionally, this process uses molecules with strong spin orbit coupling to absorb the pump light and convert the excitations to triplets prior to triplet-triplet annihilation and upconversion to the emissive singlet state. But as with phosphorescent emitters, the availability of good sensitizers tails off with the energy gap ‘law’, and demonstrations of infrared to visible upconversion, which would be most useful for many

applications, have been limited to incident light with  $\lambda < 800\text{nm}$ . Further, the exchange splitting between singlet and triplet states is typically on the order of  $0.7\text{eV}$  in molecules, thus the sensitization process can incur substantial losses, especially for infrared applications.

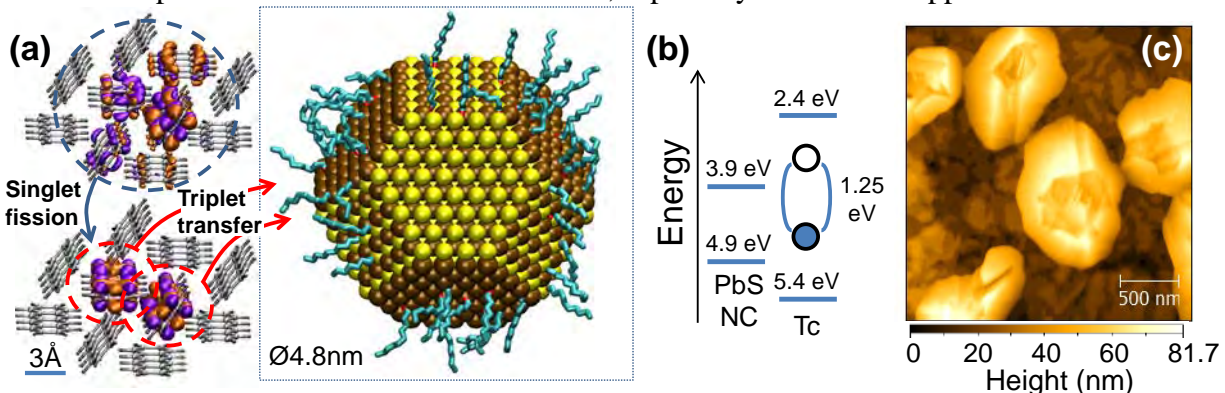


**Figure 1:** (a) Schematic of triplet exciton transfer from tetracene to a PbS nanocrystal with decanoic acid ligands. Note that the figure is not to scale; the tetracene molecules have been expanded relative to the nanocrystal to show the excitonic states. (b) Energy level diagram of the tetracene-PbS nanocrystal interface, with the tetracene HOMO energy from UPS measurements, and a lower bound for the LUMO energy obtained by adding the singlet energy from the emission peak. (c) AFM micrograph of the tetracene layer on PbS nanocrystals.

In Fig. 2, we show an example of solid-state exciton-exciton annihilation in thin films of rubrene when sensitized by PbS nanocrystals. Upconversion is achieved from beyond  $\lambda=1\mu\text{m}$  at an efficiency of 4-5%. The high triplet exciton concentrations achieved in solid state also enable operation at absorbed powers of only  $\sim 0.1$  suns. The nanocrystals are tunable to  $\lambda > 1.5\mu\text{m}$ . Thus, with matching molecular annihilators, colloidal nanocrystals promise efficient upconversion from low intensity incoherent light with wavelengths well into the near infrared.

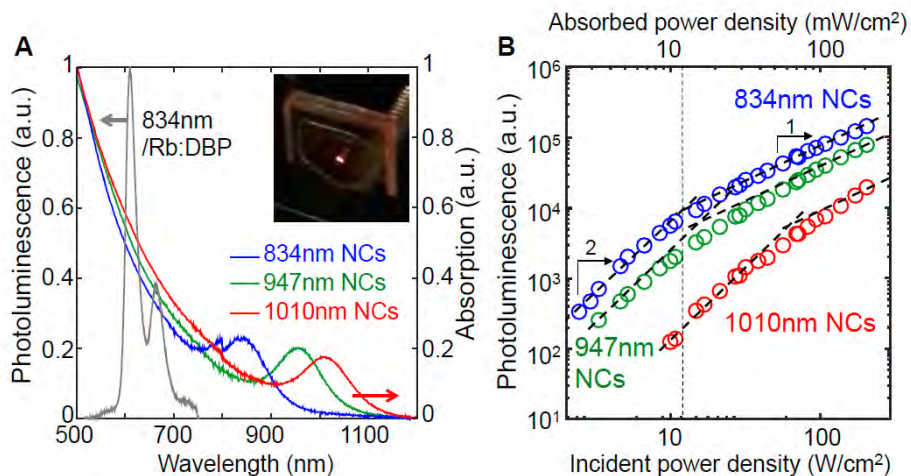


**Figure 2:** (a) The absorption and emission of the upconverting structures as a function of the excitonic peak wavelength of the colloidal nanocrystals. **Inset:** the device under excitation at  $\lambda=808\text{nm}$ . (b) The intensity dependence shows a transition from quadratic to linear when upconversion becomes the dominant process for triplet excitons.

## References

1. Thompson, N.J., M.W.B. Wilson, D.N. Congreve, P.R. Brown, J.M. Scherer, T.S. Bischof, M. Wu, N. Geva, M. Welborn, T. Van Voorhis, V. Bulović, M.G. Bawendi, and M.A. Baldo, “Energy harvesting of non-emissive triplet excitons in tetracene by emissive PbS nanocrystals”, *Nature Materials*, **13**, 1039–1043 (2014).

## Singlet Fission

Josef Michl,<sup>1,2</sup> Paul I. Dron,<sup>1</sup> Teruo Umemoto,<sup>1</sup> Yves-Marie Hervault,<sup>1</sup> Millicent B. Smith,<sup>1</sup> Cyprien Lemouchi,<sup>1</sup> Alexandre G. L. Olive,<sup>1</sup> Cecile Givelet,<sup>1</sup> Matibur Zamadar,<sup>1</sup> Zdenek Havlas,<sup>1,2</sup> Farhad Tamadon,<sup>1</sup> Lance F. Culnane,<sup>1</sup> Dean Antic,<sup>1</sup> Eric A. Buchanan,<sup>1</sup> Andrew J. Chomas,<sup>1</sup> Jonathan B. Bair,<sup>1</sup> Matthew R. Schreiber,<sup>1</sup> and Jin Wen,<sup>1,2</sup>

<sup>1</sup> Department of Chemistry and Biochemistry  
University of Colorado at Boulder  
Boulder, CO 80309-0215

<sup>2</sup> Institute of Organic Chemistry and Biochemistry  
Academy of Sciences of the Czech Republic  
16610 Prague, Czech Republic

Our goal has been a first principles formulation of structural design rules for singlet fission sensitizers. We started by using quantum mechanical principles to identify classes of organic chromophores likely to have their singlet and triplet states arranged in a way that would make singlet fission exoergic. One of these classes are alternant hydrocarbons such as tetracene, pentacene, or perylene, and their simple derivatives, which have traditionally been the mainstay of singlet fission research. We focus our attention on another much larger class, biradicaloids and their derivatives, such as isobenzofurans and indigoid heterocycles. In many cases, the lowest singlet excitation energies (band gaps) of the candidate structures then need to be adjusted by suitable substitution to approach the optimal value near 2.2 eV, and an example will be described in some detail.

We have two objectives in our search for chromophores that perform singlet fission efficiently: (i) to find very small molecules, for which very high quality calculations of molecular dynamics of the singlet fission process would then be feasible, and (ii) to find sturdy and light-fast molecules that would be practically useful. It would of course be ideal if one and the same chromophore met both objectives. Representative candidates of the biradicaloid type of structure have been selected and CASPT2 calculations of state energies were performed for them. Those compounds for which the computed results were most favorable were then used as targets for synthesis and a detailed examination of photophysics.

The next consideration is an optimization of the spatial relation between two neighboring chromophores, which is again based on simplified quantum chemical treatment with focus on the formulation of simple design rules. Ultimately, a simultaneous consideration of a larger number of chromophores may be required but has not yet been attempted. Using an approximation in which the lowest energy singlet and triplet excitations of a chromophore are represented by one-electron transitions from the highest occupied to the lowest unoccupied molecular orbital (HOMO to LUMO), we have derived somewhat complicated formulas for the relative rate of singlet fission in the diabatic representation, which go beyond results previously published in that they do not neglect intermolecular orbital overlap. A systematic introduction of physically

justifiable and numerically tested approximations yields permits a simplification of these formulas and ultimately leads to a formulation that expresses the rate as a function of the molecular orbital coefficients for HOMO and LUMO and of the overlaps between the atomic orbitals on one and the other chromophore. These formulas require almost no computational effort and qualitative results can often be guessed by inspection. Limiting cases, such as two identical chromophores, or one chromophore that is a strong electron donor and another that is a strong electron acceptor, yield particularly simple results that have been converted into structural design rules.

Using a formulation of intermediate complexity (no intermolecular overlap), numerical computations have been performed for a model consisting of two ethylenes, including a complete search of the six-dimensional space of mutual location and mutual orientation of the two chromophores. The contributions of the "direct term" were found to be entirely negligible relative to those of the "mediated term" that contains indirect interactions through virtual charge-transfer states. The results are now being examined and searched for "sweet spots" in which singlet fission is computed to be especially fast. The best mutual disposition of the two ethylenes found so far is a slip-stacked arrangement, in which the slip is in the direction of the HOMO-LUMO transition moment, and this result can be understood in very simple terms.

It is relatively rare for a highly efficient mutual arrangement of neighboring chromophores to be present in a naturally occurring crystal structure of a compound, and the next synthetic tasks are to prepare suitable covalent dimers or to use crystal engineering to arrive at the desired structures. This step carries a risk in that inter-chromophore interactions may modify state energies sufficiently to convert a case of isoergic or mildly exoergic singlet fission into an endoergic one. The simplest description of such effects is provided by exciton splitting theory and it is advisable to make a crude estimate of its magnitude using the dipole approximation. Examples of both types of approach and the associated complications will be presented.

The very first compound that was identified as a potential new candidate for singlet fission was 1,3-diphenylisobenzofuran (**1**), and we were fortunate in that one of its two crystalline modifications had neighboring molecules arranged very favorably and yielded a 200% triplet yield at liquid nitrogen temperature. In collaboration with our colleagues in the Justin Johnson group at NREL, a detailed examination of two crystalline forms of **1** was performed. We have synthesized and examined in detail a long series of its dimers and most of the results have been published. In the course of this work, it was discovered that in sufficiently polar solvents the charge transfer states referred to above as virtual contributors to the singlet fission process can actually be converted into real states and observed directly. We have also observed an interesting kind of isomerism in which two singlet or triplet excited states of a dimer differ in that one has a localized and the other a delocalized excitation and both can be observed.

### **DOE Sponsored Publications 2012-2015**

1. Akdag, A.; Havlas, Z.; Michl, J. "Search for a Small Chromophore with Efficient Singlet Fission: Biradicaloid Heterocycles", *J. Am. Chem. Soc.* **2012**, *134*, 14624.
2. Johnson, J. C.; Akdag, A.; Zamadar, M.; Chen, X.; Schwerin, A. F.; Paci, I.; Smith, M. B.; Havlas, Z.; Miller, J. R.; Ratner, M. A.; Nozik, A. J.; Michl, J. "Toward Designed Singlet

Fission: Solution Photophysics of Two Indirectly Coupled Covalent Dimers of 1,3-Diphenylisobenzofuran”, *J. Phys. Chem. B* **2013**, *117*, 4680.

3. Smith, M. B.; Michl, J. “Recent Advances in Singlet Fission”, *Annu. Rev. Phys. Chem.* **2013**, *64*, 361.

4. Johnson, J. C.; Nozik, A. J., Michl, J. “The Role of Chromophore Coupling in Singlet Fission”, *Acc. Chem. Res.* **2013**, *46*, 1290.

5. Johnson, J. C.; Michl, J. “Singlet Fission and 1,3-Diphenylisobenzofuran as a Model Chromophore”, in *Advanced Concepts in Photovoltaics*, Nozik, A. J., Conibeer, G., Beard, M. C., Eds.; Royal Society of Chemistry: Oxfordshire, UK, 2014, p. 324.

6. Schrauben, J.; Ryerson, J.; Michl, J.; Johnson, J. “The Mechanism of Singlet Fission in Thin Films of 1,3-Diphenylisobenzofuran”, *J. Am. Chem. Soc.* **2014**, *136*, 7363.

7. Ryerson, J.; Schrauben, J. N.; Ferguson, A. J.; Sahoo, S. C.; Naumov, P.; Havlas, Z.; Michl, J.; Nozik, A. J.; Johnson, J. C. “Two Thin Film Polymorphs of the Singlet Fission Compound 1,3-Diphenylisobenzofuran”, *J. Phys. Chem. C* **2014**, *118*, 12121.

8. Akdag, A.; Wahab, A.; Beran, P.; Rulíšek, L.; Dron, P. I.; Ludvík, J.; Michl, J. “Covalent Dimers of 1,3-Diphenylisobenzofuran for Singlet Fission: Synthesis and Electrochemistry”, *J. Org. Chem.* **2015**, *80*, 80.

9. Wen, J.; Havlas, Z.; Michl, J. “Captodatively Stabilized Biradicaloids as Chromophores for Singlet Fission”, *J. Am. Chem. Soc.* **2015**, *137*, 165.

10. Schrauben, J. N.; Zhao, Y.; Mercado, C.; Dron, P. I.; Ryerson, J. M.; Michl, J.; Zhu, K.; Johnson, J. C. “Singlet Fission-Induced Photocurrent in a Dye-Sensitized Solar Cell”, *ACS Appl. Mater. Interfaces* **2015**, *7*, 2286.

## Self-ordering Molecular Assemblies for Photochemical Charge Separation and Transport

Michael R. Wasielewski, Yi-Lin Wu, Patrick E. Hartnett, Kristen E. Brown, Leah E. Shoer, Daniel M. Gardner, Scott M. Dyar, Eric A. Margulies, Samuel W. Eaton, and Tobin J. Marks

Department of Chemistry  
Northwestern University  
Evanston, IL 60208-3113

Self-assembly of small electron donor-acceptor (D-A) molecules into discrete and monodisperse nanostructures provides geometrically defined platforms to emulate the photo-induced electron transfer processes in photosynthetic systems. Organization of molecules by this thermodynamically-driven method can result in architectures with unique inter-chromophore relationships that are otherwise difficult to realize by conventional covalent synthesis. In particular,  $\pi$ -stacked D-A dyads and triads can afford ordered and segregated D/A domains through which photo-generated holes and electrons can be further separated and rapidly transported to electrodes in photovoltaics or to catalysts for solar fuels formation. The design of these self-ordering molecular assemblies must ensure that charge hopping of the separated holes and electrons between the non-covalent donors and acceptors within their respective segregated conduits must be significantly faster than charge recombination (Figure 1). We will present two strategies that demonstrate that photo-induced charge separation can take place within covalent chromophoric redox partners followed by transport of photo-generated holes and electrons independently through well-ordered, segregated molecular charge conduits.

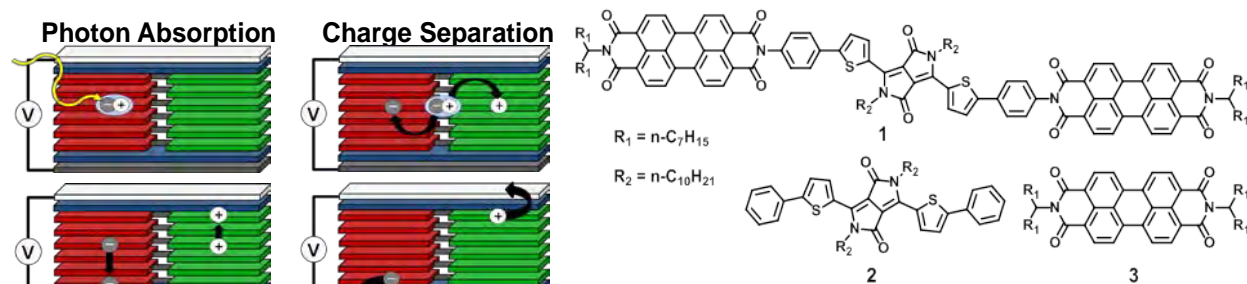


**Figure 1.** Left) Charge conduit concept. Right) Structures of PDI-DPP-PDI (**1**) and reference molecules.

To illustrate the first strategy, the photophysics of a covalently linked perylene-3,4,9,10-tetracarboxylic diimide-dipyrromethane-perylene-3,4,9,10-tetracarboxylic diimide acceptor-donor-acceptor molecule (PDI-DPP-PDI, **1**) were investigated and found to be markedly different in solution versus in unannealed and solvent annealed films. Photoexcitation of **1** in toluene results in quantitative charge separation in  $\tau = 3.1 \pm 0.2$  ps, with charge recombination in  $\tau = 340 \pm 10$  ps, while in unannealed/disordered films of **1**, charge separation occurs in  $\tau < 250$  fs, while charge recombination displays a multiexponential decay in  $\sim 6$  ns. The absence of long-lived, charge separation in the disordered film suggests that few free charge carriers are generated. In contrast, upon  $\text{CH}_2\text{Cl}_2$  vapor annealing films of **1**, grazing-incidence X-ray scattering shows that the molecules form a more ordered structure. Photoexcitation of the ordered films results in initial formation of a spin-correlated radical ion pair (electron-hole pair) as indicated by magnetic field effects on the formation of free charge carriers which live for  $\sim 4$   $\mu\text{s}$  (Figure 2). This result has significant

implications for the design of solar cells based on covalent donor-acceptor systems and shows that long-lived, charge-separated states can be achieved by controlling intramolecular charge separation dynamics in well-ordered systems.

To illustrate the second strategy, we have prepared a G-quadruplex (**GQ-1**) that incorporates an 8-(4'-aminophenylethynyl)guanine (GEAn) electron donor covalently attached to a 4-aminonaphthalene-1,8-imide (ANI) chromophore and a naphthalene-1,8:4,5-bis(dicarboximide) (NDI) electron acceptor (GEAn-ANI-NDI, **1**). In the presence of KPF<sub>6</sub> in tetrahydrofuran (THF), **1** self-assembles into a monodisperse, C<sub>4</sub>-symmetric **GQ-1** with small spatial intra-quadruplex overlap between the ANI-NDI units (Figure 3). Photoexcitation of monomeric **1** induces the two-step charge transfer GEAn<sup>-1\*</sup>ANI-NDI → GEAn<sup>++</sup>-ANI<sup>-•</sup>-NDI → GEAn<sup>++</sup>-ANI-NDI<sup>-•</sup> that occurs in τ<sub>CS1</sub> = 5 ps and τ<sub>CS2</sub> = 330 ps, respectively, while charge recombination occurs in ca. 300 ns. Sharpening of the GEAn<sup>++</sup> transient absorption and a shift of the ethynyl vibrational frequency in **1** were observed, concomitant with the stepwise electron transfer from ANI<sup>-•</sup> to NDI. Formation of **GQ-1** from **1** in THF increases the secondary charge-shifting rate (τ<sub>CS2</sub> = 110 ps), and results in no change in ethynyl vibrational frequency (Figure 4). Charge recombination in **GQ-1** is slowed by enhanced radical-pair intersystem crossing driven by the greater number of hyperfine couplings in the assembly. Moreover, time-resolved EPR spectroscopy shows that the spin-spin-exchange interaction (*J*) between the radicals of GEAn<sup>++</sup>-ANI-NDI<sup>-•</sup> within **GQ-1** is smaller than that of **1**, suggesting that the spin (charge) density in GEAn<sup>++</sup> is more dispersed in **GQ-1**. The spectroscopic results are consistent with hole sharing among the guanines within the G-quadruplex that is kinetically competitive with the formation of GEAn<sup>++</sup>. This suggests that G-quadruplexes can serve as effective hole conduits in ordered donor-acceptor assemblies.

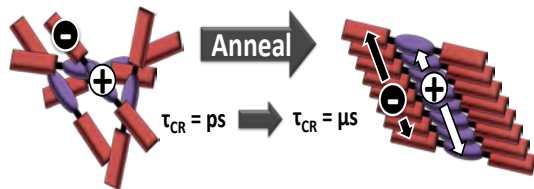


**Figure 2.** Large increase in photo-generated electron-hole pair lifetime upon structural ordering of PDI-DPP-PDI.

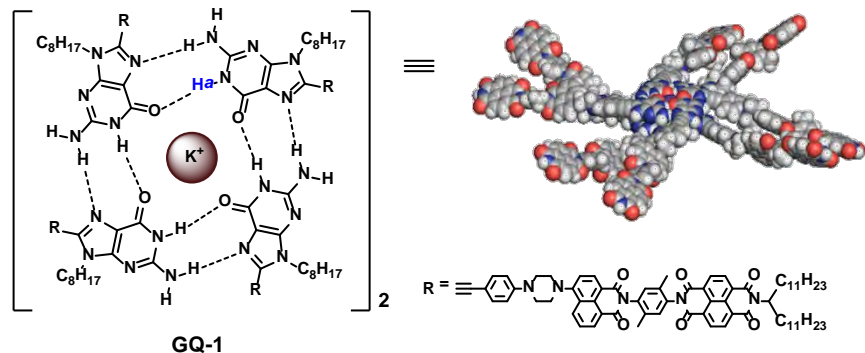


**Figure 3.** Structure of **GQ-1** obtained by NMR and SAX/WAXS.

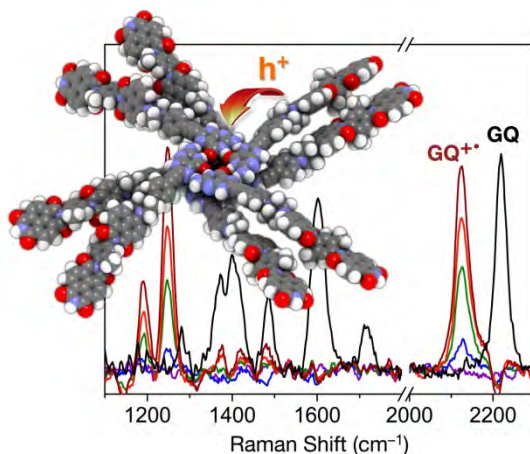


**Figure 4.** Femtosecond stimulated Raman spectra of **GQ-1** following photoexcitation.

## DOE Sponsored Publications 2012-2015

1. Polymer Matrix Dependence of Conformational Dynamics within  $\pi$ -Stacked Perylenediimide Dimer and Trimer Revealed by Single Molecule Fluorescence Spectroscopy, H. Yoo, H. W. Bahng, M. R. Wasielewski, and D. Kim, *Phys. Chem. Chem. Phys.* **14**, 2001-2007 (2012).
2. Intersystem Crossing Involving Strongly Spin Exchange-Coupled Radical Ion Pairs in Donor-Bridge-Acceptor Molecules, M. T. Colvin, A. Butler Ricks, A. M. Scott, D. T. Co, and M. R. Wasielewski, *J. Phys. Chem. A* **116**, 1923-1930 (2012).
3. Role of Bridge Energetics on the Preference for Hole or Electron Transfer Leading to Charge Recombination in Donor-Bridge-Acceptor Molecules, M. T. Colvin, A. Butler Ricks, and M. R. Wasielewski, *J. Phys. Chem. A* **116**, 2184-2191 (2012).
4. Exponential Distance Dependence of Photoinitiated Stepwise Electron Transfer in Donor-Bridge-Acceptor Molecules: Implications for Wire-like Behavior, A. Butler Ricks, D. T. Co, K. E. Brown, M. Wenninger, S. D. Karlen, Y. A. Berlin, and M. R. Wasielewski, *J. Am. Chem. Soc.* **134**, 4581-4588 (2012).
5. Electron Transfer within Self-Assembling Cyclic Tetramers using Chlorophyll-Based Donor-Acceptor Building Blocks, V. L. Gunderson, A. L. Smeigh, C. H. Kim, D. T. Co, and M. R. Wasielewski, *J. Am. Chem. Soc.* **134**, 4363-4372 (2012).
6. Supramolecular Chlorophyll Assemblies for Artificial Photosynthesis, V. L. Gunderson and M. R. Wasielewski, in "Handbook of Porphyrin Science", K. Kadish, K. M. Smith, and K. Guillard, Eds. World Scientific, Singapore, 2012, Vol. 20, pp. 45-105.
7. Vibrational Dynamics of a Perylene-Perylenediimide Donor-Acceptor Dyad Probed with Femtosecond Stimulated Raman Spectroscopy, K. E. Brown, B. S. Veldkamp, D. T. Co, M. R. Wasielewski, *J. Phys. Chem. Lett.* **3**, 2362-2366 (2012).
8. Dynamics and Efficiency of Hole Transport in LNA:DNA Hybrid Diblock Oligomers, A. Thazhathveetil, J. Vura-Weis, A. Trifonov, M. R. Wasielewski and F. D. Lewis, *J. Am. Chem. Soc.* **134**, 16434-16440 (2012).
9. Excitonic Coupling between Linear and Trefoil Trimer Perylenediimide Molecules Probed by Single-Molecule Spectroscopy, H. Yoo, S. Furumaki, J. Yang; J.-E. Lee, H. Chung, T. Oba, H. Kobayashi, B. Rybtchinski, T. M. Wilson, M. R. Wasielewski, M. Vacha, and D. Kim, *J. Phys. Chem. B* **116**, 12878-12886 (2012).
10. Self-assembly of a Chlorophyll-based Cyclic Trimer: Structure and Intramolecular Energy Transfer, V. L. Gunderson and M. R. Wasielewski, *Chem. Phys. Lett.* **556**, 303-307 (2013).
11. Photoinitiated Electron Transfer in Zinc Porphyrin-Perylenediimide Cruciforms and their Self-assembled Oligomers, S. M. Mickley Conron, L. E. Shoer, A. L. Smeigh, A. Butler Ricks, and M. R. Wasielewski, *J. Phys. Chem. B* **117**, 2195-2204 (2013).
12. Photoinitiated Multi-step Charge Separation and Ultrafast Charge Transfer Induced Dissociation in a Pyridyl-Linked Photosensitizer-Cobaloxime Assembly, B. S. Veldkamp, W.-S. Han, S. M. Dyar, S. W. Eaton, M. A. Ratner, and M. R. Wasielewski, *Energy and Environ. Sci.* **6**, 1917-1928 (2013).

13. Dynamics and Efficiency of Photoinduced Charge Transport in DNA: Toward the Elusive Molecular Wire, F. D. Lewis and M. R. Wasielewski, *Pure Appl. Chem.* **85**, 1379-1387 (2013).
14. Design, Synthesis, Characterization, and Catalytic Properties of a Large-pore MOF Possessing Single-site Vanadyl(monocatecholate) Moieties, H. G. T. Nguyen, M. H. Weston, A. A. Sarjeant, D. M. Gardner, Z. An, R. Carmieli, M. R. Wasielewski, O. K. Farha, J. T. Hupp, and S. T. Nguyen, *Crystal Growth and Design* **13**, 3528-3534. (2013).
15. Extending Photo-induced Charge Separation Lifetimes by using Supramolecular Design: Guanine-Perylenediimide G-Quadruplex, Y.-L. Wu, K. E. Brown, and M. R. Wasielewski, *J. Am. Chem. Soc.* **135**, 13322-13325 (2013).
16. Singlet Exciton Fission in Polycrystalline Thin Films of a Slip-Stacked Perylenediimide, S. W. Eaton, L. E. Shoer, S. D. Karlen, S. M. Dyar, E. A. Margulies, B. S. Veldkamp, C. Ramanan, D. A. Hartzler, S. Savikhin, T. J. Marks, and M. R. Wasielewski, *J. Am. Chem. Soc.* **135**, 14701-14712 (2013).
17. Modulation of Electronics and Thermal Stabilities of Photochromic Phosphino-Aminoazobenzene Derivatives in Weak-Link Approach Coordination Complexes, J. S. Park, A. M. Lifschitz, R. M. Young, M. R. Wasielewski, C. L. Stern, A. A. Sarjeant, and C. A. Mirkin, *J. Am. Chem. Soc.* **135**, 16988-16996 (2013).
18. Electron Sharing and Anion- $\pi$  Recognition in Molecular Triangular Prisms, S. T. Schneebeli, M. Frasconi, Z. Liu, Y. Wu, D. M. Gardner, N. L. Strutt, C. Cheng, R. Carmieli, M. R. Wasielewski, and J. F. Stoddart, *Angew. Chem. Int. Ed.* **52**, 13100-13104 (2013).
19. Ultrafast Conformational Dynamics of Electron Transfer in ExBox<sup>4+</sup>⊂perylene, R. M. Young, S. M. Dyar, J. C. Barnes, M. Juriček, J. F. Stoddart, D. T. Co, and M. R. Wasielewski, *J. Phys. Chem. A* **117**, 12423-12448 (2013).
20. Metal–Organic Framework Thin Films Composed of Free-Standing Acicular Nanorods Exhibiting Reversible Electrochromism, C.-W. Kung, T. C. Wang, J. E. Mondloch, D. Fairen-Jimenez, D. M. Gardner, W. Bury, J. M. Klingsporn, J. Barnes, R. P. Van Duyne, J. F. Stoddart, M. R. Wasielewski, O. K. Farha, and J. T. Hupp, *Chem. Mater.* **25**, 5012-5017 (2013).
21. Triplet State Formation in Photoexcited Slip-Stacked Perylene-3,4:9,10-bis(dicarboximide) Dimers on a Xanthene Scaffold, K. M. Lefler, K. E. Brown, W. A. Salamant, S. M. Dyar, K. E. Knowles, and M. R. Wasielewski, *J. Phys. Chem. A* **117**, 10333-10345 (2013).
22. Ground and Excited State Electronic Spectra of Perylenediimide Dimers with Flexible and Rigid Geometries in DNA Conjugates, P. P. Neelekandan, T. A. Zeidan, M. McCullagh, G. C. Schatz, J. Vura-Weis, R. F. Kelley, C. H. Kim, M. R. Wasielewski, and F. D. Lewis, *Chem. Sci.* **5**, 973-981 (2014).
23. Radical Anions of Trifluoromethylated Perylene and Naphthalene Imide and Diimide Electron Acceptors, V. V. Roznyatovskiy, D. M. Gardner, S. W. Eaton, and M. R. Wasielewski, *Org. Lett.* **16**, 696-699 (2014).

24. Photodriven Charge Separation and Transport in Self-assembled Zinc Tetrabenzotetraphenylporphyrin and Perylenediimide Charge Conduits, V. V. Roznyatovskiy, R. Carmieli, S. M. Dyar, K. E. Brown, and M. R. Wasielewski, *Angew. Chem. Int. Ed.* **53**, 3457-3461 (2014).
25. Gated Electron Sharing Within Dynamic Naphthalene Diimide-Based Oligorotaxanes, A.-J. Avestro, D. M. Gardner, N. A. Vermeulen, E. A. Wilson, S. T. Schneebeli, A. C. Whalley, M. E. Belowich, R. Carmieli, M. R. Wasielewski, and J. F. Stoddart *Angew. Chem. Int. Ed.* **53**, 4442-4449 (2014).
26. Electron Transfer and Multi-Electron Accumulation in ExBox<sup>4+</sup>, S. M. Dyar, J. C. Barnes, M. Juriček, J. F. Stoddart, D. T. Co, R. M. Young, M. R. Wasielewski, *Angew. Chem. Int. Ed.* **53**, 5371-5375 (2014).
27. Self-assembly of Supramolecular Light-harvesting Arrays from Symmetric Perylene-3,4-dicarboximide Trefoils, K. M. Lefler, C. H. Kim, Y.-L. Wu, and M. R. Wasielewski, *J. Phys. Chem. Lett.* **5**, 1608-1615 (2014).
28. Rh(I) as a Photoreductant in Bodipy Photoredox Switches, A. M. Lifschitz, R. M. Young, J. Mendez-Arroyo, V. V. Roznyatovskiy, C. M. McQuirk, M. R. Wasielewski, and C. A. Mirkin, *Chem. Commun.* **50**, 6850-6852 (2014).
29. Solid-State Characterization and Photoinduced Intramolecular Electron Transfer in a Nanoconfined Octacationic Homo[2]Catenane, J. C. Barnes, M. Frasconi, R. M. Young, N. H. Khadary, W.-G. Liu, S. M. Dyar, P. R. McGonigal, I. C. Gibbs-Hall, C. S. Diercks, A. A. Sarjeant, C. L. Stern, W. A. Goddard, M. R. Wasielewski, and J. F. Stoddart, *J. Am. Chem. Soc.* **2014**, *136*, 10569-10572.
30. Direct Observation of Ultrafast Excimer Formation in Covalent Perylenediimide Dimers using Near-Infrared Transient Absorption Spectroscopy, K. E. Brown, W. A. Salamant, L. E. Shoer, R. M. Young, and M. R. Wasielewski, *J. Phys. Chem. Lett.* **5**, 2588-2593 (2014).
31. Electron Delocalization in a Rigid Cofacial Naphthalene-1,8:4,5-bis(dicarboximide) Dimer, Y. Wu, M. Frasconi, D. M. Gardner, P. R. McGonigal, S. T. Schneebeli, M. R. Wasielewski, and J. F. Stoddart, *Angew Chem. Int. Ed.* **53**, 9476-9481 (2014).
32. Symmetrized Photoinitiated Electron Flow within the [Myoglobin:Cytochrome b5] Complex on Singlet and Triplet Timescales: Energetics vs Dynamics, N. Co, R. M. Young, A. L. Smeigh, M. R. Wasielewski, and B. M. Hoffman, *J. Am. Chem. Soc.* **136**, 12730-12736 (2014).
33. Excimer Formation in Cofacial and Slip-Stacked Perylene-3,4:9,10-bis(dicarboximide) Dimers on a Redox-Inactive Triptycene Scaffold, E. A. Margulies, L. E. Shoer, S. W. Eaton, and M. R. Wasielewski, *Phys. Chem. Chem. Phys.* **16**, 23735-23742 (2014).
34. Spin-Selective Charge Recombination in Complexes of CdS Quantum Dots and Organic Hole Acceptors, D. J. Weinberg, S. M. Dyar, Z. Khademi, M. Malicki, S. R. Marder, M. R. Wasielewski, and E. A. Weiss, *J. Am. Chem. Soc.* **136**, 14513-14518 (2014).

35. Energy Flow Dynamics within Cofacial and Slip-Stacked Perylene-3,4-dicarboximide Dimer Models of  $\pi$ -Aggregates, R. J. Lindquist, K. M. Lefler, K. E. Brown, S. M. Dyar, D. T. Co, R. M. Young, and M. R. Wasielewski, *J. Am. Chem. Soc.* **136**, 14912-14923 (2014).
36. Long-lived Charge Carrier Generation in Ordered Films of a Covalent Perylenediimide-Diketopyrrolopyrrole-Perylenediimide Molecule, P. E. Hartnett, S. M. Dyar, E. A. Margulies, L. E. Shoer, A. W. Cook, S. W. Eaton, T. J. Marks, and M. R. Wasielewski, *Chem. Sci.* **6**, 402-411 (2015).
37. Molecular Excited States: Accurate Calculation of Relative Energies and Electronic Coupling Between Charge Transfer and Non-Charge Transfer States, B. S. Veldkamp, X. Liu, M. R. Wasielewski, J. E. Subotnik, and M. A. Ratner, *J. Phys. Chem. A* **119**, 253-262 (2015).
38. Unusually Short Excited State Lifetimes of Indenofluorene and Fluorenofluorene Derivatives Result from a Conical Intersection, B. D. Rose, L. E. Shoer, A. G. Fix, M. R. Wasielewski, and M. M. Haley, *Chem. Phys. Lett.* **616-617**, 137-141 (2014).
39. Photoinduced Electron Transfer within a Zinc Porphyrin-Cyclobis(paraquat-*p*-phenylene) Donor-Acceptor Dyad, M. Fathalla, J. C. Barnes, R. M. Young, K. J. Hartlieb, S. M. Dyar, S. W. Eaton, B. K. Rugg, A. A. Sarjeant, D.T. Co, M. R. Wasielewski, J. F. Stoddart, *Chem. Eur. J.* **20**, 14690-14697 (2014).
40. Bias-switchable Permselectivity and Redox Catalytic Activity of a Ferrocene-Functionalized, Thin-Film Metal Organic Framework Compound, I. Hod, W. Bury, D. M. Gardner, P. Deria, V. Roznyatovskiy, M. R. Wasielewski, O. K. Farha, and J. T. Hupp, *J. Phys. Chem. Lett.* **6**, 586-591 (2015).
41. Photoinduced Hole Injection into a Self-assembled  $\pi$ -Extended G-quadruplex, Y.-L. Wu K. E. Brown, D. M. Gardner, S. M. Dyar, and M. R. Wasielewski, *J. Am. Chem. Soc.* **137**, 3981-3990 (2015).
42. Post-Assembly Atomic Layer Deposition of Ultrathin Metal-Oxide Coatings Enhances the Performance of an Organic Dye-Sensitized Solar Cell by Suppressing Dye Aggregation, H.-J. Son, C. H. Kim, D. W. Kim, N. C. Jeong, C. Prasittichai, L. Luo, J. Wu, O. K. Farha, M. R. Wasielewski, and J. T. Hupp, *ACS Appl. Mater. Interfaces* **7**, 5150-5159 (2015).
43. Electronic Interactions of Michler's Ketone with DNA Bases in Synthetic Hairpins, A. S. Jalilov, R. M. Young, S. W. Eaton, M. R. Wasielewski, and F. D. Lewis, *Photochem. Photobiol.* (in press, DOI: 10.1111/php.12360).
44. Photoinduced Electron Transfer in 2,5,8,11-Tetrakis-Donor-Substituted Perylene-3,4:9,10-bis(dicarboximides), L. E. Shoer, S. W. Eaton, E. A. Margulies, and M. R. Wasielewski, *J. Phys. Chem. B* (in press, DOI:/10.1021/jp511624s).

# Organic Macromolecular Materials for Long-Range and Efficient Transport Properties in Light Energy Conversion Applications

Goodson III, T.

Department of Chemistry, University of Michigan, Ann Arbor, Michigan 48109

The scope of this investigation is to probe the fundamental excitations in novel macromolecular organic materials with efficient energy transport and conversion properties. In order to reach these goals we have studied new organic aggregates and polymeric systems.<sup>1-4</sup> The effects of strong electronic coupling, coherent transport, through space interactions, and singlet exciton fission have been investigated with optical experiments and numerical modelling.

Utilizing novel compact porphyrin cyclic light harvesting macromolecules we have investigated the inter-chromophore coupling and the role of excitonic interactions.<sup>1</sup> The slipped

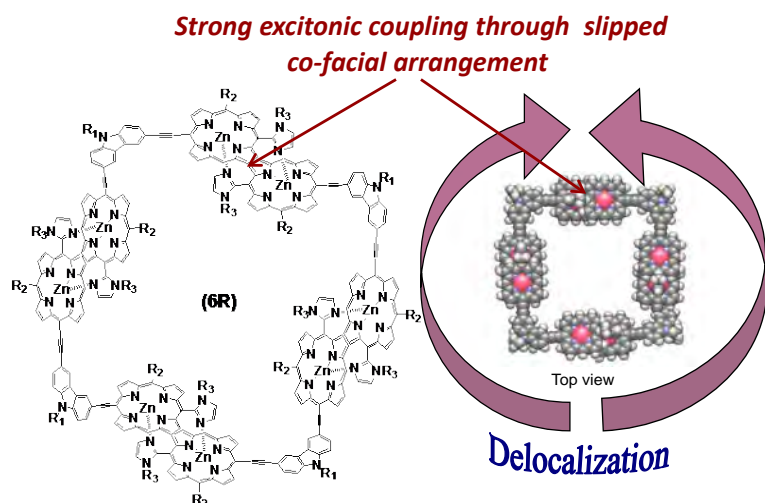


**Figure 1.** Compact porphyrin macrocycle.<sup>1</sup>

co-facial arrangement, similar to that found in the natural light harvesting complexes, provides strong inter-dimer coupling resulting in substantial enhancement in optical responses. The steady state, ultrafast dynamics, and nonlinear optical properties were probed and analyzed.<sup>1</sup> TPA cross-sections of  $\sim 3 \times 10^4$  GM for the macromolecular system of modest size (8 Zn-porphyrin units) has been achieved which clearly indicates a strong exciton coupling in the

system with the excitation delocalized over entire porphyrin

square. These results demonstrated the great potential of this macromolecule for new photovoltaic systems.

A new set of low bandgap electron-accepting polymers have been investigated to probe the structure–function relationships important to highly efficient solar cells.<sup>2</sup> One of the best organic solar cell material PTB7 has been also investigated for a comparison. Two-photon absorption measurements provided information about transition dipoles strength and a charge transfer character of the state. The TPA-diagnostics were closely correlated with time-resolved spectroscopic results as well as with electronic structure calculations for the four new conjugated photovoltaic polymers.<sup>2</sup> We have shown that the large difference in electron affinities of the comonomers of the polymers plays an important role in the improvement of the photo-physical properties necessary for efficient solar cell performance. The PECN polymer was found to possess the best combination of properties essential for PV applications.<sup>2</sup>

The effect of heteroatoms on the properties important to highly efficient organic solar cells has been investigated in low bandgap polymers featuring benzodifuran (BDF). Ultrafast

spectroscopic techniques were used to probe structure–function relationships in these donor-acceptor

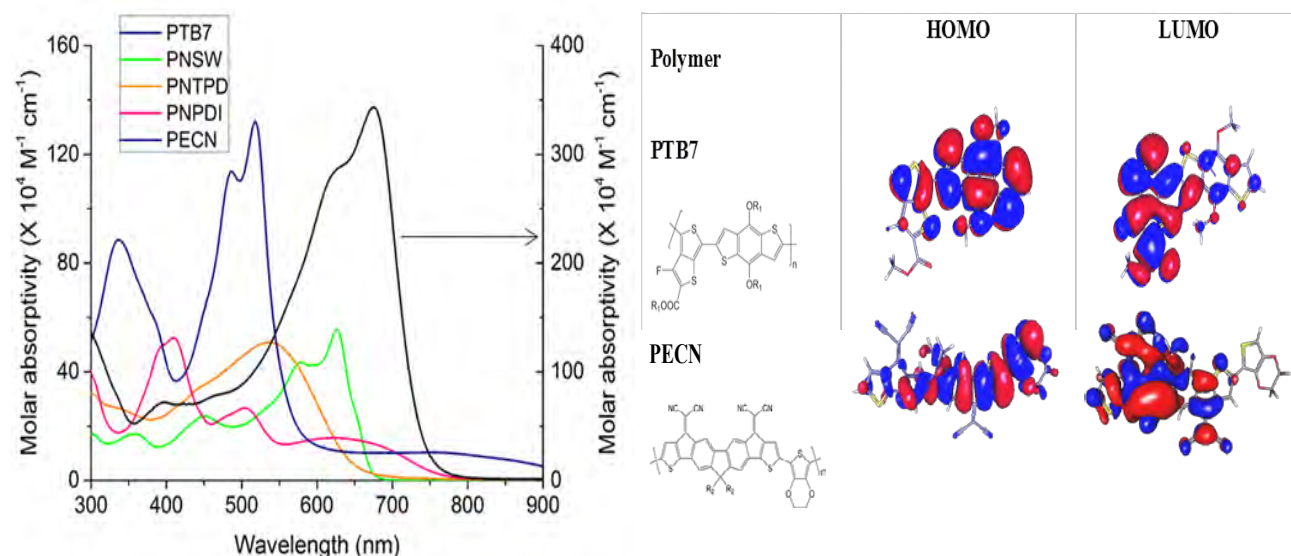


**Figure 2.** Absorption spectra of conjugated photovoltaic polymers (left).<sup>2</sup> HOMO-LUMO distributions of the repeating monomers for PTB7 and PECN (right).<sup>2</sup>

copolymers. The smaller atomic radius of oxygen in the furan relative to sulfur in thiophene, enhances planarity, conjugation, and  $\pi$ - $\pi$  stacking. Benzodifuran-Diketipyrrolopyrrole (FDPP) polymers have shown to have better potential for the solar cell applications in comparison with the BDP containing polymer.

Highly efficient intramolecular singlet-exciton fission (SEF) has been obtained in a small molecule.<sup>4</sup> Intramolecular SEF has a great potential to significantly improve photovoltaic devices via carrier multiplication. Efficient ultrafast triplet photo generation and its yield in quinoidal bithiophene are determined by photoinduced triplet-triplet absorption, flash photolysis triplet lifetime measurements, as well as by femtosecond time-resolved transient absorption and fluorescence methods. These measurements were supported by CASPT2 and RAS-2SF calculations as well as by the observation of magnetic field effects.

We are currently optimizing the deposition procedures to create regular arrays (monolayers) of porphyrin macrocycles. The square shape of the porphyrin structure is beneficial for building regular cubic 2D lattice. For the future work we plan to focus on the energy transport properties of such supramolecular structures of the porphyrin “squares”. Preliminary calculations of the inter-ring coupling based on the results obtained during the first year of the Project showed the ability to transport the excitations over the distances exceeding 100nm. We are working on the inclusion complex with the electron acceptor (bis(ethoxycarbonyl)methanofullerene) in the ring cavity and will use a broad variety of the spectroscopic tools to probe it’s properties.

DOE Sponsored Publications 2014-2015:

1. Varnavski, O.; Raymond, J.E.; Yoon, Z.S.; Yotsutuji, T.; Ogawa, K.; Kobuke, Y.; Goodson III, T. Compact Self-Assembled Porphyrin Macrocycle: Synthesis, Cooperative Enhancement, and Ultrafast Response *J. Phys. Chem. C* **2014**, *118*(50), 28474-28481.
2. Adegoke, O.O.; Jung, I.H.; Orr, M.; Yu, L.; Goodson III, T. Investigations of the Effect of the Acceptor Strength on the Optical and Electronic Properties in Conjugated Polymers for Solar Applications *J. Amer. Chem. Soc.* **2015** *137*, accepted for publication.
3. Vázquez, R.J.; Adegoke, O.O.; Jeffries-EL, M.; Theodore Goodson III, T. Ultrafast Time-resolved Spectroscopy of Donor-Acceptor Photovoltaic Copolymers Based on 2,6-di(thiophen-2-yl)benzo[1,2-b:4,5-b']difuran. *Chem. Mater.* **2015**, submitted for publication.
4. Varnavski, O.; Abeyasinghe, N.; Aragón, J.; Serrano-Pérez, J.J.; Enrique Ortí, E.; López Navarrete, J.T.; Takimiya, K.; Casanova, D.; Casado, J.; Theodore Goodson III, T. High Yield Ultrafast Intramolecular Singlet Exciton Fission in a Quinoidal Bithiophene *J. Phys. Chem. Lett.*, **2015**, *6*, Just Accepted, DOI: 10.1021/acs.jpcllett.5b00198



## *Session II*

### *Model Systems for Spectral Sensitization*



## Fundamental Studies of Illuminated Semiconductor/Electrolyte Interfaces

Meghan Kern, Laurie King, Theodore Kraus, Katarzyna Skoruspka, Kevin Watkins, Mark Spitler,\* and Bruce Parkinson

Department of Chemistry and School of Energy Resources  
University of Wyoming  
Laramie, WY 82071  
and  
\*Office of Science, SC 22.13  
Department of Energy  
Washington, D.C. 20585

I will review the work over the last funding period of our grants concerned with illuminate semiconductor electrolyte interfaces. In the first section I will discuss the doping density dependence of photocurrents that has been experimentally measured at single crystal rutile TiO<sub>2</sub> electrodes sensitized with the N3 chromophore and a trimethine dye. As the doping density of the electrodes was varied from 10<sup>15</sup> cm<sup>-3</sup> to 10<sup>20</sup> cm<sup>-3</sup>, three different regimes of behavior were observed for the magnitude and shape of the dye sensitized current-voltage curves. Low-doped crystals produced current-voltage curves with a slow rise of photocurrent with potential. At intermediate doping levels, Schottky barrier behavior was observed producing a photocurrent plateau at electrode bias in the depletion region. At highly doped electrodes tunneling currents played a significant role especially in the recombination processes. These different forms of the current-voltage curves could be fit to an Onsager-based model for charge collection at a semiconductor electrode. The fitting revealed the role of the various physical parameters that govern photoinduced charge collection in sensitized systems. I will also report on the progress in preparing homoepitaxial and heteroepitaxial layers of single crystal oxide semiconductors with controlled doping densities and our recent work on new quantum dot sensitizers.

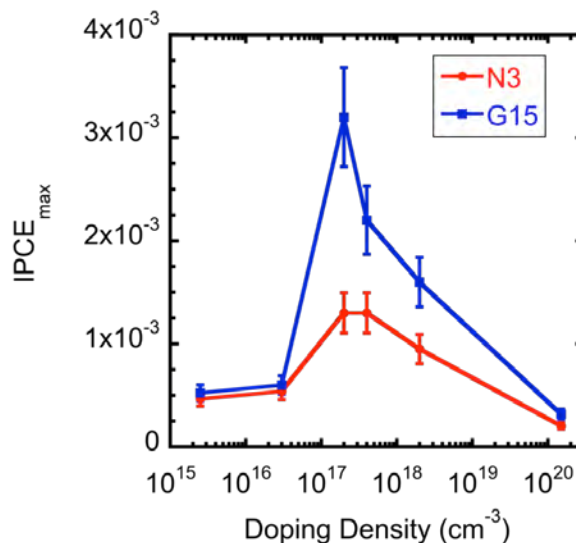


**Figure 1.** Plot of maximum IPCE for N3 and G15 sensitized TiO<sub>2</sub> over a large range of doping densities.

In the second section of the talk I will discuss the progress in identifying and characterizing new oxide semiconductors for photoelectrochemical water splitting. We reported the identification of a semiconducting p-type oxide containing iron, aluminum and chromium (Fe<sub>2-x-y</sub>Cr<sub>x</sub>Al<sub>y</sub>O<sub>3</sub>) with previously unreported photoelectrolysis activity that was discovered by an undergraduate scientist participating in the Solar Hydrogen Activity research Kit (SHARK) program. The

SHArK program is a distributed combinatorial science outreach program designed to provide a simple and inexpensive way for high school and undergraduate students to participate in the search for metal oxide materials that are active for the photoelectrolysis of water. The identified  $\text{Fe}_{2-x-y}\text{Cr}_x\text{Al}_y\text{O}_3$  photoelectrolysis material possesses many properties that make it a promising candidate for further optimization for potential application in a photoelectrolysis device. In addition to being comprised of earth abundant elements, the FeCrAl oxide material has a band gap of 1.8 eV. Current-potential measurements for  $\text{Fe}_{2-x-y}\text{Cr}_x\text{Al}_y\text{O}_3$  showed an open circuit photovoltage of nearly one volt, however the absorbed photon conversion efficiency (APCE) for hydrogen evolution was low ( $2.4 \times 10^{-4}$  at 530 nm) albeit without any deposited hydrogen evolution catalyst. X-ray diffraction of the pyrolyzed polycrystalline thin  $\text{Fe}_{2-x-y}\text{Cr}_x\text{Al}_y\text{O}_3$  film on fluorine-doped tin oxide (FTO) substrates shows a hexagonal phase (hematite structure) and scanning electron microscope (SEM) images show morphology consisting of small crystallites.

The identification of this material has spurred an international effort to “fail quickly” by quickly reproducing the fabrication of this material using in various laboratories using different synthetic techniques and evaluating the physical properties of all these samples, such as carrier lifetimes, in laboratories that specialize in such measurements. Groups in Munich and Bochum in Germany have also prepared this material by nanostructuring and sputtering resulting in higher quality films and dramatically increasing the photocurrent. We have also investigated the effects of introducing p-n and p-i-n structures to see if carrier collection can be improved in these low mobility materials. Questions remain about whether this material is stable under the reducing conditions needed to evolve hydrogen from water.

#### **DOE Sponsored Publications 2012-2015**

- 1) Dae Jin Choi, John G. Rowley and B. A. Parkinson, “Dye Sensitization of n and p type Gallium Phosphide Photoelectrodes”, J. Electrochem. Soc., 159(11), H846-852, (2012), DE-FG03-96ER14625.
- 2) B. A. Parkinson, “Combinatorial Identification and Optimization of New Oxide Semiconductors for Photoelectrochemical Hydrogen Production”, Electronic Materials: Science & Technology, Volume 102, Part 2, 173-202, (2012), DE-FG02-05ER15750.
- 3) Carrick M. Eggleston, Justin R. Stern, Tess M. Strellis and Bruce A. Parkinson, “A Natural Photoelectrochemical Cell for Water Splitting: Implications for Early Earth and Mars”, American Mineralogist, 97, 1804-1807, (2012), DE-FG02-05ER15750.
- 4) Dae Jin Choi, John G. Rowley, Mark Spitler and B. A. Parkinson, “Dye Sensitization of Four Low Index  $\text{TiO}_2$  Single Crystal Photoelectrodes with a Series of Dicarboxylated Cyanine Dyes”, Langmuir, 29, 9410–9419, (2013) DE-FG03-96ER14625.
- 5) B. Nepomnyashchii and B. A. Parkinson, “The Influence of the Aggregation of a Carbazole Thiophene Cyanoacrylate Sensitizer on Sensitized Photocurrents on  $\text{ZnO}$  Single Crystals”, Langmuir, 29, 9362–9368, (2013), DE-FG03-96ER14625.
- 6) B. Nepomnyashchii and B. A. Parkinson, “Electrogenerated Chemiluminescence of a Carbazole Thiophene Cyanoacrylate Dye: Contrasting Behavior for the Dissolved and Surface Attached Species”, Langmuir, 29(30), 9362-9368, (2013) DE-FG03-96ER14625.

- 7) John G. Rowley and B. A. Parkinson, "Simultaneous Measurement of Absorbance and Quantum Yields for Photocurrent Generation at Dye Sensitized Single-Crystal ZnO Electrodes", Langmuir, 29, 13790-13796. (2013), DE-FG03-96ER14625.
- 8) Xuzhi Zhu, Alexander B. Nepomnyashchii, Adrian E. Roitberg, Bruce A. Parkinson and Kirk S. Schanze, "Photosensitization of Single Crystal ZnO by a Conjugated Polyelectrolyte Designed to Avoid Aggregation", The Journal of Physical Chemistry Letters, 4, 3216-3220, (2013), DE-FG03-96ER14625.
- 9) Bruce Parkinson and John Turner, "The Potential Contribution of Photoelectrochemistry in the Global Energy Future", Book Chapter in Photoelectrochemical Water Splitting: Materials, Processes and Architectures, pages 1-18, H. J. Lewerenz and L. Peter, editors, RSC Publishing, (2013), DE-FG02-05ER15750.
- 10) John G. Rowley, Thanh D. Do, David A. Cleary and B. A. Parkinson, "Combinatorial Discovery Through a Distributed Outreach Program: Investigation of the Photoelectrolysis Activity of p-type Fe, Cr, Al Oxides", Applied Materials and Interfaces, 6, 9046-9052, (2014), DE-FG02-05ER15750.
- 11) Yongqi Liang, Thomas Novet, James E. Thorne and B. A. Parkinson, "Photosensitization of ZnO Single Crystal Electrodes with PbS Quantum Dots", Phys. Stat. Solidi A, 1-6, (2014), DE-FG03-96ER14625.
- 12) Yongqi Liang, Meghan Kern, James E. Thorne, B. A. Parkinson, "Sensitization of ZnO Single Crystal Electrodes with CdSe Quantum Dots", Langmuir, submitted, DE-FG03-96ER14625.
- 13) Alexander B. Nepomnyashchii and B. A. Parkinson, "Contrasting Electrogenerated Chemiluminescence for a Dissolved and Surface-Attached Carbazole Thiophene Cyanoacrylate Dye", Applied Materials and Interfaces, ASAP, DE-FG03-96ER14625.
- 14) Theodore J. Kraus, Alexander B. Nepomnyashchii and B. A. Parkinson, "Templated Homoepitaxial Growth with Atomic Layer Deposition of Single-Crystal Anatase (101) and Rutile (110) TiO<sub>2</sub>", ACS Applied Materials and Interfaces, 6, 9946-9949, (2014), DE-FG03-96ER14625.
- 15) Paul F. Newhouse and B. A. Parkinson, "Combinatorial optimization of spinel Co<sub>3-x</sub>M<sub>x</sub>O<sub>4</sub> M = (Al, Ga, In) alloyed thin films prepared by ink jet printing: photoelectrochemical, structural, and optical properties", J. Mater. Chem. A, 3, 5901-5907, (2015). DE-FG02-05ER15750.
- 16) Alexander B. Nepomnyashchii, Theodore J. Kraus and B. A. Parkinson, "Atomic Layer Deposition of Epitaxial Layers of Anatase TiO<sub>2</sub> on Strontium Titanate Single Crystals: Morphological and Photoelectrochemical Studies", Journal of Vacuum Science and Technology A, in press special ALD Issue, DE-FG03-96ER14625.
- 17) Katarzyna Skorupska, Paul Maggard, Paria Shahbazi and B. A. Parkinson, "Combinatorial Investigations of High Temperature CuNb Oxides for Photoelectrochemical Water Splitting", submitted DE-FG02-05ER15750.
- 18) Kirill Sliozberg, Helge S. Stein, Chinmay Khare, Bruce A. Parkinson, Alfred Ludwig and

Wolfgang Schuhmann, “Fe-Cr-Al containing oxide semiconductors as potential solar water splitting materials”, ACS Applied Materials and Interfaces, accepted DE-FG02-05ER15750.

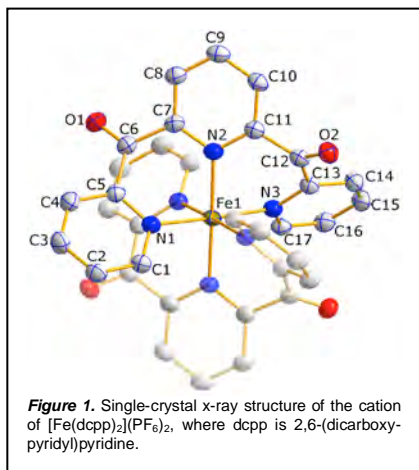
- 19) Laurie King, Meghan Kern and B. A. Parkinson, “Sensitization of Single Crystal Substrates”, Book Chapter in ACS Symposium Series "Surface Chemistry for Photocatalysis", ACS Books, 2015, DE-FG03-96ER14625.

# Synthesis and Spectroscopy of Transition Metal-based Chromophores: Tailoring First-row Photophysics for Applications in Solar Energy Conversion

James K. McCusker  
Department of Chemistry  
Michigan State University  
578 South Shaw Lane, East Lansing, MI 48824

Fundamental research on solar energy conversion – which will ultimately lead to the next generation of solar energy technologies – has sought to replicate Nature’s solution to the energy conversion problem through the creation of artificial constructs that mimic various aspects of photosynthesis. Whether it’s the creation of potential gradients to generate current (i.e., photovoltaics) or more recent efforts coupling photo-generated electrons and holes to catalysts, the first step is the absorption of light and subsequent separation of charge. Transition metal-based chromophores are particularly well suited for use in this context by virtue of the charge-transfer excited states that a majority of them possess, hence their prevalence in a wide array of solar energy conversion schemes that have been developed over the years.

When considering energy on a global scale, material availability becomes a serious consideration. While one can debate whether the use of earth-abundant elements in catalysts is critical in this regard, that same argument does not translate to the light absorption part of the problem; for metal complexes, this necessitates shifting to the first transition series. Unfortunately, the ultrafast relaxation processes that arise due to the presence of low-lying ligand-field excited states in first-row metal complexes that we first identified<sup>1</sup> then elaborated upon<sup>2</sup> through our DOE-supported research undercuts their use in virtually *any* application that relies on charge separation following photon capture. We believe this represents an important problem in fundamental science that has significant implications for solar energy conversion. The focus of our research program is therefore to understand the factors that determine the dynamics associated with charge-transfer excited states of first-row transition metal-based chromophores, with the ultimate goal of circumventing and/or redefining their intrinsic photophysics in order to make feasible their use as light-harvesting components in solar energy conversion schemes. Our research program breaks down into two main thrusts that are summarized below.



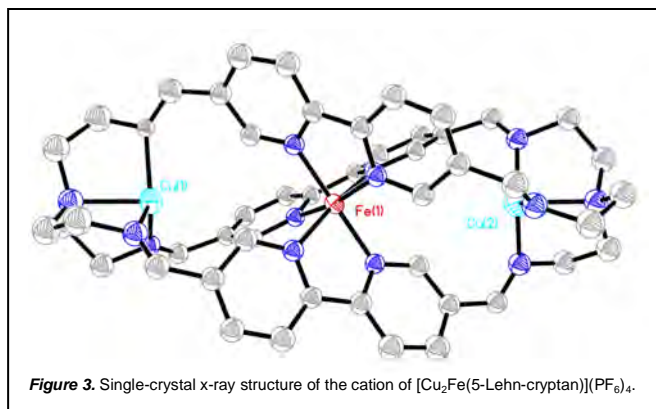
**Manipulation of Excited-State Electronic Structure: MLCT/LF-State Inversion.** We are continuing development of a new class of Fe(II) polypyridyl chromophores.  $[\text{Fe}(\text{dcpp})_2]^{2+}$  (where dcpp is 2,6-di-(carboxypyridyl)pyridine, Figure 1) represents a potential paradigm shift in Fe(II) coordination chemistry and photophysics.<sup>3</sup> As will be discussed in this presentation, this compound appears to be situated at or near the crossing point of the  ${}^3\text{T}_1/{}^5\text{T}_2$  states in the  $d^6$  Tanabe-Sugano diagram; this regime, formerly the purview of compounds such as  $[\text{Fe}(\text{bpy})(\text{CN})_4]^{2-}$  (in which bpy is 2,2'-bipyridine), presents us with the possibility of creating Fe(II)

chromophores having absorption cross-sections that span the entire visible spectrum (Figure 2) and whose lowest-energy excited states are charge-transfer (as opposed to ligand-field) in nature.

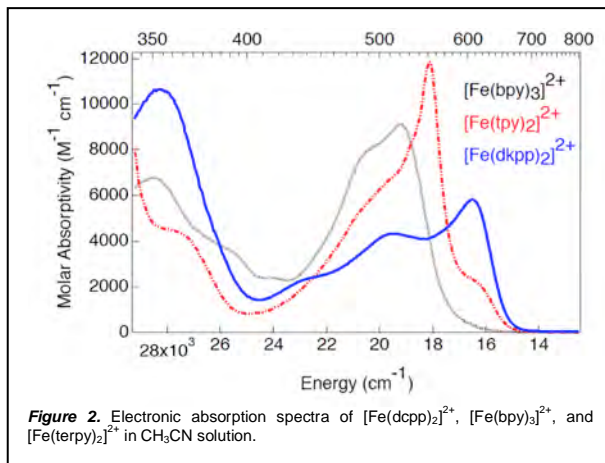
In effect, we believe we can create a compound whose excited-state electronic structure (and resulting photophysical properties) resembles that of Ru(II) polypyridyls: essentially, an Fe(II) version of  $[\text{Ru}(\text{bpy})_3]^{2+}$ . The key observations made that provide the basis for this idea will be described in addition to ongoing research coupling synthesis, steady-state and time-resolved spectroscopies, and theory, that we believe will achieve this goal.

**Controlling Charge Transfer-State Dynamics: The MLCT  $\rightarrow$  LF Coordinate.** The

second branch of our research focuses on our continuing efforts to understand the nature of the reaction coordinate(s) that defines the ultrafast conversion of charge-transfer states to lower-energy ligand-field states. Based on results we have obtained on a simple coordination compound  $(\text{Cr}(\text{acac})_3)$ ,<sup>4</sup> as well as data acquired on a series of sterically encumbered Fe(II) terpyridine complexes, we are now confident that sub-picosecond state-to-state conversion dynamics can be significantly modulated through judicious synthetic design.



computational studies designed to gain deeper insight into electronic/geometric structure-dynamic correlations. The research has already resulted in the preparation of a fascinating new Cu(I)-Fe(II)-Cu(I) heterotrimetallic compound (Figure 3) may provide the means of creating a highly reactive photoredox agent in the form of  $\text{bpy}^*$  through intramolecular reductive quenching of an Fe-based MLCT excited state.



We are therefore pursuing a range of experiments on synthetically tailored compounds that will provide us with information concerning reorganization energies associated with charge-transfer to ligand-field state conversion, electronic state-to-state coupling, identification of active vibrational modes in the charge-transfer and ligand-field manifolds, as well as direct structural information during excited-state evolution. These synthetic and experimental efforts will be supported by

1. Monat, J.E.; McCusker, J.K. *J. Am. Chem. Soc.* **2000**, *122*, 4092-4097.
2. a) Cho, H.; Strader, M.L.; Hong, K.; Jamula, L.; Gullickson, E.M.; Kim, T.K.; de Groot, F.M.F.; McCusker, J.K.; Schoenlein, R.W.; Huse, N. *Faraday Discussions* **2012**, *157*, 463-474, and references therein. b) Smeigh, A.L.; Creelman, M.; Mathies, R.A.; McCusker, J.K. *J. Am. Chem. Soc.* **2008**, *130*, 14105-14107. c) Juban, E.A.; Smeigh, A.L.; Monat, J.E.; McCusker, J.K. *Coord. Chem. Rev.* **2006**, *250*, 1783-1791. d) McCusker, J.K. *Acc. Chem. Res.* **2003**, *36*, 876-887.
3. Jamula, L.L.; Brown, A.M.; Guo, D. McCusker, J.K. *Inorg. Chem.* **2014**, *53*, 15-17.
4. Schrauben, J.N.; Dillman, K.L.; Beck, W.F.; McCusker, J.K. *Chem. Sci.* **2010**, *1*, 405-410.

## DOE Sponsored Publications 2012-2015

1. “Ligand Field Symmetry Effects in Fe(II) Polypyridyl Compounds Probed by Transient X-Ray Absorption Spectroscopy”, Hana Cho, Matthew L. Strader, Kiryong Hong, Lindsey Jamula, Eric M. Gullickson, Tae Kyu Kim, Frank M.F. de Groot, James K. McCusker, Robert W. Schoenlein, and Nils Huse, *Faraday Discussions* **2012**, *157*, 463-474.
2. “Synthesis and Characterization of a High-Symmetry Ferrous Polypyridyl Complex: Approaching the  $^5T_2/{}^3T_1$  Crossing Point for Fe(II)”, Lindsey L. Jamula, Allison M. Brown, Dong Guo, and James K. McCusker, *Inorg. Chem.* **2014**, *53*, 15-17.
3. “Enlightened State”, James K. McCusker, *Nature Physics* **2014**, *10*, 476-477.
4. “Spectroelectrochemical Identification of Charge-Transfer Excited States in Transition Metal-based Polypyridyl Complexes”, Allison M. Brown, Catherine E. McCusker, and James K. McCusker, *Dalton Transactions*, **2014**, *43*, 17635-17646.
5. “Vibrational Relaxation and Redistribution Dynamics in Ru(II) Polypyridyl-based Charge-Transfer Excited States: A Combined Ultrafast Electronic and Infrared Absorption Study”, Allison M. Brown, Catherine E. McCusker, Ana Maria Blanco-Rodriguez, Michael Towrie, Ian P. Clark, Antonin Vlcek, Jr. and James K. McCusker, *J. Am. Chem. Soc.*, submitted for publication.
6. “Experimental Methodologies for Probing Ultrafast Electron Injection in Dye-Sensitized Solar Cells”, Allison M. Brown and James K. McCusker, *J. Phys. Chem. Lett.* (Perspective), submitted for publication.
7. “Charge Transfer-State Formation and Deactivation in  $d^6$  Metal Polypyridyl Complexes: Fundamental Issues and Applications in Solar Energy Conversion”, Allison M. Brown and James K. McCusker, manuscript in preparation as an invited Feature Article in *J. Phys. Chem. A*.

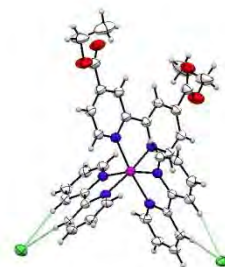
# Electron Transfer Dynamics in Efficient Molecular Solar Cells

Ke Hu, William Ward, Byron H. Farnum, Patrik Johansson, and Gerald J. Meyer  
Department of Chemistry  
University of North Carolina at Chapel Hill  
Chapel Hill, NC 27510

An important objective of this Department of Energy supported research is to provide new mechanistic insights into surface mediated photochemical processes relevant to solar energy conversion. In this past three years our research has focused on oxidation photo-redox chemistry and on the role surface electric fields play on basic spectroscopic properties of molecular-semiconductor interfaces. Although this research is purely fundamental science, the results and their interpretation have relevance to applications in dye sensitized and photogalvanic solar cells as well as in the storage of solar energy in the form of chemical bonds.

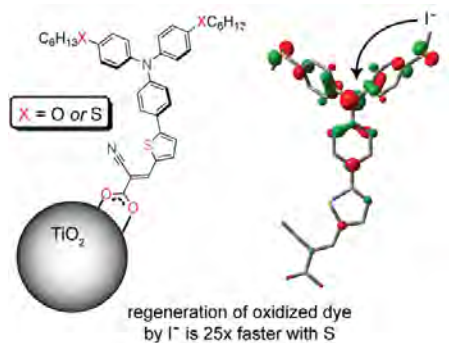
## Ruthenium Polypyridyl Site(s) for Ion-Pairing

Chloride ion-pairing with a series of four dicationic Ru(II) polypyridyl compounds of the general form  $[\text{Ru}(\text{bpy})_{3-x}(\text{deeb})_x](\text{PF}_6)_2$ , where bpy is 2,2'-bipyridine and deeb is 4,4'-diethylester-2,2'-bipyridine, was observed in dichloromethane solution. Chloride was chosen as a non-redox active surrogate for iodide to identify the site(s) of ion-pairing and to establish the fate of the excited state when ion-paired. X-ray crystal structure and  $^1\text{H}$  NMR analysis showed that when present, the H atoms at the C-3/C-3' position of bpy ligand were the preferred site for adduct formation with chloride. An example is shown in the Ortep diagram. UV-Visible absorption titration data with TBACl, where TBA is tetrabutyl ammonium, yielded equilibrium constants that ranged from  $13,700 \text{ M}^{-1}$  to  $64,000 \text{ M}^{-1}$ . A Job plot indicated a 2:1 chloride to ruthenium complex ratio in the ion-paired state. The chloride ion was found to decrease both the excited state lifetime and the quantum yield for photoluminescence, PL. The data provides insights into how one could rationally design ion-pairs to form I-I or Br-Br chemical bonds when illuminated with sunlight.



## Iodide Oxidation in Strong Electric Fields

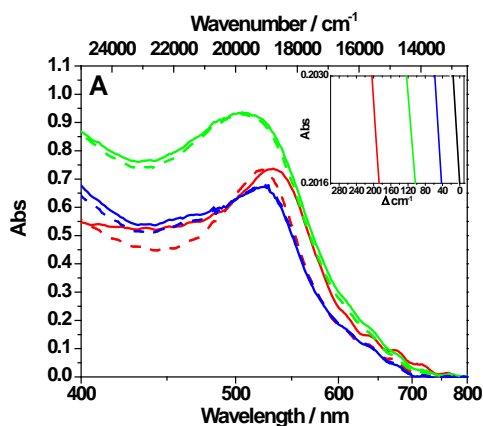
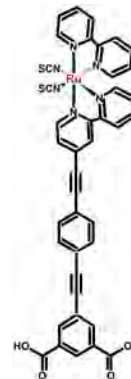
Two donor-acceptor organic dyes have been synthesized that differ only by a two-heteroatom change from oxygen to sulfur within the donor unit, (**Dye-O**) and (**Dye-S**), were subjected to comparative studies employing both  $\text{I}_3^-/\text{I}^-$  based and  $[\text{Co}(\text{bpy})_3]^{3+/2+}$  redox mediators. Despite similar optical and redox properties for the two dyes, a consistently higher open-circuit voltage ( $V_{\text{oc}}$ ) was measured for **Dye-S** relative to **Dye-O**. The improved efficiency observed with **Dye-S** in an iodide redox mediator stood in sharp contrast to the commonly held view that sulfur atoms promote charge recombination through inner-sphere donor-acceptor adducts between  $\text{I}_3^-$  and the S donor atom. No evidence for such adducts was obtained. Instead, detailed mechanistic studies revealed that after excited state injection, the regeneration rate constant was 25 times faster for **Dye-S**. The more rapid regeneration was not relevant at the short circuit condition



where the absorbed photon-to-current efficiency was within experimental error the same for the two dyes, but enhanced the regeneration yield under open circuit conditions where the number of injected electrons was high and the electric field strength was large. The data shows that a high short circuit photocurrent does not necessarily imply optimal regeneration efficiency as is often assumed. Indeed, the results indicate that the inclusion of S heteroatoms in dye molecules can enhance conversion efficiencies in dye-sensitized solar cells.

### Surface Electric Fields

In collaborative work with Professor Elena Galoppini and her research group, three ruthenium bipyridyl rigid rod *cis*-Ru(bpy)(LL)(NCS)<sub>2</sub> compounds, where LL is a 4-substituted bpy, with either zero, one or two phenylenethynylene bridge units, D0, D1, and D2, between the bipyridine ring and two carboxylic acid groups were characterized by spectroscopy and electrochemistry in fluid solution and anchored to mesoporous TiO<sub>2</sub> thin films. The structure of D2 is shown. Comparative actinometry indicated that the yields for excited state injection was near unity for D0/TiO<sub>2</sub> and decreased with additional phenylenethynylene bridge units: D0/TiO<sub>2</sub> = 0.98, D1/TiO<sub>2</sub> = 0.93, and D2/TiO<sub>2</sub> = 0.70. Charge recombination occurring on the 10<sup>-9</sup> to 10<sup>-1</sup> s time scales, was well modeled by the Kohlraush-Williams-Watt function. Recombination on the 10<sup>-4</sup> to 10<sup>-1</sup> s time scales was absent when the films were under significant forward bias, but was otherwise unaffected by temperature, irradiance, or the bridge units present in the molecular sensitizer. Recombination rates on the 10<sup>-8</sup> to 10<sup>-6</sup> s time scales increased with steady state or pulsed laser irradiance, temperature, forward bias and decreased bridge length. The bias dependence on the charge recombination was correlated with the concentration of TiO<sub>2</sub> electrons and the length of the bridge unit. At high TiO<sub>2</sub> electron concentrations, the recombination rate constants were sensitive to the bridge length and decreased with a  $\beta = 0.25 \pm 0.05 \text{ \AA}^{-1}$ .



Further evidence for a bridge dependence for interfacial electron transfer was found in Stark spectroscopic measurements. Shown are the visible absorption spectra of D0 /TiO<sub>2</sub> (red), D1/TiO<sub>2</sub> (green) and D2/TiO<sub>2</sub> (blue) in 0.3 M LiClO<sub>4</sub>/CH<sub>3</sub>CN measured at +350 mV (—) and with a bias of -300 mV vs NHE (---). Under the forward bias condition of -300 mV, about 20 electrons on average were calculated to be present in each TiO<sub>2</sub> nanocrystallite. The presence of these electrons resulted in the blue shift of the MLCT absorption. The spectral shifts were reversible upon stepping the potential back to + 350 mV. For clarity, the inset shows the long wavelength absorption edge measured at +350 mV of all three sensitized materials normalized to zero wavenumbers (black line) and the absorbance with a -300 mV applied bias represented by their respective color. The raw experimental data clearly shows that the magnitude of the spectral shift was directly correlated with the number of phenylenethynylene bridge units and hence the bridge length. Abstraction of the true distance between the Ru(NCS)<sub>2</sub>-core and the TiO<sub>2</sub> interface was complicated by the unknown location of the trapped electrons and the true interfacial dielectric constant. Nevertheless, they support the idea that the bridge units do, on average, locate the sensitizers further from the semiconductor surface.

## DOE Sponsored Publications 2012-2015:

1. **Visible Light Generation of I-I Bonds by Ru-tris(diimine) Excited-States.** Farnum, B.V.; Jou, J.J.; Meyer, G.J. *Proc. Nat. Acad. Sci.* **2012**, *109*, 15628-15633.
2. **Intramolecular Hole Transfer at Sensitized TiO<sub>2</sub> Interfaces.** Hu, K.; Robson, K.C.D.; Johansson, P.G.; Berlinguette, C.P.; Meyer, G.J. *J. Am. Chem. Soc.* **2012**, *134*, 8352–8355.
3. **Visible Light Generation of I-I Bonds by Ru-tris(diimine) Excited-States.** Farnum, B.V.; Jou, J.J.; Meyer, G.J. *Proc. Nat. Acad. Sci.* **2012**, *109*, 15628-15633.
4. **Flash-Quench Technique Studies on the One Electron Reduction of Triiodide.** Farnum, B.H.; Ward, W.M.; Meyer, G.J. *Inorg. Chem.* **2013**, *52*, 842-847.
5. **Atomic Level Resolution of Dye Regeneration in the Dye Sensitized Solar Cell.** Robson, K.C.D.; Hu, K.; Meyer, G.J.; Berlinguette, C.P. *J. Am. Chem. Soc.* **2013**, *135*, 1961-1971.
6. **Distance Dependent Electron Transfer at TiO<sub>2</sub> Interfaces Sensitized with Phenylene Ethynylene Bridged Ru<sup>II</sup>-Isothiocyanate Compounds.** Johansson, P.G.; Kopecky A.; Galoppini, E.; Meyer, G.J. *J. Am. Chem. Soc.* **2013**, *135*, 8331-8341.
7. **Panchromatic Electron Injection by Ru(II) Dipyrrinates In the Dye-Sensitized Solar Cell.** Li, G.; Hu, K.; Knappenberger, Jr., K.L.; Meyer, G.J.; Gorelsky, S.I.; Shatruk, M. *J. Phys. Chem C* **2013**, *117*, 17399-17411.
8. **Homoleptic ‘Star’ Ru(II) Polypyridyl Complexes: Shielded Chromophores to Study Charge-Transfer at the Sensitizer-TiO<sub>2</sub> Interface.** Johansson, P.G.; Zhang, Y.; Meyer, G.J.; Galoppini, E. *Inorg. Chem.* **2013**, *52*, 7947-7957.
9. **Chloride Ion-Pairing with Ru(II) Polypyridyl Compounds in Dichloromethane.** Ward W.M.; Farnum, B.V.; Siegler, M.; Meyer, G.J. *J. Phys. Chem A* **2013**, *117*, 8883-8894.
10. **Panchromatic Electron Injection by Ru(II) Dipyrrinates In the Dye-Sensitized Solar Cell.** Li, G.; Hu, K.; Yi, C.; Knappenberger, K. L.; Meyer, G. J.; Gorelsky, S. I.; Shatruk, M. *J. Phys. Chem. C* **2013**, *117*, 17399-17411.
11. **Charge Screening at Sensitized TiO<sub>2</sub> Interfaces.** O'Donnell, R. M.; Ardo, S.; Meyer, G. J. *J. Phys. Chem. Lett.* **2013**, *4*, 2817-2821.
12. **Atomic Level Resolution of Dye Regeneration in the Dye Sensitized Solar Cell.** Robson, K. C. D.; Hu, K.; Meyer, G. J.; Berlinguette, C. P. *J. Am. Chem. Soc.* **2013**, *135*, 1961-1971.
13. **Chloride Ion-Pairing with Ru(II) Polypyridyl Compounds in Dichloromethane.** Ward, W. M.; Farnum, B. H.; Siegler, M.; Meyer, G. J. *J. Phys. Chem. A* **2013**, *117*, 8883-8894.

14. **Intramolecular Hole Transfer Modulation and Lateral Hole Hopping at the Sensitized TiO<sub>2</sub> Interface.** Hu, K.; Robson, K. C. D.; Beauvilliers, E. E.; Schott, E.; Zarate, X.; Arratia-Perez, R.; Berlinguette, C. P.; Meyer, G. J. *J. Am. Chem. Soc.* **2014**, *136*, 1034-1046.
15. **Donor- $\pi$ -Acceptor Organic Hybrid TiO<sub>2</sub> Interfaces for Solar Energy Conversion.** Hu, K.; Robson, K.C.D.; Berlinguette, C.P.; Meyer, G.J. *Thin Solid Films* **2014**, *560*, 49-54.
16. **Electric Fields and Charge Screening in Dye Sensitized Mesoporous Nanocrystalline TiO<sub>2</sub> Thin Films.** O'Donnell, R.M.; Sampaio, R.N.; Barr, T.J. Meyer, G.J. *J. Phys. Chem. C* **2014**, *118*, 16976-16986.
17. **Ostwald Isolation to Determine the Reaction Order for TiO<sub>2</sub>(e<sup>-</sup>)|S<sup>+</sup>  $\rightarrow$  TiO<sub>2</sub>|S Charge Recombination at Sensitized TiO<sub>2</sub> Interfaces.** Brigham, E.C.; Meyer, G.J. *J. Phys. Chem. C* **2014**, *118*, 7886-7893.
18. **Direct Spectroscopic Evidence for Constituent Heteroatoms Enhancing Charge Recombination at a TiO<sub>2</sub>-Ruthenium Dye Interface.** Hu, K.; Severin, H.; Koivisto, B.; Robson, K.; Schott, E.; Arratia-Perez, R.; Meyer, G.J.; Berlinguette, C.P. *J. Phys. Chem. C* **2014**, *118*, 17079-17089.
19. **Electric Field Control of TiO<sub>2</sub>(e<sup>-</sup>) + I<sub>3</sub><sup>-</sup>  $\rightarrow$  Charge Recombination Relevant to Dye-Sensitized Solar Cells.** Sampaio, R.N.; O'Donnell, R.M.; Barr, T.J.; Meyer, G.J. *J. Phys. Chem. Lett.* **2014**, *5*, 3265-3268.



## *Session III*

### *New Surfaces for Dyes*



## The Relation between Structure and Photochemical Properties of Polyoxotitanate and Polysulfurcadmate Nanoparticles

Philip Coppens  
Chemistry Department  
University at Buffalo SUNY, Amherst Campus  
Buffalo, NY 14260-3000.

The project's goal is to relate the physical properties of homodisperse nanoparticles to their detailed experimental structure. Using both solution and solvothermal methods we have synthesized and crystallized a large number of homodisperse Ti- and Cd-based, 'pure', doped, and functionalized, nanoparticles of up to 3nm dimensions. Structure and properties were obtained by crystallographic, spectroscopic, theoretical and electrochemical methods. A number of the structures are shown in Fig. 1. A summary up to end 2013 is included in reference 1.

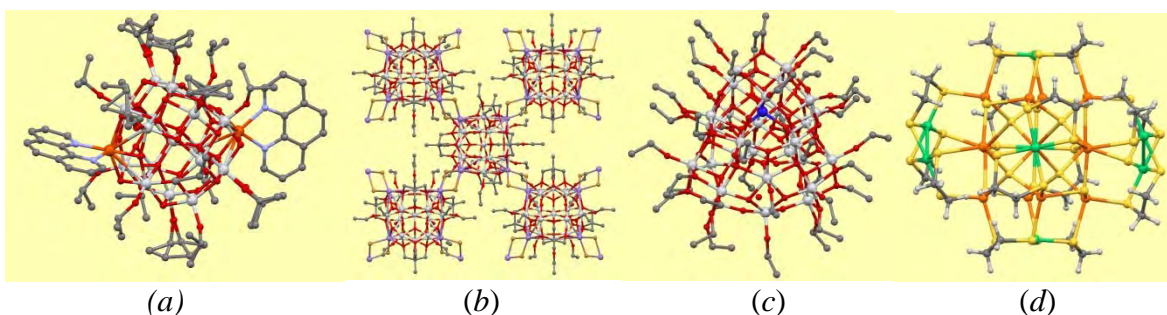
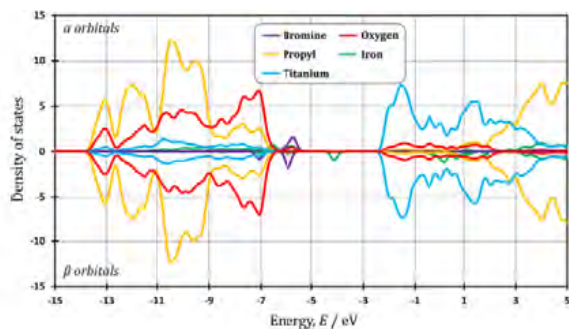


Fig. 1. Selected examples of nanoparticle structures determined during the recent grant period. (a) *functionalized*  $\text{Ti}_{17}\text{O}_{28}(\text{OiPr})_{16}(\text{Fe}^{\text{II}}\text{Phen})_2$  (Ti silver, Fe orange, oxygen red).<sup>2</sup> (b) *infinite framework*  $[\text{Ti}_{13}\text{Mn}_4\text{O}_{16}\text{Br}_4]_{\infty}$  linked by Br bridges, (Ti silver, Mn blue, Br brown).<sup>3</sup> (c) *doped*  $\text{Ti}_{28}\text{FeO}_{38}(\text{OEt})$ , (Ti silver, Fe dark blue), (d)  $\text{Cd}_{13}\text{Ni}_8\text{S}_8$  (Cd orange, Ni green, S yellow).

**Functionalization.** Functionalization with chromophores was achieved by linking a series of chromophores to the nanoparticles. They include phenylphosphonates which were found to bind in a previously unrecognized triply-bridging binding mode in  $[\text{Ti}_{25}\text{O}_{26}(\text{OEt})_{36}(\text{PhenylPO}_3)_6]$  and  $[\text{Ti}_{26}\text{O}_{26}(\text{OEt})_{39}(\text{PhenylPO}_3)_6]\text{Br}$ .<sup>4</sup> Although both bridging and chelate binding modes occur, no single chromophore was found to show both configurations, indicating high specificity.<sup>5</sup>

**Doping and mixed doping/functionalization.** Ti14 and Ti28 clusters were doped with Mn,<sup>5</sup> and with Na,<sup>7</sup> Mn<sup>8</sup> and Fe (Fig. 1c) respectively, leading for Mn and Fe to a considerable reduction in the band gap relative to the undoped Ti28 particle. Incorporation of transition metal on the surface of the particles has been accomplished with attached halogen atoms or with molecular chromophores attached to the transition metal, as shown for Fe-phenanthroline in Fig 1a. A systematic study performed for polyoxotitanate nanoclusters with formulae  $\text{Ti}_{11}(\text{MX})\text{O}_{14}(\text{OiPr})_{17}$  (M = Mn, Fe and Co; X = Cl, Br and I, O<sup>i</sup>Pr = isopropoxide) shows pronounced dopant-dependence of the spectroscopic and electronic properties.<sup>9</sup>

**Effect of nanoparticle modification on band gap and spectroscopic properties.** Long-wavelength absorption limits were measured by reflectance spectroscopy on powders and by



**Fig. 2.** HSE06/6 density of states diagram for TiFeBr.

compared with 3.43 eV for an undoped  $\text{Ti}_{28}$  cluster and 3.19 eV for the band gap of commercial anatase. Of particular interest are the results for the  $\text{Ti}_{11}\text{FeX}$  nanoparticles for which an occupied  $\text{Fe}^{2+}$ - $\beta$  orbital is located in the center of the bandgap (Fig. 2), leading for  $X = \text{Br}$  to absorption measured at 1.59 eV, confirmed by theory as involving Fe to Ti transfer. Other examples will be presented.

*Studies of electron injection by theoretical and experimental methods.* In a collaboration with Prof. Watson of our Department thin films of 4-nitrophenylacetylacetonate (NPA) functionalized  $\text{Ti}_{17}\text{O}_{24}(\text{OiPr})_{20}$  and of  $\text{Ti}_{17}\text{O}_{28}(\text{OiPr})_{16}(\text{Fe}^{\text{II}}\text{Phen})_2$  were deposited on an FTO electrode subsequently mounted in a Grätzel type photovoltaic cell.<sup>2,10</sup> The induced negative (cathodic) room temperature photocurrent for  $\text{Ti}_{17}(\text{NPA})_4$  is shown in Fig. 3. Its cathodic nature, indicative of hole-injection into the nanoparticle, is in agreement with dynamic calculations by our Yale collaborators.<sup>10</sup> The current measured for  $\text{Ti}_{17}\text{O}_{28}(\text{OiPr})_{16}(\text{Fe}^{\text{II}}\text{Phen})_2$  is on the other hand anodic and extends past 640nm exposure. The first transient spectroscopic measurements were made in collaboration

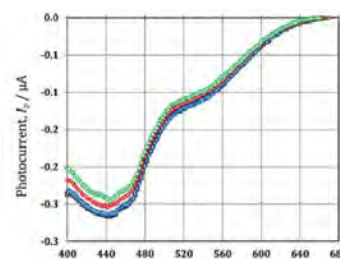


**Fig. 3.** Three successive measurements of the negative (cathodic) photocurrent recorded for  $\text{Ti}_{17}\text{NPA}_4$  at room temperature.

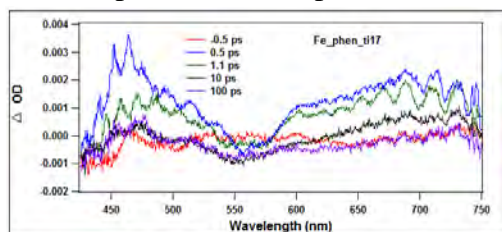


**Fig. 4** Transient absorption of a solution of  $\text{Ti}_{17}\text{O}_{28}(\text{OiPr})_{16}(\text{Fe}^{\text{II}}\text{Phen})_2$  on light exposure

with Prof. McCamant of the University of Rochester. Results shown in figure 4 show a response at both 450-500 nm and at about 700 nm, both in the 5-10 ps time range, in this case too short for time-resolved synchrotron studies, but indicating that chemical modification may allow excited state dynamic structure analysis in future research.

*Other studies.* Additional collaborative studies on excitation dynamics and excess electrons,<sup>11</sup> and on sequestration of rare elements on phosphonate monolayers<sup>12</sup> were undertaken and published.

*Future plans.* We plan to continue our synthetic work including CdS and CdSe nanoparticles. We will concentrate on the dynamics of hole and electron injection of particles with longer linking groups by transient-spectroscopic, theoretical and, if feasible, time-resolved X-ray studies at the Advanced Photon Source. We plan to study charge transfer from functionalized Cd-chalcogenide nanoparticles, and explore synthetic methods to link Cd-based

nanoparticles with polyoxotitanate clusters. In preliminary experiments we have been able to link small polyoxotitanate particles with conjugated molecules. Transient spectroscopy measurements of the dynamics of photo-induced charge transfer in a series of functionalized nanoparticles with different structure and binding modes are to be made in collaboration of Prof. Velarde of our Department. We will continue our collaboration with other research groups.

### DOE Sponsored Publications 2013-2015

- (1) Coppens, P.; Chen, Y.; Trzop, E. *Chem. Rev.* **2014**, *114*, 9645.
- (2) Jarzemska, K. N.; Chen, Y.; Nasca, J. N.; Trzop, E.; Watson, D. F.; Coppens, P. *Phys. Chem. Chem. Phys.* **2014**, *16*, 15792.
- (3) Chen, Y.; Sokolow, J. D.; Trzop, E.; Coppens, P. *Dalton Trans.* **2013**, *42*, 15285.
- (4) Chen, Y.; Trzop, E.; Sokolow, J. D.; Coppens, P. *Chem. Eur. J.* **2013**, 16651.
- (5) Sokolow, J. D., Trzop, E., Chen, Y., Tang, J., Allen, L. J., Crabtree, R. H., Benedict, J. B. & Coppens, P. (2012). *J. Am. Chem. Soc.* **134**, 11695.
- (6) Chen, Y.; Sokolow, J.; Trzop, E.; Chen, Y.-S.; Coppens, P. *J. Chin. Chem. Soc.* **2013**, *60*, 887.
- (7) Chen, Y.; Trzop, E.; Makal, A.; Sokolow, J. D.; Coppens, P. *Inorg. Chem.* **2013**, *52*, 4750.
- (8) Chen, Y.; Trzop, E.; Makal, A. M.; Chen, Y.-S.; Coppens, P. *Dalton Trans.* **2014**, 3839
- (9) Chen, Y.; Jarzemska, K.; Trzop, E.; Zhang, L.; Coppens, P. *submitted*.
- (10) Negre, C. F. A.; Young, K. J.; Oviedo, M. B.; Allen, L. J.; Sanchez, C. G.; Jarzemska, K. N.; Benedict, J. B.; Crabtree, R. H.; Coppens, P.; Brudvig, G. W.; Batista, V. S. *J. Am. Chem. Soc.* **2014**, *136*, 16420.
- (11) Bao, J.; Yu, Z.; Gundlach, L.; Benedict, J. B.; Coppens, P.; Chen, H. C.; Miller, J. R.; Piotrowiak, P. *J. Phys. Chem. B* **2013**, *117*, 4422.
- (12) Seisenbaeva, G. A.; Melnyk, I. V.; Hedin, N.; Chen, Y.; Eriksson, P.; Trzop, E.; Y. L.; Kessler, V. G. *RSC Advances* **2015**, *5*, 24575.

## Controlled Electro-Photonic Structure for Effective Solar Energy Harvesting in Dye Sensitized and Quantum Dot Solar Cells

Yukihiro Hara, Timothy Garvey, Yulan Fu, Byron Farnum, Abay Gadisa, Leila Alibabai, Rudresh Ghosh, and Rene Lopez  
Department of Physics and Astronomy  
University of North Carolina at Chapel Hill  
Chapel Hill, NC, 27713

Efficient absorption of photons and effective charge carrier extraction are the key qualities that enable good performance in a photovoltaic cell. These two functions depend primarily on material intensive properties such as optical constants, band alignments, defects, and charge mobilities and lifetimes. Morphology and geometrical factors at a large range of length scales are nevertheless decisive as light absorption and carrier extraction are frequently found to present their best performances at opposite ends of geometrical variables.

Pulsed laser deposition (PLD) is a physical thin film growing technique that enables the variation of morphology, from compact layers to nanoparticle aggregates with continuous degree of structural connectedness (Figure 1), and tunability of the electrical charge transport quality. Combined with controlled seeding of the substrate (figure 2), geometrical control can be tailored at a larger scale to affect optical absorption as well.

Armed with these parallel strategies, the overarching scope of our project is to investigate the effect of these geometrical variables in the light absorption and charge harvesting in dye sensitized and quantum dot photovoltaic systems.

In this presentation we will elucidate the mechanism by which PLD film growth gives rise to its unique materials microstructure and show its impact in dye sensitized photovoltaic systems based on  $\text{TiO}_2$  and  $\text{Sn:In}_2\text{O}_3$ . We will also describe potential and in progress electrophotonic enhancements utilizing these structural modification approaches to quantum dot photovoltaic systems.

In particular, we have developed a high surface area oxide fabrication that offers a tree-like hierarchical arrangement of nanoparticles that preserves a high surface area for dye loading while building direct highways to transport the charges toward the bottom contacts. As the technique is easily amenable to straight doping, we tested and found 1.0 atomic-% Ta in  $\text{TiO}_2$  photoanodes were 40% times superior to a pure  $\text{TiO}_2$ , we have achieved 6.7% energy conversion efficiencies

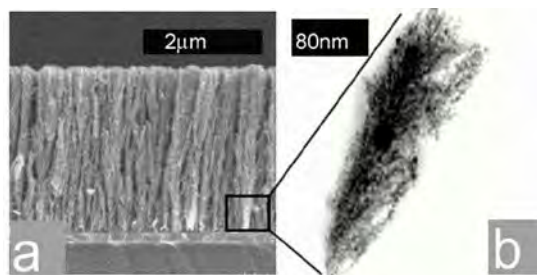


**Figure 1.** (a) Laser ablated Ta:  $\text{TiO}_2$  shows vertically aligned hierarchical nanostructure, STEM image of (b) Ta:  $\text{TiO}_2$  base of the structure.

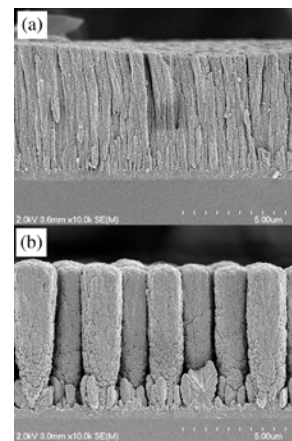


**Figure 2.** Electron cross sectional images of Ta:  $\text{TiO}_2$  nanoforest film on (a) flat FTO and (b) patterned substrates after identical Ta:  $\text{TiO}_2$  laser growth.

with N719 dye in standard cell conditions.

In order to assemble a photonic crystal structure of the Ta:TiO<sub>2</sub> nano-bushes, we patterned an array of indium tin oxide (ITO) micro-cones. The Ta:TiO<sub>2</sub> oxide layer grew in vertically separated bushes or trees out of the patterned ITO that provided a trunk-like seeds for this control growth. Dye-sensitized solar cells with the film on the patterned substrate as well as flat FTO for comparison were fabricated and tested. The devices with the patterned substrate showed 25 % increase in short circuit current ( $J_{sc}$ ) compared to the one with flat FTO substrate. The increase in  $J_{sc}$  was attributed to the enhancements of light absorption and effective electron collection by the patterned ITO.

Applying the bush-like nano-structuring directly to the ITO to form a transparent conductive layer of high surface area, we found that the ITO films develop differences in morphology as a function of the deposition conditions. The structural features led to marked changes in film sheet resistance, spanning 4 orders of magnitude from 50 to  $3 \times 10^5 \Omega/\square$ . The high resistance along the film plane is not surprising as the individual trees in the forest make progressively less contact with each other. However, the critical factor to judge the potential applicability of the nano-bush forest would be its conductivity vertically through the individual ITO structures to the substrate. Applying cyclic voltammetry in loaded samples with a ruthenium dye, we found the dye molecules are near 70% electro-active, indicating the existence of charge transport paths from every point in the individual nanostructures to the substrate.

Pulse laser perturbation transient measurements performed on the dye sensitized ITO structures in open and closed circuit conditions, showed transient photocurrents and photovoltages with time decays on the order of 100 ms and 10 s time scales, respectively. No significant transport time differences across film morphologies were observed, a good indication that the ITO nanostructured films will be able to realize the sought after fast carrier transport when employed as scaffold for thin layers of quantum dots.

In order to utilize this knowledge in a post-perovskite scientific environment, we have proceeded lately to apply our approach to PbS quantum dot system that compared to dye sensitized approaches, has the possibility to attain competitive performance levels. A two-dimensional numerical model has been developed to simulate colloidal quantum dot (CQD) solar cells with full electrophotonic properties resulting for intrinsic material properties and geometrical structure. Periodic patterned structures are shown to enhance the efficient absorption of the CQD solar cells. A series of patterned solar cell devices with different parameters are calculated, among which the optimized device achieves power convert conversion efficiency as high as 17%, with a short circuit current density of  $37.3 \text{ mA}/\text{cm}^2$ , showing great potential of these patterned CQD solar cell devices. Our ongoing efforts to fabricate these predicted structures will be discussed as well.

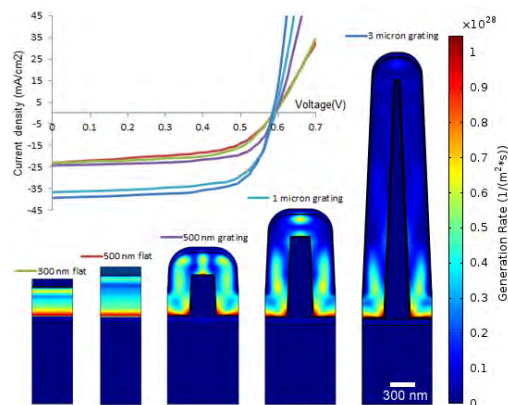


**Figure 3.** Rigorous optical and electronic simulation of TiO<sub>2</sub>:QD-PbS solar cells with different geometries. All real losses included. Layering from bottom to top: Glass, ITO, TiO<sub>2</sub>, QD-PbS, Au.

## DOE Sponsored Publications 2012-2015

1. Yulan Fu, Abay Gadisa, Yukihiro Hara, Chris Miller, Kristina T. Vrouwenvelder, Rene Lopez "Modeling Photovoltaic Performance in Periodic Patterned Colloidal Quantum Dot Solar Cells" submitted to **Optics Express** May 2015
2. A. Gadisa, Y. Hara, K. T. Vrouwenvelder, Y. Fu, J. Dempsey, R. Lopez, "Disparity in Optical Charge Generation and Recombination Processes in Upright and Inverted PbS Quantum Dot Solar Cells" **J. Phys. Chem. C**, 2015, 119 (9), pp 4606–4611, doi: 10.1021/jp512305x
3. Timothy R. Garvey, Byron H. Farnum and Rene Lopez, "Pulsed laser deposited porous nanocarpet of indium tin oxide and their use as charge collectors in core-shell structures for dye sensitized solar cells". **Nanoscale**, 2015 Feb 14;7(6):2400-2408, doi: 10.1039/c4nr05793g.
4. Yukihiro Hara, Timothy Garvey, Leila Alibabaei, Rudresh Ghosh, Rene Lopez, "Controlled Seeding of Laser Deposited Ta:TiO<sub>2</sub> Nanobrushes and Their Performance as Photoanode for Dye Sensitized Solar Cells", **ACS Applied Materials & Interfaces** 2013, 5 (24), pp 13140–13145. doi: 10.1021/am404176q
5. Rudresh Ghosh, Yukihiro Hara, Leila Alibabaei, Kenneth Hanson, Sylvie Rangan, Robert Bartynski, Thomas J. Meyer and Rene Lopez "Increasing photocurrents in dye sensitized solar cells with tantalum doped titanium oxide photoanodes obtained by laser ablation" **ACS Applied Materials and Interfaces**, 2012, 4 (9), pp 4566–4570 doi: 10.1021/am300938g

*Session IV*

*Solar Fuels*



## Towards Highly Efficient Metal Oxide Photoelectrodes for Water Splitting

Roel van de Krol, Fatwa F. Abdi, Carolin Zachäus, Sean P. Berglund  
Institute for Solar Fuels  
Helmholtz-Zentrum Berlin für Materialien und Energie GmbH  
D-14109 Berlin, Germany

In the last decade, many research efforts have been focused on developing new and improved metal oxide-based semiconductors for light-induced water splitting. There are now a handful of (modified) oxides that show photocurrents in excess of  $4 \text{ mA/cm}^2$  under 1 sun. One of these materials is  $\text{BiVO}_4$ , an n-type semiconductor with a bandgap of 2.4 eV. In the past few years, we and others have systematically identified and addressed the bottlenecks in this material. The main bottleneck is the slow surface reaction kinetics, which was readily solved by modifying the surface with a cobalt phosphate water oxidation catalyst [1]. The next bottleneck is the poor electronic conductivity of the material, which can be addressed by doping the material with W [2] or Mo [3]. However, the high doping level has the undesired effect of reducing the space charge width, thus limiting the charge separation efficiency. To tackle this, we introduced a gradient in the dopant concentration that distributes the potential drop over the entire film thickness, effectively forming a series of n-n homojunctions (Fig. 1). Although the total potential drop is limited to 59 mV per factor of 10 difference in dopant concentration, this is sufficient to achieve a significant increase in charge separation efficiency [4]. This gradient doping strategy is generally applicable and can also be used to improve other highly-doped semiconductors. By combining an optimized  $\text{BiVO}_4$  photoanode with a photovoltaic cell in a tandem configuration, we succeeded in fabricating a stand-alone water splitting device with a solar-to-hydrogen efficiency of 4.9% [4], which was further optimized to 5.2% [5].

Despite these encouraging results, the photocurrent density is still almost a factor of 2 short of the theoretical value. At least half of this is caused by the limited amount of light that is absorbed by the films. Simply increasing the film thickness will not work, since the carrier diffusion length is limited to about 70 nm [6]. We have tried to solve this by functionalizing the surface with plasmonic  $\text{Ag@SiO}_2$  core-shell nanoparticles [7]. Numerical solutions of the Maxwell equations indicate an optical absorption enhancement of up to 40% for a surface coverage of 50%. Intriguingly, we found an actual enhancement of the IPCE and AM1.5 photocurrent by a factor of  $\sim 2.5$  compared to bare (non-optimized)  $\text{BiVO}_4$  photoanodes, i.e., much larger than predicted. This was found to be caused by an enhanced injection efficiency of holes into the electrolyte by the  $\text{Ag@SiO}_2$  nanoparticles. Other groups have tackled the issue of the limited carrier diffusion length by

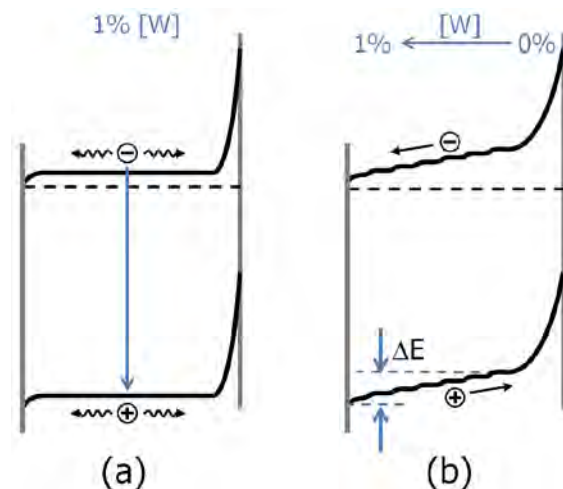


**Fig. 1.** Formation of an electric field in a highly-doped semiconductor through a gradient in the concentration of shallow dopants.

nanostructuring, resulting in impressive current densities of 5-6 mA/cm<sup>2</sup> [8-9].

Since current densities above 5 mA/cm<sup>2</sup> are now tantalizingly close, part of our efforts are now geared towards making larger-area stand-alone water splitting devices. For this, we use scalable synthesis techniques, such as magnetron sputtering. Intriguingly, we find that modification of these films with a CoPi catalyst gives no significant improvement, whereas very clear improvements were found with spray-deposited films. To gain insight into the surface reaction kinetics, we studied the films with intensity-modulated photocurrent spectroscopy (IMPS). Using the methodology developed by Peter et al. [10], we find that the main role of the CoPi ‘catalyst’ on BiVO<sub>4</sub> is to reduce the surface recombination rate. In fact, the CoPi appears to actually suppress the kinetics of hole injection into the electrolyte, in stark contrast to its supposed role as an electrocatalyst. The implications of this surprising observation will be discussed.

Although BiVO<sub>4</sub> is now considered to be a promising material by many researchers in the field, it should be realized that its theoretical efficiency is limited to ~9% due to the relatively large band gap. In order to break the 10% efficiency barrier, new and chemically stable semiconductors with band gaps between 1.7 and 2.1 eV need to be found. One way to reduce the band gap of known metal oxide semiconductors is by alloying the material with nitrogen through high-temperature exposure to NH<sub>3</sub> (ammonolysis). The N-2p orbitals are higher in energy than the O-2p orbitals, and can therefore reduce the band gap by an upward shift of the valence band. This approach has been successfully pursued by the groups of Domen [11] and others for e.g. the Ta-O-N system. It turns out that the process conditions during ammonolysis of Ta<sub>2</sub>O<sub>5</sub> need to be very precisely controlled in order to get the desired phases, such as the β-TaON phase, and that this is exceedingly difficult to reproduce across different labs and setups. To get more control over the process, we developed a setup that allows us to monitor the optical transmission of a thin metal oxide film during the high-temperature ammonolysis treatment [12]. An example of the resulting spectrum is shown in Figure 2. It clearly shows the transformation from Ta<sub>2</sub>O<sub>5</sub> (E<sub>g</sub> = 3.9 eV) to Ta<sub>3</sub>N<sub>5</sub> (E<sub>g</sub> = 2.1 eV). Analysis of samples that were cooled down quickly at various stages of the transformation showed that the film consists exclusively of a mixture of Ta<sub>2</sub>O<sub>5</sub> and Ta<sub>3</sub>N<sub>5</sub> [13]. We have recently taken this a step further, and are now able to reproducibly obtain the elusive β-TaON phase. The details of this approach will be discussed.

Finally, We will show some first results for n-type Fe<sub>2</sub>WO<sub>6</sub> and p-type CuBi<sub>2</sub>O<sub>4</sub>, two new photoelectrode candidates that have band gaps of 1.7 and 1.8 eV, respectively. We will discuss some key performance metrics, bottlenecks, and potential show-stoppers for these materials.

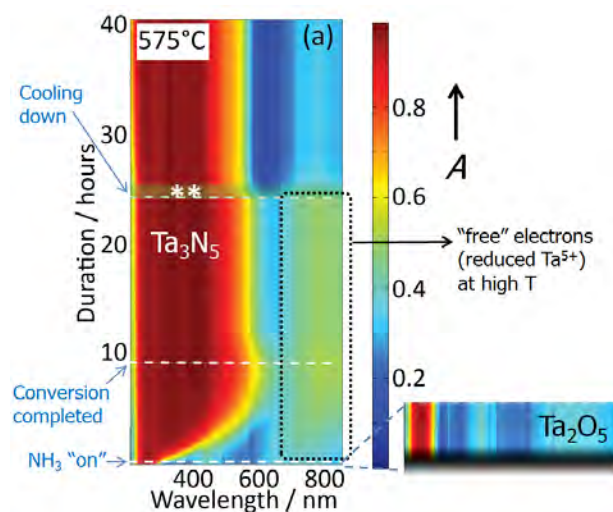


**Fig. 2.** Optical absorption spectrum as a function of wavelength and time, recorded during the conversion of a thin Ta<sub>2</sub>O<sub>5</sub> film to Ta<sub>3</sub>N<sub>5</sub> in a flow of NH<sub>3</sub> gas at 575°C [13].

## References

1. F.F. Abdi, R. van de Krol, *J. Phys. Chem. C* 116, 9398 (2012).
2. F.F. Abdi, N. Furet, R. van de Krol, *ChemCatChem* 5, 490 (2013).
3. S.P. Berglund, A.J.E. Rettie, S. Hoang, C.B. Mullins, *Phys. Chem. Chem. Phys.* 14, 7065 (2012).
4. F.F. Abdi, L. Han, A.H.M. Smets, M. Zeman, B. Dam, R. van de Krol, *Nat. Commun.* 4:2195 (2013).
5. L. Han, F.F. Abdi, R. van de Krol, R. Liu, Z. Huang, H.J. Lewerenz, B. Dam, M. Zeman, A.H.M. Smets, *ChemSusChem* 16 (2014) 15272
6. F.F. Abdi, T.J. Savenije, M.M. May, B. Dam, R. van de Krol, *J. Phys. Chem. Lett.* 4, 2752 (2013).
7. F.F. Abdi, A. Dabirian, B. Dam, R. van de Krol, *Phys. Chem. Chem. Phys.* 16, 15272 (2014).
8. T.W. Kim, K.-S. Choi, *Science* 243 (2014) 990
9. X. Shi, K. Zhang, K. Shin, M. Ma, J. Kwon, I.T. Choi, J.K. Kim, H.K. Kim, D.H. Wang, J.H. Park, *Nano Energy* 13, 182 (2015).
10. J. Li, L.M. Peter, *J. Electroanal. Chem.* 193, 27 (1985).
11. M. Hara, G. Hitoki, T. Takata, J.N. Kondo, H. Kobayashi, K. Domen, *Catal. Today* 78, 555 (2003).
12. A. Dabirian, H. van 't Spijker, R. van de Krol, *Energy Proc.* 22, 15 (2012).
13. A. Dabirian, R. van de Krol, *Chem. Mater.* 27, 708 (2015).

## Interfacial Photochemistry of Nanostructured Metal Oxide and Silicon Photoelectrodes

Nathan R. Neale  
Chemistry and Nanoscience Center  
National Renewable Energy Laboratory  
Golden, CO 80401

The production of solar fuels (*e.g.* H<sub>2</sub> from H<sub>2</sub>O, hydrocarbons from CO<sub>2</sub>) via direct photoelectrochemical (PEC) reactions is a promising approach in the pursuit of renewable energy sources. However, solar photoelectrochemical fuel production has rigid requirements – strong visible light absorption, appropriate band positions, good charge transport, fast interfacial charge transfer, stable to corrosion – that are challenging to address simultaneously. Nanostructuring semiconductors can reduce some of these requirements and thus offers one potential pathway toward this goal. We have been developing nanostructured platforms to understand and control the fundamental charge generation, separation, transport, and transfer processes toward making such PEC devices a reality.

### *Controlling Charge Generation, Separation, and Transport in a Molybdenum-Doped Bismuth Vanadate Photoanode.*

A detailed understanding of doping level, electron diffusion length and coefficient, as well as light capture and charge separation efficiencies was reported for nanoporous Mo-doped BiVO<sub>4</sub> (Mo:BiVO<sub>4</sub>) photoanodes. Efficient water oxidation was achieved by doping BiVO<sub>4</sub> with 1.8% Mo, resulting in a several-fold enhancement in photooxidation rate versus non-doped BiVO<sub>4</sub> (Fig. 1). Two methods were used to study the effect of Mo doping on the electron transport: (1) an analysis of the front/back illumination ratio of incident photon-to-current efficiency and (2) intensity modulated photocurrent spectroscopy (IMPS). These experiments showed that Mo doping improves the diffusion coefficient four-fold and increases the diffusion length to ~300 nm (*cf.* ~10 nm for the non-doped oxide), which was also the empirically-determined optimal Mo:BiVO<sub>4</sub> film thickness for photoelectrolysis. These results were consistent with IMPS measurements, which found an electron diffusion coefficient in the doped films of  $1.5 \times 10^{-7}$  cm<sup>2</sup>/s compared with just  $3.5 \times 10^{-8}$  cm<sup>2</sup>/s for non-doped films. Another important finding from this study was that we were the first to report that nanostructured, Mo-doped BiVO<sub>4</sub> films exhibit 90% charge separation

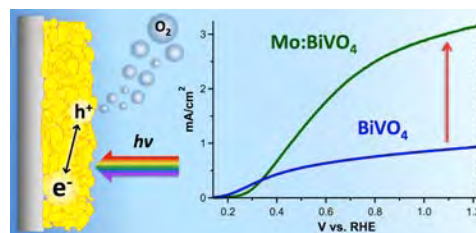


**Figure 1.** Schematic of Mo:BiVO<sub>4</sub> film (left) and *J*-*V* curves of non-doped BiVO<sub>4</sub> and Mo:BiVO<sub>4</sub> photoanodes under 1 sun front illumination in pH 7 phosphate electrolyte (right).

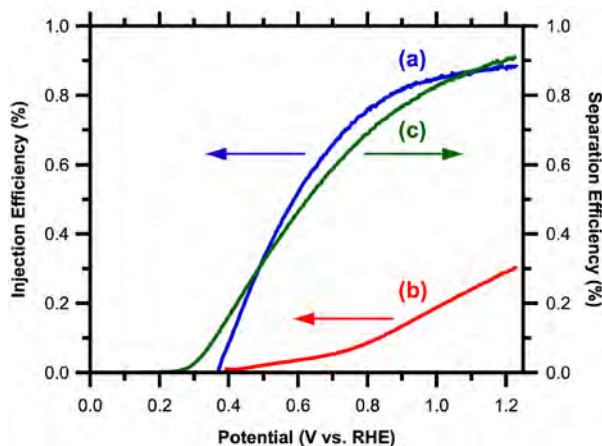


**Figure 2.** Injection efficiency of 300 nm thick Mo:BiVO<sub>4</sub> (a) with FeOOH and (b) without FeOOH. (c) Separation efficiency of 300 nm thick Mo:BiVO<sub>4</sub>. Experiments performed under 1 sun front illumination in pH 7 phosphate electrolyte.

efficiency and 80% absorbed photon-to-current efficiency (Fig. 2), excellent values for metal oxide photoabsorbers. Among the many interfacial layers explored, surface modification with iron oxyhydroxide (FeOOH) dramatically enhanced the water oxidation performance of Mo:BiVO<sub>4</sub> to an integrated IPCE of 2.41 mA/cm<sup>2</sup> and a photocurrent density of 2.77 mA/cm<sup>2</sup> in neutral phosphate at 1.23 V vs. reversible hydrogen electrode (RHE).

*New Metal Oxide Photoabsorber Based on Copper Vanadate (Cu<sub>3</sub>V<sub>2</sub>O<sub>8</sub>).* Identification of viable photoanode candidates for use in a tandem PEC water splitting system remains a significant challenge to the realization of efficient solar-driven hydrogen production. As an extension of our Mo:BiVO<sub>4</sub> work, copper vanadate (Cu<sub>3</sub>V<sub>2</sub>O<sub>8</sub>) was introduced as a new, all first row transition metal oxide with a band gap of near 2 eV that makes it suitable as a photoanode candidate in a solar water splitting system. We

established many of the key physical and PEC properties of Cu<sub>3</sub>V<sub>2</sub>O<sub>8</sub> including band gap, doping type, ability to extrinsically dope, flat-band potential, band positions, electron diffusion length, chemical stability, and O<sub>2</sub> evolution faradaic efficiency (Fig. 3). This study provided a key initial step in identifying the features that can lead to a better understanding of this new ternary metal oxide and motivate discovery of related photoanodes comprised of multicomponent oxides.

*Nanoporous Silicon Photocathode/Catalyst Interfaces.* Stable and high-performance nanoporous “black silicon” photoelectrodes with electrolessly deposited Pt nanoparticle (NP) catalysts were fabricated with two metal-assisted etching steps. The second Pt-assisted etch process buries the Pt NPs deep into the nanoporous Si surface that results in a positive shift in the proton reduction onset voltage, from 0.25 V to 0.4 V vs. RHE, as well as a reduction in the charge-transfer resistance with no performance decrease seen for at least two months (Fig. 4). The mechanism for performance enhancement was examined in detail by a number of techniques including photocurrent-voltage and capacitance-voltage measurements, scanning and transmission electron microscopies, and electrochemical impedance spectroscopy. These studies revealed that an excellent interfacial contact between the Pt NP catalysts and the crystalline silicon electrode likely cause the oxidative resistance. We will also discuss new mechanistic insights provided by elemental mapping via STEM-EELS/EDS that show oxide-

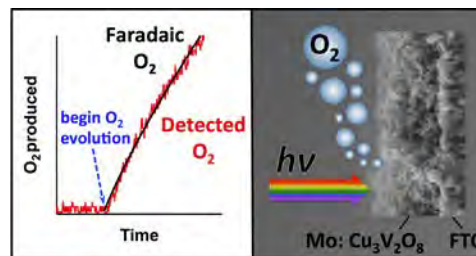


**Figure 3.** Oxygen production versus time (left) and schematic including SEM cross sectional image of a new all first row transition metal oxide photoanode based on Cu<sub>3</sub>V<sub>2</sub>O<sub>8</sub> (right).

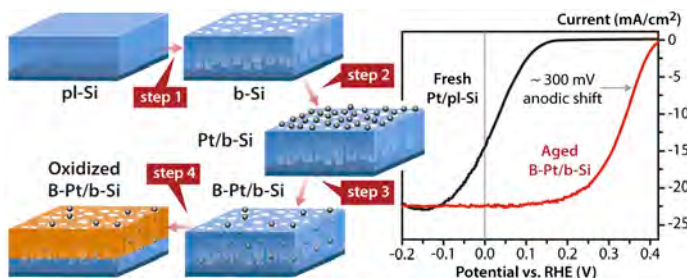


**Figure 4.** Left: Schematic of the preparation process for air-stable high-performance nanoporous black Si photocathodes modified with Pt nanoparticle (NP) catalysts buried deep within the nanopores. Right: Comparison of J–V curves for photoelectrochemical proton reduction in 0.5 M H<sub>2</sub>SO<sub>4</sub> electrolyte for a fresh planar Si electrode with Pt NPs (Pt/pl-Si) (black curve) and a black Si photocathode with buried Pt NPs (B-Pt/b-Si) aged for 1 month in air (red curve).

coated nanopore walls and a Si/Pt NP interface free from oxide contamination even after prolonged aging.

### DOE Sponsored Publications 2012-2015

1. "Overall Water Splitting using a Hydrogenase-Catalyzed Nanoporous Silicon Photoelectrode," Y. Zhao, N. C. Anderson, M. W. Ratzloff, D. W. Mulder, K. Zhu, J. A. Turner, N. R. Neale, P. W. King, H. M. Branz, *Submitted* **2015**.
2. "Surface Passivation of Silicon Nanocrystals Using Radical-Mediated Hydrosilylation," P. K. B. Palomaki, J. L. Blackburn, N. C. Anderson, L. M. Wheeler, J. C. Johnson, N. R. Neale, *Submitted* **2015**.
3. "Synthesis, Optical, and Photocatalytic Properties of Cobalt Mixed-Metal Spinel Oxides  $\text{Co}(\text{Al}_{1-x}\text{Ga}_x)_2\text{O}_4$ ," K. Lee, D. A. Ruddy, G. Dukovic, N. R. Neale, *J. Mater. Chem. A* **2015**, *3*, 8115-8122. <http://dx.doi.org/10.1039/C4TA06690A>
4. "Oxidatively Stable Nanoporous Silicon Photocathodes with Enhanced Onset Voltage for Photoelectrochemical Proton Reduction," Y. Zhao, N. C. Anderson, K. Zhu, J. A. Aguiar, J. A. Seabold, J. Oh, J. van de Lagemaat, H. M. Branz, N. R. Neale, *Nano Lett.* **2015** ASAP. <http://dx.doi.org/10.1021/acs.nanolett.5b00086>
5. "Quantum Confined Electron-Phonon Interaction in Silicon Nanocrystals," D. M. Sagar, J. M. Atkin, P. K. B. Palomaki, N. R. Neale, J. L. Blackburn, J. C. Johnson, A. J. Nozik, M. B. Raschke, M. C. Beard, *Nano Lett.* **2015**, *15*, 1511-1516. <http://dx.doi.org/10.1021/nl503671n>
6. "All First Row Transition Metal Oxide Photoanode for Water Splitting Based on  $\text{Cu}_3\text{V}_2\text{O}_8$ ," J. A. Seabold and N. R. Neale, *Chem. Mater.* **2015**, *27*, 1005-1013. <http://dx.doi.org/10.1021/cm504327f>
7. "Semiconducting Properties of Spinel Tin Nitride and Other  $\text{IV}_3\text{N}_4$  Polymorphs," C. M. Caskey, J. A. Seabold, V. Stevanovic, M. Ma, W. A. Smith, D. S. Ginley, N. R. Neale, R. M. Richards, S. Lany, A. Zakutayev, *J. Mater. Chem. C* **2015**, *3*, 1389-1396. <http://dx.doi.org/10.1039/C4TC02528H>
8. "Solar energy: Packing heat," N. R. Neale, *Nat. Chem. (News and Views)* **2014**, *6*, 385. <http://dx.doi.org/10.1038/nchem.1933>
9. "Transparent  $\text{TiO}_2$  Nanotube Array Photoelectrodes Prepared via Two-Step Anodization," J. Y. Kim, K. Zhu, N. R. Neale, A. J. Frank, *Nano Converg.* **2014**, *1*, 9. <http://dx.doi.org/10.1186/s40580-014-0009-3>
10. "Efficient Solar Photoelectrolysis by Nanoporous  $\text{Mo:BiVO}_4$  Through Controlled Electron Transport," J. A. Seabold, K. Zhu, N. R. Neale, *Phys. Chem. Chem. Phys.* **2014**, *16*, 1121-1131. <http://dx.doi.org/10.1039/C3CP54356K>
11. "Control of Plasmonic and Interband Transitions in Colloidal Indium Nitride Nanocrystals," P. K. B. Palomaki, E. M. Miller, N. R. Neale, *J. Am. Chem. Soc.* **2013**, *135*, 14142-14150. <http://dx.doi.org/10.1021/ja404599g>
12. "The effect of a metallic Ni core on charge dynamics in CdS-sensitized p-type NiO nanowire mesh photocathodes," S. H. Kang, N. R. Neale, K. Zhu, A. F. Halverson, Y. Yan, A. J. Frank, *RSC Adv.* **2013**, *3*, 13342-13347. <http://dx.doi.org/10.1039/c3ra41216d>
13. "Surface Chemistry Exchange of Alloyed Germanium Nanocrystals: A Pathway Toward Conductive Group IV Nanocrystal Films," D. A. Ruddy, P. T. Erslev, S. E. Habas, J. A. Seabold, N. R. Neale, *J. Phys. Chem. Lett.* **2013**, *4*, 416-421. <http://dx.doi.org/10.1021/jz3020875>
14. "Effects of  $\text{TiCl}_4$  Treatment of Nanoporous  $\text{TiO}_2$  Films on Morphology, Light Harvesting, and Charge-Carrier Dynamics in Dye-Sensitized Solar Cells," S.-W. Lee, K.-S. Ahn, K. Zhu, N. R. Neale, A. J. Frank, *J. Phys. Chem. C* **2012**, *116*, 21285-21290. <http://dx.doi.org/10.1021/jp3079887>
15. "Perturbation of the Electron Transport Mechanism by Proton Intercalation in Nanoporous  $\text{TiO}_2$  Film," A. F. Halverson, K. Zhu, P. T. Erslev, J. Y. Kim, N. R. Neale, A. J. Frank, *Nano Lett.* **2012**, *12*, 2112-2116. <http://dx.doi.org/10.1021/nl300399w>

## Establishing the Role of the Electrode Surface in Solar-Driven Pyridine-Catalyzed CO<sub>2</sub> Reduction

Coleman X. Kronawitter, Peng Zhao, and Bruce E. Koel  
Department of Chemical and Biological Engineering  
Princeton University  
Princeton, NJ 08540

Viable technologies that steer the U.S. energy sector away from fossil fuel use toward more sustainable solutions must address the simple fact that a large portion of U.S. power consumption derives from conversion of stored, chemical fuels. Photoelectrocatalytic CO<sub>2</sub> reduction is one such technology, since it facilitates a process whereby solar energy is used to reduce CO<sub>2</sub>, a combustion product, into chemical fuels that are compatible with the existing U.S. energy infrastructure. Catalysts play an important role in making solar-driven CO<sub>2</sub> reduction technologies feasible because they can be designed to optimize both reaction rate and selectivity.

Our project involves experimental studies of well-defined surfaces to establish the role the electrode surface in catalyzed heterogeneous CO<sub>2</sub> reduction. Specifically we investigate the role of the electrode surface in photoelectrocatalytic pyridine-catalyzed CO<sub>2</sub> reduction. It was discovered by Bocarsly and coworkers that pyridine (C<sub>5</sub>H<sub>5</sub>N) catalyzes the conversion of CO<sub>2</sub> to methanol with near-perfect Faradaic yields when used in a photoelectrochemical cell employing a p-type GaP photocathode [*J. Am. Chem. Soc.* 2008, 130, 6342]. Our experiments are designed to explain the origin of high efficiency in this model system, which is essential to the continued optimization of solar-driven CO<sub>2</sub> reduction technologies.

We have proposed surface science experiments to answer timely open questions on the role of the electrode surface and surface-bound intermediates in this chemistry. We perform surface science investigations of surface and adsorbate chemistry, based primarily on quantitative spectroscopic measurements. We utilize well-defined GaP single crystal surfaces to assess the adsorption state of relevant molecules and probe mechanisms of thermal reactions (in the dark) and the reactions that occur by illumination with light, sorting out the differences. Our studies are primarily carried out in ultrahigh vacuum (UHV), which enables the use of well-controlled amounts of adsorbed pyridine, water, CO<sub>2</sub>, formic acid, and formaldehyde, and can be performed at low temperatures which allows us to condense monolayer and multilayer films and trap reactive intermediates formed in coadsorbed and reactive environments and under illumination.

In the first several months, we have begun our investigations by characterizing adsorbed layers of surface hydride, water, and pyridine on GaP(110). These species are among the primary constituents of this catalytic system, so we began our work by establishing their baseline adsorption properties. We have used high resolution X-ray photoelectron spectroscopy (HR-XPS), ambient pressure photoelectron spectroscopy (APPES), and high-resolution electron energy loss spectroscopy (HREELS) to probe the electronic and vibrational characteristics of clean GaP(110), H<sub>2</sub>O/GaP(110), and pyridine/GaP(110).

APPES was used to spectroscopically identify *in situ* surface-bound species over ten orders of magnitude of pressure, up to 1 Torr. The data show that the interaction with water is characterized by the presence of a partially dissociated adlayer, with Ga-OH, P-H, and adsorbed molecular H<sub>2</sub>O species detected on the surface. This is consistent with published theoretical work

that predicts the presence of this layer [J. Am. Chem. Soc. 2012, 134, 13600]. Figure 1 provides P 2p APPES of GaP(110) in the presence of water, and shows the growth of the P-hydride species as a function of increasing pressure. In addition to identifying Ga-OH, P-H, and H<sub>2</sub>O on the surface, we used isobaric APPES measurements at elevated pressures to probe the thermal stabilities of adsorbed species as well as the oxidation of surface Ga and P. We observe the surface hydride to be remarkably stable in the presence of water, which is notable given the critical role of hydride transfer to catalysts and CO<sub>2</sub> during chemical fuel synthesis reactions in aqueous environments. It is hypothesized that the high observed stability of the hydride on GaP may contribute to its associated remarkable near-100% faradaic efficiency for methanol generation by solar-driven CO<sub>2</sub> reduction. This APPES work has been submitted for publication. HREELS studies are underway to further probe the chemistry of this partially dissociated layer.

We have characterized the GaP(110) surface using scanning tunneling microscopy (STM). To perform these experiments we built a sample holder that facilitated cleaving single crystals in UHV to reveal the desired surface to be probed. Figure 2 shows an atomic-resolution image of GaP(110) after cleaving (obtained at 5 K in the LT-STM facility at BNL). The Ga sublattice is evident and isolated Zn dopants are seen as bright features. Terraces are typically several hundred nanometers in extent and are ideal for exploring the interaction of co-adsorbates relevant to CO<sub>2</sub> reduction chemistry.

Using a combination of STM and density functional theory, we find that pyridine interacts with the GaP(110) surface through a dative covalent bond with surface Ga and at low coverage a tilted configuration is preferred. Our observation of the stable adsorption of both H and pyridine on this surface is important, because it characterizes the precursor state for the proposed formation of adsorbed dihydropyridine, which could be a key hydride-shuttling catalyst for heterogeneous CO<sub>2</sub> reduction. [J. Phys. Chem. Lett. 2013, 4, 4058].

Our future work entails leveraging knowledge from these baseline experiments to synthesize reactive intermediates in UHV and characterize their reactivities. Specifically we plan to synthesize surface-bound pyridine-based intermediates including pyridinium, pyridinyl, and dihydropyridine, and then establish their propensity to interact with CO<sub>2</sub> and other compounds along the CO<sub>2</sub> reduction pathway.

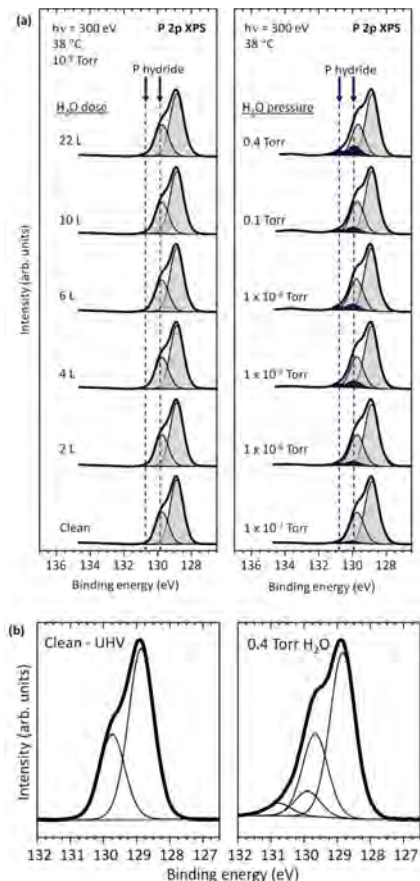


Figure 1. (a) P 2p APPES showing the formation of a negatively charged hydride on GaP(110) from the interaction with water. (b) Expanded view of the P 2p region comparing GaP(110) clean and in the presence of 0.4 Torr water.

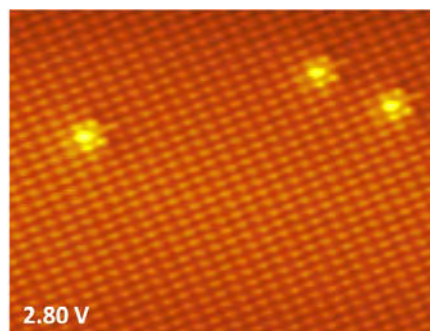


Figure 2. Constant-current STM image of the GaP(110) surface, showing atomic resolution of the Ga sub-lattice and Zn dopants (brightest features). 2.80 V, 0.04 nA, 149.1×111.8 Å.

### **DOE Sponsored Publications 2012-2015**

1. C.X. Kronawitter, M. Lessio, P. Zhao, C. Riplinger, J. A. Boscoboinik, D. Starr, P. Sutter, E.A. Carter, B.E. Koel, Observation of surface-bound negatively charged hydride and hydroxide on GaP(110) in H<sub>2</sub>O environments. *J. Am. Chem. Soc.*, 2015, submitted.



*Session V*

*Photoevents in Nanoparticles*



# Model Asymmetric Semiconductor Nanorod/Oxide Nanoparticle Hybrid Constructs

Jeffrey Pyun, S. Scott Saavedra, Neal R. Armstrong

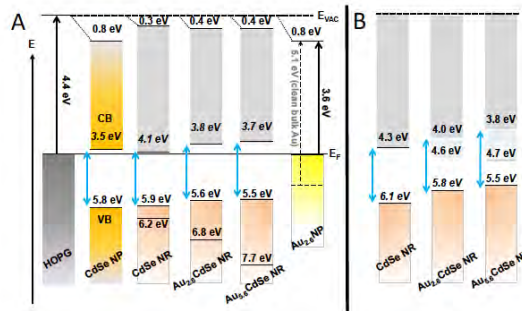
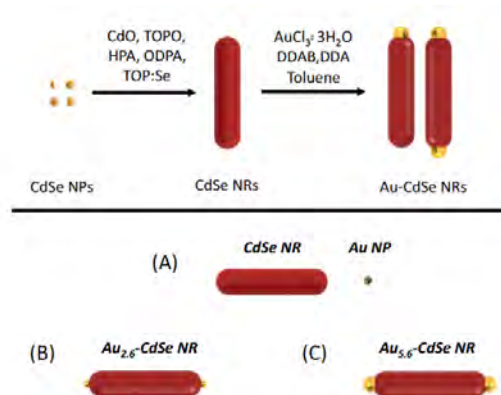
Department of Chemistry/Biochemistry

University of Arizona

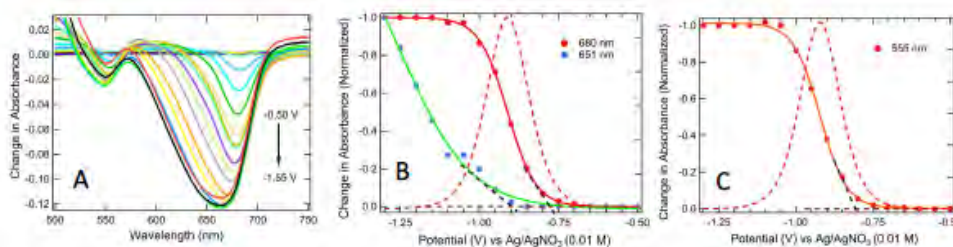
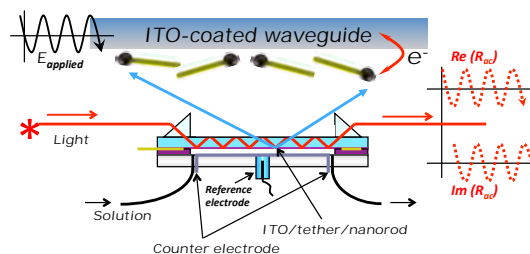
Tucson, Arizona 85721

Our collaborative research efforts have recently focused on the creation of new (symmetric and asymmetric) photoactive and photo-electrocatalytic semiconductor nanorod (NR) materials, and new approaches to the characterization of both energetics (band edge energies) and rates of heterogeneous charge transfer events for ultrathin films of these NR constructs (figures at right). These NR materials are model systems that enable the study of the compositional and structural factors that control the efficiencies of light-activated energy conversion processes in NR materials leading to fuel formation from sunlight.

Our primary focus has been on the formation and characterization of new heterostructured II-VI semiconductor NRs (CdS and CdSe NRs) with metallic and/or metal oxide ( $\text{Co}_x\text{O}_y$ ) nanoparticle (NP) “tips,” which promise to enhance photo-induced oxidation of solution donors, and ultimately oxygen evolution (OER). We envision the ultimate creation of heterostructured NRs that demonstrate the internal energy gradients that, upon illumination, ensure efficient charge separation, transport, and high rates of charge transfer (CT) processes at the NR termini, competing favorably with rates of recombination.



(upper right) CdSe NRs tipped (Au or Pt, as a precursor to addition of  $\text{Co}_x\text{O}_y$ ), (center) the band edge energies ( $E_{VB}$ ,  $E_{CB}$ ) estimated from both PES and (lower right and below) the unique ATR waveguide spectroelectrochemical construct for characterization of metal-tipped NRs, and differential absorbance data versus applied potential, demonstrating band-edge absorbance bleaching with electron injection into  $E_{CB}$ .



## 1) Formation of new semiconductor nanorods with metallic and oxide catalytic tips:

We have created a series of unique semiconductor NR materials (either CdSe@CdS, CdS, or CdSe) that have been tipped at either ends, or one end, with catalytic sites, either metallic (Pt, Au) or oxides such as  $\text{Co}_x\text{O}_y$ . The distinguishing feature of the synthetic aspects of this work has been an emphasis on developing reproducible and scalable methods to enable the preparation of materials in sub-gram quantities (100-900 mg). We have shown that the key feature in these synthetic schemes is the ability to control the deposition of either Au or Pt NP tips onto semiconductor CdSe@CdS NRs. The presence of the noble metal seeds enabled quantitative deposition of metallic Co NP tips, which were readily oxidized to form  $\text{Co}_x\text{O}_y$  tips that were still intact on the nanorod. The approach proved to be high modular and readily applied to other NR materials (CdS, CdSe) to enable spatial and energetic control in the photoactive nanocomposite. We have also prepared heterostructured CdSe nanorods that incorporate Au, Co and  $\text{Co}_x\text{O}_y$  tips. CdSe NRs are useful model constructs because they have high bandgap energies and afford ease of synthesis and tuning of the NR size, shape and functionalization in numerous ways, which leads to insights about their energetics that should be generalizable across a number of material platforms.

### ***2) Characterization of valence band energies in NCs and NRs using photoemission spectroscopies; effect of metallic tips on $E_{\text{VB}}$ :***

We have recently developed a unique approach to the characterization of  $E_{\text{VB}}$  in ultra-thin films of NCs and NRs using UV-photoemission spectroscopies (He I and He II UPS),<sup>1</sup> providing greater confidence in the energies of these band edges, especially relative to previous PES studies of related systems. These improvements have also given us confidence that we can use high sensitivity, high dynamic range forms of these UPS experiments to characterize mid-gap defect DOS in new NR materials. For NR materials based on semiconductors such as CdSe and CdS, we observe large shifts in local vacuum level (as a result of the strongly dipolar nature of these II-VI nanomaterials) large photoemission backgrounds resulting from secondary electron scattering, and large local shifts in vacuum level. Our most recent studies show that these effects can be corrected to provide reliable estimates of  $E_{\text{VB}}$  as a function of NR tipping, and our high sensitivity PES studies can be used to estimate densities-of-state (DOS) for mid-gap defects. This is especially critical for monitoring the differences in  $E_{\text{VB}}/E_{\text{CB}}$  and mid-gap DOS that result from changes in NR composition, length and tipping chemistries.

### ***3) Waveguide-based spectroelectrochemical characterization of conduction band energies and rates of heterogeneous ET in CdSe NRs with Au NP Tips:***

We have extended the use of waveguide-based spectroelectrochemistry to monitor electron injection into the conduction band ( $E_{\text{CB}}$ ) of bare and Au/Pt-tipped CdSe NRs at very low coverages on semi-transparent metal oxide contacts, for the first time. As shown in the figure above, as the applied potential is stepped negative (toward the vacuum level; electron injection into the NR film causes bleaching of the lowest energy excitonic features. Plotting  $dA$  vs  $V$  at select wavelengths provides estimates of the onset potentials for injection into the  $I\Sigma_e$  and  $III_e$  levels of the CdSe NR conduction band. As metal tips are added to the NR we see evidence of new SET levels and MSI states introduced below  $E_{\text{CB}}$  which are relevant to the possibility of recombination centers in these materials, and correspond to the same states observed in our PES experiments above  $E_{\text{VB}}$ . These spectroelectrochemical platforms have also provided a means of estimating rates of heterogeneous electron transfer,  $k_s$ , for the NR/oxide waveguide construct, showing that the addition of metal tips to these NRs enhances the electronic coupling between the NR and the oxide contact.

## DOE Sponsored Publications 2007-2015

- (1) Ehamparam, R.; Pavlopoulos, N.; Liao, M. W.; Hill, L. J.; Armstrong, N. R.; Pyun, J.; Saavedra, S. S. Characterization of Energetics and Dynamics of Charge Injection Processes in Au-Tipped CdSe Nanorod Monolayers Using Photoemission Spectroscopies and Waveguide Spectroelectrochemistry. *ACS Nano* **submitted**.
- (2) Ehamparam, R.; Pavlopoulos, N.; Richey, N.; Armstrong, N. R.; Pyun, J.; Saavedra, S. S. Characterization of Energetics in Bare and Pt-tipped CdSe@CdS Nanorod Films Using Spectroelectrochemistry. **in preparation**, manuscript in preparation.
- (3) Ehamparam, R.; Pavlopoulos, N.; Liao, M.; Hill, L. J.; Armstrong, N. R.; Pyun, J.; Saavedra, S. S. Waveguide Spectroelectrochemistry of CoxOy-tipped CdSe NRs: Determination of Band Edge Energies and Heterogeneous Electron Transfer Kinetics. **in preparation**.
- (4) Hill, L. J.; Richey, N. E.; Sung, Y.-H.; Dirlam, P. T.; Lavoie-Higgins, E.; Shim, I.-B.; Pinna, N.; Willinger, M.-G.; Vogel, W.; Char, K.; Pyun, J. Colloidal Polymers via Dipolar Assembly of Heterostructured Co-tipped CdSe@CdS Nanorods. *ACS Nano* **2014**, *8*, 3272-3284.
- (5) Hill, L. J.; Richey, N. E.; Sung, Y.-H.; Dirlam, P. T.; Lavoie-Higgins, E.; Shim, I.-B.; Pinna, N.; Willinger, M.-G.; Vogel, W.; Char, K.; Pyun, J. Synthesis and Dipolar Assembly of Heterostructured Cobalt Tipped CdSe@CdS Nanorods. *Cryst. Eng. Comm.* **2014**, *16*, 9461-9468.
- (6) Hill, L. J.; Pyun, J. Colloidal Polymers via Dipolar Assembly of Magnetic Nanoparticle Monomers. *Acs Applied Materials & Interfaces* **2014**, *6*, 6022-6032.
- (7) Hill, L. J.; Bull, M. M.; Sung, Y.; Simmonds, A. G.; Dirlam, P. T.; Richey, N. E.; DeRosa, S. E.; Shim, I.-B.; Guin, D.; Costanzo, P. J.; Pinna, N.; Willinger, M.-G.; Vogel, W.; Char, K.; Pyun, J. Directing the Deposition of Ferromagnetic Cobalt onto Pt-Tipped CdSe@CdS Nanorods: Synthetic and Mechanistic Insights. *Acs Nano* **2012**, *6*, 8632-8645.
- (8) Keng, P. Y.; Bull, M. M.; Shim, I.-B.; Nebesny, K. G.; Armstrong, N. R.; Sung, Y.; Char, K.; Pyun, J. Colloidal Polymerization of Polymer-Coated Ferromagnetic Cobalt Nanoparticles into Pt-Co(3)O(4) Nanowires. *Chemistry of Materials* **2011**, *23*, 1120-1129.
- (9) Kim, B. Y.; Shim, I.-B.; Araci, Z. O.; Saavedra, S. S.; Monti, O. L. A.; Armstrong, N. R.; Sahoo, R.; Srivastava, D. N.; Pyun, J. Synthesis and Colloidal Polymerization of Ferromagnetic Au-Co Nanoparticles into Au-Co3O4 Nanowires. *Journal of the American Chemical Society* **2010**, *132*, 3234-+.
- (10) Keng, P. Y.; Kim, B. Y.; Shim, I.-B.; Sahoo, R.; Veneman, P. E.; Armstrong, N. R.; Yoo, H.; Pemberton, J. E.; Bull, M. M.; Griebel, J. J.; Ratcliff, E. L.; Nebesny, K. G.; Pyun, J. Colloidal Polymerization of Polymer-Coated Ferromagnetic Nanoparticles into Cobalt Oxide Nanowires. *Acs Nano* **2009**, *3*, 3143-3157.
- (11) Araci, Z. O.; Shallcross, C. R.; Armstrong, N. R.; Saavedra, S. S. Potential-Modulated Attenuated Total Reflectance Characterization of Charge Injection Processes in Monolayer-Tethered CdSe Nanocrystals. *Journal of Physical Chemistry Letters* **2010**, *1*, 1900-1905.
- (12) Munro, A. M.; Zacher, B.; Graham, A.; Armstrong, N. R. Photoemission Spectroscopy of Tethered CdSe Nanocrystals: Shifts in Ionization Potential and Local Vacuum Level As a Function of Nanocrystal Capping Ligand. *Acs Applied Materials & Interfaces* **2010**, *2*, 863-869.
- (13) Shallcross, R. C.; D'Ambruso, G. D.; Pyun, J.; Armstrong, N. R. Photoelectrochemical Processes in Polymer-Tethered CdSe Nanocrystals. *Journal of the American Chemical Society* **2010**, *132*, 2622-2632.
- (14) Shallcross, R. C.; Chawla, G. S.; Marikkar, F. S.; Tolbert, S.; Pyun, J.; Armstrong, N. R. Efficient CdSe Nanocrystal Diffraction Gratings Prepared by Microcontact Molding. *Acs Nano* **2009**, *3*, 3629-3637.
- (15) Shallcross, R. C.; D'Ambruso, G. D.; Korth, B. D.; Hall, H. K., Jr.; Zheng, Z.; Pyun, J.; Armstrong, N. R. Poly(3,4-ethylenedioxythiophene) - Semiconductor nanoparticle composite thin films tethered to indium tin oxide substrates via electropolymerization. *Journal of the American Chemical Society* **2007**, *129*, 11310-+..

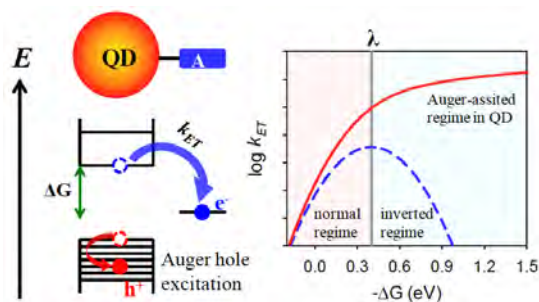
## 1D Exciton Transport and Dissociation in Semiconductor Nanorod Heterostructures

Kaifeng Wu, Haiming Zhu, Ye Yang, Zheyuan Chen, Jinquan Chen, and Tianquan Lian  
 Department of Chemistry  
 Emory University  
 Atlanta, GA 30322

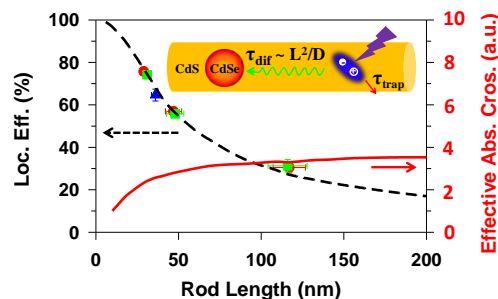
Quantum confined semiconductor nanorod heterostructures, combining two or more material components (dyads, triads, ...), offer unique opportunities to tune their properties by controlling compositions, dimensions and spatial arrangement. Further integration of catalysts forms multifunctional nano-triads capable of light-driven H<sub>2</sub> generation. The efficiency of these nano-triad-based devices depends on many fundamental processes, including light harvesting, carrier relaxation, exciton localization and transport, charge separation and charge recombination. The competition between these processes determines the overall solar energy conversion efficiency. The main objectives of our research program are 1) to provide a fundamental understanding of these charge and exciton processes in quantum dots and quantum rods, 2) to provide guideline for rational design of nano-triads for efficient solar energy conversion.

In the following, we will briefly describe the major progresses of this funding period (since Sept. 2012) and main ongoing and future efforts.

**1) Auger assisted electron transfer.**<sup>7</sup> In excitonic nanomaterials, both the electron-hole interaction and electron-phonon interactions fall between those of the bulk semiconductors and molecules and the appropriate models for describing photoinduced charge transfer remains unclear. We showed that the rates of electron transfer (ET) from CdX (X=S, Se and Te) quantum dots (QDs) quantum dots to molecular acceptors increased monotonically with the driving force (0 ~ 1.3 eV), lacking the inverted regime behavior expected from the Marcus ET theory. We proposed that electron transfer from QDs followed an Auger-assisted ET model, in which, the excess energy of the electron can be transfer to the hole, which overcomes the unfavorable Franck-Condon overlap in the Marcus inverted regime. We believe that the proposed Auger-assisted ET model is generally applicable to many excitonic nanomaterials and are currently testing this model in other quantum dots, nanorods and excitonic nanomaterials.



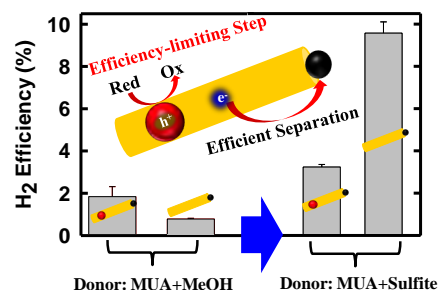
**2) Universal length dependence of exciton transport in nanorod heterostructures and mechanism for long-lived-charge separation.**<sup>2,8,12</sup> Semiconductor quantum rods are quantum confined in the radial direction and bulk like along the long axis, offering the properties of size tunable confinement energy and bulk like long distance charge/exciton transport (for long distance charge separation). We showed that strong electron-hole Coulomb interaction led to strongly bound excitons in room temperature in nanorods with type I (CdSe/CdS), quasi-type II (CdSe/CdS) and



type II (ZnSe/CdS) band alignments. Excitation of the CdS rod led to the formation of two distinct long-lived excitons that were spatially localized in the CdS rod (driven by hole trapping on the rod) and in and near the CdSe (or ZnSe) seed (driven by the large valence band offset between the core and rod), respectively. The branching ratio between these pathways decreased with the rod length and was independent of the band alignment. This universal length dependence could be well described by a model that accounted for the competition of 1-dimension exciton diffusion along the rod and hole trapping to the CdS surface. Our model predicts an optimal length for light harvesting. For example, we showed that using fast electron acceptors such as methylviologen, efficient and long-lived long distance charge separation (with hole localized in the seed and electrons on acceptors adsorbed on the rod) and high (near unity) quantum yields for photoreduction could be achieved for short CdSe/CdS and ZnSe/CdS nanorods. We are examining the rod length/band alignment dependence of photocatalytic performance and possible approaches to enhance the exciton transport properties (e.g. by reducing the hole traps).

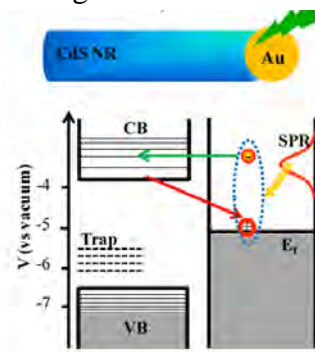
### 3) Exciton dissociation in CdSe/CdS-Pt and efficiency limiting factors in solar hydrogen generation.<sup>6,9,11</sup>

Semiconductor-metal nano-heterostructures (such as CdSe/CdS nanorods with a Pt tip at one end, or CdSe/CdS-Pt) allow rational integration of a light absorber, hole acceptor, and catalyst in an all-inorganic triadic structure with systematic control of relative energetics and spatial arrangement of the functional components. To provide design principles of such triadic nanorods, we examined the photo-catalytic H<sub>2</sub> generation quantum efficiency (QE) and the rates of elementary charge separation and recombination steps of CdSe/CdS-Pt and CdS-Pt nanorods. We showed that the steady state H<sub>2</sub> generation QEs depended sensitively on both the electron donors and the nanorods. We determined that the electron transfer efficiencies to the Pt tip were near unity for both short CdS and CdSe/CdS nanorods. Hole transfer rates to the electron donor positively correlated with the steady state H<sub>2</sub> generation quantum efficiencies, suggesting that hole transfer is a key efficiency-limiting step. We are now examining how the H<sub>2</sub> generation efficiency depends on the rod length and band alignment and possible ways for improving these efficiencies (e.g. by enhancing hole removal rates).



### 4) Plasmon induced hot electron transfer from the Au tip to CdS and CdSe nanorods.<sup>3</sup>

Quantum confined nanorod-Au also provides an excellent model system for studying the interaction of plasmonic and exciton domains. We showed that optical excitation of the plasmon band in the Au tip leads to efficient hot electron injection into the semiconductor nanorod in CdS-Au and CdSe-Au nanorod heterostructures. In the presence of sacrificial electron donors, this plasmon induced hot electron transfer process can be utilized to drive steady state photoreduction of methylviologen. Ongoing studies are examining possible mechanisms of such surprisingly efficient plasmon induced hot electron transfer processes and pathways for further improving the efficiency through controlling the size and shape of the plasmonic and excitonic domains.



## DOE Sponsored Publications 2012-2015

1. Ye Yang, Zheng Liu, and Tianquan, "Bulk Transport and Interfacial Transfer of Photogenerated Charge Carriers in Quantum Dot Solid Electrodes", **Nano Lett.** (2013), 13(8),3678-3683, DOI. 10.1021/nl401573x
2. Kaifeng Wu, William Rodríguez-Córdoba, Zheng Liu, Haiming Zhu, and Tianquan Lian, "Beyond Band Alignment: Hole Localization Driven Formation of Three Spatially Separated Long-lived Exciton States in CdSe/CdS Quasi-type II Dot-in-rod Nanorods", **ACS Nano** (2013) 7(8),7173-7185, DOI: 10.1021/nn402597p
3. Kaifeng Wu, William E. Rodríguez-Córdoba, Ye Yang, and Tianquan Lian, "Plasmon-Induced Hot Electron Transfer from the Au Tip to CdS Rod in CdS-Au Nanoheterostructures", **Nano Lett.** (2013), 13(11), 5255-5263. 10.1021/nl402730m
4. Wu, K.; Song, N.; Liu, Z.; Zhu, H.; Rodriguez-Cordoba, W.; Lian, T. Interfacial Charge Separation and Recombination in InP and Quasi-Type II InP/CdS Core/Shell Quantum Dot-Molecular Acceptor Complexes. **J. Phys. Chem. A** (2013), 117 (32), 7561-7570.
5. Kaifeng Wu, Zheng Liu, Haiming Zhu, and Tianquan Lian, "Exciton Annihilation and Dissociation Dynamics in Group II-V Cd3P2 Quantum Dots" **J. Phys. Chem. A** (2013), 117(29), 6362-6372. DOI: 10.1021/jp402511m
6. Kaifeng Wu, Zheyuan Chen, Hongjin Lv, Haiming Zhu, Craig L Hill, Tianquan Lian, "Hole Removal Rate Limits Photo-driven H<sub>2</sub> Generation Efficiency in CdS-Pt and CdSe/CdS-Pt Semiconductor Nanorod-metal tip Heterostructures", **J. AM. Chem. Soc.** (2014), 136, 7708-7716, DOI: 10.1021/ja5023893.
7. Haiming Zhu, Ye Yang, Kim Hyeon-Deuk, Marco Califano, Nianhui Song, Youwei Wang, Wenqing Zhang, Oleg V Prezhdo, Tianquan Lian, "Auger-Assisted Electron Transfer from Photoexcited Semiconductor Quantum Dots". **Nano Letters** (2014), 14(3), 1263-1269.
8. Haiming Zhu, Zheyuan Chen, Kaifeng Wu, and Tianquan Lian, Wavelength Dependent Efficient Photoreduction of Redox Mediators Using Type II ZnSe/CdS Nanorod Heterostructures", **Chem. Sci.** (2014), 5, 3905-3914.
9. Kaifeng Wu, William Rodríguez-Córdoba and Tinaquan Lian, "Exciton Localization and Dissociation Dynamics in CdS and CdS-Pt Quantum Confined Nanorods: Effect of Non-uniform Rod Diameters", **J. Phys. Chem. B** (2014), 118, 14062-14069 (DOI: 10.1021/jp504703)
10. Jing Gu, Yong Yan, Brian J. Helbig, Zhuangqun Huang, Tianquan Lian, Russell H. Schmehl, "The influence of ligand localized excited states on the photophysics of second row and third row transition metal terpyridyl complexes: Recent examples and a case study", **Coord. Chem. Rev.** (2015), 282, 100-109
11. Kaifeng Wu, Haiming Zhu, Tianquan Lian, "Ultrafast Exciton Dynamics and Light-driven H<sub>2</sub> Evolution in Colloidal Semiconductor Nanorods and Pt-tipped Nanorods", **Acc. Chem. Res.** (2015), 48, 851-859.
12. Kaifeng Wu, Lawrence J Hill, Jinqun Chen, James R McBride, Nicholas G Pavlopoulos, Nathaniel E Richey, Jeffrey Pyun, Tianquan Lian, "Universal Length-Dependence of Rod-to-Seed Exciton Localization Efficiency in Type I and Quasi Type II CdSe@ CdS Nanorods", **ACS Nano** (2015), ASAP, DOI: 10.1021/acsnano.5b01245.

# Controlled Exciton/Plasmon Interaction between Individual Colloidal Quantum Dots and Plasmonic Particles in a Liquid Crystal Matrix

Paul J. Ackerman<sup>1,2</sup>, Haridas Mundoor<sup>1,2</sup>, Ivan I. Smalyukh<sup>2</sup>, and Jao van de Lagemaat<sup>1</sup>

<sup>1</sup>Chemistry and Nanoscience Center

National Renewable Energy Laboratory

Golden, Colorado, 80401

<sup>2</sup>Department of Physics, University of Colorado

Boulder, Colorado, 80309

The possibility of impacting the excited state dynamics as well as the final fate of excitons by coupling excitons and surface plasmons, possibly leading to desirable outcomes such as increased singlet fission rates<sup>1</sup> or multiple exciton generation, has been an avenue of research within our group. In this paper, we demonstrate recent results of impacting the radiative intensity and excited state dynamics of individual quantum dots using plasmonic nanoparticles that are brought near using nanomanipulation.

In previous work, we demonstrated that similar to fluorescence blinking, individual CdSe and PbSe quantum dots exhibit “blinking” in the tunneling current in a conductive AFM microscope likely owing to trapped charge that shifts the quantum dots out of resonance in the tunneling gap.<sup>2</sup> We have also demonstrated that quantum dots on gold substrates are very strongly coupled to surface plasmons on the gold and that it is possible to transfer energy from a surface plasmon induced by tunneling current to a bound nanoparticle that then radiatively decays.<sup>3,4</sup> Before, we could not control the precise interaction between the exciton and the surface plasmon. Therefore, in the present work, we tried to understand how to manipulate individual nanoparticles and to bring them together in a controlled fashion in order to study exciton plasmon interactions in a single controlled system where we can turn on and off the interaction. One avenue that we found was to use liquid crystalline elastic traps that can be used to trap nanoparticles and laser tweezers that can be used to move particles in the medium.<sup>5-7</sup>

In this experiment, we elastically trapped a

colloidal, quantized nanoparticle (a CdSe/CdS dot-in-a-rod) in a controlled potential well formed by a topological defect in a liquid crystal. The topological elastic traps are hyperbolic point singularities in chiral nematic liquid crystals self-assembled into a solitonic configuration. The self-assembly and stability of this configuration arise due to an energetically favorable loop of double twist and result in a baby-Skyrmion mid-plane cross-section.<sup>5</sup> Using laser excitation

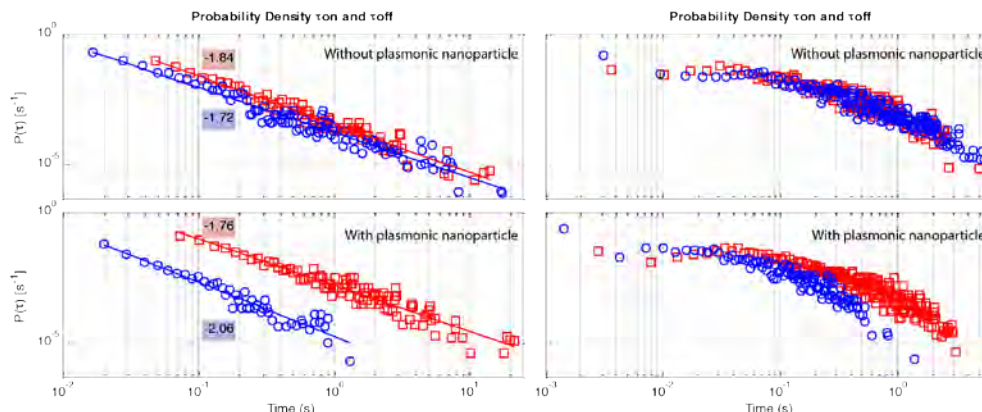


Fig. 1. Distributions of on and off times for a single quantum dot without (top) and with (bottom) plasmonic neighbor estimated using two different analysis methods. Left column:

through a microscope objective, this particle's fluorescence lifetime and intermittency can now be followed. Using laser tweezers, a second particle, such as a plasmonic nanoburst disk-like particle as used here was dropped into the same potential well and the change in intermittency as well as the change in fluorescence lifetime in the exact same particle was monitored. This is a different approach than has typically been followed where the optical behavior of quantum dots are compared with other dots with nominally the same properties in a plasmonic field or where the plasmon is delivered by the tip of a STM microscope.<sup>4</sup>

Fig. 1 shows the blinking statistics of an individual quantum rod in a topological trap with or without the plasmonic nanoburst present. Two methods of analysis of the blinking data are shown. To the left is the data analyzed using simple threshold analysis showing the typical power-law behavior of such data and that in the plasmonic field, the particle is far more often in an “on”-state than before. The same is shown using the more rigorous change-point analysis method. The “on”-state is more prevalent. A good indication of the reason behind this change is shown in Fig. 2. We compare the fluorescence lifetime of several different particles before and after adding the plasmonic nanoburst particle. It is clear that an order of magnitude increase in the fluorescence rate is observed, consistent with a Purcell effect. This also explains the increased persistence of the bright state of the particle. Because of the faster fluorescence decay, an excited particle is much less likely to lead to a trapped charge and therefore a dark quantum dot.

As shown above, the nanomanipulation of semiconductor and plasmonic nanoparticles using liquid crystalline traps is an interesting method to directly control and study the interaction of the exciton on the quantum dots with a plasmonic field. Experiments are ongoing with other shapes of particles and by controlling the energy of both exciton and surface plasmon.

## References

- (1) Johnson, J. C.; Reilly, T. H.; Kanarr, A. C.; van de Lagemaat, J. *J Phys Chem C* **2009**, *113*, 6871–6877.
- (2) Maturova, K.; Nanayakkara, S.; Luther, J. M.; van de Lagemaat, J. *Nanolett.* **2013**, *13*, 2338–2345.
- (3) Romero, M. J.; van de Lagemaat, J. *Phys. Rev. B* **2009**, *80*, 115432.
- (4) Romero, M. J.; van de Lagemaat, J.; Mora-Sero, I.; Rumbles, G.; Al-Jassim, M. M. *Nanolett.* **2006**, *6*, 2833–2837.
- (5) Ackerman, P. J.; van de Lagemaat, J.; Smalyukh, I. I. *Nature Communications* **2015**, *6*, 6012–.
- (6) Evans, J. S.; Ackerman, P. J.; Broer, D. J.; van de Lagemaat, J.; Smalyukh, I. I. *Phys. Rev. E* **2013**, *87*, 032503.
- (7) Senyuk, B.; Evans, J. S.; Ackerman, P. J.; Lee, T.; Manna, P.; Vigderman, L.; Zubarev, E. R.; van de Lagemaat, J.; Smalyukh, I. I. *Nanolett.* **2012**, *12*, 955–963.

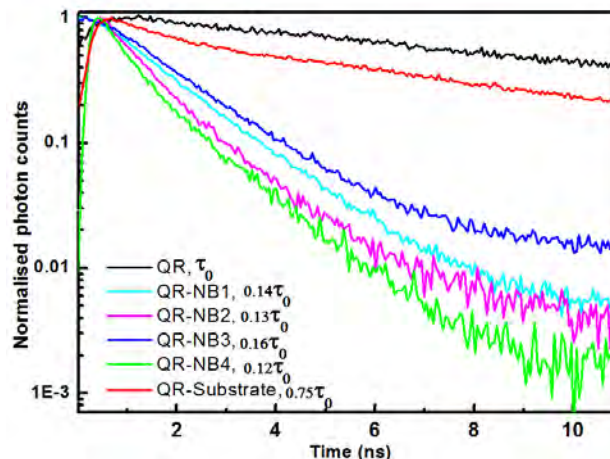


Fig 3. Fluorescence lifetime trajectories of individual quantum rods in the liquid crystal medium (black), on a glass substrate (red) and in the liquid crystalline medium close to a nanoburst plasmonic particle.

## DOE Sponsored Publications 2012-2015

1. Zhang, T.; Yang, M.; Benson, E. E.; Li, Z.; van de Lagemaat, J.; Luther, J. M.; Yan, Y.; Zhu, K.; Zhao, Y. A Facile Solvo-Thermal Growth of Single Crystal Mixed Halide Perovskite  $\text{CH}_3\text{NH}_3\text{Pb}(\text{Br}_{1-x}\text{Cl}_x)_3$ , *Chem. Commun.* **2015**, —.
2. LaCount, M. D.; Weingarten, D.; Hu, N.; Shaheen, S. E.; van de Lagemaat, J.; Rumbles, G.; Walba, D. M.; Lusk, M. T. Energy Pooling Upconversion in Organic Molecular Systems. *J. Phys. Chem. A* **2015**, *150401100642004*.
3. Zhao, Y.; Anderson, N. C.; Zhu, K.; Aguiar, J. A.; Seabold, J. A.; van de Lagemaat, J.; Branz, H. M.; Neale, N. R.; Oh, J. Oxidatively Stable Nanoporous Silicon Photocathodes with Enhanced Onset Voltage for Photoelectrochemical Proton Reduction. *Nanolett.* **2015**, *150311092822001*.
4. Ackerman, P. J.; van de Lagemaat, J.; Smalyukh, I. I. Self-Assembly and Electrostriction of Arrays and Chains of Hopfion Particles in Chiral Liquid Crystals. *Nat. Comm.* **2015**, *6*, 6012.
5. Mundoor, H.; Lee, T.; Gann, D. G.; Ackerman, P. J.; Senyuk, B.; van de Lagemaat, J.; Smalyukh, I. I. Optically and Elastically Assembled Plasmonic Nanoantennae for Spatially Resolved Characterization of Chemical Composition in Soft Matter Systems Using Surface Enhanced Spontaneous and Stimulated Raman Scattering. *J. Appl. Phys.* **2014**, *116*, 063511.
6. Ackerman, P. J.; Trivedi, R. P.; Senyuk, B.; van de Lagemaat, J.; Smalyukh, I. I. Two-Dimensional Skyrmions and Other Solitonic Structures in Confinement-Frustrated Chiral Nematics. *Phys. Rev. E* **2014**, *90*, 012505.
7. Miller, E. M.; Zhao, Y.; Mercado, C. C.; Saha, S. K.; Luther, J. M.; Zhu, K.; Stevanovic, V.; Perkins, C. L.; van de Lagemaat, J. Substrate-Controlled Band Positions in  $\text{CH}_3\text{NH}_3\text{PbI}_3$  Perovskite Films. *Phys. Chem. Chem. Phys.* **2014**, *16*, 22122–22130.
8. Maturova, K.; Nanayakkara, S.; Luther, J. M.; van de Lagemaat, J. Fast Current Blinking in Individual PbS and CdSe Quantum Dots. *Nanolett.* **2013**, *13*, 2338–2345.
9. Evans, J. S.; Ackerman, P. J.; Broer, D. J.; van de Lagemaat, J.; Smalyukh, I. I. Optical Generation, Templating, and Polymerization of Three-Dimensional Arrays of Liquid-Crystal Defects Decorated by Plasmonic Nanoparticles. *Phys. Rev. E* **2013**, *87*, 032503.
10. Nanayakkara, S. U.; Cohen, G.; Jiang, C.-S.; Romero, M. J.; Maturova, K.; Al-Jassim, M.; van de Lagemaat, J.; Rosenwaks, Y.; Luther, J. M. Built-in Potential and Charge Distribution Within Single Heterostructured Nanorods Measured by Scanning Kelvin Probe Microscopy. *Nanolett.* **2013**, *13*, 1278–1284.
11. van de Lagemaat, J.; Romero, M. J. CHAPTER 9. Light at the Tip: Hybrid Scanning Tunneling/Optical Spectroscopy Microscopy. *RSC Energy and Environment Series; Royal Society of Chemistry: Cambridge*, 2013; pp. 261–280.
12. Erslev, P. T.; Chen, H.-Y.; Gao, J.; Beard, M. C.; Frank, A. J.; van de Lagemaat, J.; Johnson, J. C.; Luther, J. M. Sharp Exponential Band Tails in Highly Disordered Lead Sulfide Quantum Dot Arrays. *Phys. Rev. B* **2012**, *15*, 155313.
13. Gregg, B. A.; van de Lagemaat, J. Solar Cells: Folding Photons. *Nat. Phot.* **2012**, *6*, 278–280.
14. Liang, Z.; Nardes, A. M.; van de Lagemaat, J.; Gregg, B. A. Activation Energy Spectra: Insights Into Transport Limitations of Organic Semiconductors and Photovoltaic Cells. *Adv. Funct. Mater.* **2012**, *22*, 1087–1091.
15. Senyuk, B.; Evans, J. S.; Ackerman, P. J.; Lee, T.; Manna, P.; Vigderman, L.; Zubarev, E. R.; van de Lagemaat, J.; Smalyukh, I. I. Shape-Dependent Oriented Trapping and Scaffolding of Plasmonic Nanoparticles by Topological Defects for Self-Assembly of Colloidal Dimers in Liquid Crystals. *Nanolett.* **2012**, *12*, 955–963.
16. van de Lagemaat, J. Plasmonic Structures for Solar Energy Harvesting. In *Encyclopedia of nanotechnology*; Bhushan, B., Ed.; *Encyclopedia of Nanotechnology: Dordrecht*, 2012; pp. 2139–2146.



*Session VI*

*Photophysics on the Nanoscale*

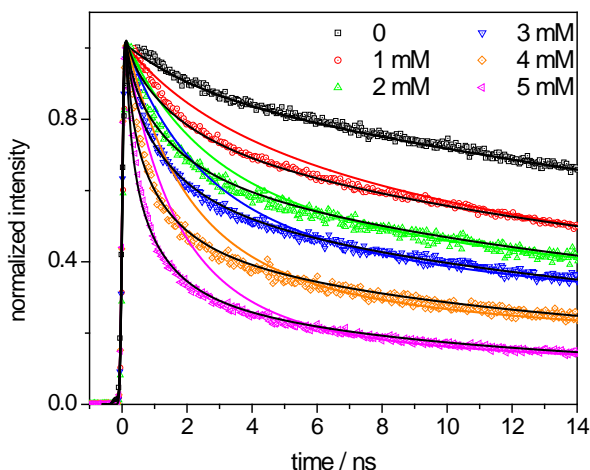


## The Role of Lattice Strain in the Photophysics of Core/Shell Quantum Dots

Ke Gong, Youhong Zeng, Zhong-Jie Jiang, Gary Beane, and David F. Kelley  
Chemistry and Chemical Biology  
University of California, Merced,  
Merced, California 95343

The role of lattice strain in controlling the photophysics and surface chemistry of II-VI core/shell quantum dots has been studied. Lattice mismatch in core/shell nanoparticles occurs when the core and shell materials have different lattice parameters. When there is a significant lattice mismatch, a coherent core-shell interface results in substantial lattice strain energy, which can affect the shell morphology. The initial system studied was ZnTe/CdSe core/shell nanoparticles, for which the pure (not alloyed) zincblende crystals have close to identical lattice parameters. However, annealing causes metal ion interdiffusion resulting in a (Cd,Zn)Te-(Zn,Cd)Se alloyed interface, which causes lattice strain. Hole tunneling from the particle core to an adsorbed hole acceptor (phenothiazine, PTZ) causes quenching of the photoluminescence (PL). The quenching rate of an extremely sensitive measure of the shell thickness and is used to determine the distribution of shell thicknesses. The hole transfer kinetics can be modeled for any quencher concentration, as shown in figure 1, below. The experimental results show that CdSe shell deposition at 215 °C on spherical ZnTe core particles is analogous to Stranski-Krastanov (S-K) growth of 2-dimensional epitaxial films. We find that the first approximately three layers of CdSe are deposited uniformly and that subsequent layers produce a rough shell surface.

Figure 1. PL kinetics of ZnTe/CdSe QDs with different PTZ concentrations. These QDs have a 2.6 nm ZnTe core and a 1.2 nm CdSe shell deposited at 215 °C. The PTZ concentrations are given in the figure. The solid (slower decaying) curves are the corresponding fitting of the experimental results assuming a uniform shell and the black curves are calculated assuming S-K growth of islands on three smooth shell monolayers.



The same method is applied to CdSe/CdSe core/shell QDs, which have a 3.9% lattice mismatch. We find that whether the shell is smooth or rough depends on the CdSe core size and the shell thickness; smaller cores can maintain smooth shells to relatively large shell thicknesses. This can be quantitatively understood in terms of a model based on elastic continuum calculations, which indicate that the lattice strain energy depends on both core size and shell thickness. The model assumes thermodynamic equilibrium, i.e., that the shell morphology corresponds to a minimum total (lattice strain plus surface) energy. Comparison with the experimental results indicates that CdSe/CdS nanoparticles undergo an abrupt transition from smooth to rough shells when the total lattice strain energy exceeds about 27eV or the strain energy density exceeds 0.59

$\text{eV}/\text{nm}^2$ . We also find that the predictions of this model are not followed for CdSe/CdS nanoparticles when the shell is deposited at very low temperature and therefore equilibrium is not established. However, if the strain energy density exceeds  $0.85 \text{ eV}/\text{nm}^2$  the shell morphology relaxes, defects are formed and the PL quantum yield drops dramatically.

We have also found that bare core CdSe particles are subject to reversible two-photon photochemistry. The two-photon nature of the chemistry is shown by varying the excitation power density while keeping the total photon flux constant, as shown in figure 2. The agreement between the calculated two-photon absorption and reaction probabilities is very good.

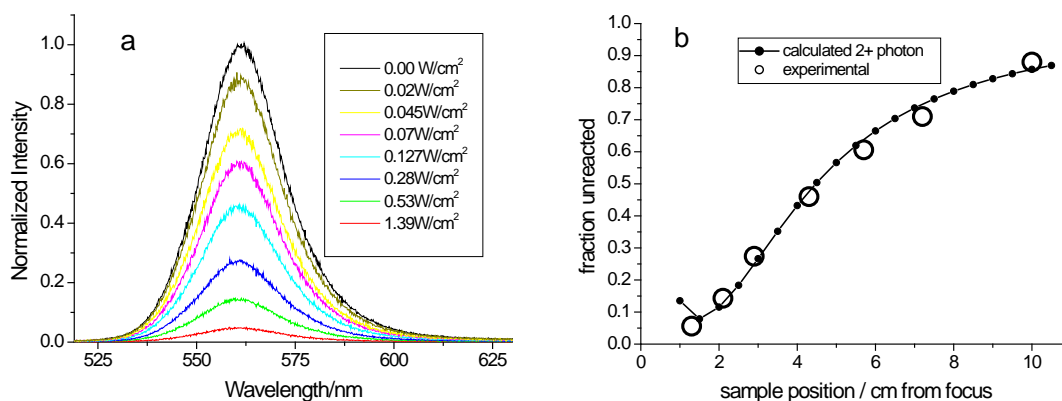
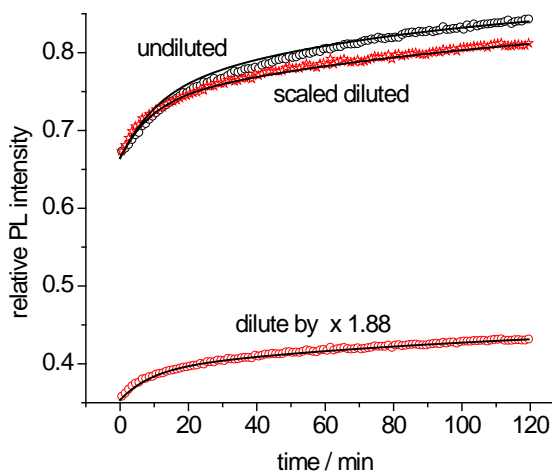


**Figure 2.** a) Emission spectra of CdSe after irradiation with different power density. b) The open circles are experimental results obtained from a), and the black dotted line is the calculated fraction of unreacted particles plotted versus the diameter of the beam.

The photodarkening reaction has a much lower quantum yield in nonpolar (hydrocarbon), compared to polar (chloroform) solvents, implying an ionic mechanism. It is reversible only if excess ligands are present the solution, and the reverse reaction takes place on the tens of minutes timescale, as shown in figure 3.

**Figure 3.** Photoluminescence recovery kinetics following two-photon irradiation of a CdSe QD sample in chloroform (black points). Also shown are the kinetics when the sample is diluted following irradiation, and the diluted kinetics scaled by the dilution factor (red points) and calculated curves from an assumed ionic mechanism (black lines).



The overall mechanism is elucidated using a classical kinetics approach. The ionization energetics and role of charged ligand dissociation and recombination are discussed.

## DOE Sponsored Publications 2012-2015

1. Ke Gong and David F. Kelley, "Surface Charging and Trion Dynamics in CdSe-based Core/Shell Quantum Dots", *J. Phys. Chem. C*, submitted
2. Ke Gong and David F. Kelley, "Lattice Strain Limit for Uniform Shell Deposition in Zincblende CdSe/CdS Quantum Dots", *J. Phys. Chem. Lett*, submitted.
3. Ke Gong and David F. Kelley, "A predictive model of shell morphology in CdSe/CdS core/shell quantum dots", *J. Chem. Phys.*, **141**, 194704 (2014).
4. Ke Gong, Youhong Zeng and David F. Kelley, "Extinction coefficients, oscillator strengths and radiative lifetimes of CdSe, CdTe and CdTe/CdSe nanocrystals", *J. Phys. Chem. C*, **117**, 20268 (2013).
5. Zhong-Jie Jiang and David F. Kelley, "Stranski–Krastanov Shell Growth in ZnTe/CdSe Core/Shell Nanocrystals", *J. Phys. Chem. C*, **117**, 6826 (2013).
6. Zhong-Jie Jiang and David F. Kelley, "Effects of Inhomogeneous Shell Thickness in the Charge Transfer Dynamics of ZnTe/CdSe Nanocrystals" *J. Phys. Chem. C*, **116**, 12958 (2012).
7. Xichen Cai, Hoda Mirafzal, Kennedy Nguyen, Valerie Leppert and David F. Kelley, "The spectroscopy of CdTe/CdSe type-II nanostructures: morphology, lattice mismatch and band-bowing effects." *J. Phys. Chem. C*, **116**, 8118 (2012).

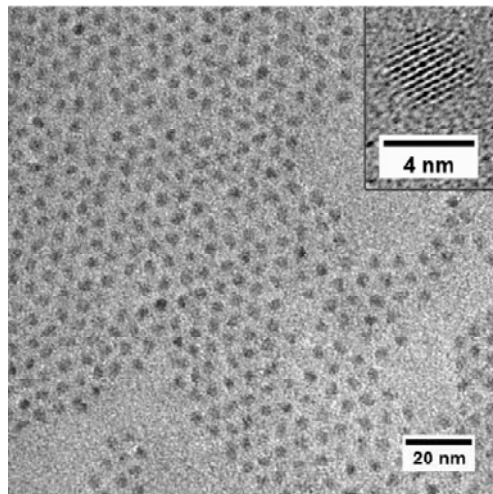
## Two-Dimensional Spectroscopy of Low Bandgap Quantum Dots

Samuel D. Park, Dmitry Baranov, Jisu Ryu, and David M. Jonas  
Department of Chemistry and Biochemistry  
University of Colorado  
Boulder, CO 80309-0215

Some time ago, Nozik proposed semiconductor quantum dots as materials that might enable higher third generation photovoltaic efficiency through either carrier multiplication or hot carrier solar cells. Multiple exciton generation has been reported in several quantum dot materials, and an external quantum efficiency exceeding unity has been reported in the ultraviolet for PbSe quantum dot solar cells. For improved efficiency, such solar cells require bandgaps in the short-wave infrared region (1-2 micron wavelength), strong interactions between carriers (for fast multiple exciton generation), weak exciton-phonon interactions (for slow carrier cooling), and a low energetic threshold for multiple exciton generation. The need to understand these interactions motivates study of low bandgap quantum dot dynamics.

We have demonstrated two-dimensional femtosecond spectroscopy in the short-wave infrared, where third generation photovoltaics must have their bandgap. The absence of broadband femtosecond beamsplitter coatings in this spectral region was overcome by designing an actively stabilized, low-dispersion, multiple-octave, Brewster's angle Mach-Zehnder interferometer. We are using it to study PbS and PbSe quantum dots with bandgaps of around 1 eV with ~15 fs time resolution. Two-dimensional Fourier transform spectroscopy spreads signals from quantum dots with different sizes (hence different bandgaps) along the diagonal, allowing a look at dynamics obscured by the size distribution in the one-dimensional techniques previously used to study these dots.

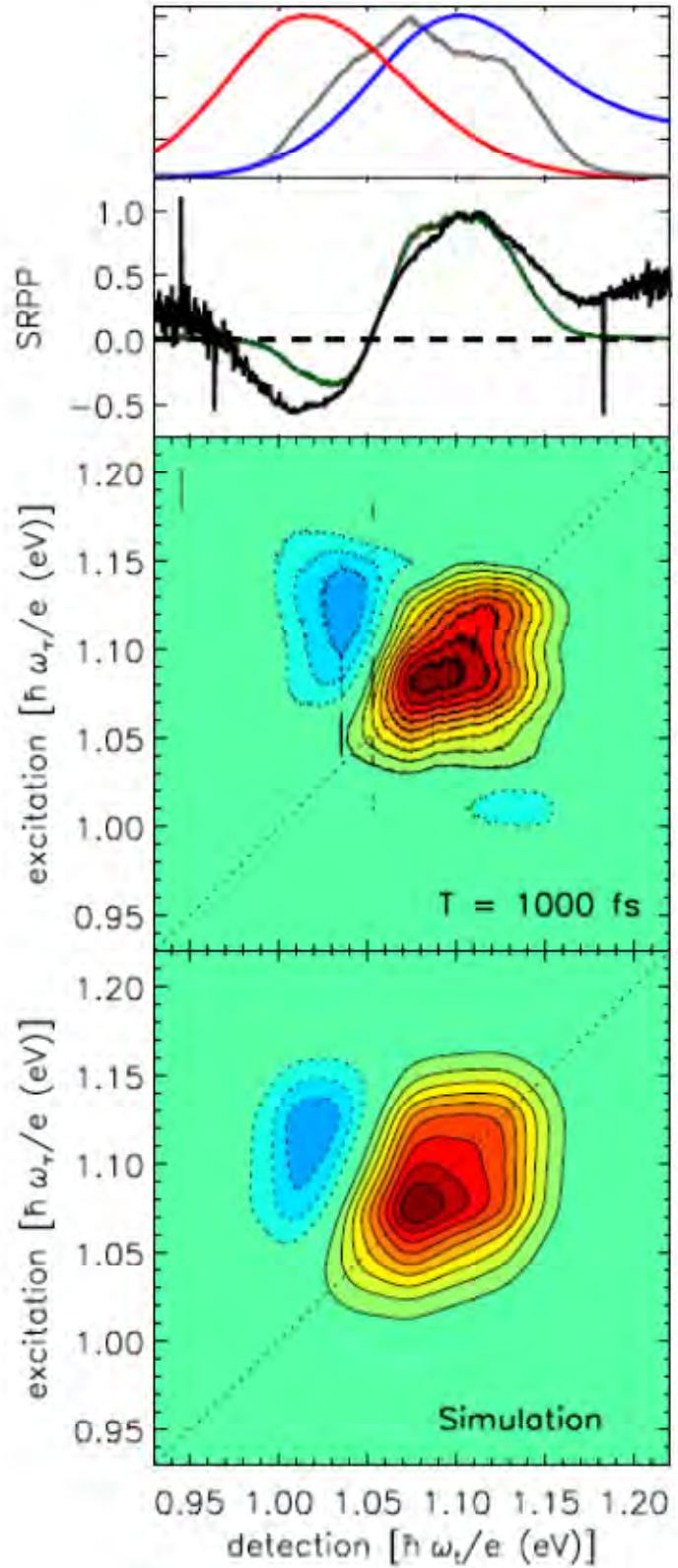
Environmental effects (exposure to oxygen or moisture) and photodegradation have been suspected as a cause of sample to sample variation in time-resolved studies of quantum dots. We have modified the lead chloride based PbS synthesis to eliminate nanocrystal exposure to protic, oxygen-containing, and potentially "wet" solvents during purification, giving photoluminescence quantum yields of ~35% and 1S-1S exciton widths of ~100 meV. High-resolution TEM reveals faceted nanocrystals. For the PbSe nanocrystals shown at right, the size distribution can be characterized as ellipsoidal, with minor and major diameters of  $3.1 \pm 0.4$  nm and  $4.2 \pm 0.5$  nm, respectively (less than a unit cell variation). ICP-MS indicates the nanocrystals used for 2D spectroscopy are lead-rich (~1.7:1). NMR indicates ~4-5 oleate ligands per nm<sup>2</sup>.



The quantum dot samples are housed in a UHV compatible sealed chamber that excludes the atmosphere and eliminates long-term blue-shifts in quantum dot absorption spectra. The sample cell spins so that each pulse sequence probes a fresh sample; this new spinning cell does not measurably disturb the  $\pm 0.6$  nm interferometer lock stability. When the cell is not spun, 2D

spectra develop a low amplitude absorption tail to the red of the bandgap that resembles the tail reported for quantum dots with surface traps.

The top panel of the figure at right shows the PbSe quantum dot absorption spectrum (blue) and photoluminescence spectrum (red) along with the laser pulse spectrum (gray) used for 2D spectroscopy. The second panel shows the spectrally resolved pump-probe signal at 1 ps pump-probe delay. The pump-induced change in transmitted probe photon number (green) is divided by the laser pulse spectrum to give the change in transmittance (black). The change in transmittance shows that the 1S-1S exciton bleach is fully captured, as is the excited state absorption to the bi-exciton state (negative feature below 1.5 eV). The third panel shows the measured 2D spectrum at 1 ps delay between excitation (vertical axis) and detection (horizontal axis), which projects onto the detection frequency axis to give the spectrally resolved pump-probe signal. The diagonal elongation of this 2D spectrum arises from the quantum dot size distribution, while the anti-diagonal broadening arises from fine structure and coupling to phonons. The red-shift of the negative feature (blue colors, dashed contours) reflects the bi-exciton binding energy. The simulation in the lowest panel assumes complete relaxation, using only size distribution broadening and the bi-exciton shift as free parameters. 2D spectra at smaller waiting times reveal dynamics that are expected to involve fine structure relaxation and coupling to optical phonons. We are working to understand and simulate these dynamics, which are unexpectedly fast.



### DOE Sponsored Publications 2012-2015

1. “Absolute femtosecond measurements of Auger recombination dynamics in lead sulfide quantum dots” B. Cho, W. K. Peters, V. Tiwari, A. P. Spencer, D. Baranov, R. J. Hill and D. M. Jonas, *EPJ Web of Conferences* **41**, 04035 (2013).
2. “Absolute Measurement of Femtosecond Pump-Probe Signal Strength”, Byungmoon Cho, Vivek Tiwari, Robert J. Hill, William K. Peters, Trevor L. Courtney, Austin P. Spencer, and David M. Jonas, *J. Phys. Chem. A* **117**, 6332-6345 (2013).
3. “Simultaneous All – Optical Determination of Molecular Concentration and Extinction Coefficient” Byungmoon Cho, Vivek Tiwari, and David M. Jonas, *Anal. Chem.* **85**, 5514-5521 (2013).

## How Light is Absorbed in a Solid State Material

Hrvoje Petek

Department of Physics and Astronomy  
University of Pittsburgh  
Pittsburgh, PA and 15215

We study the dynamical properties of solid surfaces on the femtosecond temporal and nanometer spatial scales by time-resolved photoemission and scanning tunneling microscopy methods. The chemical and physical properties at molecule-solid interfaces are fundamentally important to solar energy conversion processes.

In the field-theoretic description of light-matter interaction, the absorption of a photon to create an electron-hole pair is an instantaneous process. At the instant of interaction, a photon induces a nonadiabatic transition in a metal to create an electron-hole pair bound by the bare Coulomb interaction. This primary transition causes fast deviations from the initial charge density equilibrium of the system, which in turn couples to the dynamical polarization or screening response of the surrounding electronic density within a few lattice sites from the disturbance. The excitation evolves from this *transient excitonic* state, where a bound state of the electron-hole pair exists, to the fully screened state of the system, where a metal does not support a bound state, on the time scale of formation of the screening charge density through the virtual single-particle and collective plasma excitations. In the case of a metal surface, the self-consistent linear response to creation of an external charge has the classical analog of perfect screening in the image charge. The image charge through the associated image potential supports a Rydberg series of image potential states. The transient exciton created by the interaction of a surface state electron with a photon can recombine to regenerate the coherent field (reflection), scatter into energy conserving states (Drude absorption), or evolve into energy conserving asymptotic states such as the image potential states. In a nonlinear multiphoton photoemission experiment, additional absorption of photon can excite the electron above the vacuum level, and the resulting photoemission spectrum can capture the dynamics of the transient exciton evolving into the fully screened image potential state.

In order to study the coherent interaction of light with metals, we developed a coherent three-dimensional multi-photon photoemission (3D-*mPP*) spectroscopy technique. In the case of Ag(111), we employ 3D-*mPP* to resolve for the first time the transient excitonic response of a metal. With single color, broadly tunable <15 fs pulse excitation in the visible spectrum, we excite *mPP* from Ag(111) surfaces, and image the resulting energy vs. parallel momentum distributions. The *mPP* spectra exhibit features, which cannot be attributed to single particle excitations among the well-known surface and bulk bands of Ag. In the case of 3PP from Ag(111), a nondispersive feature, which dominates the spectra, appears when the laser is tuned near the two-photon resonant excitation from the Shockley surface state (SS) to the image potential state. The nondispersive character of the spectrum and the momentum range corresponding to the SS attribute this feature to a localized state that is created by exciting an electron from the SS, namely the transient exciton.

In order to obtain further information on this newly discovered transient exciton, we perform time-resolved *mPP* measurements with interferometric scanning of identical pump-probe pulses. Interferometric time-resolved photoemission movies with different excitation

wavelengths identify the coherent pathways and timescales for 3PP via the transient exciton resonance of Ag(111) surface. Interferograms, such as in Fig. 1 for the normal emission from Ag(111) surface, contain information on the coherent interactions leading to the 3PP process. Fourier transforming the interferograms obtains 2D photoelectron spectra, which correlate the components of the coherent polarization excited in the sample with the final state energies in the 3PP spectra. The 2D spectra manifest the evolution of the transient exciton into the fully screened image potential state on the time scale of dephasing of the surface plasmon of Ag. Remarkably, at higher excitation fluences it is possible to drive high-order processes up to 9PP via the excitation of the transient exciton in Ag. In parallel with these experimental studies, we are developing the many-body theory of the ultrafast excitonic response of metals.

In the case of SS of Cu(111) surface, the transient exciton is not observed, which is consistent with much faster screening in Cu than in Ag. Rather, we observe polaritonic effects when the excitation photon energy approaches the *d*- to *sp*-band excitation threshold. For the excitation near the interband transition onset of Cu at 2 eV, the SS band has replicas in the 3PP spectra that depend on the excitation wavelength. We attribute these replicas to polaritonic local fields associated with the slowly dephasing *d*- to *sp*-band transitions. Because electrons and holes at the Fermi level and at the top of the *d*-bands dephase slowly due to electron-electron scattering, the interband polarization builds up on the time scale of the excitation and scattering of the coupled states. Unlike the excitation field, this local field oscillates on the atomic scale, and thus is enhanced with respect to the external field. In addition to the external field, this local field can also act on the electronic system to induce the 3PP process. Thus the annihilation of multiple quanta of the interband polarization excites SS electrons at frequencies of enhancement of the interband polarization.

The transient exciton at Ag(111) surface can be observed with 15 fs laser pulses due to the unusual screening properties at Ag surfaces. We plan to explore the transient exciton response on adsorbate modified Ag surfaces and on thin metal films on semiconductor surfaces. The transient excitons and polaritonic responses of Ag and Cu surfaces are representative of the ultrafast optical responses of solid-state materials. Thus, similar coherent responses are likely to have a role in the conversion of solar to electrical and chemical energy in organic and inorganic semiconducting materials.

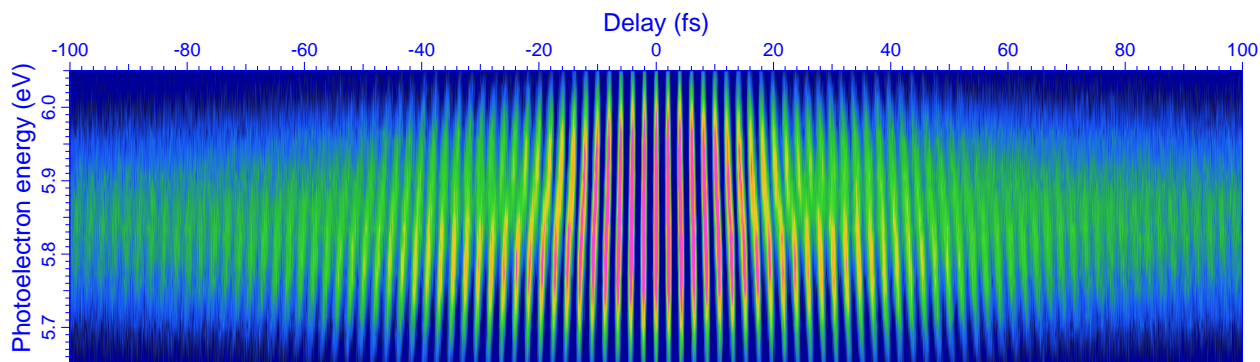


**Fig. 1.** A cross-section through a 3D movie of photoelectron counts vs. energy, momentum, and pump-probe delay time for normal emission from Ag(111) surface excited with 2.04 eV light. Fourier transform of such interferograms provides 2D spectra that correlate the induced linear and nonlinear polarization excited in the sample with specific features in the *m*PP spectra.

## DOE Sponsored Publications 2012-2015

1. U. Bovensiepen, H. Petek, M. Wolf, Eds., *Dynamics at Solid State Surfaces and Interfaces, Vol. 2: Fundamentals*, vol. 2:Fundamentals (Wiley-VCH Verlag GmbH & Co., Weinheim, ed. 1, 2012), vol. 2:Fundamentals, 1.
2. C. Lin, M. Feng, J. Zhao, P. Cabrera-Sanfeliix, A. Arnau, D. Sánchez-Portal, H. Petek, Theory of orthogonal interactions of CO molecules on a one-dimensional substrate. *Phys. Rev. B* **85**, 125426 (2012).
3. M. Feng, C. Lin, J. Zhao, H. Petek, Orthogonal Intermolecular Interactions of CO Molecules on a One-Dimensional Substrate. *Annu. Rev. Phys. Chem.* **63**, 201 (2012).
4. H. Petek, Photoexcitation of adsorbates on metal surfaces: One-step or three-step. *J. Chem. Phys.* **137**, 091704 (2012).
5. D. B. Dougherty, M. Feng, H. Petek, J. T. Yates, Jr., J. Zhao, Band Formation in a Molecular Quantum Well via 2D Superatom Orbital Interactions. *Phys. Rev. Lett.* **109**, 266802 (2012).
6. A. Winkelmann, C. Tusche, A. A. Ünal, C.-T. Chiang, A. Kubo, L. Wang, H. Petek, in *Solar Energy Conversion: Dynamics of Interfacial Electron and Excitation Transfer*, P. Piotroviak, Ed. (The Royal Society of Chemistry, Cambridge, 2013), pp. 225-260.
7. M. Feng, Y. Shi, C. Lin, J. Zhao, F. Liu, S. Yang, H. Petek, Energy stabilization of the s-symmetry superatom molecular orbital by endohedral doping of C<sub>82</sub> fullerene with a lanthanum atom. *Phys. Rev. B* **88**, 075417 (2013).
8. H. Petek, Single-Molecule Femtochemistry: Molecular Imaging at the Space-Time Limit. *ACS Nano* **8**, 5 (2014/01/28, 2014).
9. X. Cui, C. Wang, A. Argondizzo, S. Garrett-Roe, B. Gumhalter, H. Petek, Transient excitons at metal surfaces. *Nat Phys* **10**, 505 (2014).
10. J. Zhao, M. Feng, D. B. Dougherty, H. Sun, H. Petek, Molecular Electronic Level Alignment at Weakly Coupled Organic Film/Metal Interfaces. *ACS Nano* **8**, 10988 (2014/10/28, 2014).
11. M. Feng, H. Sun, J. Zhao, H. Petek, Self-Catalyzed Carbon Dioxide Adsorption by Metal–Organic Chains on Gold Surfaces. *ACS Nano* **8**, 8644 (2014/08/26, 2014).



## *Session VII*

### *Catalysis of Water Splitting*



## Water Splitting by Thin Film Metal-Oxo Catalysts

D. Kwabena Bediako, Michael X. Huynh, and Daniel G. Nocera

Harvard University Chemistry and Chemical Biology  
12 Oxford Street, Harvard University, Cambridge, Massachusetts 02138-2902

We have been interested in the development of water splitting catalysts that self-assemble from aqueous solution. Owing to the self-assembly process, oxygen-evolving catalysts of the elements of Mn, Co and Ni have been developed that are self-healing. Rate laws have been derived for each of the metal catalysts nucleation kinetics and OER. For the latter, differential electrochemical mass spectrometry, together with isotopic labeling, has been used to identify key PCET reaction intermediates. The criterion for self-healing is that these nucleation kinetics be supported at potentials at which oxygen evolution reaction (OER) catalysis occurs. The primary determinant for this interplay is the disparate pH dependences of nucleation versus OER. Figure 1 shows pH dependence of the nucleation and OER for the Co catalyst. Owing to the steeper pH dependence of catalysts self-assembly (inverse 3<sup>rd</sup> order) as compared to that of OER (inverse 1<sup>st</sup> order), a large pH-voltage window is available for self-healing. In the case of the Mn catalyst, the nucleation kinetics exhibit an inverse 4<sup>th</sup> order dependence on [H<sup>+</sup>] concentration (arising from a Mn<sup>2+</sup>/Mn<sup>4+</sup> comproportionation reaction), allowing us to perform OER under stable conditions in concentrated acid pH > -1).

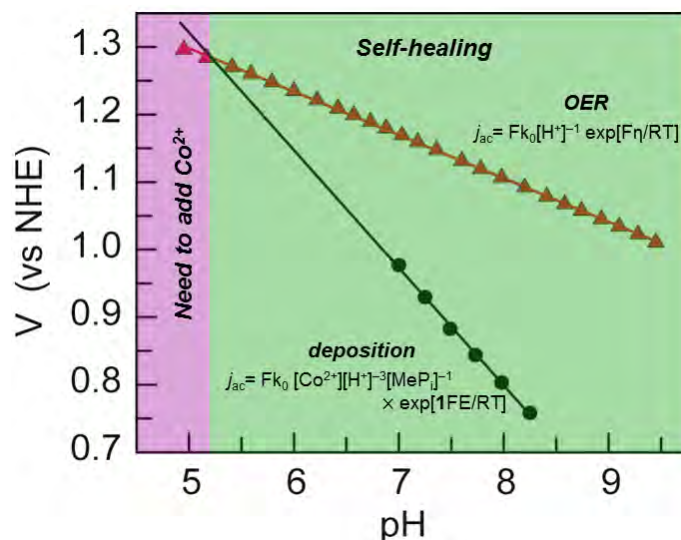


**Figure 1.** Rate laws for the deposition and OER of self-assembling Co OER catalysts from aqueous solution. The green shaded area defines the Pourbaix region of self-healing.

In a second area of study, we have examined the effect of co-dopants in the catalyst films. An especially popular co-dopant has been Fe<sup>3+</sup>. There have been many explanations for the role of enhancement of OER activity by Fe<sup>3+</sup>, ranging from special ferryl active sites to claims that Fe<sup>3+</sup> oxo-hydroxy sheets form with Co and Ni catalysts and that the sheets are extraordinary catalytic

materials. We show that Fe is not unique for enhanced catalytic activity and that a host of other metal and non0-metal ions can enhance activity (including non-redox active centers). Instead, we propose that the co-dopant increases that Co(or Ni) valency, allowing the M<sup>4+</sup> states of these metals to be achieved at lower potentials (and hence increased activity). These results offer new insight into the activity enhancement observed upon incidental or intentional Fe doping in metal oxido films.

### DOE Sponsored Publications 2013-present

“Mechanistic Studies of the Oxygen Evolution Reaction Mediated by a Nickel–Borate Thin Film Electrocatalyst”; D. Kwabena Bediako, Yogesh Surendranath and Daniel G. Nocera, *J. Am. Chem. Soc.* **2013**, *135*, 3662–74.

“Intermediate-Range Structure of Self-Assembled Cobalt-based Oxygen Evolving Catalysts”; Christopher L. Farrow, D. Kwabena Bediako, Yogesh Surendranath, Daniel G. Nocera and Simon J. L. Billinge, *J. Am. Chem. Soc.* **2013**, *135*, 6403–6.

“Proton-Electron Transport and Transfer in Electrocatalytic Films. Application to a Cobalt-Based O<sub>2</sub>-Evolution Catalyst”; D. Kwabena Bediako, Cyrille Costentin, Evan C. Jones, Daniel G. Nocera and Jean-Michel Savéant, *J. Am. Chem. Soc.* **2013**, *135*, 10492–502.

“Nucleation and Growth Mechanisms of an Electrodeposited Manganese Oxide Catalyst at Near-Neutral pH”; Michael Huynh, D. Kwabena Bediako, Yi Liu and Daniel G. Nocera, *J. Phys. Chem. C* **2014**, *118*, 17142–52.

“A Functionally Stable Manganese Oxide Oxygen Evolution Catalyst in Acid”; Michael Huynh, D. Kwabena Bediako and Daniel G. Nocera, *J. Am. Chem. Soc.* **2014**, *136*, 6002–10.

“Spectroscopic Studies of Nanoparticulate Thin Films of a Cobalt-Based Oxygen Evolution Catalyst”; Yi Liu and Daniel G. Nocera, *J. Phys. Chem. C* **2014**, *118*, 17060–6.

“Water Oxidation Catalysis by Co(II) Impurities in Co(III)<sub>4</sub>O<sub>4</sub> Cubanes”; Andrew M. Ullman, Yi Liu, D. Kwabena Bediako, Michael Huynh, Hongsen Wang, Bryce L. Anderson, David C. Powers, John J. Breen, Héctor D. Abruña and Daniel G. Nocera, *J. Am. Chem. Soc.* **2014**, *136*, 17681–8.

## Photocatalysts for H<sub>2</sub> Evolution: Combination of the Light Absorbing Unit and Catalytic Center in a Single Molecule

Travis White, Suzanne Witt, Nicholas Leed, Zhanyong, Li, Kim R. Dunbar, and Claudia Turro

Department of Chemistry and Biochemistry, The Ohio State University, Columbus OH, 43210  
 Department of Chemistry, Texas A&M University, College Station, TX 77843

New bimetallic complexes for the photocatalytic and electrocatalytic production of H<sub>2</sub> gas from acidic aqueous solutions will be presented. The approach focuses on combining the light-absorbing (LA) unit with the hydrogen-evolving center (HEC) in the same molecule in order to reduce losses in efficiency due to charge transfer reactions. This tactic also circumvents the lengthy synthesis and purification procedures required to covalently tether different chromophores in an effective geometry or at specific distances.

The photophysical properties of Rh<sub>2</sub>(II,II) compounds with formamidinate (form) bridging ligands that are highly electron donating to the metal will be presented. Complexes of the type *cis*-[Rh<sub>2</sub>(form)<sub>2</sub>(L)<sub>2</sub>]<sup>2+</sup> (L = diimine ligand) are easily oxidized, making them strong excited state reducing agents. The structures of the complexes are shown in Figure 1, which are

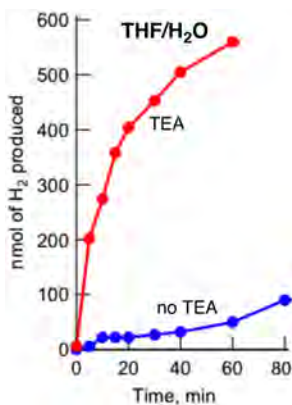


**Figure 2.** Photocatalytic production of H<sub>2</sub> by [Rh<sub>2</sub>(DTolF)<sub>2</sub>(dqp)<sub>2</sub>]<sup>2+</sup> ( $\lambda_{\text{irr}} > 395 \text{ nm}$ )

able to photocatalytically generate H<sub>2</sub> from acidic solution in the presence of a sacrificial electron donor, such as triethylamine (TEA), upon irradiation with visible light (Figure 2).

Time-resolved absorption spectroscopy and DFT calculations were used to elucidate the excited state dynamics and to gain information on the photoreactivity. Absorption of light results in the population of a singlet ligand-to-ligand charge transfer (<sup>1</sup>LLCT) excited state, followed by intersystem crossing to a triplet metal-centered (<sup>3</sup>MC) state, as shown in Figure 3. The latter is relatively long-lived (40 ns to 3  $\mu$ s) and exhibits significant electron density on the Rh<sub>2</sub>( $\sigma^*$ ) molecular orbital, which is expected to be reactive and extends to the open axial coordination sites. The <sup>1</sup>LLCT and <sup>3</sup>MC states are good excited state reducing and

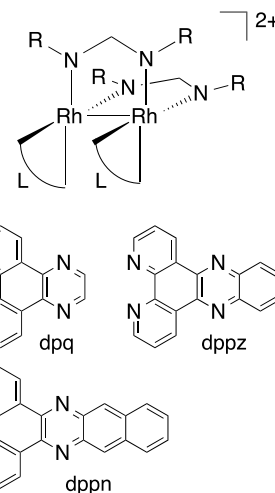


**Figure 1.** Molecular structures (R = p-toluene (DTolF) and p-fluorobenzen (F-form)).

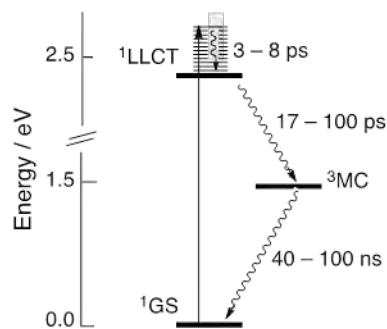


**Figure 3.** Jablonski diagram for L = dqp, dppz complexes.

oxidizing agents.

Electrochemical methods were employed to gain further understanding of the mechanism of H<sub>2</sub> generation. These experiments result in overpotentials of ~440 mV and TOFs of ~10<sup>4</sup> – 10<sup>5</sup> s<sup>-1</sup>. The mechanism of hydrogen evolution has two components, one slower and another faster; the latter requires an additional electron, as shown in Figure 5. It is important to note that following the generation of the active Rh<sub>2</sub>(II,II)-H<sub>2</sub> species (slow, right side of Figure 5), the addition of another electron into the system results in a d<sup>7</sup>-d<sup>8</sup> species with electron density in an axial Rh-H<sub>2</sub> antibonding orbital. This reduction is expected to lead to fast dissociation of H<sub>2</sub>, as depicted on the left side of Figure 5.

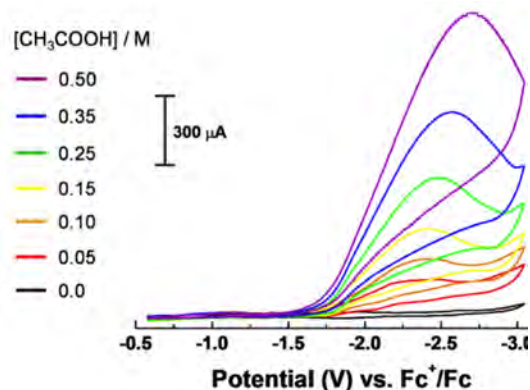


**Figure 4.** Electrocatalytic H<sub>2</sub> production by dqp complex acid (0.1 M Bu<sub>4</sub>PF<sub>6</sub> in CH<sub>3</sub>CN, 200 mV/s).

We are currently investigating the mechanism of the reaction and tuning the ligands to optimize photocatalytic properties. New complexes under investigation were designed such that ligand protonation is not possible upon electrochemical reduction and for the complexes to absorb lower energy light. Moreover, coupling to stronger absorbing units is being explored. In addition, some complexes have also been shown to catalytically reduce CO<sub>2</sub> upon reduction.

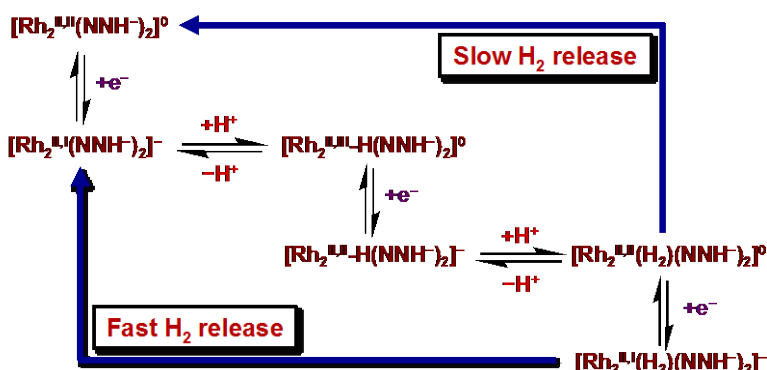


**Figure 5.** Proposed mechanism for the electrocatalytic reduction by Rh<sub>2</sub> complexes.

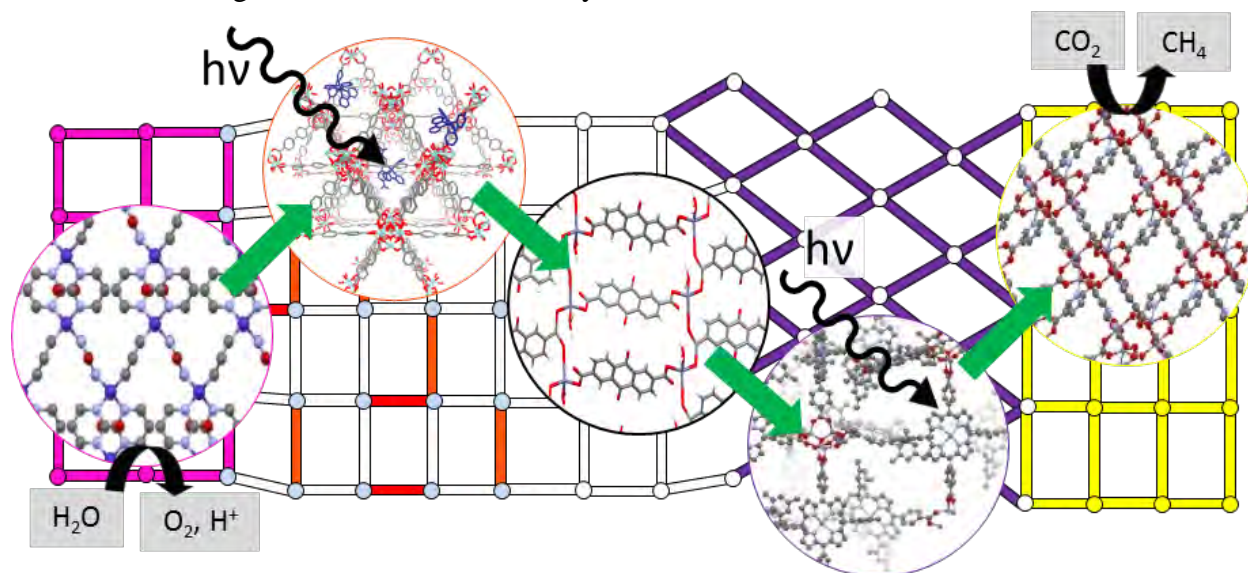
### DOE Sponsored Publications 9/1/2013 - Present

1. Li, Z.; Leed, N. A.; Dickson-Karn, N. M.; Dunbar, K. R.; Turro, C. "Directional Charge Transfer and Highly Redox Active Excited States of New Dirhodium(II,II) Complexes: Potential Applications in Solar Energy Conversion" *Chem. Sci.* **2014**, *5*, 727-737.
2. Li, Z.; David, A.; Albani, B. A.; Pellois, J.-P.; Turro, C.; Dunbar, K. R. "Optimizing the Electronic Properties of Photoactive Anticancer Oxypyridine Bridged Dirhodium(II,II) Complexes" *J. Am. Chem. Soc.* **2014**, *136*, 17058-17070.
3. White, T. A.; Witt, S. E.; Li, Z.; Dunbar, K. R.; Turro, C. "A New Rh<sub>2</sub>(II,II) Architecture for the Catalytic Reduction of H<sup>+</sup>" *Inorg. Chem.*, revisions requested.

## Electron Transport at Metal Organic Framework Donor-Acceptor Interfaces - Toward High Surface Area Photochemical Water Oxidation Catalysis

William A. Maza, Spencer R. Ahrenholtz, and Amanda J. Morris  
Department of Chemistry  
Virginia Tech  
Blacksburg, VA 24060

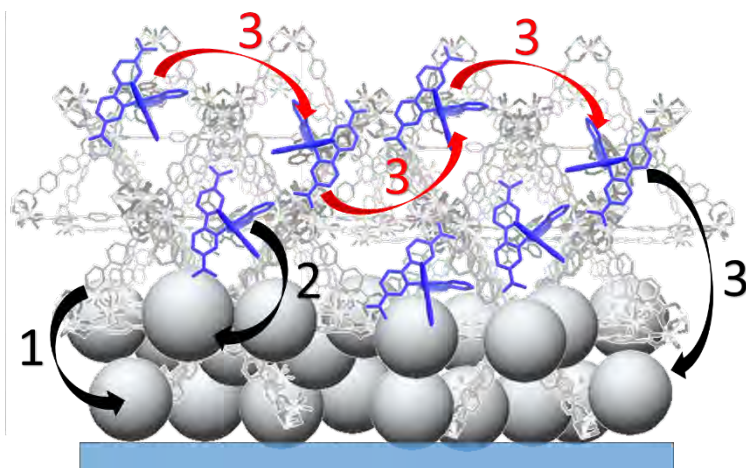
In the 2011 DOE Basic Energy Sciences Summary Report, approaches to artificial photosynthesis were identified as "critical to effectively utilizing the sun's energy". Two highlighted research efforts included the use of synthetically tunable metal organic framework materials for gas storage and inorganic catalysts for small molecule activation ( $\text{CO}$ ,  $\text{CO}_2$ ,  $\text{N}_2$ ). My research program capitalizes on these successes to look at metal organic framework (MOF) thin film assemblies capable of photo-induced heterogeneous water oxidation and carbon dioxide reduction, **Figure 1**. Specifically, the proposed work aims to provide a fundamental understanding of MOF materials utilized in photo-induced electron transport processes to elucidate the design constraints of such catalysts.



Over the past year my research program has focused on two specific thrusts toward the ultimate goal described above:

(1) *Demonstrate charge separation at a MOF donor-acceptor interface.* Toward this goal, a series of  $\text{Ru(II)L}_2\text{L}'$  ( $\text{L} = 2,2'$ -bipyridyl,  $\text{L}' = 2,2'$ -bipyridine-5,5'-dicarboxylic acid), RuDCBPY, containing zirconium(IV) MOF thin films were prepared as sensitizing materials on nanocrystalline  $\text{TiO}_2$  films. These metal organic framework (MOF) sensitized metal oxides each were shown to generate photocurrent in response to illumination under simulated 1 sun irradiation in a solar cell configuration. Emission lifetime measurements indicate the excited state quenching of RuDCBPY at the MOF- $\text{TiO}_2$  interface is extremely efficient ( $> 90\%$ ), presumably due to electron injection into  $\text{TiO}_2$ . In this geometry, there are at least three contributors to the observed photocurrent upon illumination of the MOF [see Figure]: 1) excitation of the UiO-67 or UiO-67-DCBPY followed by charge separation and electron

injection into  $\text{TiO}_2$ , 2) excitation of RuDCBPY ligands adjacent or adsorbed to the  $\text{TiO}_2$  undergoing electron injection into  $\text{TiO}_2$  from the RuDCBPY  $^1\text{MLCT}$  or  $^3\text{MLCT}$ , and 3) energy hopping/migration between RuDCBPY centers within the bulk of the MOF to the MOF/ $\text{TiO}_2$  interface with subsequent electron injection into the  $\text{TiO}_2$ . A mechanism was proposed in which RuDCBPY-centers within the MOF-bulk undergo isotropic Förster energy migration via hopping up to 25 nm from the point of origin. The energy migration process was highly dependent on synthetic preparation used to form the thin films. This work represents the first example in which a MOF sensitized interface out-performs its molecular constituent in a solar cell configuration.



(2) *Demonstrate water oxidation at a high surface MOF.* The MOF chosen as a preliminary water oxidation target was the  $\text{M}(2\text{-pymo})_2$  series, where  $\text{M} = \text{Pd}$  or  $\text{Co}$ . The MOF was deposited onto a conductive substrate and the electrocatalytic propensity for water oxidation explored. Comparison between the cyclic voltammetric response of  $\text{Co}(\text{pymo})_2$  films in aqueous and non-aqueous solutions indicated catalytic activity. Tafel analysis of the steady state potential-dependent current provided mechanistic insight and the exchange current density for comparison to reported catalysts. While the reaction rates were impressive, the material was unstable to prolonged electrolysis, and oxidation production ceased after 45 minutes. This was attributed to the large structural rearrangement that occurs about the cobalt nodes upon oxidation from  $\text{Co}(\text{II})$  to  $\text{Co}(\text{III})$ .

Our results have provided new discoveries about the structure–function relationship of MOF charge transport materials and water oxidation catalysts. Future work will grow on these initial studies to demonstrate sustained water oxidation at MOF donor-acceptor assemblies. Specifically, we are exploring the use of ruthenium polypyridyl doped-MOF thin films on  $\text{TiO}_2$  in conjunction with encapsulated solid-state water oxidation catalysts and post-synthetically incorporated molecular catalysts.

### DOE Sponsored Publications 2012-2015

1. Maza, William A.; Padilla, Roberto; Morris, Amanda J. “Concentration dependent dimensionality of resonance energy transfer in a post-synthetically doped morphologically homologous analogue of UiO-67 MOF with a ruthenium(II) polypyridyl complex.” *Submitted*.
2. Maza, William A.; Haring, Andrew J.; Ahrenholtz, Spencer R.; Epley, Charity C.; Lin, Shaoyang; Morris, Amanda J. “Ruthenium(II)-polypyridyl zirconium(IV) metal-organic frameworks as a new class of sensitized solar cells.” *Submitted*.
3. Ahrenholtz, Spencer. R.; Kolb, Benjamin; Morris, Amanda J. “Electrocatalytic water oxidation at neutral pH by a cobalt based metal organic framework.” *Submitted*.

## *Session VIII*

### *Fundamentals of Charge Separation and Transport*



## Physical Chemistry of Reaction Dynamics in Ionic Liquids

David A. Blank,<sup>1</sup> Edward W. Castner, Jr.,<sup>2</sup> Claudio J. Margulis,<sup>3</sup>  
Mark Maroncelli,<sup>4</sup> and James F. Wishart<sup>5</sup>

<sup>1</sup>Dept. of Chemistry, University of Minnesota, Minneapolis, MN 55455

<sup>2</sup>Dept. of Chemistry and Chemical Biology, Rutgers University, Piscataway, NJ 08854

<sup>3</sup>Dept. of Chemistry, University of Iowa, Iowa City, IA 52242

<sup>4</sup>Dept. of Chemistry, Penn State University, University Park, PA 16802

<sup>5</sup>Chemistry Dept., Brookhaven National Laboratory, Upton, NY 11973

The superior properties of ionic liquids (ILs) have led to their increasing use for energy related applications. However, much remains to be done to provide the physical and chemical foundations needed to rationalize the properties of ILs and guide further scientific progress. Our team has been successful at providing fundamental understanding in diverse areas ranging from solvation dynamics, chemical reactivity, anomalous transport of charged and neutral species as well as reactivity and dynamics of excess electrons. The insight gained from these studies is relevant to varied areas including photo-induced and radiation initiated reactions as well as transport processes relevant in batteries and fuel cells. Fertile topics for our collaborative research have recently included: completing a comprehensive study of solvation dynamics in ILs, comparing rates and mechanisms for intra- and bi-molecular photo-induced electron-transfer reactions in ILs, studying how transport in mixtures of ILs and conventional solvents differs from single-solvent systems, how anomalous diffusion may be related to dynamical heterogeneity and how dynamical heterogeneity may be ultimately related to nanoscale structure, and studying the properties of excess electrons in ILs.[1-24]

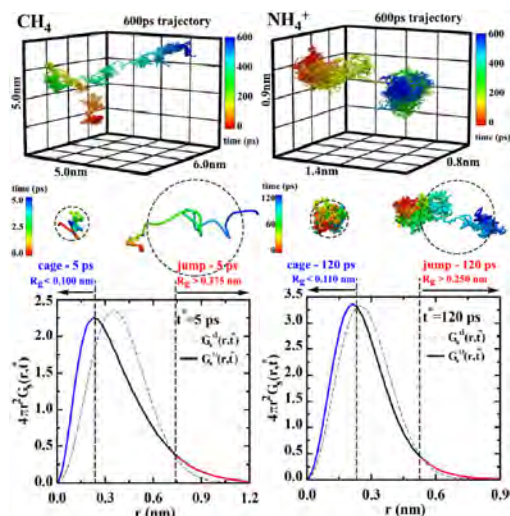


**Figure 1:** Locally stiff (high friction, high charge) and locally soft (low friction, more apolar) nanoregions are associated with solute cage and jump regimes. This is exemplified as trajectories in the upper panel and Van Hove functions in the lower panel. This behavior is linked to large deviations from hydrodynamic behavior.[24]

Recent work from the Maroncelli group unequivocally demonstrated that when charged and neutral solutes are small compared to the solvent molecular volume, significantly large deviations from Stokes-Einstein transport behavior are observed.[15] The diffusion of charged solutes becomes much slower than expected and that of neutral solutes much faster. A recent communication from the Castner group showed that dilution of an IL with hexane leaves much of the charge-ordered structure of the IL intact, even at high hexane mole fractions. Whereas simple hydrodynamic models explained diffusion rates of the ionic species, diffusion of hexane in these mixtures was found to be an order of magnitude larger than predicted.[23] Theoretical studies from the Margulis group investigated the physical reasons underpinning these deviations and found that ILs are comprised of regions of lower friction (more apolar) and regions of higher friction (more polar);[1-2] the predicted structures quantitatively

match those observed in synchrotron X-ray scattering experiments.[6,12] Such structural features directly correlate with dynamical heterogeneity and in turn with significant deviations from Stokes-Einstein predictions. Because this phenomenon is associated with the unique liquid landscape characteristic of ILs, these findings may provide the link between structural and dynamical heterogeneity in these systems.

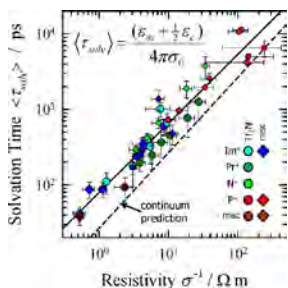


**Figure 2(a):** Correlation of integral solvation times of C153 with resistivity ( $1/\sigma$ ) in 34 varied ionic liquids.[9]

solvents like acetonitrile and water, they deviate increasingly (by up to a factor of 3) as the ionic liquid concentration increases. In the water mixture the deviations are larger, with the continuum predictions being too fast by a factor of  $\sim 7$ . Ongoing simulations suggest that preferential solvation and local frictional differences of the sort described in Fig. 1 may account for these findings.

Our team has also carried out computational and experimental work on the dynamics of excess electrons in different ionic liquids with the goal of better understanding reactivity and patterns of localization.[7,8,21] Fig. 3 is a summary of results for electron photodetachment in a series of methyl-alkyl-pyrrolidinium bis(trifluoromethylsulfonyl)amide (Pyr<sup>+</sup>/NTf<sub>2</sub><sup>-</sup>) ILs. The initial detached electron has a very large reactive radius as determined by sub-ps reactivity with the electron scavenger N<sub>2</sub>O. Simulations by the Margulis group indicate that the LUMO of the liquid accessed by photoexcitation is delocalized over several NTf<sub>2</sub><sup>-</sup> anions. When excess electrons are placed in the simulated LUMO they subsequently localize on a sub-ps time scale, in agreement with experiment. The simulations find localization of the excess electron onto an individual NTf<sub>2</sub><sup>-</sup> anion to form a dissociative dianion. In the experiments we find evidence for two competing electron localization channels, one that is consistent with the simulations, and one that produces free solvated electrons with relatively long lifetimes, in agreement with radiolysis experiments by the Wishart group. Branching between the two channels changes when increasing the alkyl chain length from hexyl to decyl, with a relative increase in the dissociative channel.[7, 27]

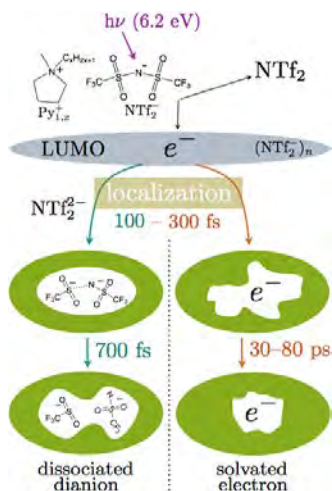


**Figure 3:** Two electron localization channels in Py<sub>1,x</sub><sup>+</sup>/NTf<sub>2</sub><sup>-</sup> ILs.[27]

Maroncelli and collaborators completed an extensive survey of the solvation response of a large group of ILs [5,9,19] and their mixtures with water[13] and acetonitrile.[16] A highlight of this work was the prediction and verification of a simple relationship between the integral solvation time  $\langle \tau_{solv} \rangle$  and ionic liquid conductivity  $\sigma_0$ , shown in Fig. 2(a). In the case of mixtures between conventional solvents and ILs, dielectric continuum predictions become increasingly worse as the IL concentration increases. Whereas continuum dielectric predictions are accurate in high-polarity conventional solvents

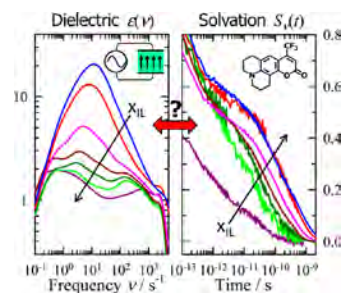


**Figure 2(b):** Dielectric dispersion data and solvation response in seven [Im<sub>41</sub>][BF<sub>4</sub>] + water mixtures.[13]

## DOE Sponsored Publications 2012-2015

1. H. K. Kashyap and C. J. Margulis, "Theoretical Deconstruction of the X-ray Structure Function Exposes Polarity Alternations in Room Temperature Ionic Liquids", *ECS Transactions*, **50**, 301 (2012).
2. H. K. Kashyap, J. J. Hettige, H. V. R. Annapureddy and C. J. Margulis, "SAXS Anti-Peaks Reveal the Length-Scales of Dual Positive/Negative and Polar/Apolar Ordering in Room-Temperature Ionic Liquids", *Chem. Commun.*, **48**, 5103 (2012).
3. D. Roy and M. Maroncelli, "Solvation and Solvation Dynamics in an Idealized Ionic Liquid Model," *J. Phys. Chem. B*, **116**, 5951 (2012).
4. M. Liang, A. Kaintz, G. A. Baker, and Mark Maroncelli, "Bimolecular Electron Transfer in Ionic Liquids: Are Rates Anomalously High?," *J. Phys. Chem. B*, **116**, 1370 (2012).
5. M. Maroncelli, X.-X. Zhang, M. Liang, D. Roy, and N. P. Ernstring, "Measurements of the Complete Solvation Response of Coumarin 153 in Ionic Liquids and the Accuracy of Simple Dielectric Continuum Predictions," *Faraday Disc.*, **154**, 409 (2012).
6. H. K. Kashyap, C. S. Santos, H. V. R. Annapureddy, N. S. Murthy, C. J. Margulis and Edward W. Castner, Jr., "Temperature-dependent structure of ionic liquids : X-ray scattering and simulations", *Faraday Disc.*, **154**, 133 (2012).
7. F. M. Domenech, B. FitzPatrick, A. T. Healy, and D. A. Blank, "Photodetachment and electron reactivity in 1-methyl-1-butyl-pyrrolidinium bis(trifluoromethylsulfonyl)amide," *J. Chem. Phys.*, **137**, 0334512 (2012).
8. C. Xu, A. Durumeric, H. K. Kashyap, J. J. Kohanoff, and C. J. Margulis, "Dynamics of Excess Electronic Charge in Aliphatic Ionic Liquids Containing the Bis(trifluoromethylsulfonyl)amide Anion", *J. Am. Chem. Soc.*, **135**, 17528 (2013).
9. X.-X. Zhang, M. Liang, N. P. Ernstring, and M. Maroncelli, "Conductivity and Solvation Dynamics in Ionic Liquids," *J. Phys. Chem. Lett.*, **4**, 1205 (2013).
10. C. Rumble, K. Rich, G. He, and M. Maroncelli, "CCVJ Is Not a Simple Rotor Probe," *J. Phys. Chem. B*, **116**, 10786 (2012).
11. H. Yennawar, G. He, C. Rumble, and M. Maroncelli, "2-Cyano-3-(2,3,6,7-tetrahydro-1*H*,5*H*-benzo[*ij*]quinolizin-9-yl)prop-2-enoic acid dimethyl sulfoxide monosolvate," *Acta Cryst.*, **E68**, o3204 (2012).
12. H. K. Kashyap, C. S. Santos, N. S. Murthy, J. J. Hettige, K. Kerr, S. Ramati, J. Gwon, M. Gohdo, S. I. Lall-Ramnarine, J. F. Wishart, C. J. Margulis, and E. W. Castner, Jr., "Structure of 1-Alkyl-1-methylpyrrolidinium Bis(trifluoromethylsulfonyl)amide Ionic Liquids with Linear, Branched and Cyclic Alkyl Groups", *J. Phys. Chem. B*, **117**, 15328 (2013).
13. X.-X. Zhang, M. Liang, J. Hunger, R. Buchner, and M. Maroncelli, "Dielectric Relaxation and Solvation Dynamics in a Prototypical Ionic Liquid + Dipolar Protic Liquid Mixture: 1-Butyl-3-Methylimidazolium Tetrafluoroborate + Water," *J. Phys. Chem. B*, **117**, 15356 (2013).
14. M. Kondo, X. Li and M. Maroncelli, "Characterization of trans-2-[4-[(Dimethylamino)styryl]benzothiazole as an Ultrafast Isomerization Probe and a Modified Kramers Theory Analysis," *J. Phys. Chem. B*, **117**, 12224 (2013).
15. Kaintz, G. A. Baker, A. Benesi, and M. Maroncelli, "Solute Diffusion in Ionic Liquids, NMR Measurements and Comparisons to Conventional Solvents," *J. Phys. Chem. B*, **117**, 11697 (2013); correction: *J. Phys. Chem. B*, **118**, 5615 (2014).

16. X.-X. Zhang, M. Liang, N. P. Ernsting, M. Maroncelli, "The Complete Solvation Response of Coumarin 153 in Ionic Liquids," *J. Phys. Chem. B*, **117**, 4291 (2013).
17. S. Khatun and E. W. Castner, Jr., "Ionic Liquid-Solute Interactions Studies by 2D NOE NMR Spectroscopy", *J. Phys. Chem. B*, 2014 ASAP. doi: 10.1021/jp509861g.
18. Jens Breffke, Brian W. Williams, and Mark Maroncelli, "The Photophysics of Three Naphthylmethylene Malononitriles," *J. Phys. Chem. B*, 2014, ASAP. doi: 10.1021/jp509882q.
19. M. Liang, X.-X. Zhang, A. Kaintz, N. P. Ernsting, and M. Maroncelli, "Solvation Dynamics in a Prototypical Ionic Liquid + Dipolar Aprotic Liquid Mixture: 1-Butyl-3-Methylimidazolium Tetrafluoroborate + Acetonitrile", *J. Phys. Chem. B*, **118**, 1340-1352 (2014). doi: 10.1021/jp412086t.
20. S. I. Lall-Ramnarine, J. A. Mukhlall, J. F. Wishart, R. R. Engel, A. R. Romeo, M. Gohdo, S. Ramati, M. Berman, and S. N. Suarez, "Cyclic phosphonium ionic liquids. Beilstein *J. Org. Chem.*, **10**, 271-275 (2014). doi: 10.3762/bjoc.10.22
21. C. Xu and C. J. Margulis, "Solvation of an Excess Electron in Pyrrolidinium Dicyanamide Based Ionic Liquids", *J. Phys. Chem. B*, **119**, 532 (2015).
22. H. Shirota, H. Matsuzaki, S. Ramati, and J. F. Wishart, "Effects of Aromaticity in Cations and Their Functional Groups on the Low-Frequency Spectra and Physical Properties of Ionic Liquids". *J. Phys. Chem. B*, 2015, ASAP. doi: 10.1021/jp509412z
23. M. Liang, S. Khatun and E. W. Castner, Jr., "Communication: Unusual structure and transport in ionic liquid-hexane mixtures", *J. Chem. Phys.*, **142**, 121101 (2015). doi: 10.1063/1.4916388.
24. J. C. Araque, S. K. Yadav, M. Shadeck, M. Maroncelli, and C. J. Margulis, "How is Diffusion of Neutral and Charged Tracers Related to the Structure and Dynamics of a Room-Temperature Ionic-Liquid? Large Deviations from Stokes-Einstein Behavior Explained", *J. Phys. Chem. B.*, *Just Accepted Manuscript*, doi: 10.1021/acs.jpcc.5b01093.

### Submitted manuscripts, 2015

25. X.-X. Zhang, J. Breffke, N. P. Ernsting, and M. Maroncelli, "Observations of Probe Dependence in the Solvation Dynamics in Ionic Liquids," *PhysChemChemPhys*, 2015, *revised version submitted*.
26. J. A. DeVine, M. Fekry, M. E. Harries, R. Abdel Malak Rached, J. Issa, J. F. Wishart and E. W. Castner, Jr., "Electron Transfer Dynamics for a Donor-Bridge-Acceptor Complex in Ionic Liquids", *submitted to J. Phys. Chem. B*, *jp-2015-03320g*.
27. F. M. Domenech, A. T. Healy, and D. A. Blank, "Photodetachment and Electron Cooling in a Series of Neat Aliphatic Room Temperature Ionic Liquids", *submitted to J. Chem. Phys.*

## Mechanism and Dynamics of Photoinduced Charge Separation in DNA

Frederick D. Lewis  
Department of Chemistry  
Northwestern University  
Evanston, IL 60201

The efficiency of photoinduced charge separation is determined by the complex kinetics of charge injection, recombination, and transport processes. The  $\pi$ -stacked base pairs that constitute the core of DNA provide a model one-dimensional system for the experimental and theoretical investigation of these processes. We have employed synthetic DNA hairpins (Figure 1) in our experimental investigations of photoinduced charge separation in DNA. The two strands of the hairpin are connected by a linker containing an organic chromophore, which upon electronic excitation can inject either a hole or an electron (positive or negative charge) into the DNA. The dynamics of the injection process have been studied by time-resolved transient absorption and fluorescence spectroscopy. A second chromophore placed either at the opposite end of the hairpin from the linker chromophore or as a replacement for a natural base within the hairpin can be employed to detect and time the arrival of the charge. These studies are carried out in collaboration with the groups of Michael Wasielewski (Northwestern) and Ferdinand Grozema (Delft, The Netherlands).

We have previously investigated the dependence of the efficiency and dynamics of hole transport on the length and base sequence of the DNA duplex. The use of poly(adenine) base sequences was found to provide for more efficient charge separation than either poly(guanine) or alternating or random base sequences. Even higher efficiency was obtained using diblock purine sequence (e.g.  $A_nG_m$ ), as a consequence of inhibited charge recombination. The effects of increased or decreased base pair conformational mobility were also investigated using analogs of the natural DNA bases. These experimental results were initially interpreted using traditional superexchange and incoherent hopping models. Recently, models specific to DNA have been developed to account for our experimental results for poly(adenine) hole transport.

This talk will begin with a description of the initial charge injection process. Advances in both the quality of the transient absorption spectra of the DNA hairpins and the analysis of two-dimensional data using global and target analysis have provided detailed information about the charge separation process in DNA which was previously unavailable. Both hole and electron injection processes can occur by either irreversible or reversible mechanisms, depending upon the free energy for conversion of the locally excited linker chromophore to a radical ion pair. The charge recombination and transport processes which determine the efficiency of hole or electron transport will then be described. The effect of placing a tunneling barrier between the chromophore and nearest base pair on hole transport dynamics will be described. Finally, the hole and electron transport processes will be compared.

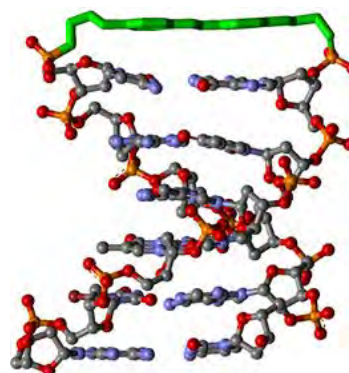


**Fig. 1** Structure of a DNA hairpin with stilbenediether linker (shown in green).

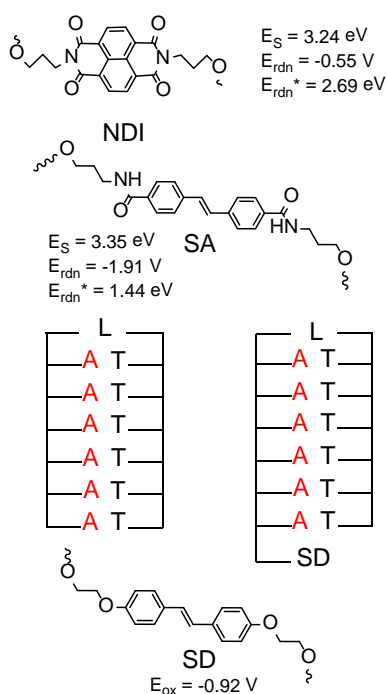


**Fig. 2** NDI, SA, and SD-linked hairpins and SD-capped hairpins having an  $A_n$  base sequence.

transport dynamics for hairpins having a SD donor and perylenediimide (PDI) acceptor separated by  $T_n$  or  $T^F U_n$  base sequences will be reported.

An artificial base pair consisting of two cyclohexane derivatives (X-X, Figure 3) has been reported to reduce the extent of fluorescence quenching of singlet PDI by an adjacent guanine. We have investigated the effect insertion of an X-X base pair between the SA, PDI, and NDI linkers and adjacent A-T or G-C. Only in the case of the strongest electron acceptor NDI is hole injection to adenine across a X-X base pair observed. A driving force of ca. 0.5 eV is required for hole injection across the X-X base pair. The dynamics of charge separation and charge recombination in systems having a NDI hole donor and SD hole trap in the absence and presence of the X-X base pair will be described.

Finally, the efficiency and dynamics of hole vs. electron transport processes in DNA will be compared. Faster hole transport is attributed to stronger electronic coupling between purine vs. pyrimidine bases.

Results for two hairpin hole injection systems (Figure 2a) will be presented (Figure 2). Hole injection using the naphthalenediimide (NDI) linker with an adjacent adenine occurs within 0.2 ps following laser excitation and is irreversible. In contrast, hole injection using the stilbenedicarboxamide (SA) linker with adenine is reversible, resulting in delayed fluorescence with a long-lived decay component of ca. 2 ns. Replacement of adenine with guanine results in fast, irreversible hole injection. In systems having a stilbenediether (SD) hole trap, transport between NDI and SD is substantially faster than between SA and SD across either a  $A_n$  or  $A_2 G_n$  diblock base sequence. This difference indicates that hole transport dynamics are dependent upon the energetics of hole injection as well as the base sequence. Possible reasons for the dependence on hole injection will be discussed.

Recent results for electron injection using SD-linked systems (Figure 2) will be presented. Rate constants for electron injection increase as the oxidation potential of the adjacent pyrimidine becomes less negative. Electron injection to cytosine is reversible; whereas injection to thymine or fluorouracil is irreversible. Base sequences having thymine followed by one or more fluoro-uracil ( $T^F U_n$ ) are best suited for electron transport beyond a single base pair. Electron

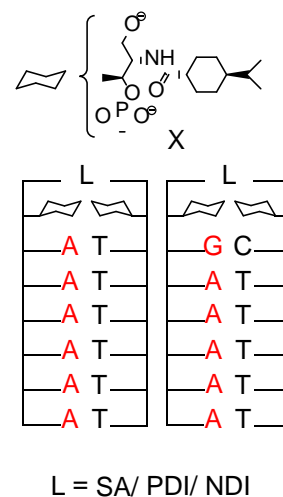


**Fig. 3** Hairpins having an X-X artificial base pair between the linker and adjacent A-T or G-C base pair .

## Sponsored Publications 2012-2015

- (1) Thazhathveetil, A. K.; Vura-Weis, J.; Trifonov, A. A.; Wasielewski, M. R.; Lewis, F. D.: Dynamics and efficiency of hole transport in LNA:DNA hybrid diblock oligomers. *J. Am. Chem. Soc.* **2012**, *134*, 16434-16440.
- (2) Lewis, F. D.; Wasielewski, M. R.: Dynamics and efficiency of photoinduced charge transport in DNA: Toward the elusive molecular wire. *Pure Appl. Chem.* **2013**, *98*, 1379-1387.
- (3) Brazard, J.; Thazhathveetil, A. K.; Vaya, I.; Lewis, F. D.; Gustavsson, T.; Markovitsi, D.: Electronic excited states of guanine-cytosine hairpins and duplexes studied by fluorescence spectroscopy. *Photochem. Photobiol. Sci.* **2013**, *12*, 1453-1459.
- (4) Chen, J.; Thazhathveetil, A. K.; Lewis, F. D.; Kohler, B.: Ultrafast Excited-State Dynamics in Hexaethyleneglycol-Linked DNA Homoduplexes Made of A·T Base Pairs. *J. Am. Chem. Soc.* **2013**, *135*, 10290-10293.
- (5) Jalilov, A. S.; Young, R. M.; Eaton, S. W.; Wasielewski, M. R.; Lewis, F. D.: Electronic Interactions of Michler's Ketone with DNA Bases in Synthetic Hairpins. *Photochem. Photobiol.* **2015**, doi:10.1111/php.12360.
- (6) Gorczak, N.; Fujii, T.; Mishra, A. K.; Houtepen, A. J.; Grozema, F. C.; Lewis, F. D.: Mechanism and Dynamics of Electron Injection and Charge Recombination in DNA. Dependence on Neighboring Pyrimidines. *J. Phys. Chem. B* **2015**.
- (7) Fujii, T.; Mishra, A. K.; Lewis, F. D.; Gorczak, N.; Grozema, F. C.; Lewis, F. D.: Mechanism and Dynamics of Electron Transport and Charge Recombination in DNA. **2015**, manuscript in preparation.
- (8) Singh, A. P. N.; Harris, M. A.; Young, R. M.; Miller, S. A.; Wasielewski, M. R.; Lewis, F. D.: Raising the Barrier for Photoinduced DNA Charge Injection with a Cyclohexyl Artificial "Base Pair". *Faraday Discussions* **2015**, submitted.

# Fundamental Studies of the Interplay of Molecular Composition, Electronic/Vibrational Characteristics, and Functional Properties of Tetrapyrrolic Chromophores and Arrays

David F. Bocian,<sup>1</sup> Dewey Holten,<sup>2</sup> Christine Kirmaier,<sup>2</sup> and Jonathan S. Lindsey<sup>3</sup>

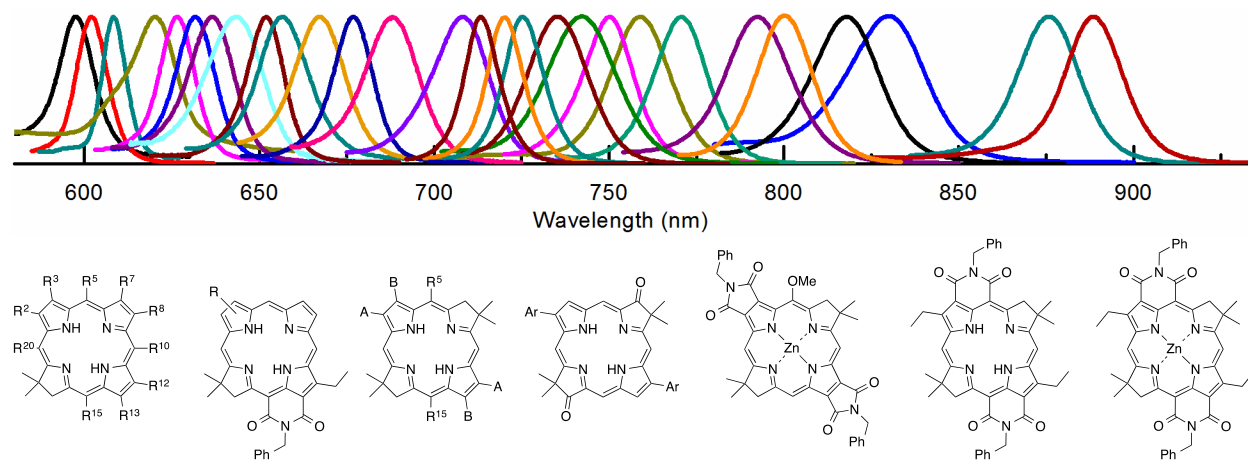
<sup>1</sup>Department of Chemistry, University of California Riverside, Riverside, CA 92521

<sup>2</sup>Department of Chemistry, Washington University, St. Louis, MO 63130

<sup>3</sup>Department of Chemistry, North Carolina State University, Raleigh, NC 27695

A long-term objective of our program is to design, synthesize, and characterize tetrapyrrole-based molecular architectures that absorb sunlight across the visible and near-infrared spectrum, funnel energy, and separate charge (hole, electron) with high efficiency and in a manner compatible with current and future solar-energy conversion schemes. Particularly noteworthy findings over the past three years are as follows:

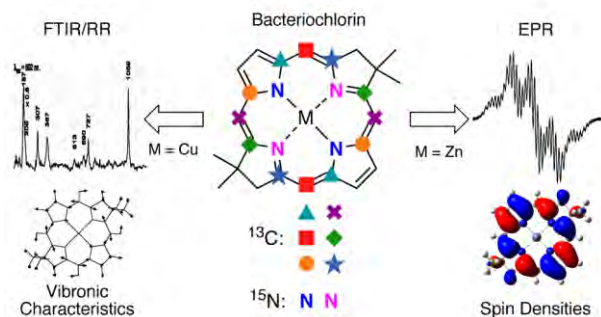
Molecular design, synthesis, and characterization (photophysical, redox, molecular orbital) studies have afforded a palette of tunable absorbers spanning the photon-rich red and near-infrared spectral regions. Recent work has (1) bridged the gap (~670-720 nm) between typical chlorins and bacteriochlorins using chlorin-imides, (2) pushed the short wavelength limit of typical bacteriochlorins to <700 nm using oxo and dioxobacteriochlorins, and (3) extended the long wavelength limit of typical bacteriochlorins first to past 800 nm using bacteriochlorin-imides and then to ~900 nm using five- and six-membered bacteriochlorin-bisimides.



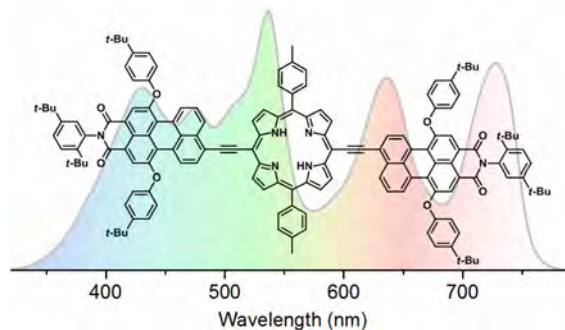
The yields and rate constants of the singlet excited-state decay pathways (fluorescence, intersystem crossing, and internal conversion) have been fully characterized. The near-ultraviolet to near-infrared absorption profiles (band energies/wavelengths and relative intensities) have been analyzed using four-orbital-model simulations based on molecular-orbital characteristics derived from density functional theory calculations. The studies provide fundamental insights into the interplay of molecular composition, electronic structure, redox, and photophysical properties spanning the main tetrapyrrole classes. Collectively the work affords molecular design principles for tunable red/near-infrared absorbers for solar-conversion systems.

The vibronic characteristics and spin-density distributions in the core bacteriochlorin macrocycle have been revealed by spectroscopic and theoretical studies of 16 isotopologues.

The vibrational modes in copper bacteriochlorin isotopologues were examined via resonance Raman and Fourier-transform infrared spectroscopy. The resonance Raman spectra exhibit an exceptional sparsity of vibronically active modes of the core macrocycle, in contrast with the rich spectra of the natural bacteriochlorophylls. The  $Q_y$ -excitation resonance Raman spectrum is dominated by a single mode at  $727\text{ cm}^{-1}$ , which calculations suggest is due to a symmetrical accordion-like deformation of the five-atom  $C_m(C_aNC_a)_{\text{pyrrole}}C_m$  portion of the ring core. This deformation also dominates the vibronic features in the absorption and fluorescence spectra. The spin-density distributions in the  $\pi$ -cation radical of the zinc bacteriochlorin isotopologues were studied by electron paramagnetic resonance spectroscopy. The spectra indicate a significant electron/spin density ( $\rho \sim 0.1$ ) on each meso-carbon atom. This observation contradicts the predictions of early calculations that have been assumed to be correct for nearly four decades. These findings have implications for how structural features that characterize native bacteriochlorophylls might influence energy- and electron-transfer processes in photosynthesis and alter the thinking on the design of synthetic, bacteriochlorin-based arrays for solar energy conversion.



A set of panchromatic absorbers exhibiting long excited-state lifetimes in both polar and nonpolar media has been prepared and characterized. The architectures are based on a porphyrin strongly coupled electronically to 1-4 perylene-monoimides via ethyne linkers. The perylene-porphyrin electronic coupling results in a substantial and unexpected redistribution of the large oscillator strength held in the typical tetrapyrrole near-ultraviolet Soret features ( $\epsilon \sim 350,000\text{ M}^{-1}\text{ cm}^{-1}$ ) into the visible, red, and near-infrared (to  $\sim 800\text{ nm}$ ) regions to afford effective panchromatic absorption. The excited-state lifetimes for the four perylene-porphyrin arrays range from 1.2 to 4.6 ns in toluene and 1.2 to 1.9 ns in benzonitrile, which is sufficient to support efficient energy or electron-transfer processes in solar-conversion systems. Such efficiency would be retained even in polar media where charge-transfer quenching within many multi-chromophore complexes can compromise utility.



Our present focus concerns several interrelated themes: (1) Gain a deeper understanding of the spectral and electronic properties of bacteriochlorins. (2) Understand the electronic origin of panchromatic absorption and associated excited-state behavior. (3) Determine the rates of ground-state hole/electron transfer between (hydro)porphyrins as a function of array architecture and molecular orbital composition. (4) Design, synthesize, and characterize integrated architectures that incorporate a panchromatic absorber and other components that afford efficient hole/electron migration and long-lived charge separation. Such architectures serve as a test-bed for successful integration of key properties and processes, some of which require rather weak coupling between constituents, some of which require very strong electronic interactions, and all of which should be tunable via control of molecular design.

## DOE Sponsored Publications 2012-2015

1. “Effects of Substituents on Synthetic Analogs of Chlorophylls. Part 3: The Distinctive Impact of Auxochromes at the 7- versus 3-Positions,” Springer, J. W.; Faries, K. M.; Diers, J. R.; Muthiah, C.; Mass, O.; Kee, H. L.; Kirmaier, C.; Lindsey, J. S.; Bocian, D. F.; Holten, D. *Photochem. Photobiol.* **2012**, *88*, 651–674.
2. “Synthesis and Physicochemical Properties of Metallobacteriochlorins,” Chen, C.-Y.; Sun, E.; Fan, D.; Taniguchi, M.; McDowell, B. E.; Yang, E.; Diers, J. R.; Bocian, D. F.; Holten, D.; Lindsey, J. S. *Inorg. Chem.* **2012**, *51*, 9443–9464.
3. “Stable Synthetic Bacteriochlorins for Photodynamic Therapy: Role of Dicyano Peripheral Groups, Central Metal Substitution (2H, Zn, Pd), and Cremophor EL Delivery,” Huang, Y.-Y.; Balasubramanian, T.; Yang, E.; Diers, J. R.; Bocian, D. F.; Lindsey, J. S.; Holten, D.; Hamblin, M. R. *ChemMedChem* **2012**, *7*, 2155–2167. *The studies utilized compounds characterized during the course of the fundamental solar-energy research sponsored by DOE. Attributions to DOE by Bocian and Holten only.*
4. “Effects of Linker Torsional Constraints on the Rate of Ground-State Hole Transfer in Porphyrin Dyads,” Hondros, C. J.; Aravindu, K.; Diers, J. R.; Holten, D.; Lindsey, J. S.; Bocian, D. F. *Inorg. Chem.* **2012**, *51*, 11076–11086.
5. “Synthesis and Characterization of Lipophilic, Near-Infrared Absorbing Metallobacteriochlorins,” Sun, E.; Chen, C.-Y.; Lindsey, J. S. *Chem. J. Chin. Univ.* **2013**, *34*, 776–781.
6. “Molecular Electronic Tuning of Photosensitizers to Enhance Photodynamic Therapy: Synthetic Dicyanobacteriochlorins as a Case Study,” Yang, E.; Diers, J. R.; Huang, Y.-Y.; Hamblin, M. R.; Lindsey, J. S.; Bocian, D. F.; Holten, D. *Photochem. Photobiol.* **2013**, *89*, 605–618. *The studies utilized compounds characterized during the course of the fundamental solar-energy research sponsored by DOE. Attributions to DOE by Bocian and Holten only.*
7. “Photophysical Properties and Electronic Structure of Bacteriochlorin–Chalcones with Extended Near-Infrared Absorption,” Yang, E.; Ruzié, C.; Kraymer, M.; Diers, J. R.; Niedzwiedzki, D. M.; Kirmaier, C.; Lindsey, J. S.; Bocian, D. F.; Holten, D. *Photochem. Photobiol.* **2013**, *89*, 586–604.
8. “Distinct Photophysical and Electronic Characteristics of Strongly Coupled Dyads Containing a Perylene Accessory Pigment and a Porphyrin, Chlorin, or Bacteriochlorin,” Wang, J.; Yang, E.; Diers, J. R.; Niedzwiedzki, D. M.; Kirmaier, C.; Bocian, D. F.; Lindsey, J. S.; Holten, D. *J. Phys. Chem. B* **2013**, *117*, 9288–9304.
9. “Serendipitous Synthetic Entrée to Tetrahydro Analogues of Cobalamins,” Deans, R. M.; Mass, O.; Diers, J. R.; Bocian, D. F.; Lindsey, J. S. *New J. Chem.* **2013**, *37*, 3964–3975.
10. “Synthesis and Photophysical Properties of Chlorins Bearing 0–4 Distinct Meso-Substituents,” Aravindu, K.; Kim, H.-J.; Taniguchi, M.; Dilbeck, P. L.; Diers, J. R.; Bocian, D. F.; Holten, D.; Lindsey, J. S. *Photochem. Photobiol. Sci.* **2013**, *12*, 2089–2109.
11. “Synthesis of 24 Bacteriochlorin Isotopologues, Each Containing a Symmetrical Pair of <sup>13</sup>C or <sup>15</sup>N Atoms in the Inner Core of the Macrocycle,” Chen, C.-Y.; Bocian, D. F.; Lindsey, J. S. *J. Org. Chem.* **2014**, *79*, 1001–1016.
12. “Probing Electronic Communication for Efficient Light-Harvesting Functionality: Dyads Containing a Common Perylene and a Porphyrin, Chlorin, or Bacteriochlorin,” Yang, E.; Wang, J.; Diers, J. R.; Niedzwiedzki, D. M.; Kirmaier, C.; Bocian, D. F.; Lindsey, J. S.; Holten, D. *J. Phys. Chem. B* **2014**, *118*, 1630–1647.

13. “Regioselective  $\beta$ -Pyrrolic Bromination of Hydrodipyrin–Dialkylboron Complexes Facilitates Access to Synthetic Models for Chlorophyll *f*,” Liu, M.; Ptaszek, M.; Mass, O.; Minkler, D. J.; Sommer, R. D.; Bhaumik, J.; Lindsey, J. S. *New J. Chem.* **2014**, *38*, 1717–1730.
14. “Photophysical Properties and Electronic Structure of Retinylidene–Chlorin–Chalcones,” Springer, J. W.; Taniguchi, M.; Krayner, M.; Ruzi , C.; Diers, J. R.; Niedzwiedzki, D. M.; Bocian, D. F.; Lindsey, J. S.; Holten, D. *Photochem. Photobiol. Sci.* **2014**, *13*, 634–650.
15. “NMR Spectral Properties of 16 Synthetic Bacteriochlorins with Site-Specific  $^{13}\text{C}$  or  $^{15}\text{N}$  Substitution,” Chen, C.-Y.; Taniguchi, M.; Lindsey, J. S. *J. Porphyrins Phthalocyanines* **2014**, *18*, 433–456.
16. “Vibronic Characteristics and Spin-Density Distributions in Bacteriochlorins as Revealed by Spectroscopic Studies of 16 Isotopologues. Implications for Energy- and Electron-Transfer in Natural Photosynthesis and Artificial Solar-Energy Conversion,” Diers, J. R.; Tang, Q.; Hondros, C. J.; Chen, C.-Y.; Holten, D.; Lindsey, J. S.; Bocian, D. F. *J. Phys. Chem. B* **2014**, *118*, 7520–7532.
17. “Panchromatic Absorbers for Solar Light-Harvesting,” Alexy, E. J.; Yuen, J. M.; Chandrashaker, V.; Diers, J. R.; Kirmaier, C.; Bocian, D. F.; Holten, D.; Lindsey, J. S. *Chem. Commun.* **2014**, *50*, 14512–14515.
18. “Effects of Substituents on Synthetic Analogs of Chlorophylls. Part 4: How Formyl Group Location Dictates the Spectral Properties of Chlorophylls *b*, *d* and *f*,” Yuen, J.; Harris, M. A.; Liu, M.; Diers, J. R.; Kirmaier, C.; Bocian, D. F.; Lindsey, J. S.; Holten, D. *Photochem. Photobiol.* **2015**, *91*, 331–342.
19. “Progress Towards Synthetic Chlorins with Graded Polarity, Conjugatable Substituents, and Wavelength Tunability,” Ra, D.; Gauger, K. A.; Muthukumaran, K.; Balasubramanian, T.; Chandrashaker, V.; Taniguchi, M.; Yu, Z.; Talley, D. C.; Ehudin, M.; Ptaszek, M.; Lindsey, J. S. *J. Porphyrins Phthalocyanines* **2015**, *19*, DOI: 10.1142/S1088424615500042.
20. “Photophysical Properties and Electronic Structure of Chlorin–Imides: Bridging the Gap between Chlorins and Bacteriochlorins,” Faries, K. M.; Diers, J. R.; Springer, J. W.; Yang, E.; Ptaszek, M.; Lahaye, D.; Krayner, M.; Taniguchi, M.; Kirmaier, C.; Lindsey, J. S.; Bocian, D. F.; Holten, D. *J. Phys. Chem. B* **2015**, DOI: 10.1021/jp511257w.
21. “Extending the Short and Long Wavelength Limits of Bacteriochlorin Near-Infrared Absorption via Dioxo- and Bisimide-Functionalization,” Vairaprakash, P.; Yang, E.; Sahin, T.; Taniguchi, M.; Krayner, M.; Diers, J. R.; Wang, A.; Niedzwiedzki, D. M.; Lindsey, J. S.; Bocian, D. F.; Holten, D. *J. Phys. Chem. B* **2015**, DOI: 10.1021/jp512818g.
22. “*De Novo* Synthesis of Gem-Dialkyl Chlorophylls for Probing and Emulating our Green World,” Lindsey, J. S. *Chem. Rev.* **2015**, *115*, submitted 02/02/2015.
23. “Access to an Unexplored Substitution Site in Synthetic Bacteriochlorins,” Zhang, N.; Jiang, J.; Reddy, K. R.; Taniguchi, M.; Lindsey, J. S. *J. Porphyrins Phthalocyanines* **2015**, *19*, submitted 03/10/2015.



*Session IX*

*Photochemistry of Complex Systems*



# Fundamental Studies of Light-induced Charge Transfer, Energy Transfer, and Energy Conversion with Supramolecular Systems

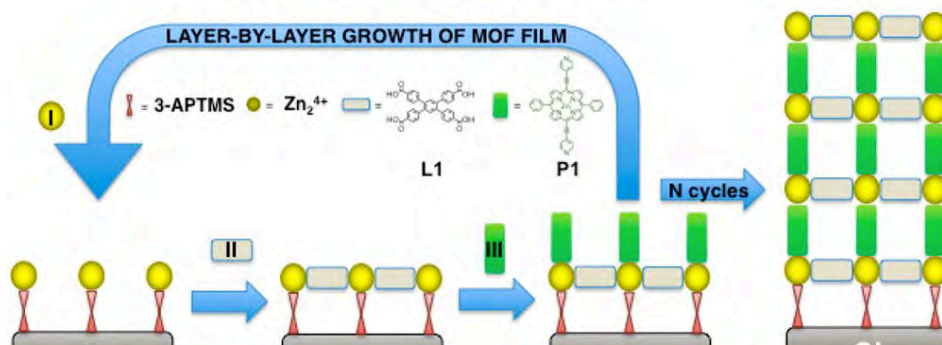
Joseph T. Hupp  
Department of Chemistry  
Northwestern University  
Evanston, IL 60208

**Summary of Project.** This project seeks to exploit supramolecular chemistry: a) to interrogate and understand fundamental aspects of light-induced charge transfer and energy transfer, and b) to construct solar energy conversion systems that make use of unique assembly motifs to address key conversion efficiency issues. The project focuses specifically on developing, investigating, and understanding at a fundamental-science level the behavior of promising new light harvesters and redox shuttles in DSC and related environments.

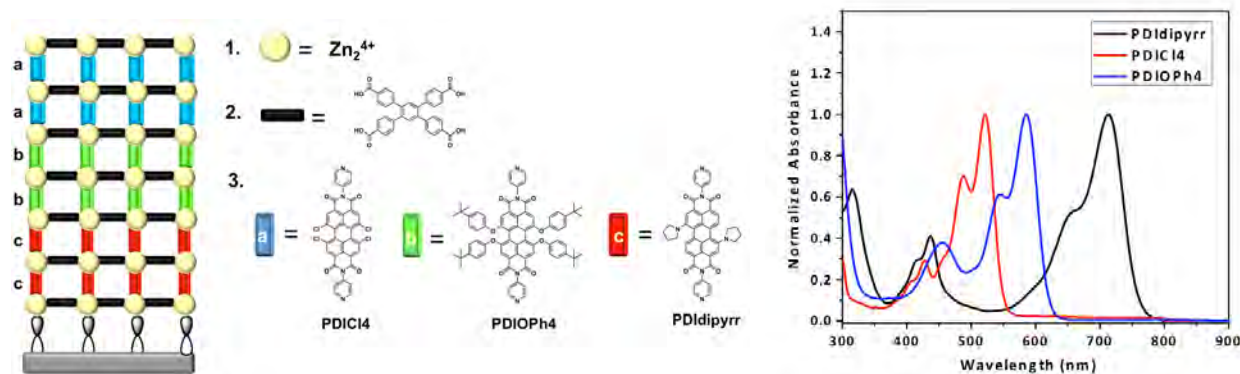
The project's focus has shifted from the chemistry of conventional dye-sensitized solar cells to metal-organic frameworks (MOFs) as components of photo electrodes and as adaptable compounds for investigations of fundamental photophysical and photo-electrochemical questions. The meeting presentation will touch on how MOFs can be used to investigate: a) long-range, directional energy-transfer, b) antenna-type light harvesting, c) directional charge-transport, including cascade-type behavior, d) charge injection into wide bandgap semiconductors, and/or e) charge transfer to external donors and acceptors. Below are outlines of a few topics.

**Electrode supported metal-organic frameworks.** We have recently reported on the synthesis of conductive-surface-supported MOFs via: 1) solvothermal chemistry, 2) electrophoretic deposition, and 3) a layer-by-layer (LbL) assembly approach. While each has its advantages, the LbL approach offers control over light-harvesting-assembly thicknesses with a precision at or near the length of a single molecular component; see figure below. In systematic studies with ditopic or tetratopic porphyrin molecules as building blocks, profilometry measurements have confirmed that the film thickness increases systematically with number of growth cycles. Polarization excitation and fluorescence measurements indicate that the porphyrin units are preferentially oriented, while X-ray reflectivity scans point to periodic ordering. Ellipsometry measurements show that the films are highly porous. Since there are currently few methods capable of yielding microporous MOFs containing accessible free-base porphyrins, it is noteworthy that the LbL growth permits direct MOF incorporation of unmetalated porphyrins.

Long-range energy transfer was demonstrated for both MOF films. The findings offer useful insights for subsequent fabrication of MOF-based solar energy conversion devices.



**Electrode supported metal-organic frameworks (E).** Layer-by-layer MOF assembly offers a way of building sequential arrays of chromophores that may be capable of displaying light-harvesting antenna behavior. With that idea in mind we have prepared a small series of peryleneimides and are using them as building blocks (see figure below). We find that we can control overall film thicknesses with close to single-molecular-layer thicknesses. We also find that we can construct three-chromophore films in predetermined chromophore order and with predetermined thicknesses for chromophore zones. The assembly process is greatly facilitated, both in terms of effort and reproducibility, by using home-built, programmable, robotic assemblers. Initial studies show that energy transfer from green absorbing to red absorbing chromophore zones readily occurs. We have yet to quantify the distance over which quantitative transfer can be observed.



**Charge-transport through MOFs.** Essential for any application of light-absorbing MOFs to the problem of light-to-electrical energy conversion is charge transport. Ideally the rate of charge transport will be directional and tunable. We have examined conductivity in a variety of electrode-supported MOFs. In the cases we have studied, transport occurs via electron or hole hopping between chemically identical sites. Under these conditions, electrical conductivity is governed by Marcus-like self-exchange behavior (or by counterion motion). We find that hopping rates can be quantified via chronocoulometry measurements, or alternatively, by appropriately designed wall-jet electrode measurements. Measurements of hopping as a function of temperature permit rate constants to be separated into reorganization-energy effects and electronic coupling effects. Initial studies point to modest free energies of activation and weak electronic coupling, resulting in highly nonadiabatic ET. The systematic tunability of MOF structures permits structure/reactivity hypotheses to be readily tested.

This presentation will include the results of studies designed to yield tunable electron transfer rates. One example is the successful modulation of charge-transport rates via reversible coupling of electron-transfer to molecular encapsulation. Other studies center on understanding how microscopic proton-coupled electron transfer behavior translates into macroscopic charge transport.

**Charge injection.** If time permits, MOF-based studies involving photo-excited linkers and metal-oxide nodes (electron acceptors) will be described, where the aim of the studies is to build up electron acceptors in atom-by-atom fashion, i.e. from molecule-like species to quantum-confined semiconductors.

## DOE Sponsored Publications 2013-2015

1. "Light Harvesting and Ultrafast Energy Migration in Porphyrin-Based Metal-Organic Frameworks," H-J. Son, S. Jin, S. Patwardhan, S. J. Wezenberg, N. C. Jeong, M. So, C. E. Wilmer, A. A. Sarjeant, G. C. Schatz, R. Q. Snurr, O. K. Farha, G. P. Wiederrecht, J. T. Hupp, *J. Am. Chem. Soc.* **2013**, *135*, 862-869.
2. "Energy Transfer from Quantum Dots to Metal-Organic Frameworks for Enhanced Light Harvesting," S. Jin, H-J. Son, O. K. Farha, G. Wiederrecht, J. T. Hupp, *J. Am. Chem. Soc.* **2013**, *135*, 955-958.
3. "Layer-by-Layer Fabrication of Oriented Porphyrin-Containing Thin Films Based on Metal-Organic Frameworks," M. So, S. Jin, H-J. Son, O. K. Farha, G. P. Wiederrecht, J. T. Hupp, *J. Am. Chem. Soc.* **2013**, *135*, 15698-15701.
4. "Metal-Organic Framework Thin Films Composed of Free-Standing Acicular Nanorods Exhibiting Reversible Electrochromism," C. W. Kung, T. C. Wang, J. E. Mondloch, D. Fairen-Jimenez, D. M. Gardner, J. M. Klingsporn, J. C. Barnes, R. P. Van Duyne, J. F. Stoddart, M. R. Wasielewski, O. K. Farha, J. T. Hupp, *Chem. Mater.* **2013**, *25*, 5012-5017.
5. "Directed Growth of Electroactive Metal Organic Framework Thin Films Using Electrophoretic Deposition," I. Hod, W. Bury, D. M. Karlin, P. Deria, C. Kung, M. J. Katz, M. So, B. Klahr, D. Jin, Y. Chung, T. W. Odom, O. K. Farha, J. T. Hupp, *Adv. Mater.* **2014**, *26*, 6295-6300.
6. "New Routes to Functional Porous Coordination Polymers," Joseph T. Hupp, *Bulletin Japan Soc. Coordination Chem.*, **2014**, submitted (invited award address article)
7. "Post-Assembly Atomic Layer Deposition of Metal-Oxide Coatings Enhances the Performance of an Organic Dye-Sensitized Solar Cell by Suppressing Dye Aggregation," Ho-Jin Son, Chul Hoon Kim, Dong Wook Kim, Nak Cheon Jeong, Chaiya Prasittichai, Langli Luo, Jinsong Wu, Omar K. Farha, Michael R. Wasielewski, and Joseph T. Hupp, *ACS Applied Materials & Interfaces*, **2015**, *7*, 5150-5159.
8. "Enhancement of the Yield of Charge Separation in Zinc Porphyrin-CdSe Quantum Dot Donor-Acceptor Complexes by a Dithiocarbamate Linkage," Shengye Jin, Mario Tagliacucchi, Ho-Jin Son, Rachel D. Harris, Kenneth O. Aruda, David J. Weinberg, Alexander B. Nepomnyashchii, Omar K. Farha, Joseph T. Hupp, and Emily A. Weiss, *J. Phys. Chem. C*, **2015**, *119*, 5195-5202.
9. "Bias-switchable Permselectivity and Redox Catalytic Activity of a Ferrocene-Functionalized, Thin-Film Metal Organic Framework Compound," Idan Hod, Wojciech Bury, Daniel M. Gardner, Pravas Deria, Vladimir Roznyatovskiy, Michael R. Wasielewski, Omar K. Farha, Joseph T. Hupp, *J. Phys. Chem. Lett.* **2015**, *6*, 586-591.

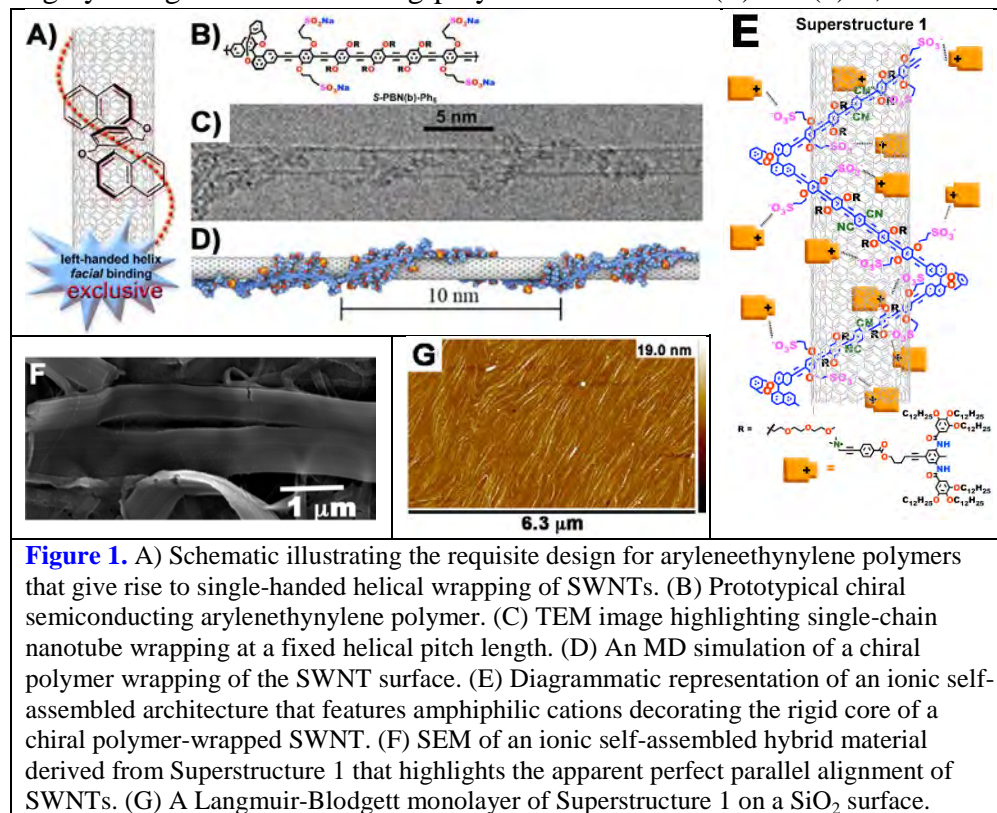
10. “Metal-organic Framework Materials for Light-Harvesting and Energy Transfer,” Monica C. So, Gary P. Wiederrecht, Joseph E. Mondloch, Joseph T. Hupp, Omar K. Farha, *Chem. Commun.* **2015**, *51*, 3501-3510 (invited feature article).
11. “Electrochemically Addressable Trisradical Rotaxanes Organized Within a Metal–Organic Framework,” Paul R. McGonigal, Pravas Deria, Idan Hod, Peyman Z. Moghadam, Alyssa-Jennifer Avestro, Noah Horwitz, Ian C. Gibbs-Hall, Anthea K. Blackburn, Dongyang Chen, Youssry, Y. Botros, Michael R. Wasielewski, Randall Q. Snurr, Joseph T. Hupp, Omar K. Farha, J. Fraser Stoddart, *Proc. Nat. Acad. Sci.*, **2015**, submitted.
12. “Porphyrin-based metal-organic framework thin films for electrochemical nitrite detection,” Chung-Wei Kung, Ting-Hsiang Chang, Li-Yao Chou, Joseph T. Hupp, Omar K. Farha, Kuo-Chuan Hoa, **2015**, manuscript submitted.

## Organic, Nanoscale, and Self-Assembled Structures Relevant to Solar Energy Conversion

Michael J. Therien  
 Department of Chemistry  
 French Family Science Center, 124 Science Drive  
 Duke University  
 Durham, NC 27708-0354

Understanding the molecular-level principles by which complex chemical systems carry out photochemical charge separation, transport, and storage will impact the design of practical solar energy conversion and storage devices. Towards this goal, this program focuses on: (i) delineating new compositions of matter relevant to solar energy conversion, (ii) elucidating factors that control charge transfer, charge migration, photoconductivity, and exciton diffusion dynamics in assemblies relevant to light-driven energy transduction, (iii) probing the extent of electronic coupling between conjugated organic materials and nanoscale structures in both ground and excited states, and (iv) engineering high quantum yield electron-hole pair production from initially prepared excitonic states in compositions that feature both molecular and nanoscale electro-optically active components. Accomplishments over the current funding period include:

***Single-Chain, Helical Wrapping of Individualized, Single-Walled Carbon Nanotubes by Ionic Poly(Arylene-ethynylene)s: New Compositions for Photoinduced Charge Transfer Reactions and Photovoltaic Applications.*** We have established aryleneethynylene polymer designs that give rise to single-handed helical wrapping of single-walled carbon nanotubes (SWNTs; **Figure 1**). Highly charged semiconducting polymers that utilize (*R*)- or (*S*)-1,1'-bi-2-naphthol components



that feature bridging 2,2'-1,3-benzyloxy tethers that restrict the torsional angle between the two naphthalene subunits, enable the production of polymer-wrapped SWNTs in which the polymer chain manifests single-handed helical wrapping (**Figure 1B-E**). The combination of single-handed helical wrapping with the ability

to modify conjugated polymer electronic structure opens up new opportunities for engineering the electro-optic functionality of nanoscale objects. Further, single-handed helical wrapping of SWNTs opens up new opportunities to organize multi-component carbon nanotube-containing ensembles over meso-to-macroscopic dimensions. We demonstrated for the first time that SWNTs, helically wrapped by a single chain of an anionic arylenethynylene polymer, can be structured into organized microscale objects through ionic self-assembly (ISA; **Figure 1F**). These microstructures are composed of rigorously aligned nanotubes at high areal density ( $2.5 \times 10^{10}$  SWNTs  $\text{cm}^{-2}$ ), and maintain the optical properties characteristic of individualized SWNTs. ISA thus offers an elegant alternative to traditional SWNT alignment methods that include horizontal SWNT growth on a single crystal surface or chemical vapor deposition under gas flow, due to the facts it: (i) is a solution-based process, and (ii) provides complex hierarchical SWNT structures based on fixed stoichiometry/fixed morphology SWNT-polymer compositions. We posit that the combination of chiral polyanionic arylenethynylene polymers, SWNTs having electronic structural homogeneity, the ability to modulate polymer electronic structure by design, and the facility of ISA to provide hierarchical organization, offers exceptional promise for the development of new types of electro-optic materials.

**Potentiometric, Electronic, and Transient Absorptive Spectroscopic Properties of Oxidized SWNTs Helically wrapped by Ionic, Semiconducting Polymers in Aqueous and Organic Media.**

We have utilized three electronically distinct semiconducting polymers, previously established to wrap SWNTs in an exclusive left-handed helical fashion to provide S-PBN(b)-Ph<sub>5</sub>-[(6,5) SWNT], S-PBN(b)-Ph<sub>4</sub>PhCN-[(6,5) SWNT], and S-PBN(b)-Ph<sub>2</sub>PZn<sub>2</sub>-[(6,5) SWNT] superstructures to interrogate the optoelectronic properties of oxidized [(6,5) SWNTs] (**Figure**

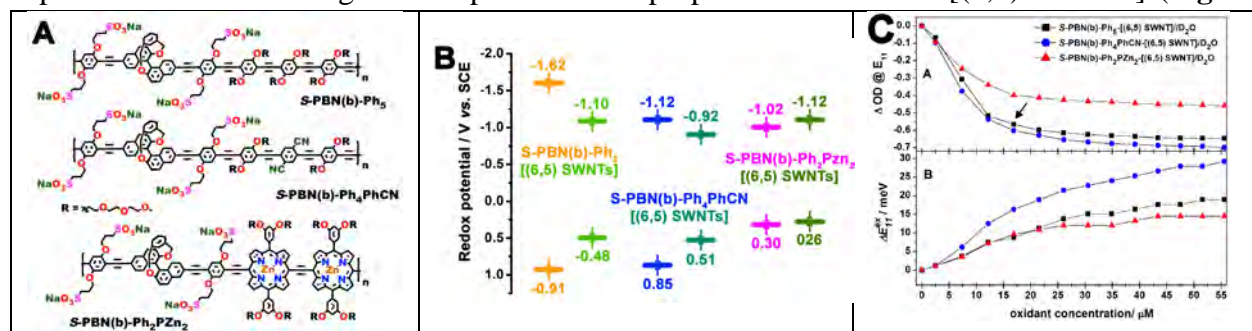


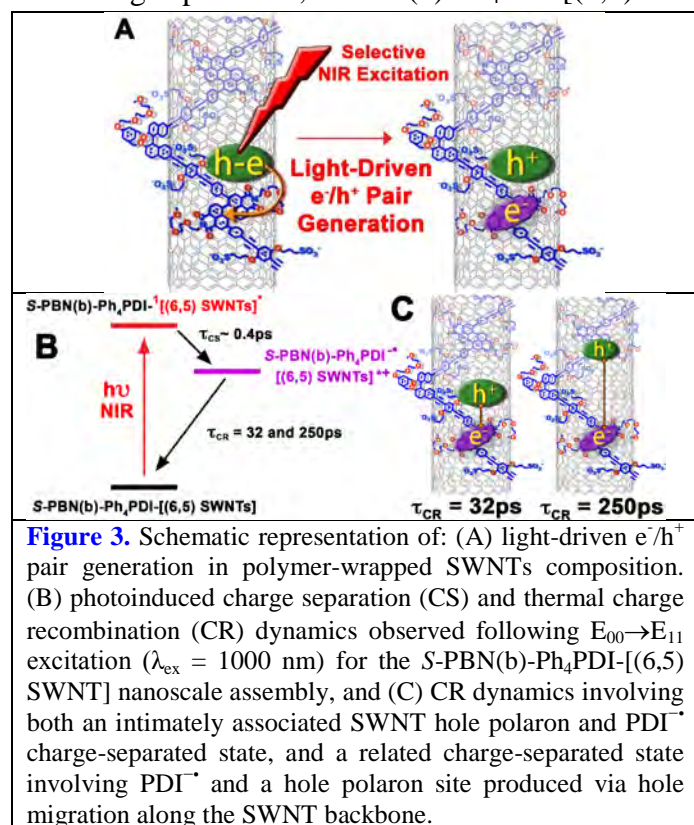
**Figure 2.** (A) Structure of arylenethynylene polymers S-PBN(b)-Ph<sub>5</sub>, S-PBN(b)-Ph<sub>4</sub>PhCN and S-PBN(b)-Ph<sub>2</sub>PZn<sub>2</sub>. (B) Potentiometrically determined HOMO and LUMO energy levels of the S-PBN(b)-Ph<sub>5</sub>, S-PBN(b)-Ph<sub>4</sub>PhCN, and S-PBN(b)-Ph<sub>2</sub>PZn<sub>2</sub> polymers, along with the valence and conduction band energies of their corresponding polymer-[(6,5) SWNT] superstructures. (C) Oxidative titration data highlighting: (i) the progressive diminution of the E<sub>00</sub> → E<sub>11</sub> transition oscillator strength and (ii) the magnitude of the E<sub>00</sub> → E<sub>11</sub> spectral blue shift observed with increasing oxidant concentration for these polymer-[(6,5) SWNT] superstructures.

2). Cyclic voltammetric experiments were used to directly determine the SWNT valence and conduction band energy levels in these assemblies (**Figure 2B**); these studies demonstrate that SWNT potentiometric properties can be modulated by the nature of the electronic structure of the semiconducting polymer that wraps its surface and thereby define a new approach by which to regulate the magnitudes of SWNT exciton binding energies. Redox titration experiments establish electronic transitions uniquely associated with the SWNT hole polaron state and determine a hole polaron delocalization length of 2.75 nm for (6,5) SWNTs (**Figure 2C**). Pump-probe TA spectroscopic data obtained for oxidized (6,5) SWNTs demonstrate: (i) a ground-state bleaching band centered at 1000 nm that is substantially broader than that

determined for the analogous ground-state bleach observed for electronically excited neutral (6,5) SWNTs at equivalent time delays; (ii) that the prominent TA spectroscopic signals characteristic of the (6,5) SWNT hole polaron state are insensitive to the solvent dielectric environment; and (iii) ground-state bleach recovery dynamics consistent with SWNT hole polarons that are both delocalized and mobile. As these findings determine steady-state and transient electronic absorptive spectroscopic signatures that are uniquely associated with the (6,5) SWNT hole polaron state, this work enables more detailed characterization of charge-transfer reactions involving SWNTs and provides new insights for engineering the electronic structural properties of hybrid semiconducting polymer–nanotube assemblies.

***First Unambiguous Diagnosis of Photoinduced Charged Carrier Signatures in a Stoichiometrically Controlled Semiconducting Polymer-Wrapped Carbon Nanotubes Assembly.***

The S-PBN(b)-Ph<sub>4</sub>PDI-[(6,5) SWNT] superstructure defines the first example of a carbon nanotube-soft matter assembly that enables the electronic signatures that distinguish electron transfer reactants and products, and corresponding analyses of charge separation (CS), charge migration, and charge recombination (CR) dynamics, to be readily elucidated (**Figure 3**). These SWNT-based nanohybrid compositions are based on (6,5) chirality enriched SWNTs [(6,5) SWNTs] and a chiral n-type polymer (S-PBN(b)-Ph<sub>4</sub>PDI) that exploits a perylenediimide (PDI)–containing repeat unit; S-PBN(b)-Ph<sub>4</sub>PDI-[(6,5) SWNT] superstructures feature a PDI electron



acceptor unit positioned at 3 nm intervals along the nanotube surface, thus controlling rigorously SWNT:electron acceptor stoichiometry and organization. Time-resolved pump-probe spectroscopic studies demonstrate that S-PBN(b)-Ph<sub>4</sub>PDI-[(6,5) SWNT] electronic excitation generates the PDI radical anion (PDI<sup>•-</sup>) via a photoinduced CS reaction ( $\tau_{\text{CS}} \sim 0.4 \text{ ps}$ ). These experiments highlight the concomitant rise and decay of transient absorption spectroscopic signatures characteristic of the SWNT hole polaron [(6,5) SWNT<sup>(•+)</sup><sub>n</sub>] and PDI<sup>•-</sup> states. Multiwavelength global analysis of these data provides two charge recombination time constants ( $\tau_{\text{CR}} \sim 31.8$  and 250 ps) that reflect CR dynamics involving both an intimately associated SWNT hole polaron and PDI<sup>•-</sup> charge-separated state, and a related charge-separated state involving PDI<sup>•-</sup> and a hole polaron site produced via hole

migration along the SWNT backbone that occurs over this timescale. This work thus defines a viable strategy to control the stoichiometry of electron (hole) acceptors at the nanotube interface, regulate the hole (electron) polaron density generated per nanotube unit length for a defined set of irradiation conditions, and engineer nanotube-soft matter assemblies in which critical energy transduction dynamical processes may be modulated.

## DOE Sponsored Solar Photochemistry Publications 2012-2015:

- 1) Electronic Transport in Porphyrin Supermolecule-Gold Nanoparticle Assemblies, D. Conklin, S. Nanayakkara, T.-H. Park, M. F. Lagadec, J. T. Stetcher, M. J. Therien, and D. A. Bonnell, *Nano Lett.* **2012**, *12*, 2414–2419.
- 2) Effect of Solvent Polarity and Electrophilicity on Quantum Yields and Solvatochromic Shifts of Single-Walled Carbon Nanotube Photoluminescence, B. A. Larsen, P. Deria, J. M. Holt, I. N. Stanton, M. J. Heben, M. J. Therien, and J. L. Blackburn, *J. Am. Chem. Soc.* **2012**, *134*, 12485–12491.
- 3) Exploiting Plasmon Induced Hot Electrons in Molecular Electronic Devices, D. Conklin, S. Nanayakkara, T.-H. Park, M. F. Lagadec, J. T. Stetcher, X. Chen, M. J. Therien, and D. A. Bonnell, *ACS Nano*, **2013**, *7*, 4479–4486.
- 4) Raman Spectroscopic Investigation of Individual Single-Walled Carbon Nanotubes Helically Wrapped by Ionic, Semiconducting Polymers, S. Bonhommeau, P. Deria, M. G. Glesner, D. Talaga, S. Najjar, C. Belin, L. Auneau, S. Trainini, M. J. Therien, and V. Rodriguez, *J. Phys. Chem. C* **2013**, *117*, 14840–14849.
- 5) Origins of the Helical Wrapping of Phenylene-Ethynylene Polymers about Single-Walled Carbon Nanotubes, C. D. Von Bargen, C. M. MacDermaid, O.-S. Lee, P. Deria, M. J. Therien, and J. G. Saven, *J. Phys. Chem. B* **2013**, *117*, 12953–12965.
- 6) The Evolution of Spin Distribution in the Photoexcited Triplet State of Ethyne-Elaborated Porphyrins, P. J. Angiolillo, J. Rawson, P. R. Frail, and M. J. Therien, *Chem. Commun.* **2013**, *49*, 9722–9724.
- 7) Ionic Self-Assembly Provides Dense Arrays of Individualized, Aligned Single Walled Carbon Nanotubes, J.-H. Olivier, P. Deria, J. Park, A. Kumbhar, M. Andrian-Albescu, and M. J. Therien, *Angew. Chemie* **2013**, *52*, 13080–13085.
- 8) Single-Handed Helical Wrapping of Single-Walled Carbon Nanotubes by Chiral, Ionic, Semiconducting Polymers, P. Deria, C. D. Von Bargen, J.-H. Olivier, A. S. Kumbhar, J. G. Saven, and M. J. Therien, *J. Am. Chem. Soc.* **2013**, *135*, 16220–16234.
- 9) Fluence-Dependent Singlet Exciton Dynamics in Length-Sorted Chirality-Enriched Single-Wall Carbon Nanotubes, J. Park, P. Deria, J.-H. Olivier, and M. J. Therien, *Nano Lett.* **2014**, *14*, 504–511.
- 10) Potentiometric, Electronic, and Transient Absorptive Spectroscopic Properties of Oxidized Single-Walled Carbon Nanotubes Helically Wrapped by Ionic, Semiconducting Polymers in Aqueous and Organic Media, P. Deria, J.-H. Olivier, J. Park, and M. J. Therien, *J. Am. Chem. Soc.* **2014**, *136*, 14193–14199.
- 11) Electron Spin Relaxation of Hole and Electron Polarons in  $\pi$ -Conjugated Porphyrin Arrays: Spintronic Implications, J. Rawson, P. J. Angiolillo, P. R. Frail, I. Goodenough, and M. J. Therien, *J. Phys. Chem. B* **2015**, *119*, DOI: [10.1021/jp5122728](https://doi.org/10.1021/jp5122728).
- 12) Extreme Electron Polaron Spatial Delocalization in  $\pi$ -Conjugated Materials, J. Rawson, P. J. Angiolillo, and M. J. Therien, *Proc. Natl. Acad. Sci. U.S.A.* Submitted.
- 13) First Unambiguous Diagnosis of Photoinduced Charged Carrier Signatures in a Stoichiometrically Controlled Semiconducting Polymer-Wrapped Carbon Nanotube Assembly, J.-H. Olivier, J. Park, P. Deria, J. Rawson, Y. Bai, A. Kumbhar, and M. J. Therien, *Angew. Chem., Int. Ed.* Submitted.

## Photoinduced Charge Separation Processes: from Natural Photosynthetic Proteins to Artificial Polymer-Fullerene Interfaces

Oleg G. Poluektov, Jens Niklas, Karen L. Mulfort, Lisa M. Utschig, and David M. Tiede

Chemical Sciences and Engineering Division, Argonne National Laboratory

Argonne, IL 60439

Kristy L. Mardis

Department of Chemistry & Physics, Chicago State University

Chicago, IL 60628

The ultimate goal of our solar energy conversion research is to mimic photosynthesis and devise integrated systems that can capture, convert, and store solar energy. The development and improvement of these systems relies on understanding the inherent, fundamental mechanisms for coupling captured photons to solar energy conversion and fuel generation. Specifically our research is focused on: (1) photoinduced charge separation in natural and artificial photosynthetic systems and photo-active organic interfaces, (2) structure-function relationships in novel biohybrid systems for H<sub>2</sub>-production, (3) electronic structure of molecular catalysts for proton reduction and water oxidation.

In natural photosynthesis light-induced long-lived charge separation occurs with a quantum yield that approaches 100%. This efficiency is so far unmatched by any artificial system. In natural photosynthetic systems, this efficient separation of charges is achieved with the aid of a cascade of energy levels and charge screening. Semiconductor polymer-fullerene blends, usually used in organic photovoltaic systems, by contrast, seem to possess none of these elements, yet surprisingly some organic photovoltaic devices are very efficient. While photovoltaic cells are highly promising man-made devices for direct solar energy utilization, a number of fundamental questions about how the organic bulk heterojunction cell enables efficient long-lived and long-range charge separation remain unanswered.

To address these questions we investigate semiconductor polymer-fullerene interfaces by employing an advanced suite of experimental and theoretical techniques originally developed for the study of photochemical reactions in natural and artificial photosynthetic systems. Thus, we utilize multifrequency EPR spectroscopy in combination with DFT calculations to study charge separation and stabilization mechanisms in photo-active polymer-fullerene systems. The polymers include the “reference” polymer P3HT and representatives of two series of high-performance, low bandgap polymers, PCDTBT and PTB7. The fullerenes include derivatives of C<sub>60</sub>, C<sub>70</sub>, and the heterodimer C<sub>60</sub>:C<sub>70</sub>. Structures of selected molecules are depicted in Figure 1.

Upon illumination, two paramagnetic species are formed in these complexes due to photo-induced

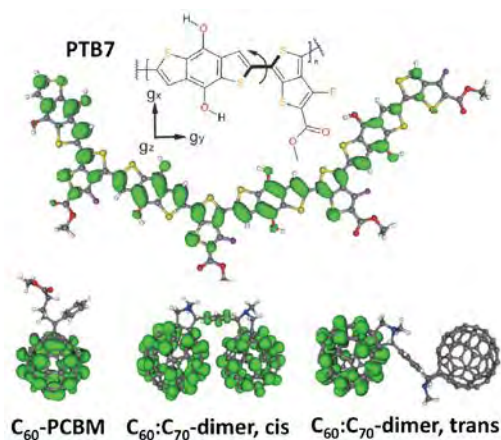


**Figure 1.** Charge distribution in the high-performance low band gap polymer donor PTB7 (top) and on the fullerene derivative acceptors (bottom).

electron transfer (ET) between the conjugated polymer and the fullerene derivative. These species are the positive,  $P^+$ , and the negative,  $P^-$ , polarons on the polymer backbone and fullerene cage, respectively, and correspond to radical cations and radical anions. To address the question of charge delocalization within the polarons, we performed high-frequency EPR (130 GHz) and pulsed ENDOR experiments which allow unambiguous determination of g-tensors and hyperfine (hf) interactions of magnetic nuclei with the unpaired electron. The g-tensors and hf-interactions are a sensitive probe of the electronic wave function and provide an excellent reference for validation of our current and future theoretical calculations, and as a result, for reconstruction of the electronic structures of the respective polarons. Our comprehensive EPR/DFT study revealed that, in all three systems, the positive polaron is distributed over distances of 40 - 60 Å along the polymer chain. This corresponds to about 15 thiophene units for P3HT, approximately three units for PCDTBT, and about three to four units for PTB7. No charge delocalization over several fullerene cages was observed in polymer-monomeric fullerene films. In contrast, in the novel covalently linked  $C_{60}:C_{70}$ -heterodimer fullerene it was found that the anion state is delocalized over both cages in the films, but is predominantly localized on either the  $C_{60}$  or  $C_{70}$  cage of the dimer in the solution. Electronic structure calculations demonstrated that different delocalization pattern in the dimers are related to the presence of two nearly iso-energetic minima, essentially the *cis* and *trans* conformers, which are separated by a thermodynamically accessible rotational barrier (Figure 1).

Time-resolved EPR spectra show a strong polarization pattern for all polymer-fullerene blends after light-induced charge separation. This polarization is caused by a non-Boltzmann population of the electron spin energy levels in the radical pairs. Similar polarization patterns were first reported in natural and artificial photosynthetic assemblies, and were understood within the models of spin-correlated radical pairs and sequential ET. The same models can help us describe a charge separation process that occurs via electron jumps or tunneling between neighboring fullerene molecules. The first step of the charge separation process is exciton dissociation and ET to the fullerene molecule at the polymer interface. The life time of this state is less than a few picoseconds. Importantly, efficient delocalization of the positive polaron on the polymer, which has been reported to happen on the same time scale, is a major mechanism for overcoming the

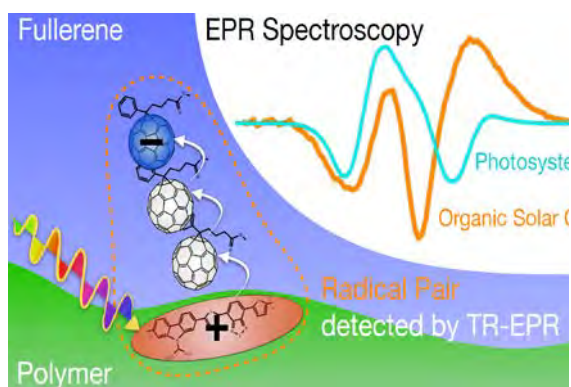


**Figure 2.** Simplified scheme of the charge separation steps near the polymer/fullerene interface. Overlapping TR-EPR spectra of P3HT/ $C_{60}$ -PCBM and Photosystem I reveals similar spin-polarization patterns.

Coulomb attraction and thus recombination, and thereby facilitating forward electron transfer. Forward ET forms an intermediate radical pair, with a separation distance within 15-20 Å. The third step is ET to the secondary, long-lived (up to tens to hundreds of ms), radical pair with a separation of 25-30 Å (Figure 2).

This charge delocalization upon photoinduced ET is similar to that in natural photosynthetic systems. In the latter, upon initial charge separation, the positive charge is delocalized over at least two large chlorophyll molecules to reduce the Coulomb interaction and enable forward electron transfer - the photosynthetic analogue of photocurrent.

## DOE Sponsored Publications 2012-2015

1. S. R. Soltau, J. Niklas, P. D. Dahlberg, D. M. Tiede, O. G. Poluektov, K. L. Mulfort, and L. M. Utschig, "Aqueous light-driven hydrogen production by a Ru-Ferredoxin-Co biohybrid", *J. Amer. Chem. Soc.*, 2015, submitted.
2. Poluektov, O. G., Utschig, L. M. "Low Temperature Bidirectional Electron Transfer in F<sub>x</sub> removed photosystem I", *J. Phys. Chem. B*, 2015, submitted.
3. J. Niklas, M. Westwood, K.L. Mardis, T. Brown, A. Pitts-McCoy, M.D. Hopkins, O.G. Poluektov, "X-Ray Crystallographic, Multifrequency EPR, and DFT Characterization of the Ni(P<sup>Cy</sup><sub>2</sub>N<sup>tBu</sup><sub>2</sub>)<sub>2</sub><sup>n+</sup> Hydrogen Oxidation Catalyst in the Ni(I) Oxidation State", *Inorganic Chemistry*, 2015, submitted.
4. Niklas, J., Mardis, K. L., Dyakonov, A., Beaupré, S., Leclerc, M., Xu, T., Yu, L., Poluektov, O. G. "Dynamics of Charge Separation in Polymer-Fullerene Bulk-Heterojunctions: A time-resolved Multi-Frequency EPR Study", *J. Phys. Chem. B*, 2015, DOI: 10.1021/jp511021v.
5. D. Basu, S. Mazumder, X. Shi, H. Baydoun, J. Niklas, O. Poluektov, H. B. Schlegel, C. N. Verani, "Ligand Transformations and Efficient Proton/Water Reduction with Cobalt Catalysts Based on Pentadentate Pyridine-Rich Environments", *Ang. Chem. Int. Ed.*, 2015, 54, 2105–2110.
6. J. Camacho-Bunquin, N. A. Siladke, G. Zhang, J. Niklas, O. G. Poluektov, S. T. Nguyen, J. T. Miller, and A. S. Hock, "Synthesis and Catalytic Hydrogenation Reactivity of a Chromium Catecholate Porous Organic Polymer", *Organometallics*, 2015, 34 (5), 947–952.
7. J. Zadrozny, J. Niklas, O.G. Poluektov, D. Freedman, "Multiple Quantum Coherences from Hyperfine Transitions in a Vanadium(IV) Complex", *J. Amer. Chem. Soc.*, 2014, 136, 15841-15844.
8. I.A. Shkrob, A.J. Kropf, T.W. Marin, Y. Li, O.G. Poluektov, J. Niklas, D.P. Abraham, "Manganese in Graphite Anode and Capacity Fade in Li-Ion Batteries", *J. Phys. Chem. C*, 2014 18, 24335-24348.
9. B. Hu, A. Getsoian, N.M. Schweitzer, U. Das, H.S. Kim, J. Niklas, O.G. Poluektov, L.A. Curtis, P.C. Stair, J.T. Miller, A.S. Hock, "Selective Propane Dehydrogenation with Single Site Co(II) on SiO<sub>2</sub> by a Non-redox Mechanism", *Journal of Catalysis*, 2015, 322, 24-37
10. K.K. Tanabe, M.S. Ferrandon, N.A. Siladke, S.J. Kraft, G. Zhang, J. Niklas, O.G. Poluektov, S.J. Lopykinski, E.E. Bunel, T.R. Krause, J.T. Miller, A.S. Hock, S.T. Nguyen, "Discovery of highly selective alkyne semi-hydrogenation catalysts based on 1st-row transition metallated porous organic polymers", *Ang. Chem. Int. Ed.*, 2014, 53, 1-5.
11. M. Bacchi, G. Berggren, J. Niklas, E. Veinberg, M.W. Mara, M.L. Shelby, O.G. Poluektov, L.X. Chen, D.M. Tiede, C. Cavazza, M.J. Field, M. Fontecave, V. Artero, "Cobaloxime-Based Artificial Hydrogenases", *Inorganic Chemistry*, 2014, 53, 8071-8082.
12. J. D. Megiatto, D. D. Méndez-Hernández, M. E. Tejada-Ferrari, A.-L. Teillout, O. G. Poluektov, T. Rajh, V. Mujica, T. L. Groy, D. Gust, T. A. Moore and A. L. Moore, "A bioinspired construct that mimics radical interactions of the Tyr-His pairs of photosystem II", *Nature Chemistry*, 2014, 6, 423-428.
13. Poluektov, O. G.; Niklas, J.; Mardis, K. L.; Beaupré, S.; Leclerc, M.; Villegas, C.; Erten-Ela, S.; Delgado, J. L.; Martin, N.; Sperlich, A.; Dyakonov, V. "Electronic Structure of Fullerene Heterodimer in Bulk-Heterojunction Blends", *Advanced Energy Materials*, 2014, 4(7), 1301517.

14. Niklas, J., Holt, J. M., Mistry, K., Rumbles, G., Blackburn, J., and Poluektov, O. G. "Charge Separation in SWNT:P3HT Blends Studied by EPR: Spin Signature of the Photoinduced Charged State in SWCNT", *J. Phys. Chem. Lett.*, 2014, 5, 601-606.
15. S. C. Silver, J. Niklas, P. Du, O. G. Poluektov, D. M. Tiede, L. M. Utschig, "Protein Delivery of a Ni Catalyst to Photosystem I for Light-Driven Hydrogen Production." *J. Amer. Chem. Soc.*, 2013, 135, 13246-13249.
16. R. Chatterjee, C. S. Coates, S. Milikisoyants, C-I. Lee, A. Wagner, O. G. Poluektov, and K. V. Lakshmi "High-Frequency Electron Nuclear Double-Resonance Spectroscopy Studies of the Mechanism of Proton-Coupled Electron Transfer at the Tyrosine-D Residue of Photosystem II" *Biochemistry*, 2013, 52 (28), 4781-4790.
17. J. Niklas, K.L. Mardis, B.P. Banks, G.M. Grooms, A. Sperlich, V. Dyakonov, S. Beaupre, M. Leclerc, T. Xu, L. Yu, O.G. Poluektov "Highly-Efficient Charge Separation and Polaron Delocalization in Polymer-Fullerene Bulk-Heterojunctions: A Comparative Multi-Frequency EPR & DFT Study" *Phys. Chem. Chem. Phys.*, 2013, 15 (24), 9562 – 9574.
18. Antipov, S., Poluektov, O., Schoessow, P., Kanareykin, A., Jing, C. "Photoinduced Spin Polarization and Microwave Technology" *Nuclear Inst. and Methods in Physics Research, A*, 2013, 700, 171-178.
19. A. Abouimrane, W. Weng, H. Eltayeb, Y. Cui, J. Niklas, O. Poluektov, and K. Amine "Sodium insertion in carboxylate based materials and their application in 3.6 V full sodium cells" *Energy Environ. Sci.*, 2012, 5, 9632-9638.
20. Donald M. Crokek, Anja Metz, Astrid M. Müller, Harry B. Gray, Toyketa Horton, Dorothy C. Horton, Oleg Poluektov, David Tiede, Ralph T. Weber, William L. Jarrett, Joshua D. Phillips, and Alvin Holder "A novel ruthenium(II)-cobaloxime supramolecular complex for photocatalytic H<sub>2</sub> evolution: Synthesis, characterisation, and mechanistic studies", *Dalton Trans.*, 2012, 41, 13060-13073.
21. F. A. Beckford, J. Thessing, A. Stott, A. A. Holder, O. G. Poluektov, L. Li, N. P. Seeram, "Anticancer activity and biophysical reactivity of copper complexes of 2-(benzo[d][1,3]dioxol-5-ylmethylene)-N-alkylhydrazinecarbothioamides", *Inorg. Chem. Comm.*, 2012, 15, 225-229.
22. T. Berthold, E. D. von Gromoff, S. Santabarbara, P. Stehle, G. Link, O. G. Poluektov, P. Heathcote, C. F. Beck, M. C. Thurnauer, and G. Kothe "Exploring the Electron Transfer Pathways in Photosystem I by High-Time Resolution Electron Paramagnetic Resonance: Observation of the B-side Radical Pair P<sub>700</sub><sup>+</sup>A<sub>1B</sub><sup>-</sup> in Whole Cells of the Deuterated Green Alga *Chlamydomonas reinhardtii* at Cryogenic Temperatures", *J. Amer. Chem. Soc.*, 2012, 134(12) 5563-5576.
23. R. Chatterjee, C. Coates, S. Milikisoyants, O. G. Poluektov, and K. V. Lakshmi "The Structure and Function of Quinones in Biological Solar Energy Transduction: A High-Frequency D-Band EPR Spectroscopy Study of Model Benzoquinones" *J. Phys. Chem. B*, 2012, 116(1), 676-682.
24. Niklas, J., Mulfort, K. L., Rakhimov, R. R., Mardis, K. L., Tiede, D. M., and Poluektov, O. G. "The Hydrogen Catalyst Cobaloxime – a Multifrequency EPR and DFT Study of Cobaloxime's Electronic Structure" *J. Phys. Chem. B*, 2012, 116(9) 2943-2957.

## Photoinduced Electron Transfer Processes in Doped Conjugated Polymer Films

Garry Rumbles, Jessica Ramirez, Hilary Marsh, Jaehong Park, and Obadiah Reid  
Chemistry and Nanoscience Center  
National Renewable Energy Laboratory  
Golden, Colorado and 80401

Unlike molecular Donor- $\pi$ -Acceptor systems where the product of photoinduced electron transfer is a charge-separated (CS) state, in fullerene-doped conjugated polymer films or blends, the primary product of excited state dissociation is separated charges and, frequently, with quantum yields that can approach unity. In addition to these high yields, the rate constant for the photoinduced electron transfer step is often significantly faster than 1 ps and the recombination time can be as long as milliseconds – all in a medium with a low dielectric constant. These differences make the fullerene-doped conjugated polymer systems worthy of study and are the primary focus of this work.

One of the specific topics of interest is the role of intermediate states between the initially excited state, frequently called an exciton, in the donor system and the free carriers that are produced by the dissociation of this exciton using a suitable acceptor, frequently a substituted fullerene. There is growing evidence in the literature that the intermediate species is a charge-transfer (CT) state that can be excited directly in the sub-bandgap region, and that can also emit when the carriers recombine. The properties of this so-called CT state are markedly different from the charge-separated CS state of the molecular systems, and it is this difference that is examined in this research.

We will present results on studies of the kinetics of photoinduced electron transfer processes in conjugated polymers that are doped lightly with a number of molecular acceptors. These studies aim to understand the role of the driving force in controlling the yield and recombination kinetics of free carriers and the impact of the solid-state microstructure of the host conjugated polymer on these processes. Results from flash photolysis, time-resolved microwave conductivity (*fp*-TRMC); femtosecond (*fTA*) and nanosecond transient absorption spectroscopy (*nTA*); and time-resolved photoluminescence spectroscopy (TRPL) are reported.

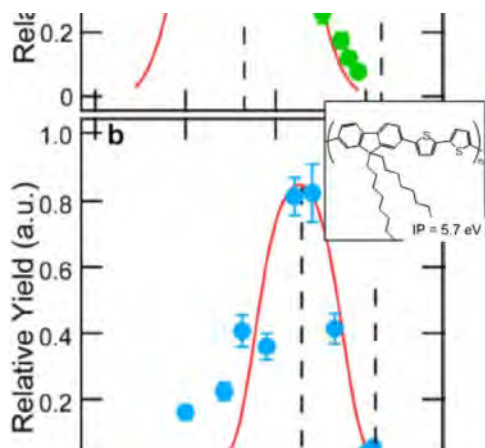


Figure 1 - Free carrier yield measured with *fp*-TRMC as a function of driving force for photoinduced electron transfer. Inset is structure of host polymer F8T2.

Recently, a series of perfluoroalkyl-substituted fullerenes (PFAFs) were used to systematically increase the electron affinity of the basic fullerene molecule that enabled the driving force for the electron transfer process to be varied over a range of  $\sim 0.9$  eV. The fullerenes were doped into three different conjugated polymers at low concentration and the yield of photoinduced, separated carriers detected using *fp*-TRMC. With increasing driving force the carrier yield was seen to increase, reaching a maximum and then decreasing (Figure 1), an observation that appears to be consistent with a Marcus formulation for electron transfer. However, this is only correct if the other

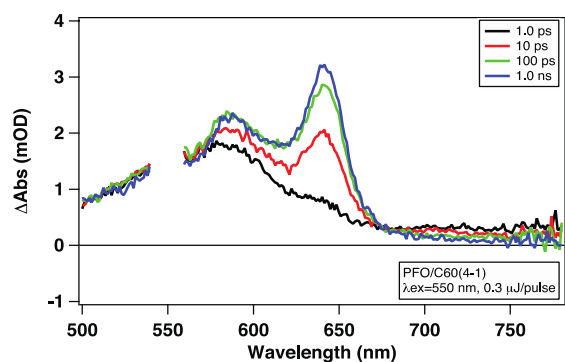


Figure 2 - FTA spectra of the PFAF C<sub>60</sub>-4-1 (Popov et al, DOI:10.1021/ja073181e) dispersed in PFO at low concentration. The broad spectrum at 585 nm corresponds to positive polarons in the amorphous phase, while the sharper peak at 630 nm corresponds to positive polarons in the beta-phase of PFO.

geminate carrier recombination. Using *f*TA spectroscopy, the production of positive holes (polarons) in the PFO polymer was investigated for these two particular fullerenes on a faster timescale than available with the *fp*-TRMC experiment. In these experiments, two characteristic polaron features were observed: one broad feature that appeared on a sub-picosecond timescale and a second, sharper feature that took up to 300 ps to appear (see Figure 2). These two features are consistent with polarons in the amorphous and so-called beta phases, respectively, on the PFO polymer.

Although the fullerenes are well known to be excellent electron acceptors, the low absorption coefficient associated with the lowest singlet state make the selective excitation required for the aforementioned experiments difficult. To overcome this issue, we have recently demonstrated that using simple molecular chromophores, such as phthalocyanines and perylenes, with the appropriate electron affinity (reduction potential) can serve the same role as the fullerenes, but provide a distinct, sharper absorption profile with a larger extinction coefficient. Using a silicon phthalocyanine (Gust et al, DOI:10.1142/S1088424611003847), which has a strong Q-band absorption in the near-IR, photoinduced electron transfer with three different thiophene-containing polymers was investigated. The three polymers provide control over the solid-state microstructure with the number and size of the crystallite regions readily controlled through subtle changes in the molecular structure, as well as control of processing. The *fp*-TRMC transients for the phthalocyanine at low concentration in regioregular and regiorandom poly(3-hexylthiophene) are shown in Figure 3. Long-lived carriers are only observed in the regio-regular film, where crystallites exist, and not in the amorphous-only regio-random sample. TRPL data, however, show that the excited states are quenched in both cases. These data indicate the importance of delocalizing the charges in prolonging the lifetime of the separated carriers where, in this instance, it is delocalization of the holes in the crystalline phase of the polymer.

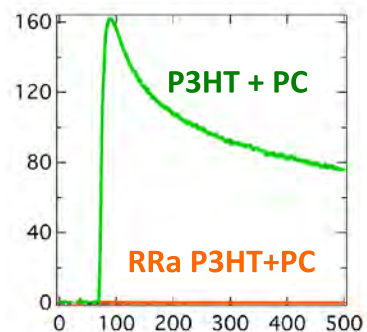


Figure 3 - *Fp*-TRMC transients of SiPc dispersed at low concentration in regio-regular (green) and regio-random (orange) poly(3-hexylthiophene).

## DOE Sponsored Publications 2012-2015

- (1) LaCount, M. D.; Weingarten, D.; Hu, N.; Shaheen, S. E.; van de Lagemaat, J.; Rumbles, G.; Walba, D. M.; Lusk, M. T. Energy Pooling Upconversion in Organic Molecular Systems. *J Phys Chem A* **2015**, 150401100642004.
- (2) Dayal, S.; Zhong, H.; Kopidakis, N.; Scholes, G. D.; Rumbles, G. Improved Power Conversion Efficiency for Bulk Heterojunction Solar Cells Incorporating CdTe-CdSe Nanoheterostructure Acceptors and a Conjugated Polymer Donor. *J. Photon. Energy* **2015**, 5, 057409.
- (3) San, L. K.; Bukovsky, E. V.; Larson, B. W.; Whitaker, J. B.; Deng, S. H. M.; Kopidakis, N.; Rumbles, G.; Popov, A. A.; Chen, Y.-S.; Wang, X.-B.; Boltalina, O. V.; Strauss, S. H. A Faux Hawk Fullerene with PCBM-Like Properties. *Chem Sci* **2015**, 6, 1801–1815.
- (4) Wojciechowski, K.; Stranks, S. D.; Abate, A.; Sadoughi, G.; Sadhanala, A.; Kopidakis, N.; Rumbles, G.; Li, C.-Z.; Friend, R. H.; Jen, A. K.-Y.; Snaith, H. J. Heterojunction Modification for Highly Efficient Organic–Inorganic Perovskite Solar Cells. *Acs Nano* **2014**, 141209140910005.
- (5) Marsh, H. S.; Reid, O. G.; Barnes, G.; Heeney, M.; Stingelin, N.; Rumbles, G. Control of Polythiophene Film Microstructure and Charge Carrier Dynamics Through Crystallization Temperature. *Journal of Polymer Science Part B-Polymer Physics* **2014**, Submitted, 700–707.
- (6) O'Connor, B. T.; Reid, O. G.; Zhang, X.; Kline, R. J.; Richter, L. J.; Gundlach, D. J.; DeLongchamp, D. M.; Toney, M. F.; Kopidakis, N.; Rumbles, G. Morphological Origin of Charge Transport Anisotropy in Aligned Polythiophene Thin Films. *Adv Funct Mater* **2014**, 24, 3422–3431.
- (7) Niklas, J.; Holt, J. M.; Mistry, K.; Rumbles, G.; Blackburn, J. L.; Poluektov, O. G. Charge Separation in P3HT:SWCNT Blends Studied by EPR: Spin Signature of the Photoinduced Charged State in SWCNT. *The Journal of Physical Chemistry Letters* **2014**, 5, 601–606.
- (8) Callahan, R. A.; Coffey, D. C.; Chen, D.; Clark, N. A.; Rumbles, G.; Walba, D. M. Charge Generation Measured for Fullerene–Helical Nanofilament Liquid Crystal Heterojunctions. *Acs Appl Mater Inter* **2014**, 6, 4823–4830.
- (9) Larson, B. W.; Whitaker, J. B.; Popov, A. A.; Kopidakis, N.; Rumbles, G.; Boltalina, O. V.; Strauss, S. H. Thermal [6, 6]→[6, 6] Isomerization and Decomposition of PCBM (Phenyl-C61-Butyric Acid Methyl Ester). *Chem Mater* **2014**, 26, 2361–2367.
- (10) Spencer, S.; Cody, J.; Mixture, S.; Cona, B.; Heaphy, P.; Rumbles, G.; Andersen, J.; Collison, C. Critical Electron Transfer Rates for Exciton Dissociation Governed by Extent of Crystallinity in Small Molecule Organic Photovoltaics. *The Journal of Physical Chemistry C* **2014**, 118, 14840–14847.
- (11) Bird, M. J.; Reid, O. G.; Cook, A. R.; Asaoka, S.; Shibano, Y.; Imahori, H.; Rumbles, G.; Miller, J. R. Mobility of Holes in Oligo- and Polyfluorenes of Defined Lengths. *The Journal of Physical Chemistry C* **2014**, 118, 6100–6109.
- (12) Larson, B. W.; Whitaker, J. B.; Wang, X.-B.; Popov, A. A.; Rumbles, G.; Kopidakis, N.; Strauss, S. H.; Boltalina, O. V. Electron Affinity of Phenyl-C 61–Butyric Acid Methyl Ester (PCBM). *J Phys Chem C* **2013**, 117, 14958–14964.
- (13) Reid, O. G.; Rumbles, G. Quantitative Transient Absorption Measurements of Polaron Yield and Absorption Coefficient in Neat Conjugated Polymers. *The Journal of Physical*

- Chemistry Letters* **2013**, *4*, 2348–2355.
- (14) Treat, N. D.; Nekuda Malik, J. A.; Reid, O.; Yu, L.; Shuttle, C. G.; Rumbles, G.; Hawker, C. J.; Chabinyo, M. L.; Smith, P.; Stingelin, N. Microstructure Formation in Molecular and Polymer Semiconductors Assisted by Nucleation Agents. *Nat Mater* **2013**, *12*, 628–633.
- (15) Savenije, T. J.; Ferguson, A. J.; Kopidakis, N.; Rumbles, G. Revealing the Dynamics of Charge Carriers in Polymer: Fullerene Blends Using Photoinduced Time-Resolved Microwave Conductivity. *The Journal of Physical Chemistry C* **2013**, *117*, 24085–24103.
- (16) Reid, O. G.; Pensack, R. D.; Song, Y.; Scholes, G. D.; Rumbles, G. Charge Photogeneration in Neat Conjugated Polymers. *Chem Mater* **2013**, *26*, 561–575.
- (17) Coffey, D. C.; Larson, B. W.; Hains, A. W.; Whitaker, J. B.; Kopidakis, N.; Boltalina, O. V.; Strauss, S. H.; Rumbles, G. An Optimal Driving Force for Converting Excitons Into Free Carriers in Excitonic Solar Cells. *J Phys Chem C* **2012**, *116*, 8916–8923.
- (18) Blackburn, J. L.; Holt, J. M.; Irurzun, V. M.; Resasco, D. E.; Rumbles, G. Confirmation of K-Momentum Dark Exciton Vibronic Sidebands Using <sup>13</sup>C-Labeled, Highly Enriched (6,5) Single-Walled Carbon Nanotubes. *Nano Lett* **2012**, *12*, 1398–1403.
- (19) Dayal, S.; Kopidakis, N.; Rumbles, G. Photoinduced Electron Transfer in Composites of Conjugated Polymers and Dendrimers with Branched Colloidal Nanoparticles. *Faraday Discuss* **2012**, *155*, 323.

## *Posters*



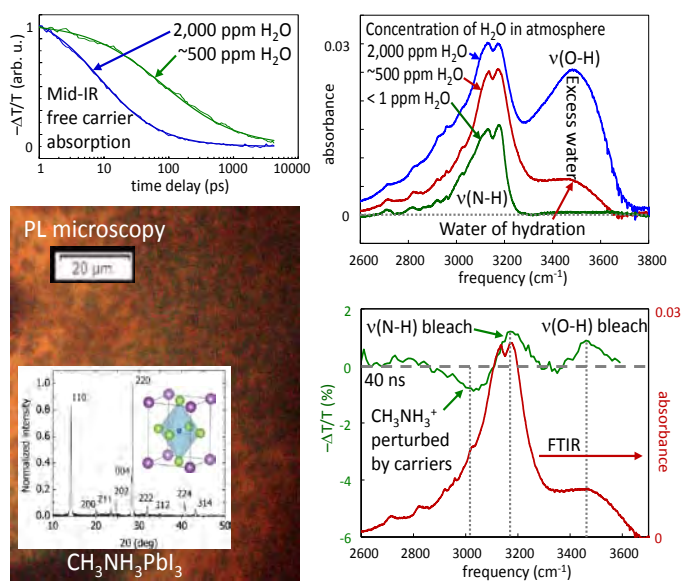
## Molecular Origins of Electronic Structure in Inorganic Systems for Solar Photoconversion

Robert J. Stewart, Christopher Grieco, Adam Rimshaw, and John B. Asbury  
 Department of Chemistry  
 The Pennsylvania State University  
 University Park, PA 16802

The influences that molecular species have on the electronic structure and charge recombination mechanisms of inorganic semiconducting heterostructures are investigated using time-resolved infrared spectroscopy in conjunction with electronic spectroscopy and microscopy. Two chemical systems of interest for solar photoconversion are investigated in parallel.

In the first example, organic-inorganic interactions are examined in ligand exchanged lead sulfide nanocrystals by probing the molecular species on nanocrystal surfaces that are associated with the formation of long-lived transient electronic states following optical excitation of their bandgap transitions. The influence of quantum confinement on the electronic states is investigated through temperature and size-dependent studies of ligand exchanged lead sulfide nanocrystals densely packed into solid films.

In the second example, nanostructured organohalide lead perovskites are examined in an effort to elucidate fundamental mechanisms of photoconversion in these systems that exhibit surprisingly high photoluminescence quantum yields. However, organohalide perovskites exhibit marked degradation and instability with origins that are not well understood. A study was undertaken to examine the factors affecting stability such as exposure to water and oxygen and non-stoichiometric compositions leading to interstitial defects and anti-site substitutions. Exposure of organohalide perovskite films to controlled amounts of moisture introduces water into the crystal that is assigned to water of hydration. Inclusion of such limited quantities of water does not markedly decrease the photoluminescence quantum yield or lifetime. However, inclusion of water in excess of this amount results in rapid degradation of the photoluminescence quantum yield and lifetime. Furthermore, ultrafast infrared transient absorption spectroscopy reveals that the time scale for free carrier cooling to the band edges decreases markedly as the concentration of water increases. Infrared transient absorption spectra reveal that the water of hydration and ammonium groups are perturbed by the presence of photogenerated charge carriers. This molecular polarization may be the underlying origin of hysteresis that has been observed in similar organohalide perovskite films.



## Photodetachment and Electron Dynamics in Aliphatic Ionic Liquids

Francesc Molins i Domenech, Andrew T. Healy, and David A. Blank  
Department of Chemistry, University of Minnesota, Minneapolis, MN 55455

Room temperature ionic liquids (RTILs) have experienced very rapid adoption in a number of applications related to energy generation and storage. These include fuel cells, solar energy capture, supercapacitors, and treatment of radioactive materials. Critical to these applications is a better understanding of the behavior of free electrons in RTILs. Aliphatic cations tend to demonstrate good stability in the presence of free electrons. One of the most commonly employed anion is bis(trifluoromethylsulfonyl)amide ( $\text{NTf}_2^-$ ). However, simulations and radiolysis experiments provide evidence for rapid fragmentation of  $\text{NTf}_2^-$  in the presences of excess electrons. At the same time, radiolysis experiments demonstrate long-lived absorption spectra consistent with stable solvated electrons.

We have investigated photodetachment in a series of methyl-alkyl-pyrrolidinium ( $\text{Py}1,x^+$ ) [ $\text{NTf}_2^-$ ] ILs, Fig 1. In the neat liquid, photodetachment creates an electron with substantial reactive reach. The observed reactivity is consistent with placing an electron in the LUMO of the liquid, which simulations indicate is delocalized over a set of the  $\text{NTf}_2^-$  anions. Sub-ps loss of reactivity follows ultrafast localization. Our experiments find evidence for two competing channels, one onto an individual  $\text{NTf}_2^-$  anion to create an unstable dianion, as indicated by simulations, and one into a cavity followed by reorganization to form a stable solvated electron, in agreement with radiolysis experiments. Branching between the two channels is sensitive to the size of the cation, as are the cooling dynamics and depth of the solvation trap. This can be correlated with changes in the structure of the liquid. Cooling of the solvated electron is similar to that observed in the radiolysis experiments, however it takes place slower reflecting the lower initial energy of the detached electrons.

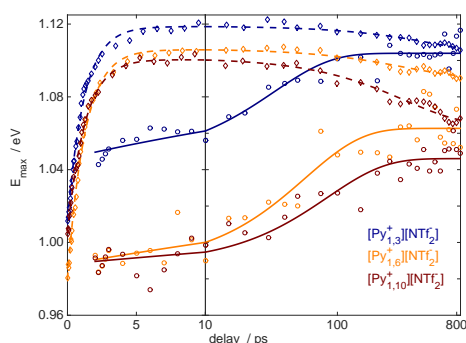


**Fig 2.** The peak absorption energy for the free electron detached from the neat liquid (circles) and  $\text{I}^-$  (diamonds)

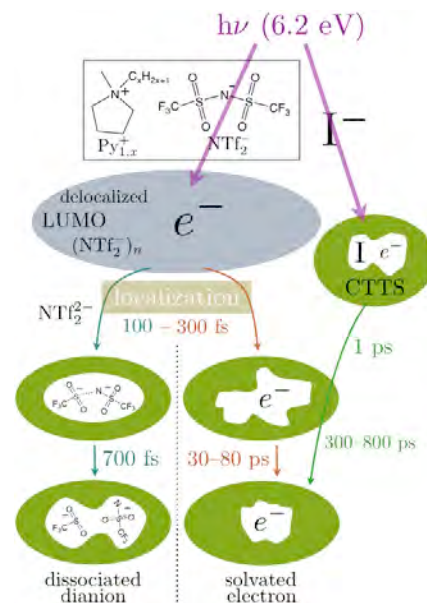


**Fig 1.** Diagram of the electron detachment channels.

We also investigated the photodetachment of iodide dissolved in the  $[\text{Py}1,x^+][\text{NTf}_2^-]$ . Photoexcitation results in electron detachment via a charge-transfer-to-solvent (CTTS) state of the iodide rather than the LUMO of the liquid. The only observed product is the free solvated electron. The transient absorption spectra in the near-IR are qualitatively similar, but exhibit very different dynamics, Fig. 2. Rather than a consistent increase in the energy of the absorption, iodide detachment exhibits a very rapid one ps increase followed by a subsequent decrease that converges to the same spectrum as the solvated electron detached in the neat liquid.

## Linker Rectifiers for Covalent Attachment of Catalysts to Semiconductor Surfaces

W. Ding<sup>1,2</sup>, M. Koepf<sup>2</sup>, C. Koenigsmann<sup>2</sup>, A. Batra<sup>3</sup>, L. Venkataraman<sup>3</sup>, C. F. A. Negre<sup>1,2</sup>,  
G. W. Brudvig<sup>1,2</sup>, R. H. Crabtree<sup>1,2</sup>, C. A. Schmuttenmaer<sup>1,2</sup>, and V. S. Batista<sup>1,2</sup>

<sup>1</sup>Department of Chemistry, Yale University, New Haven, CT, USA, <sup>2</sup>Energy Sciences Institute, Yale University, Yale University, West Haven, CT, 06516-7394, USA, and <sup>3</sup>Department of Applied Physics and Applied Mathematics, Columbia University, NY 10027, USA

Linkers that favor rectification of interfacial electron transfer are likely to be required for efficient photo-driven catalysis of multi-electron reactions at electrode surfaces [1-5]. Design principles are discussed, together with the synthesis and characterization of a specific pair of molecular frameworks, related by inversion of the direction of an amide bond at the heart of the molecule. The linkers have a terpyridyl group that can covalently bind Mn as in a well-known water oxidation catalyst and an acetylacetonate group that allows attachment to TiO<sub>2</sub> surfaces. The appropriate choice of the sense of the amide linkage yields directionality of interfacial electron transfer, essential to enhance electron injection and slow back-electron transfer. Support comes from electron paramagnetic resonance, terahertz spectroscopic, computational modelling characterizing the asymmetry of electron transfer properties, and conductance measurements based on the scanning tunnelling microscope break-junction (STM-BJ) technique.

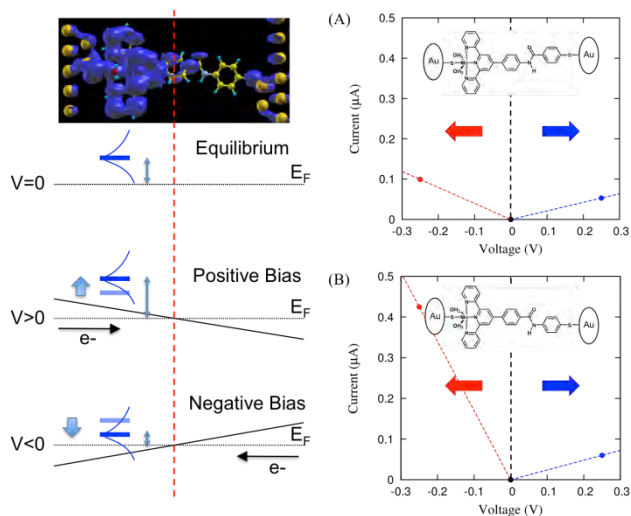


**Fig. 1** – (Left) Schematic representation of the state responsible for electron transport (LUMO) and alignment relative to the Fermi level under equilibrium ( $V=0$ ), positive ( $V>0$ ) and negative bias ( $V<0$ ). (Right) Calculated I-V curves for Mn-terpy-L1 (A) and Mn-terpy-L2 (B). The red and blue lines represent the current under negative and positive bias, respectively. Mn-terpy-L2 shows significant rectification.

### References

- [1] W. Ding, C. F.A. Negre, L. Vogt, V. S. Batista, “High Conductance Conformers in Histograms of Single-Molecule Current-Voltage Characteristics”, *J. Phys. Chem. C* (2014) **118**, 8316.
- [2] W. Ding, C. F. A. Negre, J. L. Palma, A. C. Durrell, L. J. Allen, K. J. Young, R. L. Milot, C. A. Schmuttenmaer, G. W. Brudvig, R. H. Crabtree and V. S. Batista, “Linker Rectifiers for Covalent Attachment of Transition Metal Catalysts to Metal-Oxide Surfaces”, *ChemPhysChem* (2014) **15**: 1138
- [3] W. Ding, C.F.A. Negre, L. Vogt, V. S. Batista, “Single Molecule Rectification Induced by the Asymmetry of a Single Frontier Orbital”, *J. Chem. Theory Comput.* (2014) **10**: 3393.
- [4] C. F. A. Negre, K. J. Young, M. B. Oviedo, L. J. Allen, C. G. Sánchez, K. N. Jarzemska, J. B. Benedict, R. H. Crabtree, P. Coppens, G. W. Brudvig, V. S. Batista, “Photoelectrochemical hole injection revealed in polyoxotitanate nanocrystals functionalized with organic adsorbates”, *J. Am. Chem. Soc.* (2014) **136**, 16420.
- [5] A. C. Durrell, G. Li, M. Koepf, K. J. Young, C. F. A. Negre, L. J. Allen, W. R. McNamara, H. Song, V. S. Batista, R. H. Crabtree, G. W. Brudvig, “Photoelectrochemical Oxidation of a Turn-On Fluorescent Probe Mediated by a Surface Mn(II) Catalyst Covalently Attached to TiO<sub>2</sub> Nanoparticles”, *J. Catalysis* (2014) **310**, 37.

## Intramolecular Photo-Induced Electron Transfer in Ionic Liquids

Jessalyn A. Devine,<sup>1</sup> Marissa Saladin,<sup>2</sup> Mark Maroncelli,<sup>2</sup> Gary A. Baker,<sup>3</sup> James F. Wishart,<sup>4</sup> and Edward W. Castner, Jr.<sup>1</sup>

<sup>1</sup>Dept. of Chemistry and Chemical Biology, Rutgers University, Piscataway, NJ 08854

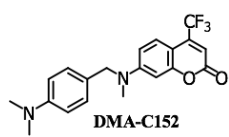
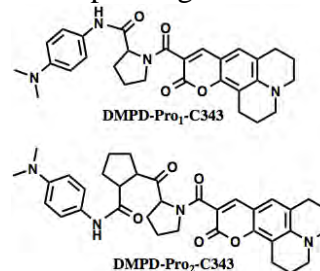
<sup>2</sup>Department of Chemistry, The Pennsylvania State University; University Park PA 16802

<sup>3</sup>Department of Chemistry, University of Missouri-Columbia, Columbia, Missouri 65211

<sup>4</sup>Department of Chemistry, Brookhaven National Laboratory, Upton, NY 11973-5000

Ionic liquids (ILs) continue to find increasing use as solvents and electrolytes for a number of fields of energy research, including solar photoelectrochemical cells and photocatalysis, electrochemical applications such as batteries and super-capacitors, chemical separations, and pre-treatment of lignocellulosic biomass for application to liquid fuels. One of our recent collaborations has focused on understanding how the unique properties of ionic liquids can lead to different outcomes for photo-induced electron-transfer reaction rates and mechanisms when compared to conventional solvents such as water or CH<sub>3</sub>CN. To this end, we are studying the rates and mechanisms of photo-induced charge separation for donor-acceptor dyads<sup>1</sup> and donor-bridge-acceptor molecules where the bridging molecules are proline or diproline,<sup>2,3</sup> shown below. The solvent reorganization dynamics for a number of classes of ILs are known to include both an ultrafast ~1 ps relaxation together with a broad distribution of relaxation rates spanning several orders of magnitude, with a centroid of ~1 ns.<sup>4</sup>

In all cases we have observed to date, intramolecular photo-induced electron-transfer does not display well defined rates, but rather a broad distribution of rates that spans 2-3 orders of magnitude.<sup>2,3</sup> For the DMPD-Pro<sub>1</sub>-C343 donor-bridge-acceptor molecule, a primary low energy conformation determines the donor-acceptor coupling H<sub>DA</sub>, which is found to be in the strongly-coupled regime. When the diproline linker is used, five low energy conformations are found, with estimated for the lowest three energy conformations having smaller values of H<sub>DA</sub> and the two higher energy conformations having quite strong coupling values.



Similar studies have been initiated with the dyad DMA-C152. Characterization in conventional solvents shows higher electron transfer rates than the proline bridged systems, which will enable us to probe faster portions of the ionic liquid response.

1. X. Li, M. Liang, A. Chakraborty, M. Kondo, and M. Maroncelli, *J. Phys. Chem. B* **115**, 6592 (2011).
2. J. A. Devine, M. Fekry, M. E. Harries, R. A. M. Rached, J. Issa, J. F. Wishart and E. W. Castner, Jr., *J. Phys. Chem. B*, 2015 *submitted*.
3. H. Y. Lee, J. B. Issa, S. S. Isied, E. W. Castner, Jr., Y. Pan, C. L. Hussey, K. S. Lee, and J. F. Wishart, *J. Phys. Chem. C* **116**, 5197 (2012).
4. X.-X. Zhang, M. Liang, N. P. Ernstring, and M. Maroncelli, *J. Phys. Chem. B* **117**, 4291 (2013).

## Hot Carriers in Lead Iodide Perovskites and Si Nanostructures

Ye Yang, Matthew R. Bergren, Jao van de Lagemaat, Kai Zhu, Nathan R. Neale, and Matthew C. Beard

Chemical and Material Sciences Center  
National Renewable Energy Laboratory  
Golden, Co, 80401

We studied hot-carrier relaxation in planar lead iodide perovskite films (Fig., left) using transient absorption spectroscopy and in Silicon Nanostructures using time-resolved THz spectroscopy (Fig., right). We find a surprisingly efficient hot-phonon bottleneck in methylammonium lead tri-iodide perovskite films that slows down cooling of hot-carriers by 3-4 orders of magnitude. The cooling times found in solution deposited perovskite films are an order of magnitude better than in highly crystalline GaAs layers and comparable to highly engineered III-V based multiple quantum wells which also achieves slowed cooling. We also developed a model that fully reproduces the TA-spectrum and explains the role of free-carrier compared to exciton bleaching. We measure the exciton dissociation time to be  $\sim 150$  fs at room temperature. We also show that time-resolved THz spectroscopy (TRTS) can distinguish between hot-carriers and excitons in silicon nanostructures and measured the exciton formation time in silicon quantum dots (QDs) as a function of QD diameter. We find an increase in the exciton formation time from  $\sim 600$  fs to  $\sim 1$  ps as the QD diameter is reduced from 6.3 to 3.5 nm consistent with a phonon-bottleneck in quantum confined systems.

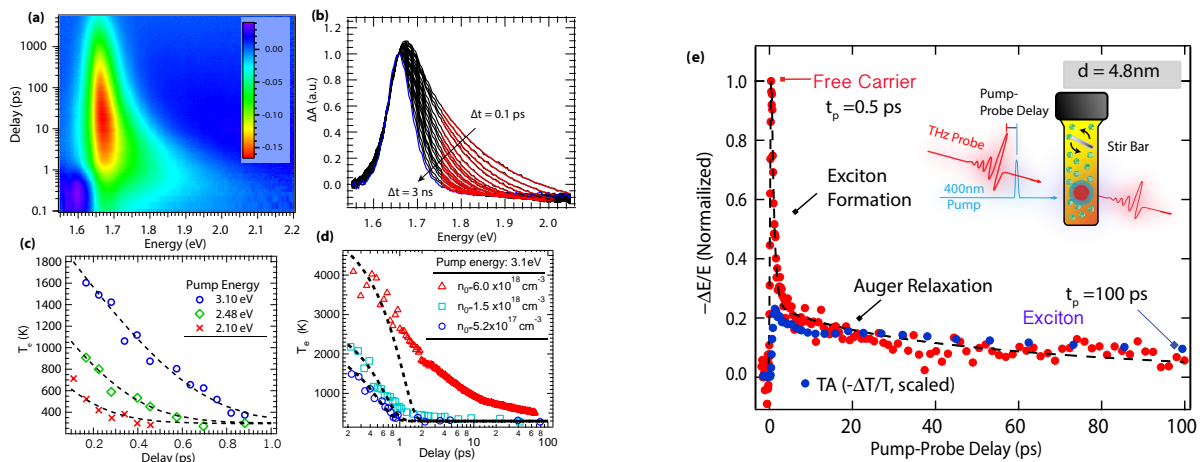


**Figure.** (a) Pseudocolor representation and (b) normalized perovskite TA spectra for  $n_0$  of  $6.0 \times 10^{18} \text{ cm}^{-3}$  and  $\hbar\omega_{pump}$  of 3.10 eV. The amplitude at  $\hbar\omega_{probe} = 1.66 \text{ eV}$  are normalized to 1. The higher energy tails are fit by Maxwell-Boltzmann distribution (red lines) to extract the carrier temperature,  $T_e$ . Time-dependent  $T_e$  (c) the same  $n_0$  but varying  $\hbar\omega_{pump}$  (d) the same  $\hbar\omega_{pump}$  but varying  $n_0$ . Above a critical carrier density the thermalization increases from 30 fs to over 20 ps. (e) Time-resolved THz spectroscopy (TRTS) dynamics for 4.8 nm Si QDs (red circles) compared to transient absorption dynamics (blue circles). The initial decay of the TRTS dynamics follows the formation of excitons from hot-charge carriers. Once excitons are formed the decay of the TRTS dynamics follows the exciton decay dynamics similar to transient absorption.

## Dynamics of Charged and Neutral Species in Ionic Liquids: From Molecules to Electrons

J. C. Araque<sup>†</sup>, C. Xu<sup>†</sup>, S. K. Yadav<sup>†</sup>, M. Shadeck<sup>‡</sup>, M. Maroncelli<sup>‡</sup>, and C. J. Margulis<sup>†</sup>  
<sup>†</sup>Department of Chemistry, University of Iowa, Iowa City, IA 52242 and <sup>‡</sup> Department of Chemistry, The Pennsylvania State University; University Park PA 16802

As often organic, yet charged media, Ionic Liquids (ILs) possess unique characteristics suitable for various energy processes involving electron transfer and charge transport. Applications range

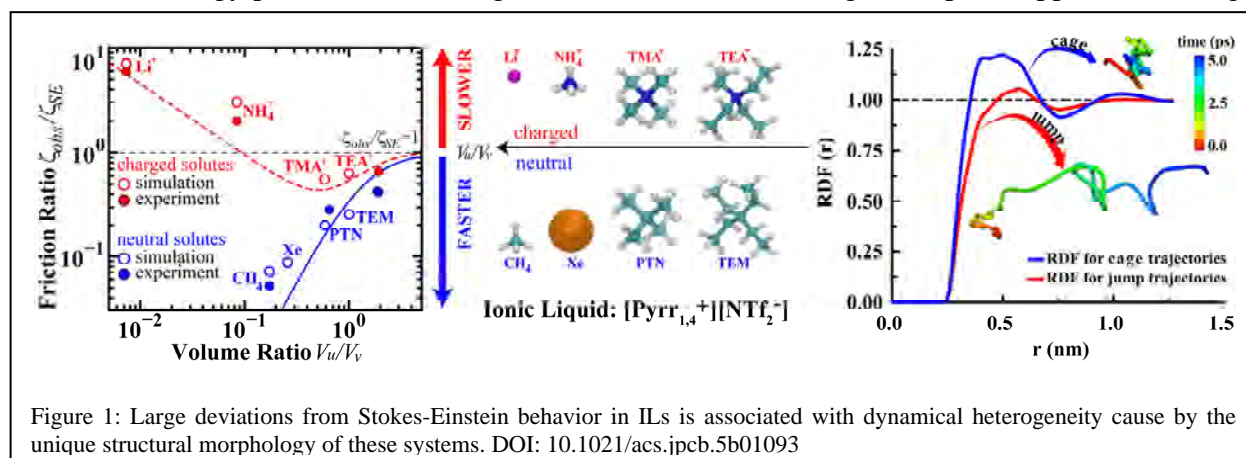


Figure 1: Large deviations from Stokes-Einstein behavior in ILs is associated with dynamical heterogeneity cause by the unique structural morphology of these systems. DOI: 10.1021/acs.jpcc.5b01093

from solar energy processing and electrochemical applications to nuclear fuel recycling. The optimal use of these novel liquids in energy related tasks requires a fundamental understanding of their structure, dynamics and solvation characteristics. In particular, an understanding of the behavior of solutes that are charged or neutral, or that of excess electrons and holes is still at an infancy stage. A set of recent articles from our groups have provided insight into all such processes. Ionic liquids are known to be structurally heterogeneous on a nanoscale level; they are also known to be dynamically heterogeneous. A firm link between these two types of heterogeneities has been elusive, but recent work from the Maroncelli and Margulis groups (DOI: 10.1021/acs.jpcc.5b01093) has shown that for charged and neutral solutes, large deviations with respect to Stokes-Einstein behavior are linked to dynamical heterogeneity for which the origin can be traced to structural heterogeneity intrinsic of ILs (Fig. 1). ILs have regions that are stiff (high friction) and soft (low friction) associated with charged and apolar liquid components respectively.

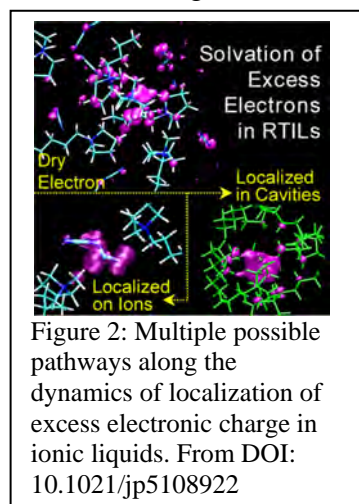


Figure 2: Multiple possible pathways along the dynamics of localization of excess electronic charge in ionic liquids. From DOI: 10.1021/jp5108922

In the case of excess electronic charge, recent theoretical work from our group has proposed that different pathways of localization may co-exist after a dry excess electron is injected into aliphatic ILs based on the dicyanamide anion. Each of the pathways should have clearly different spectroscopic signatures. One pathway is associated with the localization on ions, the other with localization in cavities that give rise to characteristic s-to-p type cavity-electron transitions. Similar theoretical predictions we made in the case of ILs based on the bis(trifluoromethylsulfonyl)-amide anion are consistent with latest experiments performed by the Blank group.

## CO<sub>2</sub> and H<sub>2</sub>O Reduction in an Aqueous Photoelectrochemical Environment

Yuan Hu, Yong Yan, Elizabeth L. Zeitler, Jing Gu, Anna Wuttig, and Andrew B. Bocarsly  
 Department of Chemistry  
 Frick Laboratory, Princeton University  
 Princeton, New Jersey 08544

We previously demonstrated that the kinetic limitations associated with the multielectron reduction of CO<sub>2</sub> can be overcome by employing aqueous pyridinium as an electrocatalyst at an illuminated p-GaP photocathode. At pH = 5.2 and using the (100) face of GaP, methanol has been observed with 96% faradaic efficiency at a ~300mV underpotential. Based on this finding, our current studies focus on a mechanistic understanding of this chemistry, along with an expansion of the process to other photoelectrodes and co-catalysts. In general, the observed chemistry is surface sensitive, yet the details of this coupling are ill defined at present. To attack this problem, we are investigating the related III-V semiconductors: p-GaAs and p-GaInP<sub>2</sub>, both, which efficiently reduce CO<sub>2</sub> in the presence of aromatic amines. In these cases, the observed product distribution varies from that obtained using p-GaP/pyridinium systems, with the latter two systems, forming carbon-carbon bonded products along with C<sub>1</sub> products.

We have also launched an investigation of p-type metal oxides as potential photocathodes, focusing on delafossite-structured materials. This class of semiconductors represents a relatively overlooked materials regime when it comes to photoelectrochemistry. Separately, we have synthesized and characterized several p-type delafossites, including p-CuFeO<sub>2</sub>, p-CuRhO<sub>2</sub>, and p-AgRhO<sub>2</sub>. These layered materials, as shown in Figure 1, consist of Fe(III) or Rh(III) centers octahedrally coordinated to oxygens to form one layer that is interwoven with Cu(I) or Ag(I) oxide layers. We obtain a measured band gap of 1.36eV with a conduction band edge at -1.1 V vs. SCE for Mg doped CuFeO<sub>2</sub>. This material selectively reduces CO<sub>2</sub> to formate without the need for a dissolved co-catalyst. The system develops ~800 mV of underpotential.

The analogous delafossite, p-CuRhO<sub>2</sub>, has a band gap of 1.9 eV with a conduction band edge at -1.5 V vs. SCE at neutral pH. This material is inept at CO<sub>2</sub> reduction. Rather, it efficiently splits water. Experimentally, we find that that material splits water under zero bias, with reasonable stability in basic electrolytes containing dissolved oxygen. Faradaic efficiencies for H<sub>2</sub> production reach 80%, even in the presence of O<sub>2</sub>. The Ag(I) analog, p-AgRhO<sub>2</sub>, provides a band gap of 1.7eV, yielding an improved spectral match to the solar spectrum. It too is efficient at splitting water at basic pH values with a conduction band edge at -1.1 V vs. SCE at neutral pH. This material shows enhanced current-voltage properties with a greater underpotential for water splitting (fill factor ~50%), and an increased current density compared to the copper system due to improved bulk carrier mobilities. This latter effect appears due to improved hole transport between the rhodium oxide layers.

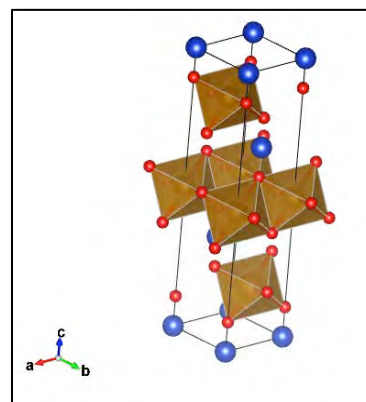


Figure 1: Powder x-ray determined structure of p-MM'O<sub>2</sub> containing alternating planes of M=Cu or Ag (blue) and O<sub>h</sub> M'O<sub>2</sub> units M=Fe or Rh (brown).

## Solvent and Solute Dynamics in Ionic Liquid + Conventional Solvent Mixtures

Min Liang<sup>1,2</sup>, Brian Conway<sup>1</sup>, Xin-Xing Zhang<sup>3</sup>, Edward W. Castner, Jr.<sup>2</sup>, and Mark Maroncelli<sup>1</sup>  
<sup>1</sup>Department of Chemistry, The Pennsylvania State University; University Park PA 16802, and  
<sup>2</sup>Department of Chemistry and Chemical Biology, Rutgers University, Piscataway, NJ 08854  
<sup>3</sup>Department of Chemistry, Humboldt Universität zu Berlin, D-12489 Berlin, Germany

Ionic liquids are finding increasing use in myriad applications, including many in energy-related fields.<sup>1</sup> Mixtures with conventional solvents are often used as a means of tuning properties for such applications, and to support these efforts we have been examining structural, energetic, and dynamical aspects of two types of ionic liquid + conventional solvent mixtures.

In one set of studies, the energetics and time-dependence of solvation of coumarin 153 have been measured in two prototypical mixtures of a simple ionic liquid, [Im<sub>41</sub>][BF<sub>4</sub>], with acetonitrile<sup>2</sup> and water<sup>3</sup> and compared to dielectric solvation models. Whereas the energies and dynamics in the acetonitrile mixture evolve in a simple manner with composition, with water the solvation properties appear to be dominated by the ionic liquid component. Preliminary simulation results indicate preferential solvation in the latter case and differences in mixture structure are responsible for these differences. Ongoing simulations are providing molecular insights into the nature of solvation in such mixtures.

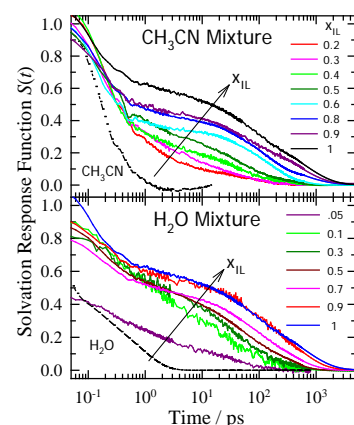


**Fig. 1:** Solvation response functions of C153 in [Im<sub>41</sub>][BF<sub>4</sub>] + CH<sub>3</sub>CN mixtures.

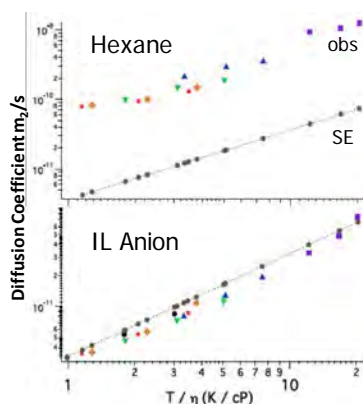


**Fig. 2:** Component self-diffusion coefficients in [P<sub>14,666</sub>][Tf<sub>2</sub>N] + hexane mixtures.

In other work, the structure and dynamics of mixtures of [P<sub>14,666</sub>][Tf<sub>2</sub>N] with n-hexane

have been studied.<sup>4</sup> Ionic liquids formed with the P<sub>14,666</sub><sup>+</sup> cation, which has one tetradecyl and four hexane substituents, are unusual for their extreme degree of apolar domain formation. Addition of hexane (with which the IL is nearly miscible) expands the size of these domains and is expected to lead to even more unusual behavior. Initial experiments show that the n-hexane component diffuses roughly 10-fold faster than would be expected based on hydrodynamic models, whereas the cation and anion diffusion rates nearly equal to these predictions. Computer simulations are just beginning to reveal the origins of this unusual behavior.

### References:

1. Wishart, J. F. *Energy Environ. Sci.* **2009**, *2*, 956-961.
2. Liang, M.; Zhang, X.-X.; Kaintz, A.; Ernsting, N. P.; Maroncelli, M. *J. Phys. Chem. B* **2014**, *118*, 1340.
3. Zhang, X.-X.; Liang, M.; Hunger, J.; Buchner, R.; Maroncelli, M. *J. Phys. Chem. B* **2013**, *117*, 15356.
4. Liang, M.; Khatun, S.; Castner, E. W. *J. Chem. Phys.* **2015**, *142*, 121101.

## Semiconductor-Electrocatalyst Contacts: Theory, Experiment, and Applications to Solar Water Photoelectrolysis

Shannon W. Boettcher, Fuding Lin, Thomas J. Mills, and Benjamin F. Bachman

Department of Chemistry and the Materials Science Institute

University of Oregon, Eugene, Oregon 97403

Semiconductor photoelectrodes coated with electrocatalysts are key components of photoelectrochemical (PEC) energy conversion and storage systems. Despite an intense effort aimed at optimizing these materials, there has been little systematic work focused on the semiconductor-electrocatalyst (SC|EC) interface. The SC|EC interface is important because it is responsible for collecting the photoexcited electron-hole pairs generated in the semiconductor. To understand interfacial electron transfer between electrocatalysts and bulk semiconductors, we developed a new experimental technique, dual-working-electrode photoelectrochemistry, allowing for direct electrical measurement of the SC-EC interface *in situ*.<sup>1</sup> We also developed the first theory of the SC|EC interface and applied the theory through numerical simulation to explain the measured interfacial charge transfer properties of the SC|EC junction.<sup>2</sup> We discovered that porous, ion-permeable, redox-active catalysts such as Ni-(Fe) oxyhydroxides form “adaptive” junctions where the effective interfacial barrier height for electron transfer depends on the charge state of the catalyst. This is in sharp contrast to interface properties of dense ion-impermeable catalysts, which we found form buried junctions that could be described by simple equivalent electrical circuits. These results elucidated a design principle for catalyzed photoelectrodes - high-performance photoelectrodes with direct SC|EC junctions use soft deposition techniques that yield ion-permeable catalysts.<sup>3</sup>

In the last year we have expanded this work to analyze a range of common OER catalysts.<sup>4</sup> For all catalysts deposited by electrodeposition on TiO<sub>2</sub> (hydrous IrO<sub>x</sub>, CoOOH, FeOOH, and NiOOH) the photovoltage output and fill factor of the combined system was *independent* of the catalyst identity. When the catalysts were deposited in a solid nanocrystalline form, the junction properties varied dramatically for the different catalysts and in all cases were worse than the ion-permeable catalysts. These results are important because they confirm the key prediction that the activity of the catalyst does not affect current-voltage response in the adaptive junction limit. We also developed a new general model describing semiconductor photoelectrodes with both catalyst layers and surface states. Simulations show how catalyst activity affects the charge stored in the surface states and hence the response of the photoelectrode.<sup>5</sup>

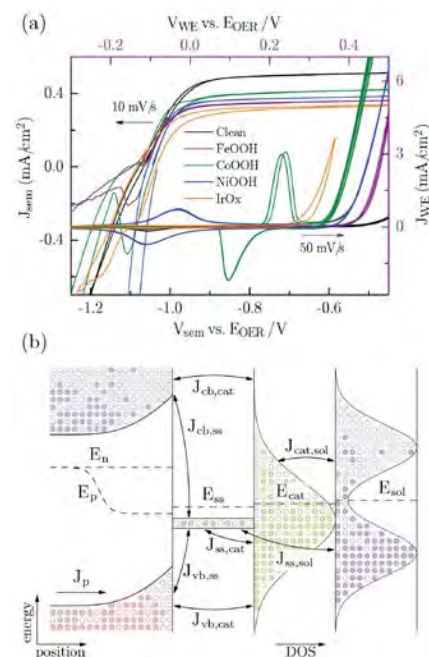


**Figure 1.** (a) Dark and light  $J$ - $E$  curves of catalyzed TiO<sub>2</sub> in the adaptive junction limit. (b) Schematic of photoelectrode simulation containing surface states.

(1) Lin, F.; Boettcher, S. W. *Nat. Mater.* **2014**, *13*, 81. (2) Mills, T. J.; Lin, F.; Boettcher, S. W. *Phys. Rev. Lett.* **2014**, *112*, 148304. (3) Lin, F.; Boettcher, S. W. In *Photoelectrochemical Solar Fuel Production: From Basic Principles to Advanced Devices*; Bisquert, J., Gimenez, S., Eds.; Springer: 2016. (submitted) (4) Lin, F.; Bachman, B.; Boettcher, S. W. *In revision.* **2015**. (5) Mills, T. J.; Boettcher, S. W. *In prep.* **2015**.

## Nanotechnological and Biological Systems for Light-Driven Hydrogen Evolution

Kara L. Bren, Richard Eisenberg, and Todd D. Krauss

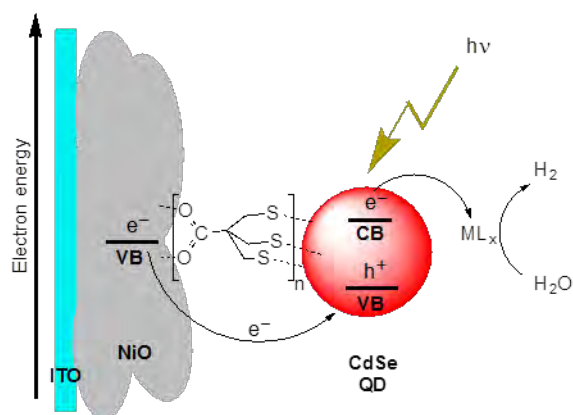
Department of Chemistry

University of Rochester

Rochester, NY 14627-0216

Solar energy has great potential for long-term impact, but efficient and economical means of storing solar energy are needed to support its wider implementation. One attractive approach is to photochemically drive the reduction of aqueous protons to form hydrogen ( $H_2$ ) as an energy carrier. In this project, systems that convert light energy into the formation of hydrogen are being developed. The approach draws on advances in synthetic chemistry, nanotechnology, and biochemistry to develop integrated systems for solar hydrogen production.

A major advance in photochemical hydrogen production consisted of the use of CdSe-DHLA (dihydrolipoic acid) quantum dot photosensitizers and an in situ formed Ni-DHLA catalyst to produce over 600,000 turnovers of hydrogen with a quantum yield of ~36% and a durability of weeks. The photocatalytic  $H_2$  production activity of various CdSe semiconductor nanoparticles was compared including CdSe and CdSe/CdS quantum dots (QDs), CdSe quantum rods (QRs), and CdSe/CdS dot-in-rods (DIRs). With equivalent photons absorbed, the  $H_2$  generation activity orders as: CdSe QDs  $\gg$  CdSe QRs  $>$  CdSe/CdS QDs  $>$  CdSe/CdS DIRs, consistent with ultrafast transient absorption measurements of the electron transfer processes but opposite of the electron-hole separation efficiency.



DHLA dissociation was problematic in assessing other molecular catalysts because of DHLA exchange with catalyst ligands. Consequently, exchange-inert tripodal trithiolate capping agents have been synthesized and the resultant quantum dots were found to operate with different Co bis(dithiolate) complexes as catalysts. The work was further advanced in the fabrication of photocathodes in which the exchange-inert CdSe QDs were attached to NiO films on a conductive surface, thereby eliminating the need for ascorbic acid as a sacrificial electron donor (see Figure).

Biomolecular catalysts provide proton shuttles, second-sphere interactions, and protection of the metal active site to enhance efficiency and activity. As part of this effort, metalloproteins are being engineered into artificial hydrogenases so that these properties of proteins can be incorporated into the catalysts. The first-generation biocatalyst is a cobalt-porphyrin-peptide that provides  $>20,000$  turnovers of hydrogen electrocatalytically. The poor stability of this catalyst, which degrades after 20 minutes of electrolysis, is a major drawback. To improve on this catalyst, the full-length protein Co-HtM61A was prepared. This artificial hydrogenase maintains high activity for 3 hours and provides  $>100,000$  turnovers of hydrogen. In ongoing work, this catalyst is being modified with the goal of lowering overpotential.

## Lateral Charge Transport Along a Surface Dye Monolayer and Applications for Solar Light-Driven Water Oxidation

Gary W. Brudvig, Bradley J. Brennan, Alec C. Durrell, Matthieu Koepf, Robert H. Crabtree, Charles A. Schmuttenmaer, and Victor S. Batista

Department of Chemistry  
Yale University  
New Haven, CT 06520-8107

Molecular systems for photoelectrocatalysis involve converting light into electrical charge that can then be used to drive an electrochemical reaction. The water splitting reaction affords a storable and transportable source of energy, and is therefore an ideal solar-to-fuels system. However, current molecular water-oxidation photoelectrocatalytic cells have substantial kinetic limitations under normal solar photon flux. In these systems, electron-hole recombination processes out-compete charge build-up on the catalytic centers for the  $4e^-$  electrochemical reaction. One method of overcoming these limitations is to design a system where multiple light-harvesting photosensitizers work cooperatively with a single catalyst. We devised a model system consisting of a monolayer of porphyrin molecules bound to  $\text{SnO}_2$  semiconductor nanoparticles. Absorbed photons initiate a photo-induced charge separation, whereby an electron is injected into the semiconductor and an oxidized porphyrin species (hole) is produced. This hole is capable of traversing the monolayer surface via a series of electron self-exchanges with neighboring molecules. When a dyad molecule, acting as a thermodynamic trap and model for a catalyst, is embedded in the porphyrin monolayer, it is efficiently oxidized even when embedded as a relatively low percentage of the monolayer. Computational modelling of transient absorption spectroscopy data revealed that the rate of electron self-exchange was  $\sim 40$  per microsecond. This general concept of hole hopping and localization effectively concentrates oxidizing equivalents at a predetermined site. These model studies are being extended to investigate photochemical turnover of molecular water-oxidation catalysts by using a catalyst embedded in an array of high-potential porphyrin photosensitizers on a metal oxide semiconductor surface.

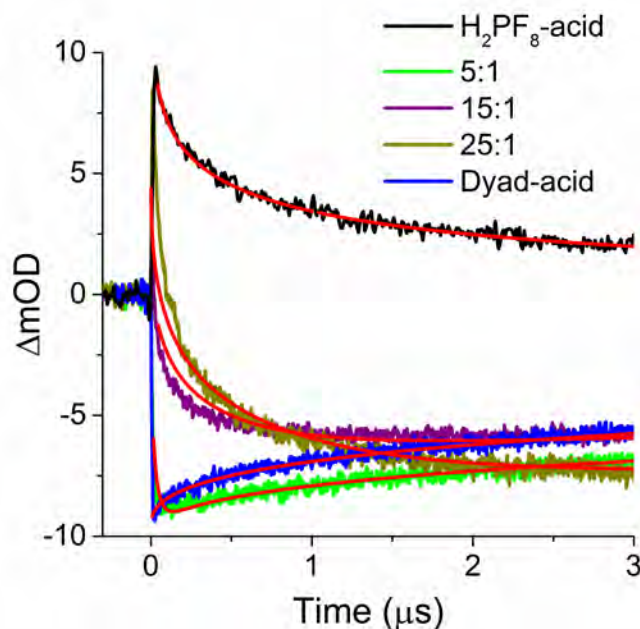


**Figure 1.** Transient absorption traces for varying monomer/dyad ratios with fits shown in red. Samples were photoexcited at 515 nm and probed at 560 nm.

## Photoinduced Formation of Transient Ni(I) Porphyrin Captured by X-ray Snapshots and Theoretical Modeling

M. L. Shelby,<sup>1,2</sup> M. W. Mara,<sup>1,2</sup> N. E. Jackson,<sup>1,2</sup> A. B. Stickrath,<sup>1</sup> and L. X. Chen,<sup>1,2</sup>

<sup>1</sup>Chemical Sciences and Engineering Division, Argonne National Laboratory, Lemont, IL 60439

<sup>2</sup>Department of Chemistry, Northwestern University, Evanston, IL 60208

P. J. Lestrage<sup>3</sup> and X. Li<sup>3</sup>

<sup>3</sup>Department of Chemistry, University of Washington, Seattle, WA 98195

Despite having very interesting photophysics and photochemistry, Ni(II) tetramesitylporphyrin (NiTMP), like other nickel(II) porphyrins, has not been considered useful in solar energy conversion processes involving photoinduced electron transfer at the metal center or the macrocycle, which yield transient redox equivalents for potential catalytic reactions. Ni(II) porphyrins are not known to undergo nickel oxidation state changes due to photoexcitation. However, nickel is considered to be a catalytic center in many systems. Then the questions are 1) can Ni(II) undergo a photoinduced redox reaction, 2) how fast does the reaction occur, 3) what is the transient oxidation state of the Ni center, and 4) can we control the lifetime of the metal center with structural factors to enable its function as a photocatalyst? These questions are fundamentally important for us to understand the interplay between the electronic and nuclear structure as these molecules are photoexcited, from which the guidance of molecular design for photocatalyst can be optimized. In the past, we measured the electronic and nuclear structures of NiTMP in its excited state with 100-ps time resolution, which revealed the electronic configuration change from  $3d^8 (d_{z^2})^2(d_{x^2-y^2})^0$  (**A**) to  $3d^8 (d_{z^2})^1(d_{x^2-y^2})^1$  (**B**). In our recent study at the Linac Coherent Light Source (LCLS) with 100-fs time resolution, an intermediate state with only a 2-ps lifetime was captured by X-ray transient absorption spectroscopy (XTA). This state was assigned as Ni(I) or  $3d^9 (d_{z^2})^2(d_{x^2-y^2})^1$  (**C**) and showed a red-shifted  $1s \rightarrow 4p_z$  transition and a single peak in the pre-edge region. Theoretical calculations using TDDFT methods resulted in a ruffled Ni(I)TMP with longer Ni-N distances than those of **A** but shorter than **B**. Further, the ES-TDDFT calculations showed that when Ni(II) is reduced to Ni(I), the effective repulsive potential felt by the  $1s$  electron is increased, raising its energy, and reducing the  $1s \rightarrow 4p_z$  transition energy. These calculations also corresponded well with the single peak in the  $1s \rightarrow 3d$  transition pre-edge region. These results inspire molecular design with planar macrocyclic coordination geometry and proper Ni-N distances which could prolong the Ni(I) transient state lifetime to enable photocatalytic functions.

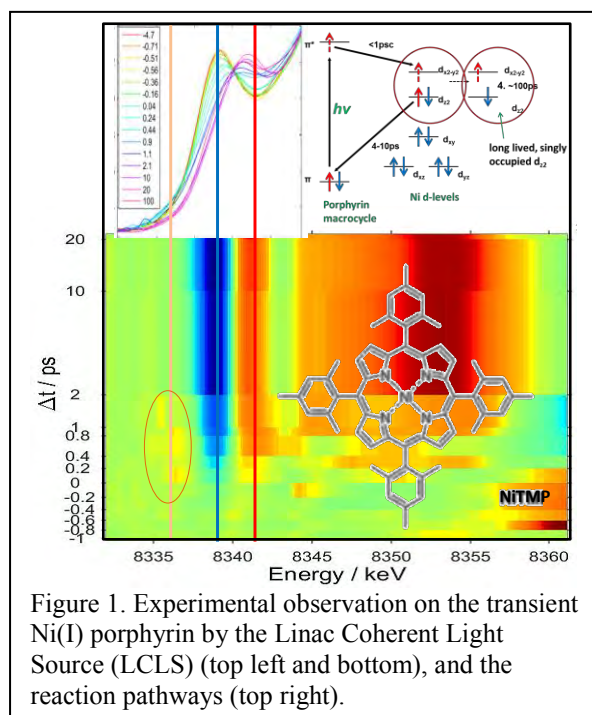


Figure 1. Experimental observation on the transient Ni(I) porphyrin by the Linac Coherent Light Source (LCLS) (top left and bottom), and the reaction pathways (top right).

## Understanding Roles of Ultrafast and Coherent Electronic and Atomic Motions in Photochemical Reactions

L. X. Chen,<sup>1,2</sup> F. N. Castellano,<sup>3</sup> X. Li,<sup>4</sup> K. L. Mulfort,<sup>1</sup> M. A. Ratner,<sup>2</sup> R. D. Schaller,<sup>1,2</sup> G. C. Schatz,<sup>2</sup> T. Seideman,<sup>2</sup> D. M. Tiede,<sup>1</sup> L. Young,<sup>5</sup> and their coworkers

<sup>1</sup>Chemical Sciences and Engineering Division, <sup>5</sup>the Advanced Photon Source, Argonne National Laboratory, Lemont, IL 60439; <sup>2</sup>Department of Chemistry, Northwestern University, Evanston, IL 60208; <sup>3</sup>Department of Chemistry, North Carolina State University, Raleigh, NC 27695; <sup>4</sup>Department of Chemistry, University of Washington, Seattle, WA 98195

Understanding the quantum dynamics of molecular excited states is an important area of chemical science. The newly formed research team aims at investigating the significance of coherent electronic or nuclear motions in the fundamental steps of photochemical reactions and energetic, structural and dynamic factors pertinent to these coherent motions. The research activities in our multi-disciplinary team (Figure 1) are focused on A) identifying, characterize and compute functionally important coherent electronic and nuclear motions in the excited state properties of transition metal complexes (TMCs) with one or multiple metal centers. B) understanding and engineering ultrafast two-electron transfer reactions in chromophore-catalyst-chromophore supramolecular TMC assemblies and C) elucidating structure-function relationships between plasmonic structures and coherent ultrafast lattice “breathing modes” in gold nanoparticles and exploring their effects on the interfacial electron and energy transfer processes of TMC-nanoparticle hybrids.

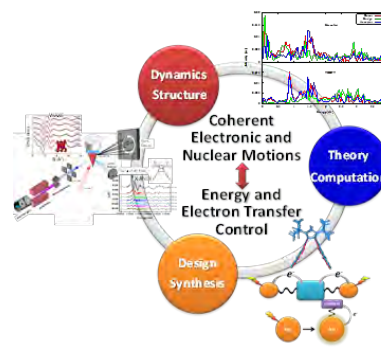


**Figure 1.** Research focuses and methods.

Preliminary results have been obtained and will be collectively presented. In each project, synthesis, characterization and theoretical calculations are combined to answer specific questions. In particular, we will present the following preliminary results on:

1. Ultrafast electronic and atomic motions transition metal complexes. As one example, local and global structural analysis in CO bound iron porphyrins in myoglobin has been carried out using simultaneous detection of ultrafast X-ray transient absorption and small angle scattering, implementing the optical polarization selected X-ray transient absorption (OPS-XTA) spectroscopy. The polarization selection effect and molecular dynamics have been simulated.
2. Correlations of structural factors with coherent lattice motions in nearly uniformly sized gold bipyramidal nanoparticles and theoretical simulations have shown the size dependent lattice coherent motions which effect on energy and electron transfer will be investigated. We have characterized the acoustic modes of these nanoparticles using the *abaqus* continuum mechanics program, and this provides a quantitative description of the experiments.
3. Developing computational methods in calculation of excited state structures, core level transitions and dynamics. The combination of ultrafast visible excitation and transient x-ray measurements provides significant challenges for electronic structure theory due to the production of doubly excited states, but we are developing new TDDFT approaches to handle this capability, with applications being made to the TMC's being studied in the experiments.

## Combined Biomass Valorization and Hydrogen Production in a Photoelectrochemical Cell

Hyun Gil Cha, and Kyoung-Shin Choi  
 Department of Chemistry  
 University of Wisconsin-Madison  
 Madison, WI 53706, USA

In a typical hydrogen-producing photoelectrochemical cell (PEC), water reduction at the cathode (producing hydrogen) is accompanied by water oxidation at the anode (producing oxygen). This anode reaction is, however, not kinetically favorable. In this presentation, we discuss the possibility of utilizing solar energy for biomass conversion by performing oxidation of 5-hydroxymethylfurfural (HMF) to 2,5-furandicarboxylic acid (FDCA) at the anode of a PEC (Figure 1). HMF is a key intermediate in biomass conversion, and FDCA is an important monomer for the production of numerous polymers. Using 2,2,6,6-tetramethylpiperidine-1-oxyl as a mediator, we obtained near quantitative yield and 100% Faradaic efficiency at ambient conditions without the use of precious metal catalysts. This reaction is also thermodynamically and kinetically more favorable than water oxidation. Our results suggest that solar driven biomass conversion can be a viable anode reaction that has the potential of increasing the efficiency as well as the utility of PECs constructed for solar fuel production.

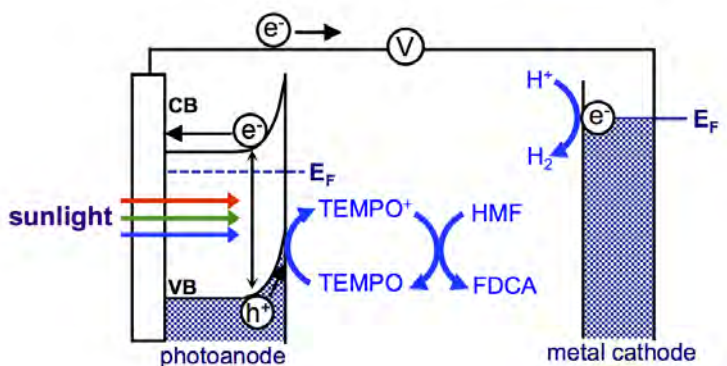
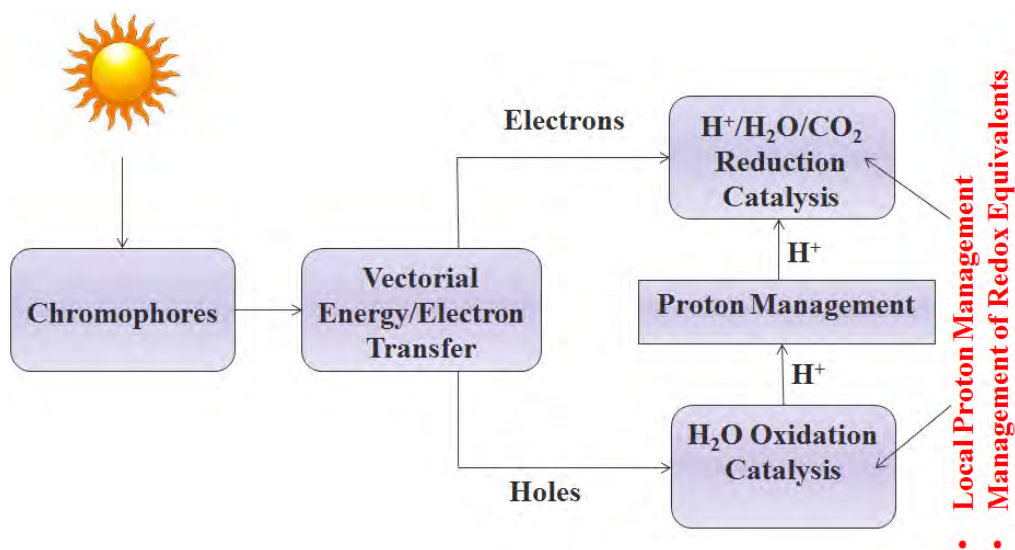


**Figure 1.** Schematic representation of a photoelectrochemical TEMPO-mediated HMF oxidation coupled with H<sub>2</sub> production.

## Chromophores and Molecular Catalysts for Oxidation and Reduction Reactions Relevant to Artificial Photosynthesis

Javier J. Concepcion, David W. Shaffer, Yan Xie, Gerald Manbeck, and Mehmed Z. Ertem  
 Chemistry Department  
 Brookhaven National Laboratory  
 Upton, NY 11973-5000

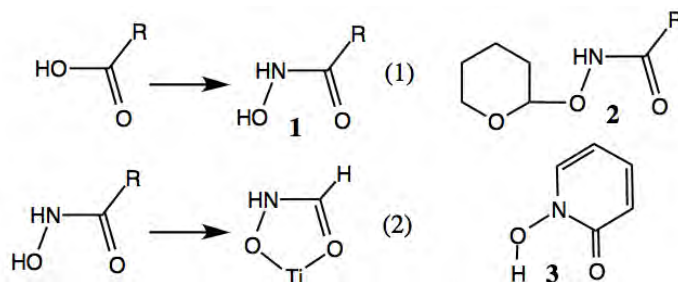
The generation of solar fuels *via* artificial photosynthesis requires integrated systems that combine light absorption, excited state quenching with vectorial energy/electron transfer leading to charge separation, water oxidation and water/CO<sub>2</sub> reduction catalysis. Proton management and product separation are also key requirements for efficient and safe operation. In addition, local proton management as well as redox potential leveling at the oxidative and reductive catalytic sites needs to be taken into account. In this presentation we will discuss new chromophores with tyrosine-histidine mimics for light absorption and vectorial charge separation as well as new families of fast, robust and efficient water oxidation catalysts. For the latter, we will present a combined study that includes kinetic and mechanistic results in solution and with the catalysts anchored to metal-oxide electrodes, pH-dependent electrochemistry and spectroelectrochemistry and DFT calculations. In addition, new catalytic pathways that take into account the need for careful management of redox equivalents for efficient catalysis will be discussed. These new pathways provide unprecedented access to the rational design of better catalysts and to the generation and characterization of catalytic intermediates.



## Hydroxamate as Water-Stable Anchors for Water-Splitting Solar to Fuel Strategies

Gary W. Brudvig, Bradley J. Brennan, Jeffrey Chen, Matthieu Koepf, Robert H. Crabtree, Subhajyoti Chaudhuri, Benjamin Rudshiteyn, Charles A. Schmuttenmaer, and Victor S. Batista  
 Department of Chemistry and Energy Sciences Institute  
 Yale University  
 New Haven, CT 06520-8107

Water splitting can lead to a storable source of energy, and is therefore often considered in solar-to-fuels work. In aiming to attach molecular components to semiconductor electrodes for photoelectrocatalysis in aqueous solutions, we obviously need water-stable anchors. The commonest anchor in regular use is carboxylate; its big advantage is the ready availability of carboxylate dyes and catalysts, such as MK2 or N719. Carboxylates tend to detach in aqueous media, however. We have tried to leverage the availability of carboxylates by converting them to hydroxamates (**1** in eq. 1), an anchor that is much more solidly bound to semiconductor oxides (eq. 2). A number of siderophores bind Fe(III) via hydroxamate groups and so our proposal might be considered biomimetic. Several conventional carboxylate to hydroxamate conversion strategies have proved possible, such as EDC coupling of RCOOH with NH<sub>2</sub>OH or spontaneous coupling of RCOCl with NH<sub>2</sub>OH. On occasion it is useful to have a protected form of the hydroxamate, in which case we find THP is an excellent protecting group. In addition THP-protected molecules (**2**) spontaneously deprotect on, and attach to, TiO<sub>2</sub> surfaces. Extensive physical data show that the monodeprotonated form binds and that the anchor efficiently conducts electrons well during photoinjection. MK-2 has been converted to the hydroxamate and incorporated into a DSSC with the result that the system works significantly better in 10% aqueous MeCN than in dry MeCN, in contrast with the standard MK-2 carboxylate. Cyclic hydroxamates, such as **3**, have also proved useful. By synthesis of model compounds, such as trinuclear **4** (XRD structure shown below), we can spectroscopically compare IR data with those of surface-bound analogues. DFT work has been a valuable help in interpreting the data.



## Exploring How Symmetry and Vibration Impact Singlet Fission in Molecular Dimers

Niels H. Damrauer, Jamie Snyder, Thomas Carey, Jasper Cook, and Tarek Sammakia  
 Department of Chemistry and Biochemistry  
 University of Colorado at Boulder  
 Boulder, Colorado 80309

This work explores fundamental underpinnings of singlet fission (SF) and is motivated by previous observations from our group that SF yields in thin film systems may be impacted by spectroscopies that drive low-frequency inter-chromophore motions. We will focus on recent explorations of molecular dimers where two tetracene-derived chromophores are held in a partially co-facial geometry by a structurally well-defined bicyclic alkyl bridge. We will describe the outcome of our synthetic efforts including a final strategy to generate the dimer BT1 (see Fig. 1) wherein Diels-Alder cycloaddition reactions are followed by multiple oxidation and reduction steps. In Fig. 1 is shown UV-Vis spectra comparing the tetracene dimer BT1 to a one-chromophore model complex Tc-e. Band splitting in the UV (260–320 nm) as well as in higher-energy vibronic transitions within the near-UV (see inset) indicate interchromophore electronic coupling for BT1. We will describe the outcome of static and time-resolved photoluminescence studies as well as ultrafast transient absorption measurements designed to characterize the SF rate and yield for this dimer.

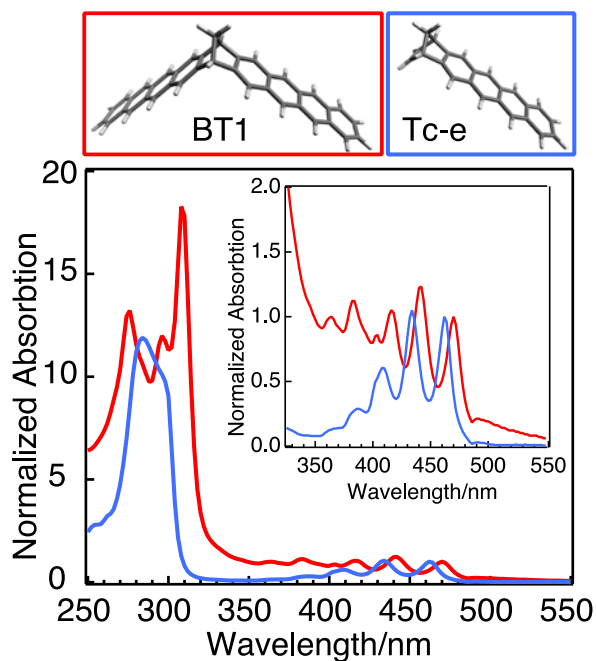


**Figure 1.** Normalized UV-Vis absorption spectra for BT1 (red) and monomer model complex Tc-e (blue) in room temperature chloroform.

We will also describe recent theoretical efforts (in collaboration with Subotnik’s group at the University of Pennsylvania) to calculate key one-electron coupling matrix elements that enable a rapid but accurate estimation of diabatic coupling between singlet and multiexcitonic excited states in the SF photoreaction. These methods use a Boys localization unitary transformation as a starting point, and with them we are able to study how vibrational motions of the BT1 dimer impact diabatic coupling for the photoreaction. A specific outcome has been an understanding of which normal modes of motion – in terms of symmetry and frequency – can be expected to impact the SF rate. Interestingly, very specific rules emerge that are based on orbital phase and how it impacts the constructive versus destructive interference of hole-transfer versus electron-transfer quantum mechanical pathways to SF. These ideas will play into our quantum control efforts based on pulse shaping. Finally, we will touch on proposed aza-tetracene dimers that exploit these symmetry rules in ground state structures to achieve large diabatic coupling for SF.

## Mono- and Dinuclear Cobalt Complexes with O-Donor Ligands for WOC

J. L. Steele, L. Tahsini, M. K. Youmans, Chen S. Sun, and L. H. Doerr

Chemistry Department

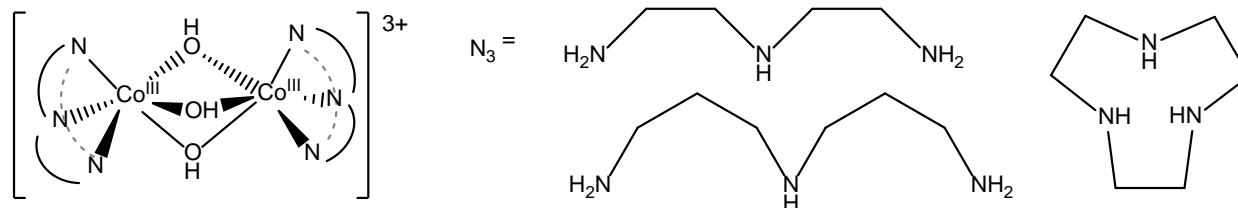
Boston University

Boston, MA 02215

The current global energy demand for low-cost, clean, and sustainable energy has prompted intensive development of earth-abundant transition metal complexes as potential catalysts for water oxidation. Our group has focused on complexes with O-donor ligands because so many effective WOC systems are dominated by O-donor ligands including Photosystem II, Co-Pi, perovskites, and layered-double hydroxides. We are interested not only in effective catalysis, but particularly in the detailed coordination environments of the metal atoms at which the oxygen oxidation and O-O bond formation steps occur.

The first of two systems to be presented is our most recent work with the perfluoropinacolate ( $\text{pin}^{\text{F}}$ ) ligand and its derivatives.<sup>1</sup> Previously we have presented work on  $[\text{Co}^{\text{II}}(\text{OH}_x)(\text{pin}^{\text{F}})_2]^{n-}$  and  $[\text{Ni}^{\text{II}}(\text{OH}_x)(\text{pin}^{\text{F}})_2]^{n-}$  as molecular precursors for water oxidation. We have recently characterized a new oxidized intermediate, namely  $[\text{Co}^{\text{III}}(\text{pin}^{\text{F}})_2]^-$  and will present data that shed light on its conversion, via proposed OH radicals, to  $[\text{Co}^{\text{II}}(\text{Hpfa})_4]^{2-}$  in which (Hpfa)- is monodeprotonated hexafluoropropane-2,2-diol. We are also investigating the related manganese system, including the new compounds  $[\text{Mn}^{\text{II}}(\text{pin}^{\text{F}})_2]^{2-}$  and  $[\text{Mn}^{\text{III}}(\text{OH}_x)(\text{pin}^{\text{F}})_2]^{n-}$ , the latter of which has been structurally characterized as the  $\{\text{K}(\text{18C6})\}[\text{Mn}(\text{THF})(\text{pin}^{\text{F}})_2]$  derivative. This synthetic and structural data will be presented as well as pH-dependent UV-vis and electrochemical data in a Pourbaix format to delineate the electron and proton transfer behavior within this aqueous system.

The other system under investigation is a series of old dinuclear Co compounds with bridging hydroxide ligands, as shown in the scheme.



Given the prevalence of polynuclear species in earth-abundant WOC, models that can test mechanistic dinuclear hypotheses with O-donor ligands are needed. During our investigative studies, we found that some of these complexes are capable of evolving oxygen from water at neutral pH at  $\sim 1.2$  V vs Ag/AgCl. Some of these complexes produce a catalytic current under more acidic and reducing conditions implying that these compounds can catalyze both water reduction and water oxidation in a pH-dependent manner. Electrochemical and UV-vis spectroscopic data will be presented to put these compounds in the context of the literature.

<sup>1</sup>Tahsini, L., Specht, S. E., Lum, J. S., Nelson, J. J. M., Long, Alexandra F. Golen, J.A., Rheingold, A. L., Doerr, L. H. *Inorg. Chem.* **2013**, 52, 14050-14063

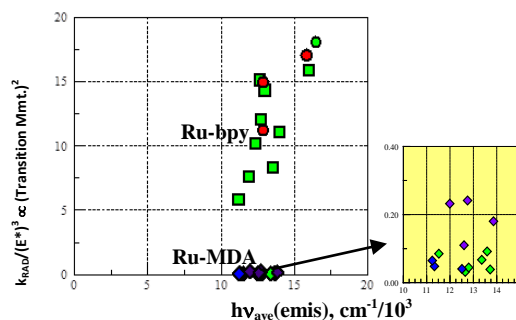
## Spectroscopic and DFT Studies Related to the Design of Transition Metal Solar Photosensitizers

Ryan A. Thomas,<sup>‡</sup> Chia Nung Tsai,<sup>†</sup> Shivnath Mazumder,<sup>‡</sup> Yuan Jang Chen,<sup>†</sup> H. Bernhard Schlegel,<sup>‡</sup> Claudio N. Verani,<sup>‡</sup> and John F. Endicott<sup>‡</sup>

Departments of Chemistry  
<sup>‡</sup>Wayne State University and <sup>†</sup>Fu-Jen Catholic University  
 Detroit, MI 48202 (USA) and New Taipei City 24205 (Taiwan, R.O.C)

Among the important criteria for selecting photosensitizers are: (a) the efficiency of the transduction of light energy into chemical processes; and (b) the long term functional stability of the sensitizer. We have used spectroscopic and computational triplet state modeling approaches to examine pathways of sensitizer deactivation and/or degradation that compete with charge transfer to a substrate in several series of [Ru(II) donor]-[acceptor ligand] complexes. We are searching for patterns of these excited state properties that are relevant to the design of efficient, durable sensitizers. Factors that contribute to the overall efficiency of a sensitizer include: (a) radiative (RAD) and (b) non-radiative relaxation (NRD) to the ground state; (c) internal conversion (IC) to a triplet metal centered state (<sup>3</sup>MC); (d) <sup>3</sup>MLCT photochemistry. Factors (a)-

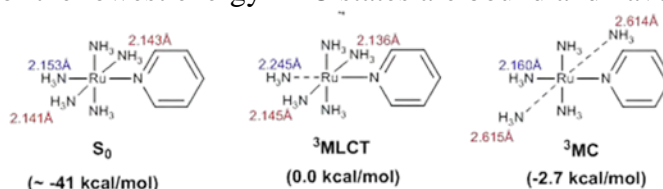
(c) usually determine intrinsic excited state lifetimes ( $\tau = (k_{\text{RAD}} + k_{\text{NRD}} + k_{\text{IC}})^{-1}$ ). We find that  $k_{\text{RAD}}$  for Ru-(bipyridine) chromophores increases more strongly with excited state energy ( $E^* = h\nu_{\text{max}}(\text{emis})$ ) at 77 K) than the expected  $(E^*)^3$  dependence implying MLCT/ $\pi\pi^*(\text{bpy})$  mixing (Thomas, et al. J. Phys. Chem. B, 2015; [dx.doi.org/10.1021/jp510949x](https://doi.org/10.1021/jp510949x)). In contrast Ru-MDA chromophores (MDA = py, pz, 4,4'-bpy, etc.) so far show only the  $(E^*)^3$  dependence. Surprisingly, several Ru-bpy



chromophores have large emission quantum yields at 77 K even though  $E(\text{MC}) < E(\text{MLCT})$  (Mazumder, et al., Can. J. Chem., 2014; [doi.org/10.1139/cjc-2014-0155](https://doi.org/10.1139/cjc-2014-0155)) while most Ru-MDA chromophores emit very weakly even if  $E(\text{MC}) > E(\text{MLCT})$ . Many  $[\text{Ru}(\text{NH}_3)_5\text{MDA}]^{2+}$  have very weak emissions from <sup>3</sup>MLCT excited states and these complexes provide models for intrinsic excited state distortions in the limit of no stereochemical constraints on Ru-ligand motions. DFT modeling indicates that many of the lowest energy <sup>3</sup>MC states are bound and have very large distortions in both bonds along a

single L-Ru-L axis in the plane orthogonal to the Ru-MDA axis. Stereochemical constraints on the donor ligand distortions can alter the pattern of distortions and raise the <sup>3</sup>MC state energies.  $E(^3\text{MC})$  for the

$[\text{Ru}(\text{NH}_3)_5\text{MDA}]^{2+}$  and  $\text{trans-}[\text{Ru}(\text{NH}_3)_4(\text{MDA})_2]^{2+}$  complexes is nearly MDA independent (about 45 kcal/mol); a little less than the energy calculated for breaking two Ru-NH<sub>3</sub> bonds of the ground state (about 54 kcal/mol). Variations found for  $E(^3\text{MC})$  have been small, but there may be increases with Ru-L bond energy and with stereochemical constraints.

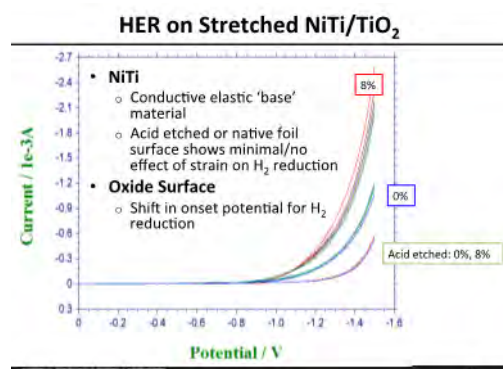


## Tuning Optoelectronic and Catalytic Properties with Dynamic Strain

Drazenka Svedruzic, Eric Benson, Brian A. Gregg, and Sue Ferrere  
 Chemistry and Nanoscience Center  
 National Renewable Energy Laboratory  
 Golden, Colorado 80401

We are probing the use of dynamic strain to strain bonds and access a continuum of fundamental properties, including more reactive, non-equilibrium conformations relevant to catalysis, photochemistry, and photovoltaics. The ability to dynamically and reversibly tune optoelectronic properties by stretching bonds or distorting lattices allows access to multiple variations on a system, and has the potential to eliminate the time and resource-intensive methods normally required to change properties (e.g., altering a functional group, changing out a metal, growing a new film). Strain thus becomes a proxy for chemical composition.

Elastic strain is a well established technique in device physics for changing electronic properties, e.g. to boost carrier mobility in field effect transistors; however, systems typically employ a built in (“static”) stress via lattice mismatch. Our approach employs dynamic tensiometry coupled to analytical techniques (e.g. electrochemistry, UV-Vis, fluorescence, raman - “spectrotensiometry”) that can monitor changes in optoelectronic and catalytic properties as we reversibly stretch metals, chromophores, and semiconductors.



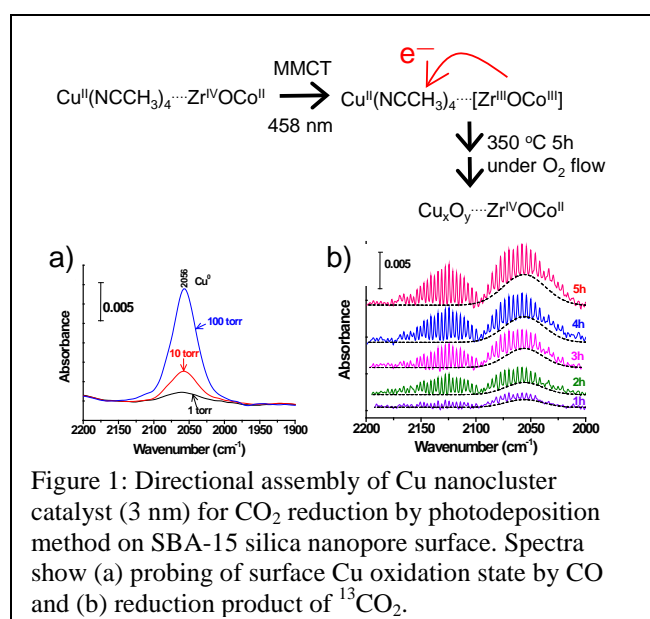
Using dynamic tensiometry coupled to electrochemistry, recent results indicate a reduction in the overpotential for the hydrogen evolution reaction (HER) when a TiO<sub>2</sub>-coated NiTi (“Nitinol”) electrode is stretched (see Figure). We are also preparing 2D semiconductors, like MoS<sub>2</sub>, on elastic substrates and using spectrotensiometry to characterize its optoelectronic and catalytic properties under strain. The reduced dimensionality imparts greater mechanical strength, and it is also catalytic for the HER. Both of these systems will be presented.

## Photo-driven Hierarchical Assembly of Inorganic Light Absorber – Nanocluster Catalyst Units for CO<sub>2</sub> Reduction and H<sub>2</sub>O Oxidation

Wooyul Kim, and Heinz Frei

Physical Biosciences Division, Lawrence Berkeley National Laboratory  
Berkeley, CA 94720

Addressing the gap of multi-electron photoreduction of CO<sub>2</sub> beyond 2-electron reduction products like CO to more deeply reduced, liquid products such as methanol is among the most challenging tasks of artificial photosynthesis. Our approach is to couple an all-inorganic binuclear light absorber to a multi-electron catalyst for CO<sub>2</sub> activation. To accomplish the coupling between acceptor metal of the charge-transfer chromophore and the catalyst, a photodeposition method was developed to achieve the proper spatial arrangement of the components on a silica nanopore surface.



Taking a similar synthetic approach as recently shown for the assembly of an Ir oxide nanocluster coupled to a Zr<sup>IV</sup>OCu<sup>II</sup> metal-to-metal charge-transfer (MMCT) chromophore for accomplishing the photosynthetic cycle of CO<sub>2</sub> reduction by H<sub>2</sub>O on the nanoscale,<sup>1</sup> we have developed a photodeposition method for assembling a cuprous oxide nanocluster (3 nm according to TEM analysis and EDX) adjacent to the Zr acceptor center (Figure 1). Electron transfer coupling of the ZrOCu unit with the catalyst cluster was demonstrated by visible light driven reduction of surface Cu centers to metallic Cu<sup>0</sup> probed by adsorbed CO (Fig. 1a).<sup>2</sup> Photocatalytic yields measured by <sup>13</sup>CO evolution from <sup>13</sup>CO<sub>2</sub> (Fig. 1b) were found to depend on the state of reduction of

the surface Cu centers. For Cu<sub>x</sub>O<sub>y</sub> clusters coupled to Ti<sup>IV</sup>OCu<sup>II</sup> MMCT chromophore, visible light driven electron transfer (458 nm) resulted in the formation of Cu<sup>I</sup> surface centers only, while use of higher energy UV photons (355 nm) gave a mixture of Cu<sup>0</sup> and Cu<sup>I</sup> surface centers. These results indicate that the reduction potential of the acceptor center and excitation energy of the MMCT chromophore strongly influence the electronic state of the cluster accessed by the light driven electron transfer.

Search for reduction products beyond CO, and of transient reaction intermediates at the Cu<sub>x</sub>O<sub>y</sub> nanoparticle surface by transient FT-IR spectroscopy at the gas-solid interface and in aqueous suspension for elucidating the catalytic mechanism currently in progress will be discussed.

1. Kim, W.; Yuan, G.; McClure, B. A.; Frei, H. *J. Am. Chem. Soc.* **2014**, *136*, 11034-11042.
2. Kim, W.; Frei, H., to be submitted.

## Quantum Chemical Modeling of Transition Metal Containing Systems

Andrew Weisman, Louis Brus, Mike Steigerwald, Steve Jerome, and Richard A. Friesner  
Department of Chemistry  
Columbia University  
New York, NY 10027

Our current efforts are focused in two principal directions: (1) develop density functional theory (DFT)-based methods for accurate treatment of transition metal containing systems, particularly redox potentials, pKa's, and other quantities of importance in reactions important for solar energy conversion such as charge separation and water splitting; (2) application of these methods to understand charge separation, trapping, and transport in the Gratzel cell. Progress in both areas is described below.

In previous work, we have shown that a simple, ligand based correction scheme, in the framework of a general approach to improving DFT based on localized orbital corrections (LOCs), reduces the mean unsigned error (MUE) for redox potentials in transition metal complexes from  $\sim 0.4\text{eV}$  to  $\sim 0.1\text{eV}$ . We have also calculated pKa's for hexaaquo metal complexes, reducing the MUE from 5.7 pKa units for the B3LYP functional to 0.9 pKa units when the LOC corrections are utilized. In this calculation, only one adjustable parameter was employed; the raw pKa value was scaled to optimize the fit to experiment. The remaining parameters were all taken from the existing B3LYP-LOC model for transition metals (DBLOC). We have also applied the redox corrections from DBLOC to the calculation of barrier heights in the extraction of a hydrogen atom by the heme groups of the enzymes methane monooxygenase and P450; the DBLOC corrections significantly improve agreement with experimental data. Finally, we are engaged in a large scale comparison of DBLOC with alternative DFT functionals such as PBE and M06 for spin splittings and redox potentials. This comparison provides an essential benchmark with regard to the degree of improvement obtained by the DBLOC model.

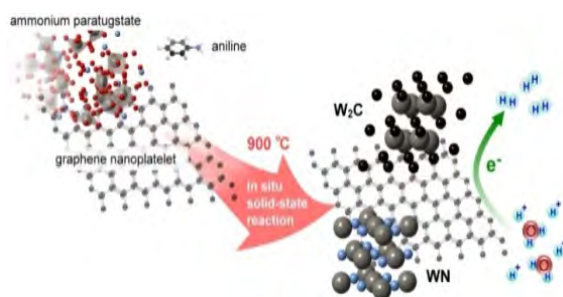
In previous work, we investigated an ambipolar model for electron transport in the Gratzel cell, achieving good agreement with experiment for various energetic and transport properties, and providing a physical model for the electron trapping site. These calculations used the lithium cation as the ion stabilizing an excess electron in a reduced Ti (III) site. We have now investigated what happens if a proton is used in the model rather than lithium. The calculations show that the proton binds differently to the  $\text{TiO}_2$  than lithium; it forms a covalent bond with an oxygen atom, as opposed to an ion pair. This leads to a greater trap depth and larger activation energy for transport, in good agreement with experimental measurements of these quantities. These results demonstrate the consistency and predictive capabilities of our model.

Most recently, we have been studying anatase (as opposed to rutile) models of  $\text{TiO}_2$ , to investigate the effects of the structure of the material on the energy and transport properties computed previously. We also have initiated an effort to calculate kinetics for a water splitting reaction at the surface of a  $\text{TiO}_2$  particle. This work builds on our water splitting calculations for ruthenium complexes, and the development of cluster  $\text{TiO}_2$  models discussed above.

## Artificial Photosynthesis for the Generation of Fuels using Molecular Catalysts and Metal Carbide-Nitride Composites

Etsuko Fujita, James T. Muckerman, and Kotaro Sasaki  
 Chemistry Department  
 Brookhaven National Laboratory  
 Upton, NY 11973-5000

The electrolysis of water presents an environmentally responsible alternative for hydrogen generation when electricity is produced by renewable energy. However, carrying out the hydrogen evolution reaction (HER,  $2\text{H}^+ + 2\text{e}^- \rightarrow \text{H}_2$ ) requires alternatives to noble metal catalysts. We synthesized graphene-supported molybdenum and tungsten carbide-nitride nanocomposites by using either soybeans or aniline as the source of carbon and nitrogen, and the ammonium salt of the metal oxide to produce active, durable electrocatalysts with very low overpotentials for the HER in acidic environments (*Energy Environ. Sci.*, **2013**, *6*, 1818-1826; *ChemSusChem*, **2014**, *7*, 2414-2418).



Despite the potential for production of solar-generated hydrogen, the problems of storage and transport remain. Another approach to solar fuels generation is based on  $\text{CO}_2$  hydrogenation using catalysts for recycling  $\text{CO}_2$  combined with the use of solar-generated  $\text{H}_2$ . Proton-responsive ligands offer control of catalytic reactions through modulation of pH-dependent properties, second coordination sphere stabilization of transition states, or by providing a local proton source for multi-proton, multi-electron reactions. We present our recent investigations using metal complexes with proton-responsive ligands on: (1)  $\text{CO}_2$  hydrogenation to formate; (2) formic acid (FA) dehydrogenation; and (3) interconversion of  $\text{CO}_2$  and formic acid. We have recently shown significant breakthroughs for formic acid dehydrogenation to  $\text{CO}_2$  and  $\text{H}_2$  using Ir complexes bearing hydroxy substituted pyrimidine-imidazole ligands (TOF up to 322,000  $\text{h}^{-1}$  and TON greater than 1,200,000) in water (*ACS Catal.* in revision).

We have also prepared Re and Ru complexes with proton-responsive ligands such as 6,6'-dihydroxy-2,2'-bipyridine for electrochemical and photochemical  $\text{CO}_2$  reduction. However, contrary our hypothesis that the local proton source might facilitate protonation of a  $\text{CO}_2^-$  ligand or accelerate catalysis through secondary coordination sphere interactions, we discovered that ligand-based reactivity for electrochemical  $\text{CO}_2$  reduction impedes catalysis (*J. Phys. Chem. B*, **2015**, ASAP).

We thank our collaborator Dr. Yuichiro Himeda (AIST, Tsukuba, Japan).

## Model Dyes for the Study of Molecule/Metal Oxide Semiconductor Interfaces and Electron Transfer Processes

E. Galoppini,<sup>a</sup> R. A. Bartynski,<sup>b</sup> L. Gundlach,<sup>c</sup> A. Batarseh,<sup>a</sup> H. Fan,<sup>a</sup> S. Rangan,<sup>b</sup>  
J. Nieto-Pescador,<sup>c</sup> and B. Abraham<sup>c</sup>

<sup>a</sup> Chemistry Department, Rutgers University-Newark, Newark, NJ 07102

<sup>b</sup> Department of Physics and Astronomy, Rutgers University-New Brunswick, Piscataway, NJ 08854

<sup>c</sup> Department of Physics, University of Delaware, Newark, DE 19716

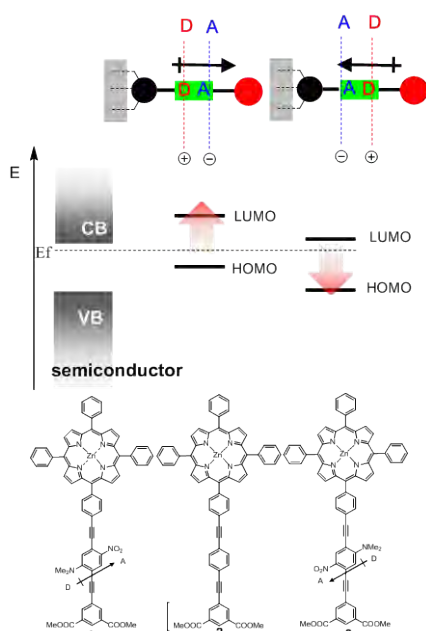


**Figure 1.** Schematic representation of the dyes and energy level shifts.

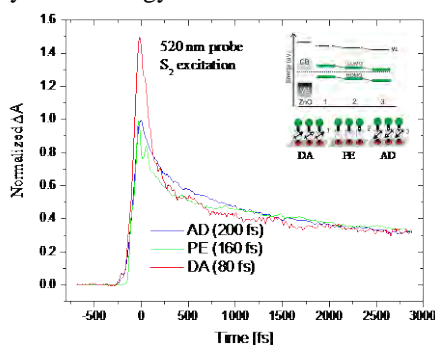


**Figure 2.** Normalized electron injection for **1-3** bound to TiO<sub>2</sub> films.

The poster describes the synthesis and study of porphyrin dyes made of an anchor group, a bridge and a chromophore, with a built-in dipole in the bridge that, when bound to TiO<sub>2</sub> or ZnO is aligned parallel or antiparallel to the semiconductor surface normal. The dipole in the bridge enabled us to establish a desired energy level alignment between the semiconductor and the chromophore. Briefly, porphyrins **1** and **3** formed a monolayer and an electrostatic potential that shifted the HOMO and LUMO of the porphyrin chromophore by ( $\pm$ )  $\sim$ 100 meV with respect to the band edges of the semiconductor, when compared with **2**, as in Figure 1. When the direction of the dipole in the linker was reversed, the shift direction was reversed by the same amount. Electron injection for **1**, **2**, and **3** bound to nanostructured TiO<sub>2</sub> films is being studied by the Gundlach group. It was recently observed that fast electron injection following Soret excitation has a different rate for the different dyes, as shown in Figure 2. The porphyrin dyes lying above in conduction band have a faster injection process than the ones at the bottom of the conduction band, in accordance with the observed dipole-induced shift ( $\tau_{inj1} > \tau_{inj2} > \tau_{inj3}$ ). The poster will describe the synthesis of **1-3**, the ultraviolet photoemission spectroscopy (UPS) and inverse photoemission spectroscopy (IPS) studies, the electrochemical and spectroelectrochemical properties, the ultrafast charge transfer studies and future directions for this project.

*Synthesis of Zinc Tetraphenylporphyrin Rigid-Rods with a Built-in Dipole* K. Chitre, A. Batarseh, A. Kopeccky, H. Tang, R. Lalancette, R. A. Bartynski, E. Galoppini, J. Phys. Chem. B. **2015**, in press

*Tuning Energy Level Alignment At Organic/Semiconductor Interfaces Using a Built-In Dipole in Chromophore-Bridge-Ancor Compounds* S. Rangan, A. Batarseh, K. P. Chitre, A. Kopeccky, E. Galoppini, R. A. Bartynski, J. Phys. Chem. C **2014** 118, 12923-12928

## Ionic Liquid-Enhanced Electrocatalytic Reduction of CO<sub>2</sub> with a Homogeneous Catalyst

David C. Grills

Chemistry Department, Brookhaven National Laboratory, Upton, NY, 11973-5000, USA

We recently reported a new strategy for improving the efficiency of electrocatalytic CO<sub>2</sub> reduction with a homogeneous catalyst, using an ionic liquid (IL) as both the solvent and electrolyte.<sup>1</sup> With 1-ethyl-3-methylimidazolium tetracyanoborate ([emim][TCB]) as the IL and *fac*-ReCl(bpy)(CO)<sub>3</sub> as the catalyst, the onset potential for the catalytic reduction of CO<sub>2</sub> to CO shifts positive by ~0.45 V compared to when acetonitrile solvent is used in the presence of a

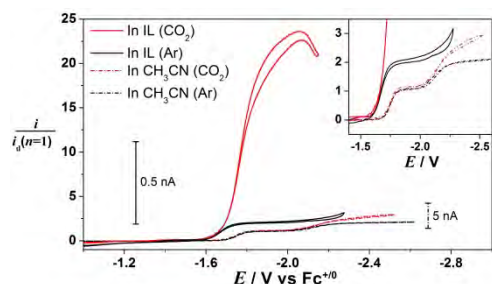


**Fig. 1.** CV's of ReCl(bpy)(CO)<sub>3</sub> recorded in [emim][TCB] (solid lines, 10 mV/s) and in CH<sub>3</sub>CN containing 0.1 M [Bu<sub>4</sub>N][PF<sub>6</sub>] (dashed lines, 100 mV/s) after argon (black) and CO<sub>2</sub> (red) purging. Currents are normalized against a diffusion-limiting current for one-electron reduction.

conventional electrolyte ([Bu<sub>4</sub>N][PF<sub>6</sub>]), see Fig. 1. Furthermore, the apparent CO<sub>2</sub> reduction rate constant,  $k_{app}$ , in [emim][TCB] exceeds that in acetonitrile by over one order of magnitude ( $k_{app} = 4000$  vs  $100$  M<sup>-1</sup> s<sup>-1</sup>) at  $25 \pm 3$  °C, as can be seen by the much greater catalytic current in Fig. 1. The two separate one-electron reduction waves of the catalyst that occur in acetonitrile combine into a single two-electron reduction wave at more positive potential in the IL.

In very recent work,<sup>2</sup> we performed a more detailed investigation of the thermodynamic parameters for the reduction of CO<sub>2</sub> to CO in acetonitrile in the presence of an imidazolium IL, and in neat imidazolium IL. This led to a  $-0.28$  V revision of the previously-estimated<sup>3</sup>

standard electrode potential for the reduction of CO<sub>2</sub> to CO in wet acetonitrile (1 M H<sub>2</sub>O), to  $E^\circ = -1.55$  V vs Fc<sup>+0</sup>. In the presence of an imidazolium IL, the same standard electrode potential applies. Experiments in acetonitrile in the presence of an acid-base buffer revealed the bifunctionality of imidazolium cations for homogeneous electrochemical CO<sub>2</sub> reduction, i.e., as proton donors and catalytic promoters. Future work is aimed at clarifying the nature of the interaction between the IL and the catalyst that results in catalytic promotion. We will also investigate a range of diverse IL cations and anions to determine structure-property relationships to maximize CO<sub>2</sub> reduction efficiency, and will explore the development of new Re- and Ru-based homogeneous electrocatalysts for use with ILs.

1. Grills, D. C.; Matsubara, Y.; Kuwahara, Y.; Golisz, S. R.; Kurtz, D. A.; Mello, B. A. *J. Phys. Chem. Lett.* **2014**, *5*, 2033-2038.
2. Matsubara, Y.; Grills, D. C.; Kuwahara, Y. *ACS Catal.*, submitted.
3. Costentin, C.; Drouet, S.; Robert, M.; Savéant, J.-M. *Science* **2012**, *338*, 90-94.

**Acknowledgements:** We thank our collaborators on this project, Dr. Yasuo Matsubara (Kanagawa University, Japan) and Dr. Yutaka Kuwahara (Kumamoto University, Japan), and also Drs. Dmitry Polyansky and Etsuko Fujita for helpful discussions.

## Complex Photochemistry in a Molecular Artificial Photosynthetic Reaction Center

Antaeres Antoniuk-Pablant, Gerdenis Kodis, Ana L. Moore, Thomas A. Moore, Devens Gust  
 Department of Chemistry and Biochemistry  
 Arizona State University  
 Tempe, AZ 85287-1604

Since our first report of the use of fullerenes as acceptors for photoinduced electron transfer in artificial photosynthetic reaction centers, C<sub>60</sub> derivatives have been used in this capacity by many investigators due to favorable properties such as suitable redox potentials, small reorganization energies for electron transfer, and low sensitivity of their ions to solvent stabilization, relative to acceptors such as quinones. These same properties make fullerenes potentially attractive as electron relays in multicomponent photoinduced electron transfer molecules, but they have not been studied in this capacity, in part because doing so requires a very strong electron acceptor to serve as the final site in a transport chain.

Recently, we have developed new synthetic methodology for the preparation of substituted tetra-β-cyanoporphyrins. These porphyrins have high oxidation potentials, and are also very strong electron acceptors due to the electron withdrawing effects of the cyano groups. The availability of these porphyrins allowed us to design and synthesize molecular triad **1**, which consists of a fullerene (C<sub>60</sub>) linked to both a porphyrin (P) and a tetra-β-cyanoporphyrin (CyP) via a pyrrolidine group. The molecule was studied using a variety of steady-state and time-resolved spectroscopic techniques in order to determine how it responds to illumination. As each of the three chromophores can absorb light and in principle act as a donor or acceptor for either excitation or electrons one might expect a rich photochemistry, and indeed this is the case.

In toluene, only singlet-singlet energy transfer among the chromophores is observed, whereas in benzonitrile both energy and electron transfer are seen. In benzonitrile, excitation of the porphyrin yields <sup>1</sup>P-C<sub>60</sub>-CyP, which decays by electron transfer to the fullerene to give a P<sup>+</sup>-C<sub>60</sub><sup>-</sup>CyP charge-separated state and by singlet energy transfer to yield both the cyanoporphyrin first excited singlet state and a small amount of the fullerene excited singlet. The fullerene excited state undergoes photoinduced electron transfer to give P<sup>+</sup>-C<sub>60</sub><sup>-</sup>CyP and energy transfer to the cyanoporphyrin. The P<sup>+</sup>-C<sub>60</sub><sup>-</sup>CyP species evolves by electron transfer to the cyanoporphyrin, yielding P<sup>+</sup>-C<sub>60</sub>CyP<sup>-</sup>. The same final state is reached by photoinduced electron transfer to P-C<sub>60</sub>-<sup>1</sup>CyP. The P<sup>+</sup>-C<sub>60</sub>CyP<sup>-</sup> state has a lifetime of 350 ps and is formed from <sup>1</sup>P-C<sub>60</sub>-CyP with a quantum yield of 0.85. Roughly half of the charge separation is due to electron transfer via the fullerene acting as an electron relay, and the other half comes from the cyanoporphyrin excited state.

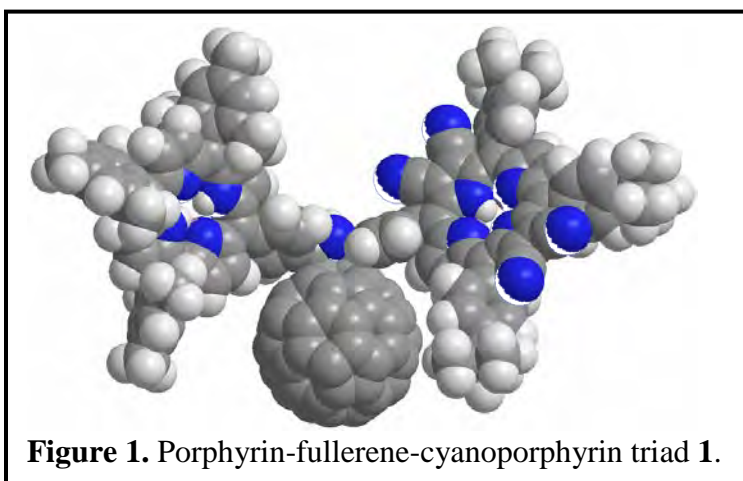


## Photo-Injection of High Potential Holes into $\text{Cu}_5\text{Ta}_{11}\text{O}_{30}$ Nanoparticles by Porphyrin Dyes

Ian Sullivan,<sup>†</sup> Chelsea Brown,<sup>‡</sup> Manuel J. Llansola-Portoles,<sup>‡</sup> Miguel Gervaldo,<sup>§</sup> Gerdenis Kodis,<sup>‡</sup> Thomas A. Moore,<sup>‡</sup> Devens Gust,<sup>‡</sup> Ana Moore,<sup>‡</sup> and Paul Maggard<sup>†\*</sup>

<sup>†</sup> Department of Chemistry, North Carolina State University, Raleigh, NC 27695-8204 USA

<sup>‡</sup> Department of Chemistry and Biochemistry, Arizona State University, Tempe, AZ 85287-1604 USA

<sup>§</sup> Departamento de Química, Universidad Nacional de Río Cuarto. Agencia Postal Nro. 3, X5804BYA Río Cuarto, Córdoba, Argentina

Excited-state hole injection (Fig. 1a, step 2) into the valence band of  $\text{Cu}_5\text{Ta}_{11}\text{O}_{30}$  nanoparticles (NP- $\text{Cu}_5\text{Ta}_{11}\text{O}_{30}$ ) was investigated through sensitization with zinc porphyrin dyes using

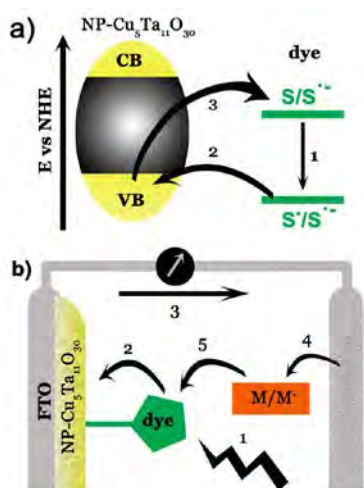


**Figure 1** a) sensitized p-type nanoparticle; b) p-type sensitized DSSC

and recombination (Fig. 1a, step 3 shown as  $\text{h}^+$  transfer) rates were obtained by transient absorption measurements.

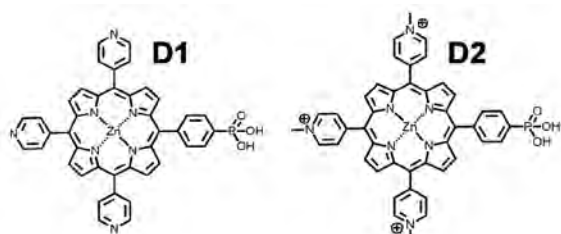


**Figure 2** Zinc porphyrins used as p-type sensitizers

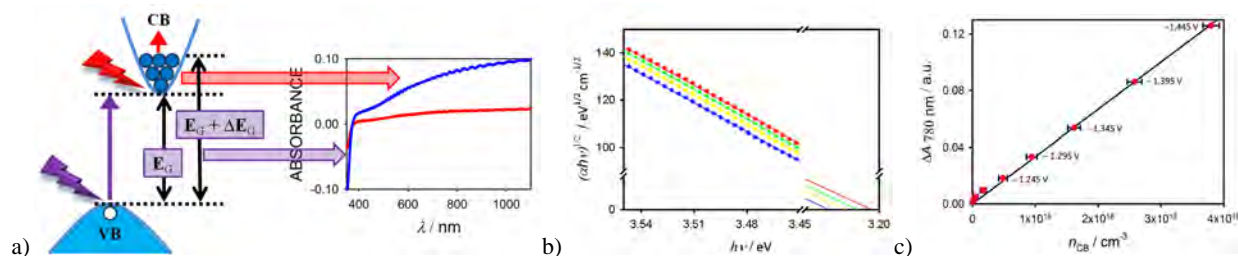
Investigating the use of NP- $\text{Cu}_5\text{Ta}_{11}\text{O}_{30}$  as a new p-type semiconductor with a VB more positive than the water oxidation potential and an extremely negative CB is a step in the development of new materials for p-DSSCs, which could lead to more efficient ways to carry out solar water splitting. This work has been submitted to the *Journal of Physical Chemistry*.

## Molecular and Material Approaches to Overcome Kinetic and Energetic Constraints in Dye-Sensitized Solar Cells

Josh Baillargeon, Dhritabrata Mandal, Yuling Xie, Thomas W. Hamann  
Department of Chemistry, Michigan State University, East Lansing, MI 48824

The general goal of this project is to understand the fundamental role of the relevant dye-sensitized solar cell, DSSC, components (redox shuttle, photoanode and sensitizer) involved in key efficiency-determining processes. Ultra-fast electron injection from a photoexcited sensitizer into a photoanode produces a charge separated state with typically high quantum efficiency. We are primarily interested in developing a detailed picture of the subsequent processes of dye regeneration and recombination which control charge collection.

The photoanode plays a central role as the donor species in recombination. One potential way to control recombination is therefore to alter the photoanode material. A detailed general kinetic model of recombination from a semiconductor to redox shuttles and/or sensitizers requires knowledge of the energy and concentration of both trapped and free electrons. Results of a new simple spectroelectrochemistry method to directly and accurately determine the absolute band energies of nanostructured semiconductor materials, as well as the concentration of free and trapped electrons, will be presented.<sup>1</sup> In this method Tauc plots are used to quantify the Burstein shift and determine the concentration of conduction band electrons as a function of potential. Once this concentration is known, the conduction band can be calculated directly. Further, the conduction band concentration can be used to calculate the extinction coefficient of these electrons (as opposed to trapped). Charge extraction measurements determine the total electron concentration, thus simple subtraction yields the concentration of trapped electrons. While this method was benchmarked with measurements on TiO<sub>2</sub>, results from other nanoparticles semiconductor materials, including SrTiO<sub>3</sub> and SrSnO<sub>3</sub>, will be presented.



a) Scheme depicting assignments of bleach and absorbance features observed in spectroelectrochemistry measurements b) Tauc plots showing bandgap shift with applied potential and c) determination of extinction coefficient of conduction band electrons in a TiO<sub>2</sub> nanoparticle electrode

The primary limitations of most redox shuttles are a large driving force required to achieve quantitative regeneration and fast recombination which limits charge collection. We are attempting to overcome these limitations by moving the redox shuttles to a new potential regime. Results of photoelectrochemical measurements of a new series of cobalt complexes based on derivatives of the pentadentate ligand 2,6-bis(1,1-bis(2-pyridyl)ethyl)pyridine, where the sixth coordination spot allows fine tuning of the redox shuttle properties, will therefore also be presented. This combination of systematic variation of redox shuttle and photoanode in tandem will ultimately allow for design rules to control recombination to redox shuttles capable of quantitative regeneration with minimal overpotential losses.

1. Mandal, D., Hamann, T.W.; *Physical Chemistry Chemical Physics* 2015, DOI: 10.1039/C5CP01714A

## Photochemical Fates of Oxygen on a Mixed Fe+Cr Oxide Surface: Desorption, Dissociation and Stabilization by Coadsorbed Water

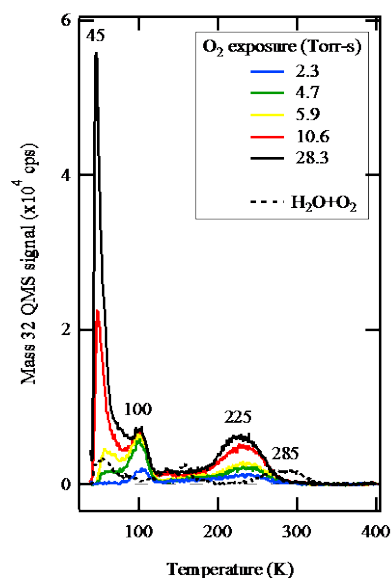
Michael A. Henderson  
 Physical Sciences Division  
 Pacific Northwest National Laboratory  
 PO Box 999, MS K8-87  
 Richland, WA 99352

The key mechanistic steps by which O<sub>2</sub> is formed during the water oxidation reaction on oxide photocatalysts are not known. A potentially important step, sometimes overlooked, is the liberation of O<sub>2</sub> from the interface. The bonding between O<sub>2</sub> and many metal cations can be strong, requiring temperatures in excess of standard operating conditions to rapidly evolve O<sub>2</sub>. In this study, the thermal and photochemical desorption of O<sub>2</sub> from a model mixed oxide surface has been explored under ultrahigh vacuum conditions. In particular, the possibility is explored that light induced desorption of O<sub>2</sub> constitutes an important process for removing product from the surface without initiated reverse reactions (e.g., O-O bond cleavage). The mixed oxide surface, which possesses a magnetite-like structure, is composed of 60% iron and 40% chromium. Identification of the binding sites of O<sub>2</sub> on this surface is a complex undertaking of its own, as interfacial characterization of mixed oxides is challenging.

Molecular oxygen is chemisorbed in two main binding states, as revealed by temperature programmed desorption, at 100 and 225 K (see adjacent figure). Another feature at 45 K represents the physisorbed state. Irradiation of the O<sub>2</sub>-covered surface with visible light results in both O<sub>2</sub> photodesorption *and* the unfortunate reverse reaction of O<sub>2</sub> photodissociation. Competition between these two channels is site-dependent.

The impact of water-coadsorption on the chemistry and photochemistry of O<sub>2</sub> on this surface was also explored. In concept, a water covered photocatalyst surface should prevent O<sub>2</sub> molecules from revisiting active sites that could promote unproductive back reactions. This, in fact, is shown to be the case. However, water also stabilizes O<sub>2</sub> on this surface to 285 K, which adversely affects the thermal evolution of O<sub>2</sub> from the catalyst. More remarkably, the H<sub>2</sub>O-O<sub>2</sub> interaction on the surface renders O<sub>2</sub> as photoinactive for desorption. These results suggest that the chemical and photochemical properties of O<sub>2</sub> on the catalyst surface must be tuned to limit accumulation of product during the water oxidation reaction.

This work was supported by the US Department of Energy, Office of Basic Energy Sciences, Division of Chemical Sciences, Geosciences & Biosciences. Pacific Northwest National Laboratory (PNNL) is a multiprogram national laboratory operated for DOE by Battelle. The research was performed using EMSL, a national scientific user facility sponsored by the Department of Energy's Office of Biological and Environmental Research and located at Pacific Northwest National Laboratory.



## Integrated Synthetic, Computational, Spectroelectrochemical and Spectroscopic Study of Polyoxometalate Water Oxidation Catalyst-Based Photoanodes

Craig L. Hill, Tianquan Lian, and Djamaladdin G. Musaev

Department of Chemistry

Emory University

Atlanta, GA 30322

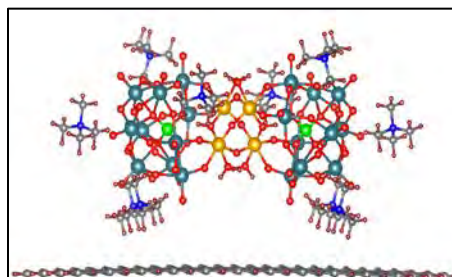
The team has obtained significant results in 3 interlinked areas:

I. New molecular water oxidation catalysts (WOCs) based on polyoxometalates (POMs) that are (a) very fast, (b) stable to O<sub>2</sub> (carbon-free) and H<sub>2</sub>O over a range of pH values, (c) stable to high temperatures, and perhaps most importantly (d) amenable to detailed structural and mechanistic investigation over a range of experimental conditions. Additional experimental studies on the POM WOC, [Co<sub>4</sub>(H<sub>2</sub>O)<sub>2</sub>(VW<sub>9</sub>O<sub>34</sub>)<sub>2</sub>]<sup>10-</sup> (“**Co<sub>4</sub>V<sub>2</sub>**”) clarify its detailed structural and magnetic properties. However, the origins of the very fast turnover of this catalyst (~1000 s<sup>-1</sup> in homogeneous catalytic reactions) relative to the isostructural phosphorus-centered analogue we reported earlier, [Co<sub>4</sub>(H<sub>2</sub>O)<sub>2</sub>(PW<sub>9</sub>O<sub>34</sub>)<sub>2</sub>]<sup>10-</sup> (“**Co<sub>4</sub>P<sub>2</sub>**”), are not yet fully clear but being probed currently by mechanistic and computational studies.

II. Robust immobilization of POM WOCs on photoelectrodes; preparation and study of dyadic and triadic POM-containing catalytic photoanodes. Electrostatic and hydrophobic methods have been shown to work for most POM WOCs. In very recent work, (a) the WOC, [Ru<sub>4</sub>(μ-O)<sub>4</sub>(μ-OH)<sub>2</sub>(H<sub>2</sub>O)<sub>4</sub>(γ-SiW<sub>10</sub>O<sub>36</sub>)<sub>2</sub>]<sup>10-</sup> (“**Ru<sub>4</sub>Si<sub>2</sub>**”), was electrostatically bound to TiO<sub>2</sub> nanoparticles (NPs), (b) a photocatalytic anode was made from the resulting TiO<sub>2</sub>-**Ru<sub>4</sub>Si<sub>2</sub>** NPs, (c) this electrode was used for 24 hours of continual photocatalytic water oxidation, and (d) several techniques were used to establish that the NP-surface-bound **Ru<sub>4</sub>Si<sub>2</sub>** POMs are still intact after this extended use. There are very few studies that show convincing evidence that a molecular WOC remains intact after extended use when immobilized on a photoelectrode. Two TiO<sub>2</sub>-Sensitizer-POMWOC triadic photoanodes with [Ru(bpy)<sub>2</sub>(H<sub>4</sub>dpbpy)]<sup>2+</sup> (**P2**) and a novel crown ether functionalized [Ru(5-crownphen)<sub>2</sub>(H<sub>2</sub>dpbpy)] (**C2P2**) sensitizers have been prepared and characterized. In addition to the observation of enhanced photocurrent upon catalyst attachment, fundamental charge separation and recombination kinetics in the triads have also been studied. Finally BiVO<sub>4</sub>-POMWOC dyadic photoanodes have been made and successfully used to catalytically oxidize water using visible light.

III. Computational methods for structure and charge transfer dynamics at POM-electrode interface have been developed. We reported a hybrid method for computing charge transfer at quantum dot-charge acceptor interface, in which quantum dots were treated by an infinite order discrete variable representation of an effective mass Hamiltonian and molecular acceptors were treated at DFT level. DFT electronic structures of new POM catalysts have been elucidated, and the interaction of POM WOCs on graphene surfaces have been probed using density functional theory (Figure 1). In these calculations, the polyanionic POM is neutralized by 10 tetramethyl ammonium (TMA) cations.

Figure 1. Bonding of the charge-neutralized POM WOC, **Ru<sub>4</sub>Si<sub>2</sub>**, on a graphene surface.



## Using Morphology to Tune Triplet Formation in Films of Singlet Fission Chromophores

Justin C. Johnson, Joseph L. Ryerson, Dylan Arias, Paul I. Dron, Josef Michl, Arthur J. Nozik  
 Dept. of Chemistry and Biochemistry, University of Colorado, Boulder, CO 80309  
 National Renewable Energy Laboratory, Golden, CO 80401

The role of interchromophore coupling on singlet fission rates and yields remains an important yet poorly understood topic. Systematic control of key intermolecular geometric variables is challenging, thwarting attempts at comprehensive fundamental understanding that can be compared with various levels of theory. We are approaching this challenge with improved methods for depositing and characterizing films or aggregates by controlling growth conditions and annealing. The most commonly employed singlet fission chromophores are 1,3-diphenylisobenzofuran (DPIBF) and its derivatives as well as tetracene. Both molecular types have been shown to undergo singlet fission with nearly 100% efficiency in certain situations. For the DPIBF monomer, sandwich or slip-stacked geometries (Fig 1, top) appear to lead to the highest triplet yield. However, we have found that thermally evaporated film polymorphs with similar slip-stacking have different singlet/triplet energetics and contain different propensities for excimer formation (Fig 1, center). Excimer formation can reduce the available energy for singlet fission in DPIBF, rendering it highly endoergic and inefficient.

Linearly linked dimers of DPIBF have yet to show high triplet yield, and the lack of any considerable  $\pi$  stacking is the likely reason. In order to investigate covalently bound chromophores that have additional flexibility to form  $\pi$ -stacked aggregates, a nonconjugated polymer of DPIBF has been studied. Polymer chains adopt various configurations depending upon the solvent (Fig 1, bottom) and film casting conditions. Up to this point, triplet formation is relatively slow while excimer formation appears fast. A conjugated version of the polymer and other methods of film formation are being investigated as strategies to induce better defined stacking geometries to enhance triplet yield and inhibit excimer formation.

Although crystalline tetracene is known to exist in two polymorphs, only one of these polymorphs has been extensively investigated. Our spectroscopic results for the lesser studied polymorph suggest that while the singlet fission process itself is unaffected by the altered morphology, differences in exciton diffusion, important for reducing the parasitic triplet-triplet fusion process, are significant. Intermolecular packing dictates the anisotropic diffusion rates and can be correlated with observed dynamics.

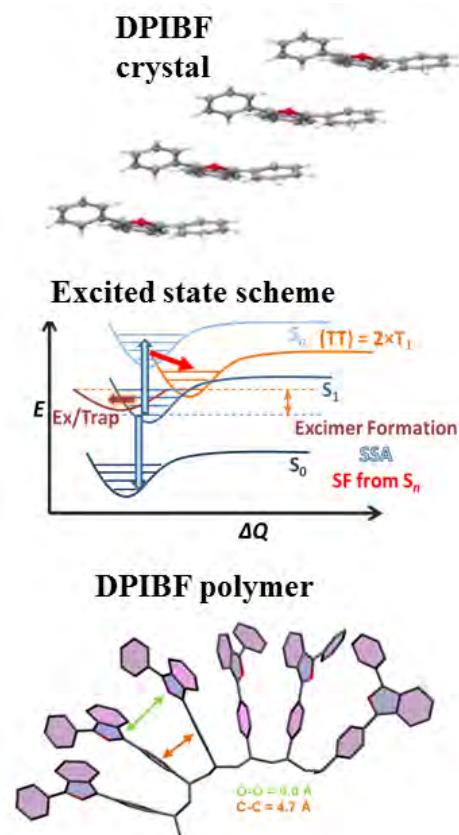


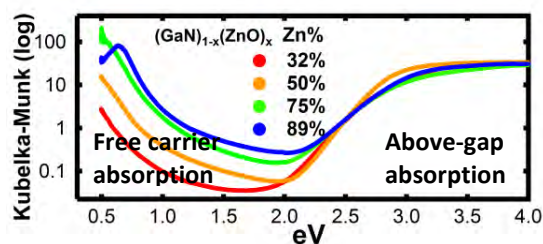
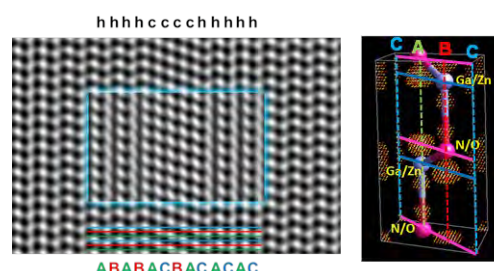
**Figure 1.** Top to bottom: slip-stacking geometry, complex dynamics with excimer formation and altered energetics, calculated interchromophore coupling in an oligomer.

## Fundamental Properties of Wurtzite $(\text{GaN})_{1-x}(\text{ZnO})_x$ Semiconductors

Peter Khalifah  
 Department of Chemistry  
 Stony Brook University  
 Stony Brook, NY 11794-3400

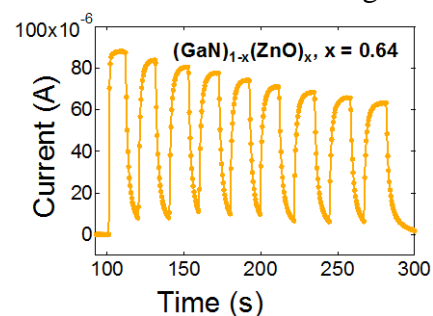
In the search for efficient semiconductors for solar water splitting, there is a paradox in that direct measurements of water splitting activity are the only measure by which the success of semiconductor design efforts can be judged, but these activity measurements provide no useful feedback about the maximum efficiency that a semiconductor material can achieve and give no direct guidance about the specific steps needed to improve the efficiency of semiconductor systems. Complementary measurements of key physical properties (absorption, carrier transport) are therefore required if semiconductors with high quantum efficiencies ( $> 10\%$ ) are to be realized, measurements which we have pursued for  $(\text{GaN})_{1-x}(\text{ZnO})_x$  semiconductors.

We have developed synthesis methods for producing bulk powders across essentially the entire width of the  $(\text{GaN})_{1-x}(\text{ZnO})_x$  solid solution ( $0.05 < x < 0.95$ ), and find that the minimum band gap of this system is about 2.6 eV, with small gaps found for samples with about 40 – 70% Zn. Depending on the synthesis method, we have observed that the nominally hexagonal  $(\text{GaN})_{1-x}(\text{ZnO})_x$  samples can contain up to about 10% of a cubic close packed intergrowth that is typically four layers (1.04 nm) in width, and the influence of composition and synthesis method on intergrowth formation has been explored.



samples, a system for which the production of single crystal or thin films is particularly problematic. Also, optical methods for investigating the carrier concentration in  $(\text{GaN})_{1-x}(\text{ZnO})_x$  samples through measurements of  $\alpha(E)$  below the band gap energy have been developed, enabling the carrier concentration to be tuned independently of the Ga:Zn ratio and allowing the influence of these two variables on photoactivity to now be independently evaluated. In initial photoelectrodes, significant photocurrents for water oxidation can be seen though there are clear losses in activity over time, a result attributed to adhesion problems. Our well-characterized  $(\text{GaN})_{1-x}(\text{ZnO})_x$  samples provide a rigorous platform for systematically understanding factors controlling the photoactivity of this system.

Although the determination of the absolute values for  $\alpha(E)$  typically requires single crystal or thin film samples, we have been able to access this information by carrying out powder measurements in a biaxial reflectance geometry, and have applied appropriate mathematical transforms in order to evaluate for the first time the absolute absorption of  $(\text{GaN})_{1-x}(\text{ZnO})_x$



## Photophysics of Doped Individual Single Walled Carbon Nanotubes

Sebastian Schäfer, Nicole M. B. Cogan, and Todd D. Krauss  
 Department of Chemistry  
 University of Rochester  
 Rochester, New York 14627-0216

Semiconducting single-walled carbon nanotubes (SWNTs) are fundamentally interesting and technologically relevant materials with size tunable absorption and emission across a range of visible and near infrared wavelengths. However, several important aspects of their photophysical properties are not known in enough depth to predict how SWNTs will behave as part of a larger integrated solar photochemical system. In particular, the energetics and dynamics of photoexcited excitons on SWNTs doped with extra electrons or holes, relevant to the state of a NT after a charge transfer event, is not well understood.

We will present results from optical spectroscopic measurements of individual SWNTs that are doped with extra electrons or holes. Photoluminescence (PL) studies of single (6,5) chirality SWNTs were performed while their charge state was controlled electrochemically. The

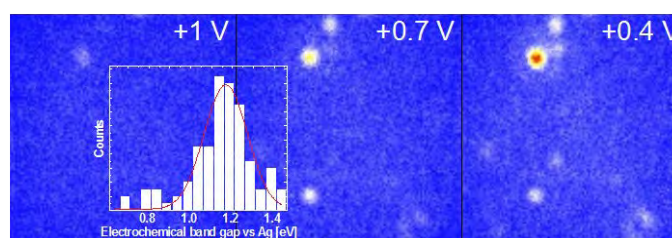


Figure 1: PL images from single SWNTs as a function of applied electrochemical potential. As the potential is made more positive individual NTs start to bleach.

PL of the SWNTs was found to be quenched at positive and negative potentials, although surprisingly the onset and offset varied substantially for each individual SWNT (Figure 1). Small differences in the local environment of the individual SWNT lead to dramatic shifts of the Fermi energy, resulting in a wide distribution of the oxidation and reduction potentials. The exciton emission energy was found to correlate with the oxidation and reduction potential, which was found by deliberately doping individual SWNTs and monitoring their PL spectral shift.

Also, low temperature (10 K) PL measurements from single (7,5) SWNTs that have been doped with holes via exposure to tetrafluoro-tetracyanoquinodimethane will be presented. At 300 K, hole doping causes a quenching of the PL from the band edge exciton (S1) state for the majority of SWNTs, and the emergence of a long-wavelength PL feature attributed to a “trion” (Figure 2). Like the PL from the S1 state, the trion PL intensity was found to be “non-blinking.” Interestingly, at 10 K the S1 PL partially recovers its intensity, while the majority of SWNTs show an increase in the trion PL intensity. Another unexpected finding was that the average PL linewidth of the trion peak hardly changed between 300 K and 10 K, while the exciton S1 PL narrowed considerably.

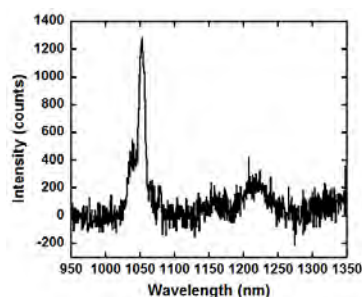


Figure 2: PL spectrum from doped NTs at 10K showing the S1 and trion PL at 1050 and 1225 nm, respectively.

These findings suggest that the “trion” PL arises from recombination of an exciton at a charged defect, rather than from a delocalized three-particle “trion” state.

## Investigation of Performance Losses in p-WSe<sub>2</sub> Layered Photocathodes and Surface Functionalization of Single Layer MoS<sub>2</sub>

Jesus M. Velazquez, Joshua D. Wiensch, Jimmy John, and Nathan S. Lewis  
 Department of Chemistry and Chemical Engineering  
 California Institute of Technology  
 Pasadena, CA 91125

Transition metal dichalcogenide semiconductors of the type MX<sub>2</sub> where M = Mo, W and X = S, Se, Te have long been studied as good light absorbers for solar energy conversion with desirable band gaps of between 1.2 and 1.5 eV. However, only high quality single-crystals with low edge-site density allow for the efficient collection of generated charge carriers. We have explored the

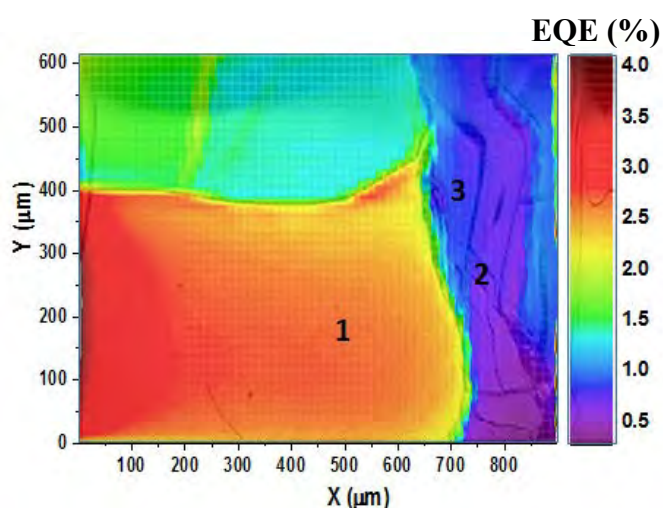


Figure 1. External Quantum Efficiency (EQE) map of  $\text{Ru}(\text{NH}_3)_6^{3+}$  reduction on p-WSe<sub>2</sub>

phenomena controlling the external quantum efficiency (EQE) of p-WSe<sub>2</sub> photocathodes by scanning photocurrent microscopy (SPCM). We have discovered a surface inhomogeneity with different terraces on a single crystal possessing significantly different EQEs in a solution of  $\text{Ru}(\text{NH}_3)_6^{3+}$ . An EQE map (Figure 1) of the surface was generated to display the difference in reduction efficiencies between terraces. Three numbered terraces are visible within the figure. An area which is redder indicates a higher EQE while a bluer area indicates a lower EQE. Terrace one is larger in area and possesses a higher EQE than the two smaller labeled terraces. Larger area terraces often provided higher conversion efficiencies than smaller terraces, which is consistent with past findings of lower edge-site density crystals providing the highest photo-conversion efficiencies. However terrace area was not the only predictor to EQE.

We propose the existence of sub-bandgap states within the low efficiency terraces as the reason for lower overall EQE. Figure 2 shows local spectral response data for the three terraces in figure 1. A high density of microstructural defects leads to the introduction of surface states, acting as recombination centers. High resolution STM reveals the presence of selenium vacancies on the surface of p-WSe<sub>2</sub>. Additionally, Kelvin probe force microscopy showed deviations in contact potential difference (CPD) at various locations on the photoelectrode, indicating differences in local electronic structure.

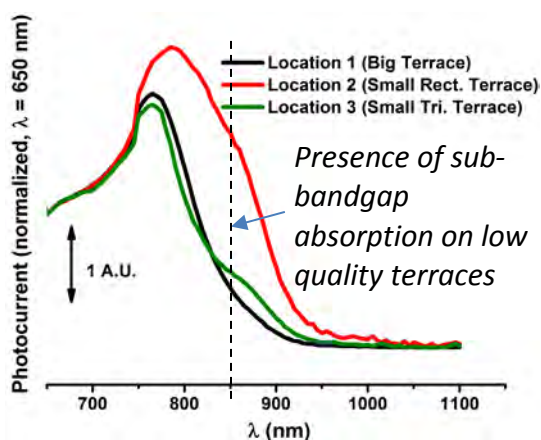


Figure 2. Local Spectral Response Measurements showing sub-bandgap absorption on low quality terraces.

## Electron/Hole Selectivity in Organic Semiconductor Contacts for Solar Energy Conversion

Chris Weber, Ethan Walker, Colin Bradley, and Mark Lonergan

Department of Chemistry and Biochemistry

University of Oregon

Eugene, OR 97403

The selective collection of electron and holes at separate contacts to an absorber material are critical steps in systems for the direct conversion of solar energy into electricity. We present numerical calculations quantifying the selectivity characteristics needed to maximize the efficiency of solar energy conversion for systems based on various absorbers and at various light intensities, results on quantifying the selectivity of organic semiconductors, and a previously unrecognized interaction between ion-containing organic semiconductors and more traditional semiconductors that lead to unusual charge injection characteristics that impact charge selectivity.

A central system for both our numerical and experimental treatment of selectivity is the point-contact solar cell or Swanson cell (see portion of Figure 1 bounded by red dashed line). Making a third contact to the near intrinsic silicon absorber in this cell enables a differential measurement of energy conversion characteristics between a contact of interest and both  $n^+$  and  $p^+$  back contacts in a single system. We demonstrate that the resulting differential measurement provides a quantitative measure of selectivity that is isolated from contributions from surface recombination. We present experimental results on the selectivity of common fullerene derivatives and conjugated polymers currently being explored as contacts in emerging photovoltaic systems.

Figure 2 (solid circles) shows density of charge injected into an ion-containing conjugated polymer based on polyacetylene, which is a mixed ionic electronic conductor (MIEC). Surprisingly, the density of holes injected from an Ohmic metal contact and extracted from a semiconductor (SC) contact (positive applied voltage) is significantly less than when the electrode roles are reversed (negative applied voltage). We present a quantitative model of extracting electrode space-charge-limited charge injection that accurately describes this observation (see solid line in Figure 2). The space charge generated in the semiconductor contact limits the potential drops available to drive electrochemical charge injection at the injecting electrode.

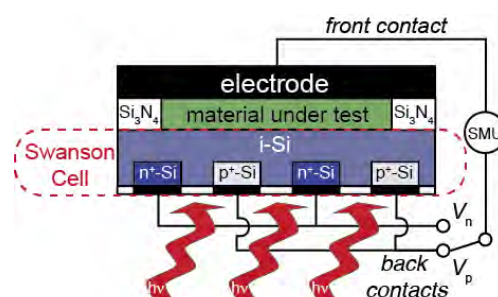


Figure 1 - Swanson Cell for Selectivity Characterization

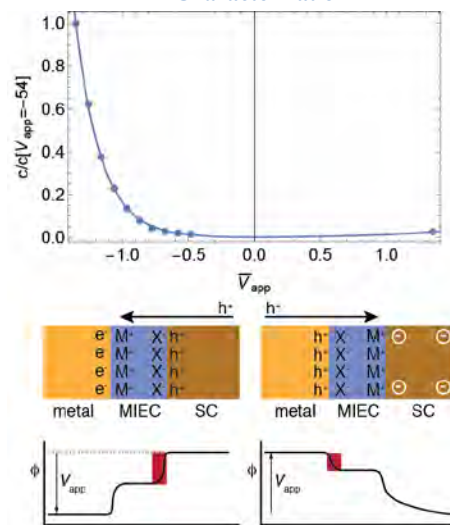


Figure 2 - Asymmetric charge injection into mixed ionic/electronic conducting conjugated polymers.

## Light-Stimulated Hole Injection at Dye-Sensitized Phosphide Photocathodes: Attaching Molecular Sensitizers and Catalysts to p-GaP Photocathodes

Elizabeth Brown, and Stephen Maldonado

Department of Chemistry  
University of Michigan  
Ann Arbor, MI 48109-1055

This poster presentation describes our latest advancements on the design and assembly of p-GaP electrodes for use in aqueous photoelectrochemical cells. Previous work in the group demonstrated the concept of using chemical attack of atop Ga atoms on GaP(111)A surfaces by strong nucleophiles as a means to introduce secondary surface reactivity through interfacial groups bound through putative Ga-C surface bonds. In this phase, we present data showing amide bond formation between organic dyes and surficial amine groups grafted onto GaP(111)A through a Grignard reaction with 3-[bis(trimethylsilyl)amino]phenylmagnesium bromide. Using a series of organic dyes with lifetimes varying between 3 and 3000 ps (donated by the Glusac group at Bowling Green State University), we present data showing high net quantum yields for sensitized hole injection into p-GaP under strong depletion with dyes possessing lifetimes as short as 600 ps.

Separately, an alternative route to bind molecular species to any crystallographic surface plane of GaP has been explored. Based on recent demonstrations of graphene coatings as universal semiconductor modifying layers, we have explored graphene adlayers as a means to couple strongly aromatic molecular species to an electrode surface with interfacial properties otherwise incongruent with their adsorption. Figure 1 illustrates the concept through the adsorption of a Co bis(dithiolate) compound on to p-GaP coated with a graphene adlayer. The graphene layer was first floated off a growth substrate and deposited onto a CH<sub>3</sub>-terminated p-GaP(111)A. The modified p-GaP substrate was then immersed into a saturated solution of Co bis(dithiolate) in acetonitrile. X-ray photoelectron spectra obtained for this sample and control (i.e. no graphene adlayer) samples treated in the same way are shown. Evidence of persistent adsorption of the Co complex was only observed for p-GaP surfaces coated with graphene. The electrocatalytic activity of these species for H<sup>+</sup> reduction will be presented.

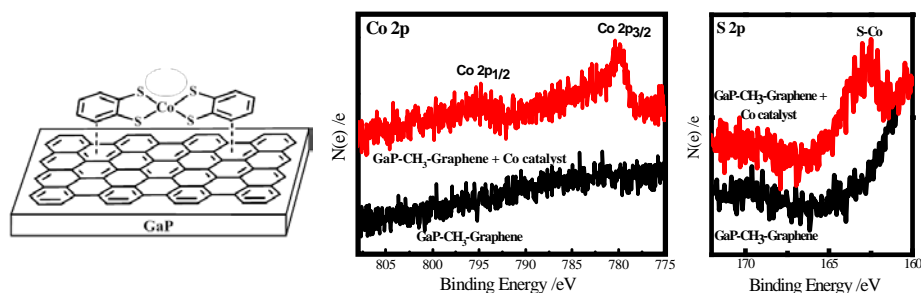


**Figure 1.** (left) Schematic depiction of planar Co bis(dithiolate) adsorbed onto GaP through  $\pi$ - $\pi$  interactions with a graphene adlayer. (middle) High resolution Co 2p XP spectra for CH<sub>3</sub>-terminated p-GaP(111) substrates immersed in a saturated Co bis(dithiolate) solution. The red and black traces correspond to experiments with and without a graphene adlayer, respectively. (right) High resolution S 2p XP spectra for the same substrates treated in the same manner.

## Nanostructured Photocatalytic Water Splitting Systems

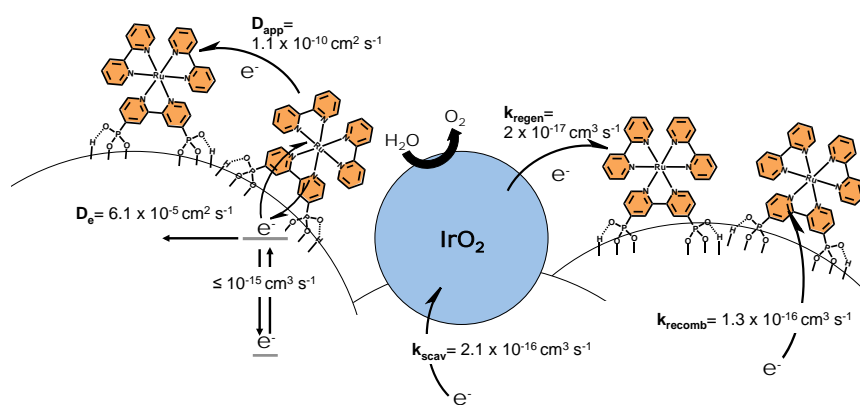
John R. Swierk, Nella M. Vargas-Barbosa, Nicholas S. McCool, Pengtao Xu, Yuguang Li, Megan E. Strayer, and Thomas E. Mallouk

Department of Chemistry, The Pennsylvania State University, University Park, PA 16802

Ana L. Moore, Thomas A. Moore, and Devens Gust

Department of Chemistry and Biochemistry, Arizona State University, Tempe AZ 85281

Our DOE-supported research investigates problems associated with overall water splitting in molecular photoelectrochemical systems. We are studying anode assemblies based on the architecture of the dye-sensitized solar cell (DSSC) and cathode assemblies grown layer-by-layer from oxide nanosheets and photoredox molecules. We are also studying anion- and cation-exchange membranes in the context of complete water splitting systems.



A key problem in these systems is to control the relative rates of charge injection, transport, and recombination at the catalyzed DSSC anode. Recently, we have used a complementary set of spectro- and photoelectrochemical methods to measure the rates of these

processes, which are summarized above for electrodes catalyzed by  $\text{IrO}_2$  nanoparticles sintered onto the nanocrystalline  $\text{TiO}_2$  surface. The dominant recombination pathway is back electron transfer to the oxidized dye, but photocurrents in the  $\text{mA}/\text{cm}^2$  range can be obtained under AM 1.5 conditions by dispersing the catalyst to shorten the distance of charge transfer diffusion. The kinetic model sketched above also explains the polarization that is universally observed at water-splitting photoanodes with different water oxidation catalysts, now studied by a number of groups. Polarization occurs on a timescale of seconds, involving a gradual build up of trapped electrons and oxidized sensitizer, and this suggests strategies for further improving the architecture and efficiency of the system. In related work we have studied metal-free porphyrins as sensitizers with a broader photoaction spectrum across the visible than  $\text{Ru}(\text{bpy})_3^{2+}$  derivatives. The photocurrents are lower with these sensitizers because of slow charge transfer diffusion.

We have used the Mott-Schottky method to measure the flat-band potentials of layered metal oxide semiconductors that are components of photocathodes made by Langmuir-Blodgett and layer-by-layer assembly. We are studying the kinetics of photoinduced electron transfer in these lamellar nanosheet/redox polymer films by transient spectroscopic techniques.

Proton transport from the anode to the cathode is also a significant system-level problem in water splitting cells. Ordinary cation- and anion-exchange membranes result in substantial energy losses in cells that operate near neutral pH. Bipolar membranes enable stable operation of acid/base electrolysis cells that can utilize earth-abundant anode and cathode materials. We are now studying water and  $\text{CO}_2$  electrolysis and photoelectrolysis using this approach.

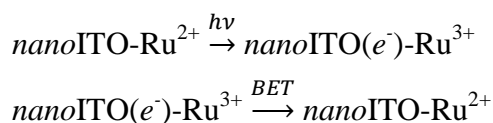
## Photoinduced Interfacial Electron Transfer at *nano*ITO

Byron H. Farnum<sup>†</sup>, Animesh Nayak<sup>†</sup>, Akinobu Nakada<sup>‡</sup>, M. Kyle Brennaman<sup>†</sup>, Osamu Ishitani<sup>‡</sup>,  
 Thomas J. Meyer<sup>†</sup>

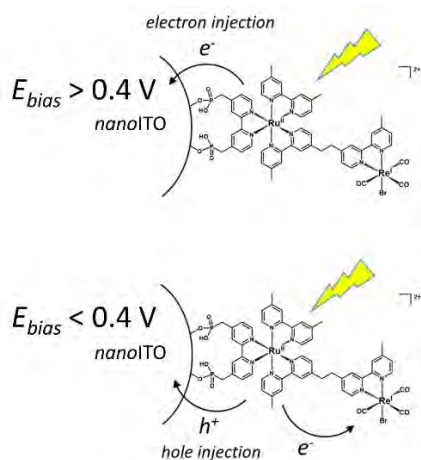
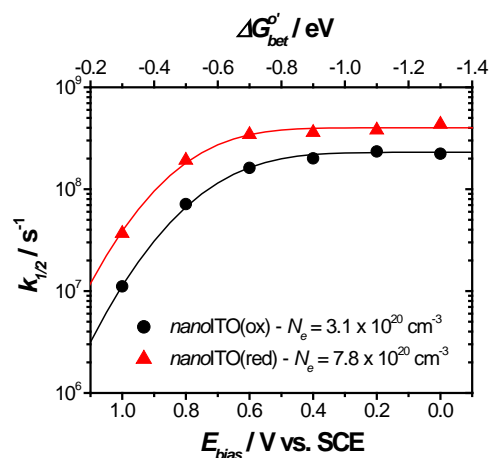
<sup>†</sup>Department of Chemistry, University of North Carolina at Chapel Hill, Chapel Hill, NC 27599

<sup>‡</sup>Department of Chemistry, Tokyo Institute of Technology, Meguro-ku, Tokyo, Japan 152-8550

Interfacial electron transfer to and from transparent, conductive Sn-doped In<sub>2</sub>O<sub>3</sub> semiconductor nanoparticles in mesoporous thin films (*nano*ITO) has been investigated by transient absorption measurements with phosphonate-bound Ru-polypyridyl chromophores. Metal-to-ligand charge transfer excitation of the chromophore is followed by highly efficient electron injection on the picosecond timescale with efficiencies of ~100%. Injection is followed by back electron transfer (BET) which occurs on the nanosecond time scale.



The conducting properties of the films have been exploited to investigate the influence of applied bias and, with it, the Fermi level in the nanoparticle films, on both injection and back electron transfer. The figure at the right shows BET rate constants ( $k_{1/2}$ ) as a function of applied bias ( $E_{\text{bias}}$ ) and driving force ( $\Delta G_{\text{bet}}^{\circ}$ ) for *nano*ITO films having different electron densities ( $N_e$ ) as measured in 0.1 M LiClO<sub>4</sub> acetonitrile. The fit to the data was based on Marcus-Gerischer theory giving an interfacial reorganization energy of  $\lambda = 0.56$  eV for the single-site, surface-bound  $-\text{Ru}^{3+/2+}$  couple, comparable to values obtained in fluid solution.



At  $E_{\text{bias}} < 0.4$  V, reductive quenching, with electron transfer from the oxide to the excited state, (*i.e.* hole injection) is evident by the appearance of remote, reduced  $\text{Re}^{\text{I}}(\text{bpy}^{\bullet-})$  in transient absorption spectra. Back electron transfer between  $-\text{Re}^{\text{I}}(\text{bpy}^{\bullet-})$  and  $\text{nanoITO}(h^+)$  occurs in  $>500$  ns.

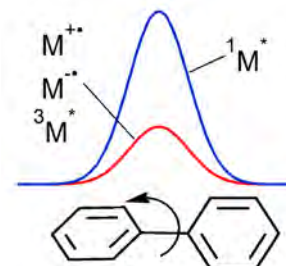
These initial results are important in demonstrating the use of an applied bias to control photo-induced electron transfer events at the surface of *nano*ITO opening a door to potential applications in optoelectronics, sensors, and dye-sensitized solar energy conversion.

## Exciton and Charge Transport in Conjugated Chains

T. Mani, M. J. Bird, A. R. Cook, L. Zaikowski, R. Holroyd, G. Mauro, X. Li., G. Rumbles,  
J. Blackburn, O. G. Reid, and J. R. Miller

Chemistry Department, Brookhaven National Laboratory, Upton, NY 11973  
National Renewable Energy Laboratory, Golden, CO 80401

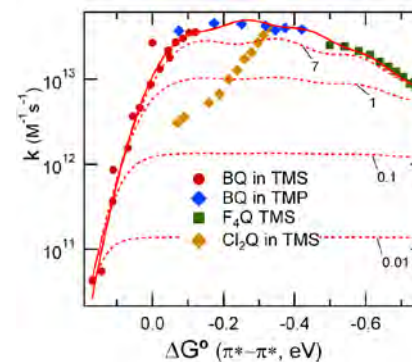
Better transport of singlet excitons has potential to benefit organic photovoltaics, but we lack understanding of what limits singlet transport. Unfavorable “bad” dihedral angles, which constitute barriers for transport of charges and excitons, may be one factor. Via synthesis we intentionally introduced large dihedral angles. Measurements and DFT calculations find that the barriers due to “bad” dihedrals are of similar heights for holes, electrons and triplet excitons, but are about three times larger for singlet excitons. Nevertheless intrachain transport of singlet excitons to traps at the ends of polyfluorene (pF) chains gave an exciton diffusion length  $L_D = 34$  nm, far longer than 7 nm reported for polythiophenes. Excitons reaching the ends traps produced charge transfer excited states and polarity-dependent fluorescence. Future work will seek to understand this difference in exciton transport, examine transport in a variety of structures, and seek to understand how to improve it.



The possibility that dihedrals may limit transport due to higher barriers for singlets point to triplet transport as an interesting and potentially important subject to enable basic understanding of transport. Fortunately pulse radiolysis offers abilities to rapidly create triplets in molecules having low triplet quantum yields. That ability, including fast creation of triplets, possibly without singlet precursors, is under investigation in another part of our program. While it is only partly understood, it enabled observations that triplets in (pF) chains completely span pF chains with lengths to >100 repeat units. Although the method could say only that this transport occurred in <1  $\mu$ s, earlier results found transport in <40 ns, and current results suggest it may be much faster. New methods will perform measurements with high time resolution, and will seek to couple understanding of exciton transport with charge transport. The current results on triplets showed that defects were rare in the pF chains and measured of the completeness of end capping by acceptor groups.

Closely related experiments on electrons and holes in conjugated chains measure their transport by similar end trapping methods and by transient microwave conductivity (TRMC), which can operate without end traps. Future experiments will evaluate effects of dihedral angles and medium polarity and will seek to measure transport in single-walled carbon nanotubes using TRMC.

Radiation chemistry methods also observe the inverted region for bimolecular electron transfer reactions, where the free energy change can be continuously adjusted over an  $\sim 300$  meV range. The rate vs.  $\Delta G^\circ$  relation is free from the effects of the diffusion-controlled limit due to the very high mobilities of the electrons in these fluids.



Rate constants for electron attachment to benzoquinones in nonpolar liquids.

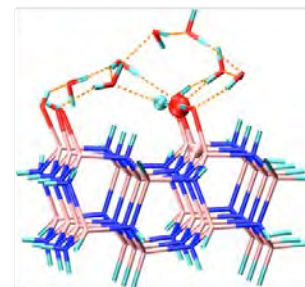
## Photocatalytic Water Oxidation at the Semiconductor-Aqueous Interface: GaN, ZnO and the GaN/ZnO Alloy

James T. Muckerman  
Chemistry Department  
Brookhaven National Laboratory  
Upton, NY 11973-5000

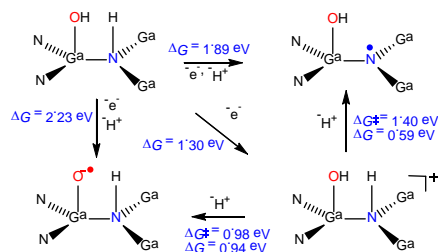
Domen's group has reported that the band gap of GaN can be reduced to absorb visible instead of UV light by alloying GaN with ZnO. The band-gap-narrowed GaN/ZnO alloy is an efficient visible-light photocatalyst, although microscopic models for reaction sites and mechanisms remain as important open questions.

We recently constructed an accurate cluster expansion model to reproduce the energetics of a large number of relaxed configurations of the GaN/ZnO alloys, and used it in Monte Carlo calculations of equilibrated configurations of a large supercell of the alloy as a function of ZnO concentration and temperature [1]. This allowed the construction of a phase diagram of the two-component system that revealed a homogeneous high-temperature phase (characteristic of synthesis conditions) that has only very short-range order and a low-temperature 1:1 phase with ordered layers of the four elements. The structural information from the disordered high-temperature phase of the 1:1 GaN/ZnO alloy was used to explore the interfacial acid/base behavior of water at the GaN/ZnO-aqueous solution interface through DFT-MD simulations and to compare it to that at the pure GaN and ZnO (10 $\bar{1}$ 0) interfaces [2]. At the equilibrated interfaces, most of the surface anions are protonated, while many surface cations are bonded to hydroxide ions, similar to that of the GaN(10 $\bar{1}$ 0)-water interface.

Most recently, we have employed these simulations to investigate the water oxidation mechanism using a large molecular cluster model. In addition to coupled electron-transfer (ET) and proton-transfer (PT) reactions, the cluster model also allowed us to investigate the sequential steps with the PT step following the ET step. We found that photo-generated holes localize on surface -NH sites and PT from -NH sites is thermodynamically favorable [3,4]. However, proton transfer from -



OH sites and subsequent localization of holes on oxygen atoms occurs at a faster rate because of hydrogen bonding interactions at the GaN(10 $\bar{1}$ 0)-water interface [4], confirming that the catalytic reaction proceeds through a sequence of four proton-coupled electron-transfer steps starting with \*OH $^-$  (the "dark" state where \* is a surface Ga site) and then through \*O $^{\bullet-}$ , \*OOH $^-$ , and \*O $_2^{\bullet-}$  before returning to the initial state by the elimination of O $_2$  and the addition of H $_2$ O accompanied by the dissociation of a proton.



### References

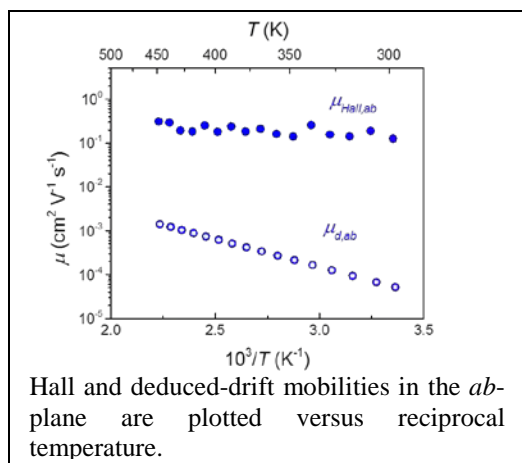
- [1] Li, Muckerman, Hybertsen & Allen, *Phys. Rev. B* **2011**, 83, 134202.
- [2] Kharche, Hybertsen & Muckerman, *Phys. Chem. Chem. Phys.* **2014**, 16, 12057-12066.
- [3] Akimov, Muckerman & Prezhdo, *J. Am. Chem. Soc.* **2013**, 135, 8682-8691.
- [4] Ertem, Kharche, Hybertsen, Batista, Tully & Muckerman, *ACS Catal.* **2015**, ASAP, DOI 10.1021/acscatal.5b00054.

We thank our collaborators M. S. Hybertsen (BNL), P. B. Allen (Stony Brook U.), M. V. Fernandez-Serra (Stony Brook U.), O. V. Prezhdo (USC), V. S. Batista (Yale U.) and J. C. Tully (Yale U.).

## Small-Polaron Hopping in W:BiVO<sub>4</sub> and Ni-Doped FeOOH OER Electrocatalyst

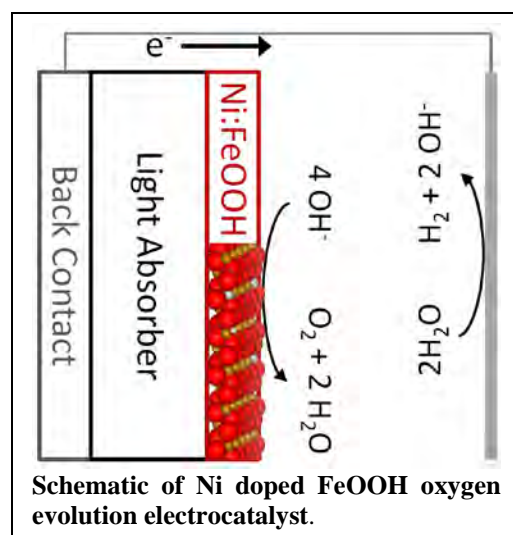
Alexander J. E. Rettie, William C. Chemelewski, Allen J. Bard, and C. Buddie Mullins  
 Departments of Chemistry and Chemical Engineering  
 University of Texas at Austin  
 Austin, TX 78712

DC electrical conductivity, Seebeck and Hall coefficients were measured between 300-450 K on single crystals of monoclinic bismuth vanadate that are doped *n*-type with 0.3% tungsten donors (W:BiVO<sub>4</sub>). Strongly activated small-polaron hopping is implied by the activation energies of the Arrhenius conductivities (about 300 meV) greatly exceeding the energies characterizing the fall of the Seebeck coefficients' magnitudes with increasing temperature (about 50 meV). Small-polaron hopping is further evidenced by the measured Hall mobility in the *ab*-plane ( $10^{-1} \text{ cm}^2 \text{ V}^{-1} \text{ s}^{-1}$  at 300 K) being larger and much less strongly activated than the deduced drift mobility (about  $5 \times 10^{-5} \text{ cm}^2 \text{ V}^{-1} \text{ s}^{-1}$  at 300 K). The conductivity and *n*-type Seebeck coefficient is found to be anisotropic with the conductivity larger and the Seebeck coefficient's magnitude smaller and less temperature dependent for motion within the *ab*-plane than that in the *c*-direction. These anisotropies are



addressed by considering highly anisotropic next-nearest-neighbor ( $\approx 5 \text{ \AA}$ ) transfers in addition to the somewhat shorter ( $\approx 4 \text{ \AA}$ ), nearly isotropic nearest-neighbor transfers.

We also report on the electrodeposition of Ni-doped FeOOH (Ni:FeOOH) as an OER electrocatalyst. The deposition method is applicable to a wide range of photoanodes and catalytic films as thin as a few nanometers can be easily grown. The Ni:FeOOH films with 5-20% Ni content reach  $10 \text{ mA/cm}^2$  in 0.1 M NaOH at an overpotential ranging from 420-460 mV initially, and improve with anodization at  $10 \text{ mA/cm}^2$  to below 400 mV. Deposition on triple junction solar cells results in a full PEC system with higher performance and a more cathodic peak power potential compared to undoped FeOOH electrocatalysts. We successfully grew Ni-doped FeOOH via anodic electrodeposition. The Ni doping is achieved despite no active oxidation of Ni ions in the deposition bath, which leads to low incorporation efficiency. Despite this, the activity is quite high, on par with other Fe/Ni oxide materials recently investigated elsewhere. The films are stable under high current OER conditions, and show high activity for very thin layers (on the order of 10 nm), which should allow low parasitic light absorption compared to other OER catalysts for PEC water oxidation applications.



## Extension of Hopfield's Electron Transfer Model to Accommodate Site-Site Correlation

Marshall D. Newton

Department of Chemistry, Brookhaven National Laboratory, Upton, NY 11973

By elegant analogy with the Förster Excitation Energy Transfer (EET) rate constant expression, Hopfield (JH) derived the following rate constant for nonadiabatic electron transfer of the charge separation (CS) type,  $DA \rightarrow D^+A^-$ :

$$k_{ET} = (2\pi/\eta) (H_{DA})^2 \int_{-\infty}^{+\infty} P_D(\Delta) P_A(-\Delta) d\Delta,$$

where  $P_D(\Delta_d)$  and  $P_A(\Delta_a)$  are taken as independent Gaussian thermal probability densities of, respectively, the vertical gaps for electron detachment (d) from site D and electron attachment (a) at site A, subject only to the constraint of resonance,  $\Delta \equiv \Delta_d = -\Delta_a$ , and where the integral is the classical Franck-Condon weighted density of states (FCWD). This approach (an alternative route to the Marcus model) has been useful for studies of long distance ET (*eg.*, in proteins), but for shorter D/A separations it cannot accommodate site-site correlations due to D/A coulomb terms arising in the reorganization energy for polar media and the driving force for CS (and charge recombination (CR)). We have extended the model to include the site-site terms, considering for illustration of our approach, the same 2-site/2-mode/3-state framework used by JH, yielding generalized expressions for the resonant gap at the CS transition state (TS),  $\Delta^{TS}$ , which provide values for the mean absolute redox potential ( $\Delta^{TS}/q$ , with  $q$  the electron charge magnitude) of the system at the TS. The same approach is also applied to a related process, bridge (B)-mediated CS,  $DBA \rightarrow D^+BA^-$ , where the corresponding resonant TS gap now controls the electron (e) or hole (h) superexchange (se) coupling element.

If the virtual (vertical) processes at each site were independent (uncorrelated), then the same result for the FCWD would be obtained for either order of d and a: *ie.*,  $DA \rightarrow D^+A + e \rightarrow D^+A^-$  (da) or  $DA + e \rightarrow DA^- \rightarrow D^+A^- + e$  (ad), where the virtual electron (e) is placed at infinity. With coulombic 'correlation' terms, the resonant TS gaps for the da and ad sequences (respectively,  $\Delta^{TS(da)}$  and  $\Delta^{TS(ad)}$ ) are distinct:

$$\Delta^{TS(da)} = \{IP_D(\lambda_A + \lambda_{DA}) + (EA_A - C_{DA})(\lambda_D + \lambda_{DA})\} / (\lambda_D + \lambda_A + 2\lambda_{DA}) - \lambda_{DA},$$

while  $\Delta^{TS(ad)} = \Delta^{TS(da)} + 2\lambda_{DA} - C_{DA}$ . For the case where the 2 modes are inertial solvent polarization modes,  $\lambda_D$ ,  $\lambda_A$ , and the off-diagonal (correlating) term  $2\lambda_{DA}$  (as defined here) may be taken, for example, as the 3 terms in the Marcus 2-sphere model for solvent reorganization energy, while  $\lambda_D$  and  $\lambda_A$  may also have solute molecular contributions. The adiabatic  $IP_D$  and  $EA_A$  terms (respectively, ionization potential of D and electron affinity of A) include solvation contributions, and the coulomb term  $C_{DA}$  (defined as negative for CS) includes solvent screening. In either case (da or ad), neglect of the  $\lambda_{DA}$  and  $C_{DA}$  terms leads to the result for the original JH model (discussed in work with D. Beratan). The present model yields the full Marcus FCWD, including the  $\lambda_{DA}$  and  $C_{DA}$  terms. For the case of B-mediated CS, the  $\Delta^{TS}$  is now referenced to the unoccupied (e) or occupied (h) B level. The model also yields expressions for the 'direction cosines' of the different pairs of reaction coordinates (taken as) vertical gaps.

## Pendant Proton Relays and Proton-Coupled Electron Transfer in Electrocatalytic Hydrogen Generation by Ni Hangman Porphyrins

D. Kwabena Bediako<sup>a</sup>, Brian H. Solis<sup>b</sup>, Dilek Dogutan<sup>a</sup>, Sharon Hammes-Schiffer<sup>b</sup>, and Daniel G. Nocera<sup>a</sup>

<sup>a</sup>Harvard University Chemistry and Chemical Biology  
12 Oxford Street, Harvard University, Cambridge, Massachusetts 02138-2902

<sup>b</sup>University of Illinois at Urbana-Champaign  
Department of Chemistry, University of Illinois at Urbana-Champaign, Urbana, Illinois 61801

The efficient conversion of solar energy into fuels requires the catalytic promotion of complex multi-electron multi-proton transformations. Understanding the mechanism for coupling proton transfer to electron transfer is therefore central to the discovery of new catalysts that give access to a solar-to-fuels conversion schemes. To this end, we have set out to synthesize and interrogate a class of porphyrin-based compounds possessing a proton relay (Hangman group).

We report a new nickel hangman porphyrin (**1-Ni**, Figure 1, left) that catalyzes the generation of H<sub>2</sub> from weak acids in acetonitrile. The improved activity of this catalyst relative to its previously reported cobalt analogue is manifest in cyclic voltammetry (CV) as a “total catalysis” wave—a wave that is well separated from the reduction wave of the catalyst in the absence of substrate (Figure 1-right). CV data and simulations together with computational studies using density functional theory (DFT) suggest the shift in electrokinetic zone between these Co and Ni porphyrins is attributed to a change in proton-coupled electron transfer (PCET) mechanism. We conclude that protonation likely occurs at the Ni(I) state followed by reduction, in a stepwise proton transfer followed by electron transfer, PTET, pathway. CV modeling and DFT calculations implicate the subsequent reduction of this nickel(II) hydride intermediate to yield a formal nickel(I) hydride from which thermal hydrogen production proceeds.

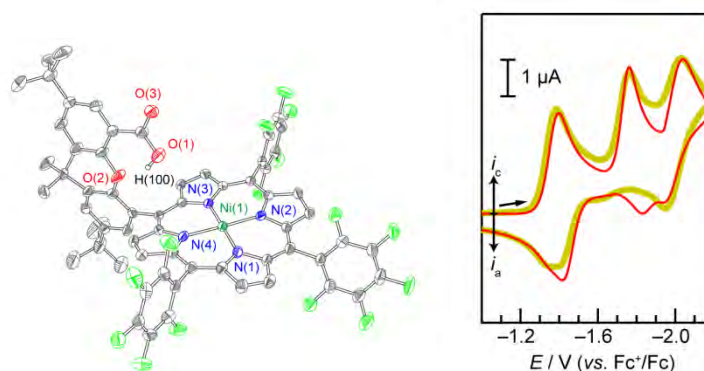


**Figure 1.** Left. Crystal structure of **1-Ni**. Experimental (thick green curves) and simulated (thin red curves) cyclic voltammograms of a 0.4 mM solution of **1-Ni** at a scan rate of 30 mV/s. The CV was simulated according to a mechanistic framework consisting of an ETPT pathway.

## Z-Scheme Dye Cells for Solar Fuels *Buried Junctions vs. Chromophore-Catalyst Assemblies*

Arthur J. Nozik

Department of Chemistry and Biochemistry  
University of Colorado, Boulder, CO 80309  
National Renewable Energy Laboratory, Golden, CO 80401  
University of No. Carolina Energy Frontier Research Center for Solar Fuels 27599

In general, the redox reactions that yield fuels require greater photopotentials than can be created by absorption of a single photon. As a result, cell architectures for solar fuels are under study that utilizes a two-photon configuration (Z-scheme), in which one pair of photogenerated charge carriers from each of the two photosystems recombine to up-convert their energy into additional photopotential (Fig. 1). In one scheme (at UNC EFRC) based on molecular chromophores and molecular catalysts combined in a dyad structure (Fig.1(b)), the photopotential for photoelectrosynthesis to fuel is determined by the difference between the oxidative and reductive potentials of molecular catalysts rather than the difference between the Fermi levels within the semiconductors. In a second alternative configuration the photopotential needed for photoelectrosynthesis is generated in a buried-junction Z-scheme configuration, as depicted in Fig. 1(a). In this cell, the photon-absorbing and voltage-generating region is encapsulated (within the dashed dark red lines in Fig 1(a)) using TCO and 3 other insulating layers and isolated from the solution redox chemistry. The important fundamental differences and advantages vs disadvantages of these two architectures are presented and discussed.

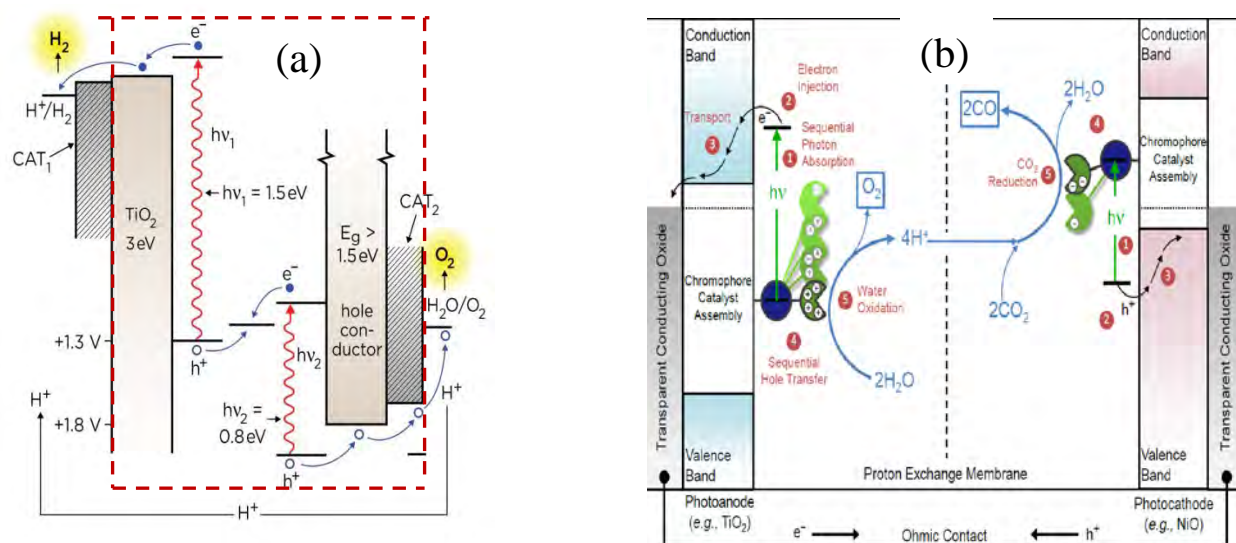


Figure 1. Dye sensitized Z-scheme solar cells for  $\text{H}_2\text{O}$  splitting. (a) Buried junction architecture. (b) Unburied junction chromophore-catalyst assembly (from University of North Carolina EFRC).

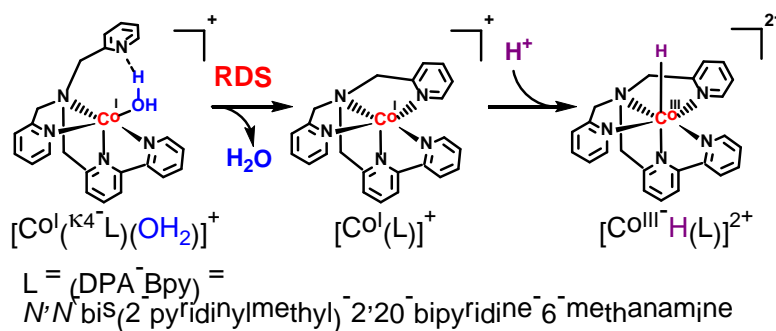
## The Effect of Solvent Coordination on the Mechanism of Formation of a Metal (Co, Ru) Hydride Bond

Dmitry E. Polyansky, Etsuko Fujita, and James T. Muckerman  
 Chemistry Department  
 Brookhaven National Laboratory  
 Upton, NY 11973-5000

Metal hydride species (M–H) of coordination compounds are crucial intermediates in catalytic CO<sub>2</sub> reduction or H<sub>2</sub> production. However, their regeneration from solvent-coordinated species using electrons and protons in water remains challenging owing to the fairly negative reduction potentials of the starting complexes. This also creates a mechanistic challenge in studying the properties and reactivity of M–H species under catalytic conditions because of their transient nature. In our studies, we focus on a mechanistic understanding of the formation of M–H species in water using a combination of theoretical and experimental methods, such as transient pulse radiolysis, laser flash photolysis and electrochemical studies.

In one example, we describe the formation of [Ru(tpy)(bpy)H]<sup>+</sup> in water. Our results indicate that the formation of the ruthenium hydride requires two-electron reduction of [Ru(tpy)(bpy)(H<sub>2</sub>O)]<sup>2+</sup> in a pH independent process. The loss of the aqua ligand takes place only after the second reduction, resulting in neither electron transfer step being coupled to the protonation reaction. The modest weakening of the Ru–OH<sub>2</sub> binding upon the first reduction is explained by poor electronic communication between the π\* orbitals of the reduced tpy ligand and the molecular orbitals involved in the formation of the Ru–O bond.

In another example we present our studies of intermediates produced during catalytic proton reduction in aqueous solution promoted by the [(DPA-Bpy)Co(OH<sub>2</sub>)]<sup>n+</sup> complex ([Co(OH<sub>2</sub>)]<sup>n+</sup>). Our results show that while the water ligand is strongly coordinated to the metal center in the oxidation state 3+, one-electron reduction of the complex to form a Co<sup>II</sup> species results in weakening the Co–O bond. The further reduction to a Co<sup>I</sup> species leads to the loss of the aqua ligand and the formation of [Co<sup>I</sup>–VS]<sup>+</sup> (VS = vacant site). Both electrochemical and kinetic results indicate that the Co<sup>I</sup> species must undergo some structural change prior to accepting the proton and this transformation represents the rate determining step (RDS) in the overall formation of [Co<sup>III</sup>–H]<sup>+</sup>. We propose that this RDS may originate from the slow removal of a solvent ligand in the intermediate [Co<sup>I</sup>(κ<sup>4</sup>-L)(OH<sub>2</sub>)]<sup>+</sup> in addition to the significant structural reorganization of the metal complex and surrounding solvent resulting in a high free energy of activation.



**Acknowledgements:** We thank our coworkers A. Lewandowska-Andralojc, W. Ward and J. Concepcion for their assistance. We also thank our collaborator X. Zhao (University of Memphis).

## Excited State Dynamics in Complex Systems for Solar Energy Harvesting: Time-Domain Ab Initio Studies

Oleg Prezhdo  
 Department of Chemistry  
 University of Southern California  
 Los Angeles, CA 90089

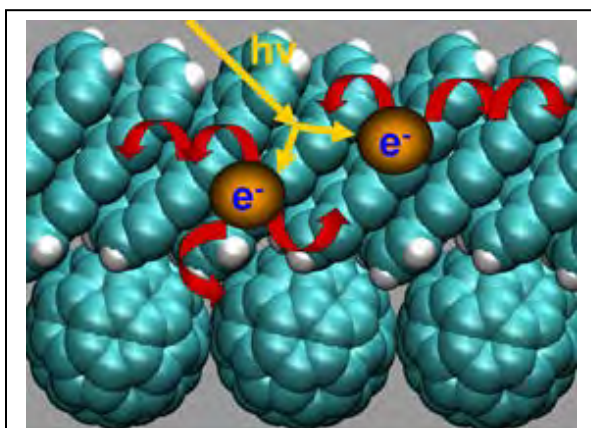


**Figure 1.** An interface between pentacene and  $C_{60}$  layers. The photoinduced dynamics at the interface is much more complex than in isolated singlet fission material (pentacene), since it involves a variety of interfacial charge transfer states, in addition to the pentacene states.

GaN/water interface, carbon nanotube bundles, interfaces of  $C_{60}$  with pentacene and inorganic particles, etc. Photoinduced charge separation across such interfaces creates many challenges due to stark differences between molecular and periodic, and organic and inorganic systems. Our simulations provide a unifying description of quantum dynamics on nanoscale, characterize the rates and branching ratios of competing processes, resolve debated issues, and generate theoretical guidelines for development of novel systems for solar energy harvesting.

Photo-induced processes at various interfaces form foundation of photovoltaic and photocatalytic applications. They require understanding of dynamical response of novel materials on atomic and nanometer scales. Our non-adiabatic molecular dynamics techniques, implemented within time-dependent density functional theory, allow us to model such non-equilibrium response in real time. We focus on photo-initiated charge and energy transfer at interfaces involving organic and inorganic nanoscale materials. Examples include  $TiO_2$  sensitized with organic molecules, water, semiconductor quantum dots and graphene,

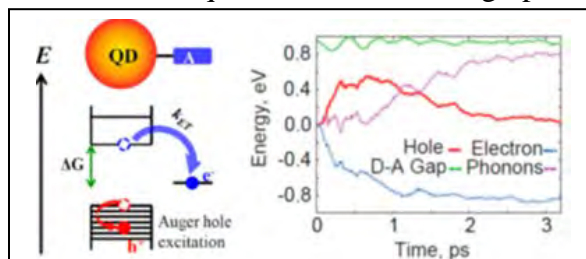


**Figure 2.** Auger-assisted electron transfer (ET) strongly influences ET rate and eliminates the Marcus inverted regime. Significant electron-hole coupling and high density of states available in nanomaterials allows hole excitation during electron transfer. Our time-domain atomistic study will provide a detailed description of Auger-assisted ET. It shows that the hole supporting the Auger mechanism is excited only transiently and restores its initial energy within several picosecond by transferring energy to phonons.

## Interfacial Processes between Gas-Phase Molecules and Ga-based Surfaces Probed by Near-Ambient Pressure X-ray Photoelectron Spectroscopy

Sylwia Ptasińska, and Xueqiang Zhang  
 Radiation Laboratory and Department of Physics  
 University of Notre Dame  
 Notre Dame, IN 46556

Current research in material sciences is focused on enhancing the efficiency of photoelectrochemical (PEC) cells using various semiconductor photoanodes for water splitting. Such photoanodes should have good stability in aqueous media, as well as suitable band-edge and band-gap energies to match both the potential for water oxidation-reduction reactions and the solar spectrum, respectively. Ga-based semiconductors fulfill these criteria, but their solar-to-hydrogen efficiency has still not reached the performance expectations for a PEC cell. Therefore, knowledge of interfacial reactions on the surface of Ga-based material at various conditions is essential to improve our understanding of water-splitting mechanisms and of the stability of PEC devices.

In this study, we focused on fundamental understanding the surface interaction between Ga-based materials, i.e., GaAs and GaP, and common gaseous molecules, mainly H<sub>2</sub>O and O<sub>2</sub> [1,2]. In work presented here, *in situ* near-ambient pressure x-ray photoelectron spectroscopy was used to track the evolution of surface chemistry at elevated pressures and elevated temperatures. The obtained spectra revealed the nature of the molecular interactions and allowed the detection of changes in the electronic structure of surface Ga, As/P, and O atoms under the reaction conditions. Dynamic changes in chemical evolution at the gas phase/semiconductor interfaces were reflected in Ga 2p<sub>3/2</sub>, O 1s, and As/P 2p spectra. A “phase diagram” of GaP oxidation under various O<sub>2</sub> (Fig. 1) and H<sub>2</sub>O pressures and temperatures allowed us visualize transition states and gain more insight into the chemical pathways leading to the final products of surface oxidation and hydroxylation. Further, an estimation of work function changes of the oxidized surface and activation energies for oxide formation were obtained under near-ambient conditions.

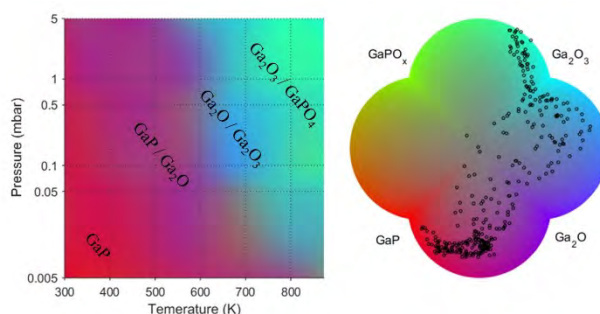


Fig. 1. Transition between four states: GaP, Ga<sub>2</sub>O, Ga<sub>2</sub>O<sub>3</sub>, and GaPO<sub>4</sub> as the temperature and pressure are changed.

### References

1. X. Zhang, S. Ptasińska, J. Phys. Chem. C 119, 262 (2015)
2. X. Zhang, S. Ptasińska, Phys. Chem. Chem. Phys. 17, 3909 (2015)

## Ru Complexes under Catalytic Condition of Water Oxidation

Yulia Pushkar, Guibo Zhu, Lifen Yan, and Yuliana Smirnova  
 Department of Physics  
 Purdue University  
 West Lafayette, Indiana 47907

Achieving new energy solutions based on concept of artificial photosynthesis requires understanding the mechanisms of water oxidation. X-ray spectroscopic analysis allows to follow water oxidation catalysis *in situ* under working conditions. We studied the simplest and one of the most analyzed model water oxidation catalyst:  $[\text{Ru}(\text{tpy})(\text{bpy})\text{H}_2\text{O}]^{2+}$  and its modification  $[\text{Ru}(\text{tpy})(\text{bpy})\text{I}]^+$  for which improved catalytic performance was reported.<sup>1-3</sup>

Improved catalytic activity of iodide complex was attributed to the formation of 7-coordinated Ru species.<sup>3</sup> We tested this hypothesis by EPR and X-ray spectroscopy (XAS) and found that  $[\text{Ru}^{\text{II}}(\text{bpy})(\text{tpy})\text{I}]^+$  only serves as a precursor for formation of  $[\text{Ru}^{\text{IV}}(\text{bpy})(\text{tpy})=\text{O}]^{2+}$ . Upon oxidation with excess of  $\text{Ce}^{\text{IV}}$  the Ru-I bond quickly dissociates with formation of  $[\text{Ru}^{\text{III}}(\text{bpy})(\text{tpy})\text{H}_2\text{O}]^{3+}$  and  $[\text{Ru}^{\text{IV}}(\text{bpy})(\text{tpy})=\text{O}]^{2+}$  complexes, Figure 1. The catalytic steady state of  $[\text{Ru}(\text{tpy})(\text{bpy})\text{I}]^+$  was composed of 95%  $[\text{Ru}^{\text{IV}}(\text{bpy})(\text{tpy})=\text{O}]^{2+}$  species. Thus,  $[\text{Ru}(\text{tpy})(\text{bpy})\text{I}]^+$  catalyst is not capable of forming 7-coordinated complexes. Introducing the Ru-I bond into initial catalysts cannot serve to improve catalyst design as it dissociates within 30 sec under catalytic conditions of water oxidation.

To avoid restrictions of the  $\text{Ce}^{\text{IV}}$  as an oxidant we developed *in situ* XAS for electrochemical water oxidation. X-ray damage analysis at Ru K-edge shown that inside electrochemical cell solutions of Ru complexes can be exposed for extended periods of time (up to 24 hours) to 22-23 keV X-ray beam without causing changes to Ru oxidation state or ligand environment. This stability is due to low absorption of Ru K-edge X-rays by water and sufficient sample volume (5-10 ml) of the cell. Applying 1.8 V (relative to NHE) potential to initiate water oxidation we quickly achieved sample oxidation and catalytic current. In spite of the claims that  $\text{Ru}^{\text{V}}=\text{O}$  species should be dominant at such high oxidizing potential, measured Ru oxidation state does not increase above  $\text{Ru}^{\text{IV}}$  while ligand environment of  $[\text{Ru}(\text{tpy})(\text{bpy})\text{H}_2\text{O}]^{2+}$  catalyst undergoes significant modification. After this period of initial quick oxidation and EXAFS spectral changes spectroscopic signatures of solution remain unchanged for up to 24 hours of electrolysis. No new Ru-O-Ru bridge signatures were observed in EXAFS. Sample remains catalytically active. Clear solutions show no signs of sample degradation.

### References

1. Y. Pushkar, D. Moonshiram, V. Purohit, L. Yan, I. Alperovich, J. Am. Chem. Soc., 136 (2014) 11938–11945.
2. J.J. Concepcion, M.K. Tsai, J.T. Muckerman, T.J. Meyer, J. Am. Chem. Soc., 132 (2010) 1545-1557.
3. N. Kaveevivitchai, R.F. Zong, H.W. Tseng, R. Chitta, R.P. Thummel, Inorg. Chem., 51 (2012) 2930-2939.

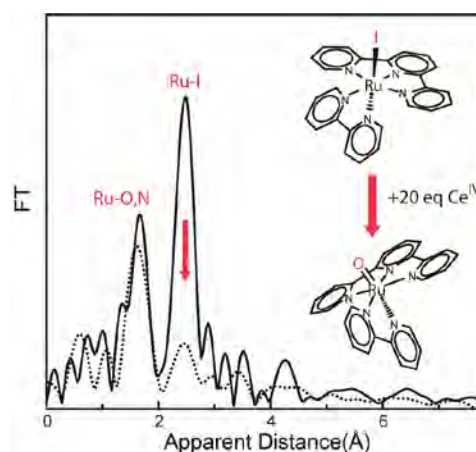


Figure 1. Ru K-edge EXAFS shows how very strong Ru-I absorber-backscatter interaction is quickly lost after addition of 20 equivalent of  $\text{Ce}^{\text{IV}}$  to initiate water oxidation catalysis. 30 sec is sufficient to form predominantly  $[\text{Ru}^{\text{IV}}(\text{bpy})(\text{tpy})=\text{O}]^{2+}$  catalytic steady state.

## Facet-Dependent Photoelectrochemical Performance of TiO<sub>2</sub> Nanostructures: An Experimental and Computational Study

Charles A. Schmuttenmaer, Christopher Koenigsmann, Chuanhao Li,<sup>a</sup> Wendu Ding, Benjamin Rudshiteyn, Ke R. Yang, Kevin P. Regan, Steven J. Konezny, Gary W. Brudvig, Victor S. Batista, and Jaehong Kim<sup>a</sup>

Department of Chemistry

<sup>a</sup>Department of Chemical and Environmental Engineering

Yale University

New Haven, CT 06520-8107

The behavior of crystalline nanoparticles depends strongly on which facets are exposed. Some facets are more active than others, but it is difficult to selectively isolate particular facets. This study provides fundamental insights into photocatalytic and photoelectrochemical performance of three types of TiO<sub>2</sub> nanoparticles with predominantly exposed {101}, {010}, or {001} facets, where 86% to 99% of the surface area is the desired facet. Photodegradation of methyl orange reveals that {001}-TiO<sub>2</sub> has 1.79 and 3.22 times higher photocatalytic activity than {010} and {101}-TiO<sub>2</sub>, respectively. This suggests that the photochemical performance is highly correlated with the surface energy and density of under-coordinated Ti<sup>4+</sup> sites. In contrast, the photoelectrochemical performance of the faceted TiO<sub>2</sub> nanoparticles sensitized with the commercially available MK-2 dye was highest with {010}-TiO<sub>2</sub> which yielded an overall cell efficiency of 6.1%, compared to 3.2% for {101}-TiO<sub>2</sub> and 2.6% for {001}-TiO<sub>2</sub> prepared under analogous conditions.

Measurement of desorption kinetics and accompanying computational modeling suggest a stronger covalent interaction of the dye with the {010} and {101} facets compared with the {001} facet. Time-resolved THz spectroscopy and transient absorption spectroscopy measure faster electron injection and recombination dynamics when MK-2 is bound to {010} compared to other facets, consistent with extensive computational simulations which indicate that the {010} facet provides the most efficient and direct pathway for interfacial electron transfer. Our experimental and computational results establish for the first time that photoelectrochemical performance is dependent upon the binding energy of the dye as well as the crystalline structure of the facet, as opposed to surface energy alone.

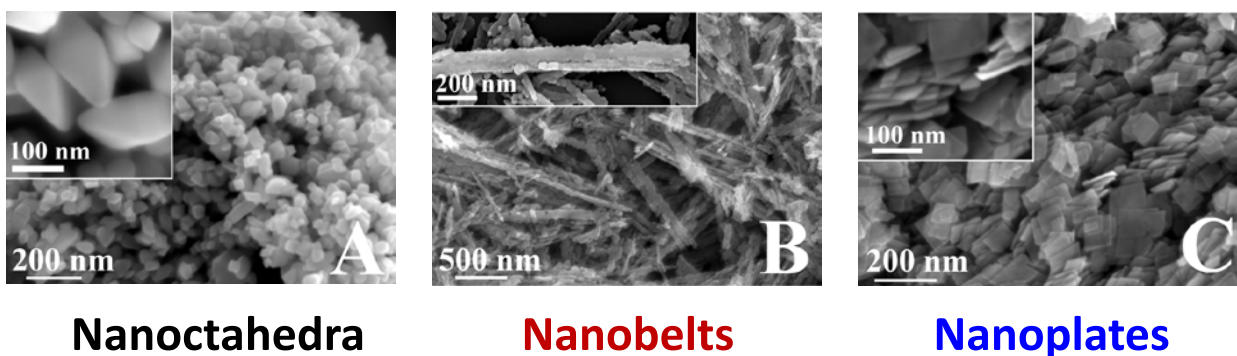


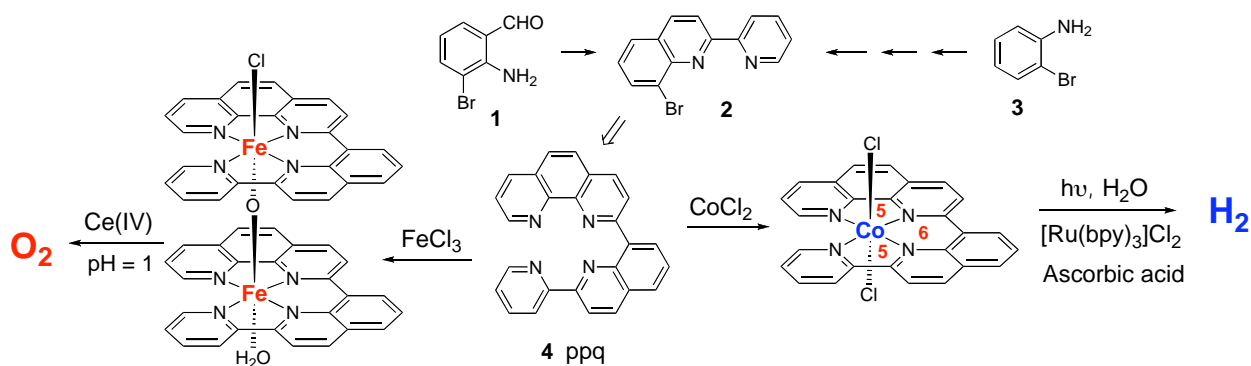
**Figure 1.** Examples of different facets studied. The nanooctahedra have primarily {111} facets exposed, the nanobelts are primarily {001}, and the nanoplates are primarily {100}.

## Earth Abundant Metal-based Catalysts for Artificial Photosynthesis

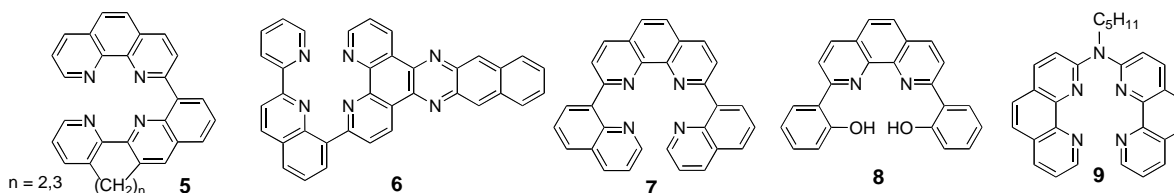
Lianpeng Tong, Lars Kohler, Ruifa Zong, Rongwei Zhou, Lanka Wickramasinghe, Andrew Kopecky, and Randolph P. Thummel  
 Department of Chemistry, 112 Fleming Building, University of Houston,  
 Houston, TX 77204-5003

Homogeneous metal-based catalysts for photochemical water decomposition often involve surrounding ligand systems that can be modified to improve catalytic activity. We are slowly beginning to understand the steric and electronic features that are desirable in such ligands. There is also an effort to use more earth abundant metals for these catalytic processes. Until recently we have almost exclusively examined more precious Ru(II)-based systems.

In binding to a metal, polypyridines form 5-membered chelate rings and present fairly spacious coordination environments that are more favorable to the larger second and third row transition elements. We have prepared 2-(pyridin-2'-yl)-8-(1'', 10''-phenanthroline-2''-yl)quinoline (**4**, ppq) starting either from 2-amino-3-bromobenzaldehyde (**1**) or 2-bromoaniline (**3**). The additional  $sp^2$  center embodied by the C8 of quinoline allows for the formation of tetradentate (5-6-5) chelation geometry that will accommodate the smaller first row transition metals.



The ppq ligand reacts with  $\text{CoCl}_2$  to form a complex with the ppq occupying the equatorial plane. The axial Co-Cl bonds are quite long and thus readily replaced by water. Upon irradiation with blue light, using  $[\text{Ru}(\text{bpy})_3]\text{Cl}_2$  as a photosensitizer and ascorbic acid as a sacrificial electron donor, the complex generates  $\text{H}_2$  with a TOF =  $1400 \text{ h}^{-1}$  at pH = 4.5. When ppq is treated with  $\text{FeCl}_3$ , it forms a complex in which the X-ray structure indicates that two  $\text{Fe}(\text{ppq})$  subunits are linked as an oxo-bridged dimer. When exposed to  $\text{Ce}(\text{IV})$  in aqueous solution this system generates oxygen with a TOF =  $4320 \text{ h}^{-1}$ . In either case no evidence was found for nanoparticle formation. Variations on ppq, such as **5-9**, will be discussed with regard to synthesis, structure, and catalytic activity.

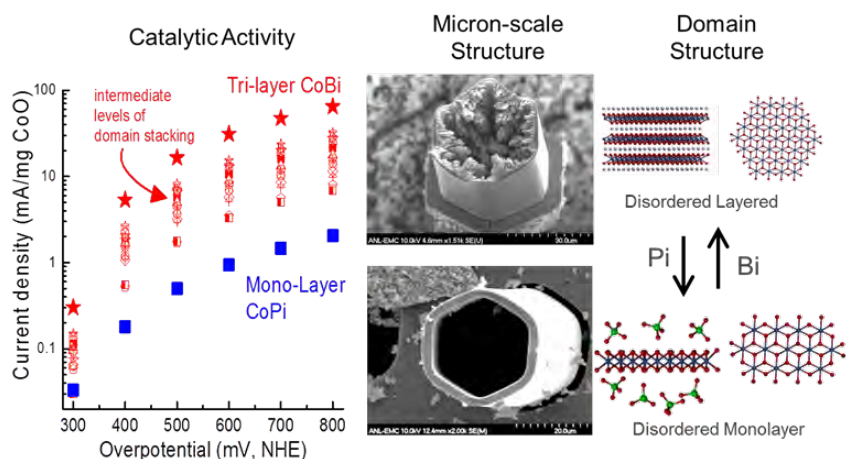


## High Valence Homogeneous and Amorphous Metal Oxide Clusters as Biomimetic Water-Oxidation Catalysts: Exploring Ligand Dependencies on Domain Structure and Function Using *In-Situ* X-Ray Structure Characterization

Gihan Kwon<sup>1</sup>, Diego Fazi<sup>1</sup>, Jonathan D. Emery<sup>2</sup>, Alex B. F. Martinson<sup>2</sup>,  
Lin X. Chen, Karen L. Mulfort<sup>1</sup>, and David M. Tiede<sup>1</sup>

<sup>1</sup>Chemical Sciences and Engineering and <sup>2</sup>Material Sciences Divisions,  
Argonne National Laboratory, Lemont, IL 60439

The assembly of homogeneous and amorphous metal oxide catalytic clusters by photo- and electro-oxidative chemistry is of wide-spread interest for applications in solar energy conversion and the development of artificial leaf assemblies. High valence transition metal-oxo chemistries also underlie mechanisms for the water-splitting catalyst assembly, repair, and function in photosynthesis. As an approach for resolving structures, coordinating ligand dependencies, and mechanisms for metal oxide cluster assembly and catalytic chemistries, we have been developing techniques for resolving both homogeneous and amorphous oxide catalyst structures using synchrotron high energy (60 keV) X-ray scattering and atomic pair distribution function (PDF) analyses. PDF measurements offer the opportunity to resolve pair correlations across the complete length scale of catalytic domains with 0.2 Å spatial resolution, and with a precision that allows discrimination between coordinate models. We have developed high surface area porous electrodes that allow *in-situ* X-ray PDF measurements for characterization of both molecular catalysts and catalytic films. This presentation will compare domain structures resolved for amorphous cobalt oxide films formed electrolytically in the presence of different oxyanions. The results show that phosphate is unique in restricting domain size to a small 13-cobalt atom, single layer domain where defects and edge distortions can be resolved. However, the highest catalytic currents are found associated with films having larger, layered domains, and higher conductivity.



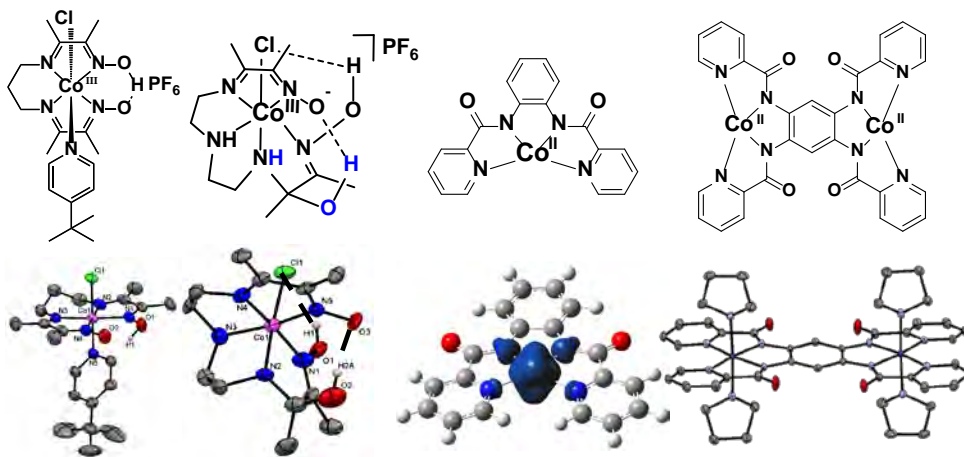
Further, we have used this work to demonstrate the sensitivity PDF measurements to about  $10^{14}$  metal-oxo clusters in the X-ray beam volume. This work establishes a foundation for extending the X-ray PDF method for the analysis of atomic structure changes in molecular catalysts driven by excited-state, sequential single electron photo-chemistry.

## Concerted Experimental and Theoretical Efforts towards the Design of New Cobalt-based Catalysts for Proton/Water Reduction

Debashis Basu, Shivnath Mazumder, Habib Baydoun,  
H. Bernhard Schlegel,\* and Claudio N. Verani\*

Department of Chemistry  
 Wayne State University  
 Detroit, MI, 48202

The Verani and Schlegel groups have been partners in the development of groundbreaking work toward the design of new architectures based on Earth-abundant transition metals and capable of water splitting. The work prioritizes the design of cobalt species with new ligands, the understanding of their electronic and electrochemical behavior and their testing toward proton and water reduction. In this poster we will focus on current efforts as follows: (i) the examination of the energetics of axial ligand dissociation in cobalt oximes, where the order of redox *vs.* chemical events leading to the catalytic Co(I) species is reconsidered; (ii) the development of a new cobalt catalyst with a pentadentate oxime ligand and the investigation of its behavior in organic media with mild acids and in water, where it yields turnover numbers of 6,500;<sup>1</sup> (iii) the investigation of new ligand designs inspired by our recently published<sup>2</sup> pendant-arm [N<sub>2</sub>N'<sub>3</sub>] amido polypyridyl ligand, where we observe turnover numbers of up to 7,000.



For each of these cases we will discuss the syntheses, characterizations, redox and electronic behavior, and catalytic properties as determined by experimental and theoretical approaches.

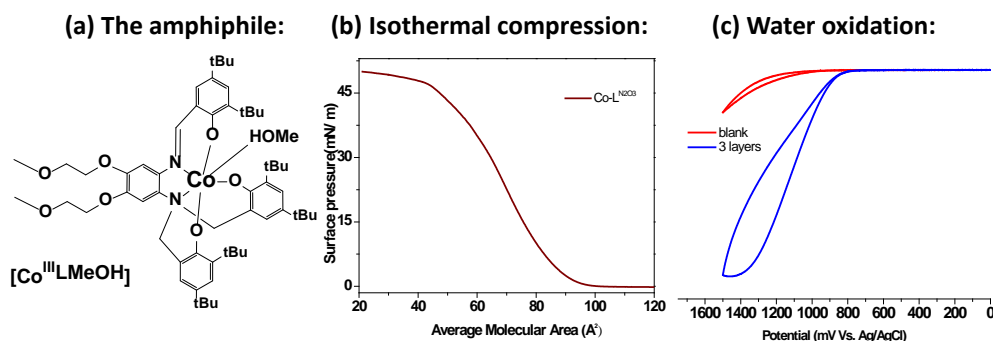
1. D. Basu, S. Mazumder, X. Shi, H. Baydoun, J. Niklas, O. Poluektov, H. B. Schlegel,\* C. N. Verani\* "Ligand Transformations and Efficient Proton/Water Reduction with Cobalt Catalysts Based on Pentadentate Pyridine-Rich Environments" *Angew. Chem. Int. Ed.* **2015**, *54*, 2105–2110
2. D. Basu, S. Mazumder, X. Shi, R. J. Staples, H. B. Schlegel,\* C. N. Verani\* "Distinct Proton and Water Reduction Behavior with a Cobalt(III) Electrocatalyst Based on Pentadentate Oximes" *Angew. Chem. Int. Ed.* **2015**, *accepted* DOI: 10.1002/anie.201501410R2

## Water Oxidation with Langmuir-Blodgett Films of Cobalt [N<sub>2</sub>O<sub>3</sub>] Amphiphiles

Sunalee Gonawala, Habib Baydoun, and Claudio N. Verani\*

Department of Chemistry  
Wayne State University  
Detroit, MI, 48202

The Verani group published recently the use of cobalt-containing phenolate-rich systems for proton reduction.<sup>1,2</sup> Structurally related [Co(salen)] complexes are able to catalyze light-driven water oxidation in solution,<sup>2,3</sup> and these results led us to hypothesize that conductive substrates can be functionalized using LB methods to drive heterogeneous water oxidation. In order to test this hypothesis, we synthesized the phenolate-rich amphiphilic cobalt complex [LCo<sup>III</sup>MeOH], then deposited three layers of this amphiphile on an electrically conductive fluorine-doped tin oxide (FTO) electrode via Langmuir-Blodgett isothermal compression. Cyclic voltammetry reveals the appearance of a catalytic peak at a potential of  $\sim 0.80$  V<sub>Ag/AgCl</sub>, which corresponds to an overpotential of 0.47 V in a 50 mmol.L<sup>-1</sup> K-triflate aqueous solution at pH 12.



In order to validate that this peak is indeed due to film-catalyzed water oxidation, bulk electrolysis was performed at an applied potential of +1.2 V for 1 hour. Using atmospheric nitrogen as an internal standard, an increase in the amount of oxygen present in the headspace was observed. Based on the assumption that each molecule on the surface occupies an area of 97 Å<sup>2</sup> (derived from direct reading of the  $\pi$  vs. A isothermal plot), it can be estimated that the electrode has a surface coverage of  $1.03 \times 10^{14}$  molecules/(layer.cm<sup>2</sup>). As such, we preliminarily estimate a TON of 11,000 with Faradaic efficiency of 98%. This catalytic activity cannot be observed by FTO substrates nor by simple drop-cast films with the same amphiphile, as these yield no or only marginal results. The stability of the deposited film towards mechanical stress was assessed by placing the modified electrode in an aqueous potassium triflate solution under stirring for 3 h. The CVs were measured at regular time intervals and remained constant, leading to the conclusion that the LB film is mechanically robust. In order to verify whether oxidation is metal- or ligand-centered, a gallium-containing analogue, [LGa<sup>III</sup>MeOH], was deposited onto FTO and a voltammogram was measured. The results reveal the absence of any catalytic current, thus confirming the metal involvement in catalysis.

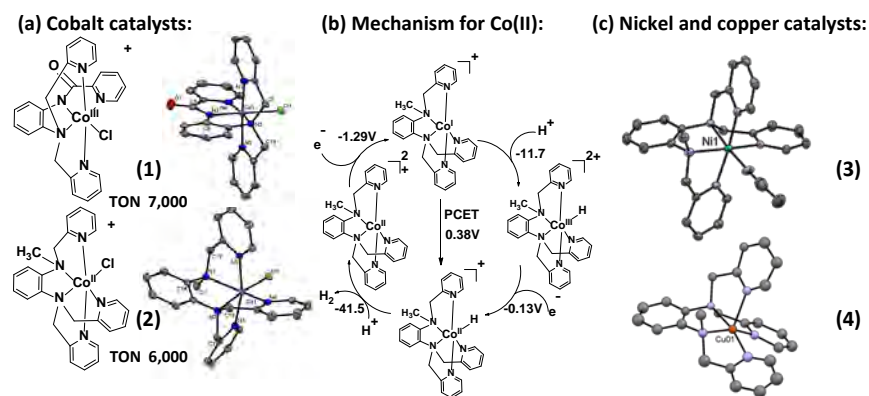
1. Allard, Heeg, Schlegel, Verani *Eur. J. Inorg. Chem.* **2012**, 4622
2. Basu, Allard, Xavier, Heeg, Schlegel, Verani *Dalton Trans.* **2015**, 44, 3454
3. Pizzolato, Natali, Posocco, Montellano, Bazzan, Valentin, Galloni, Conte, Bonchio, Scandola, Sartorel, *Chem. Commun.* **2013**, 49, 9941

## Water Reduction with Cobalt, Nickel, and Copper Complexes Based on an [N<sub>2</sub>N'<sub>3</sub>] Ligand

Debashis Basu, Pavithra Kankanamalage, Danushka Ekanayake, Shivnath Mazumder,  
H. Bernhard Schlegel,\* and Claudio N. Verani\*

Department of Chemistry  
 Wayne State University  
 Detroit, MI, 48202

The Verani and Schlegel groups have been evaluating the catalytic properties of cobalt complexes based on pentadentate [N<sub>2</sub>N'<sub>3</sub>] pyridine rich ligands. We recently published<sup>1</sup> on two catalysts, the Co(III) amide species [Co<sup>III</sup>L<sup>1</sup>Cl] (**1**) and the N-methyl protected complex [Co<sup>II</sup>L<sup>2</sup>Cl] (**2**). Electrochemical experiments at -1.7 V<sub>Ag/AgCl</sub> reveal H<sub>2</sub> generation with TONs of 15.44 and 14.35, respectively after 3 h and in presence of mild acetic acid in MeCN. Remarkably, **1** and **2** are excellent water reduction catalysts with TONs of 7,000 and 6,000, respectively after 18 h and Faradaic efficiencies of 95%. The present TONs insert these two species among a select group of top catalysts for water reduction. The catalytic mechanisms obtained by DFT calculations involve the formation of a Co<sup>III</sup>-H species that undergoes further reduction followed by protonation of the hydride on the cobalt center. Recent photocatalytic activity was also observed.



These results led us to consider the viability of using nickel and copper species. Kankanamalage & Ekanayake have synthesized the complexes [Ni<sup>II</sup>L<sup>2</sup>MeCN] (**3**) and [Cu<sup>II</sup>L<sup>2</sup>] (**4**) with the methylated ligand used for the cobalt catalyst **2**. Species **3** shows redox processes at 1.08 and -1.71 V<sub>Fc+/Fc</sub> tentatively associated with the Ni<sup>III/II</sup> and Ni<sup>II/I</sup> couples, whereas **4** displays a Cu<sup>II/I</sup> couple at -0.48 V<sub>Fc+/Fc</sub>. Both species revealed moderate to good catalytic activity in preliminary 2 h BE runs at pH 7 in phosphate buffer; the nickel-containing **3** presents an onset overpotential of 0.85 V, yielding a TOF of ca. 430 h<sup>-1</sup> and a modest Faradaic efficiency of ca. 70%, while the copper-containing **4** shows a similar catalytic behavior with an onset overpotential of 0.80 V yielding a TOF ~ 285 after 2 hours and Faradaic efficiency of 90 % at -1.7 V<sub>Ag/AgCl</sub>. This poster discusses the electro and photocatalytic behavior of **2**, **3**, and **4**.

1. D. Basu, S. Mazumder, X. Shi, H. Baydoun, J. Niklas, O. Poluektov, H. B. Schlegel, C. N. Verani "Ligand Transformations and Efficient Proton/Water Reduction with Cobalt Catalysts Based on Pentadentate Pyridine-Rich Environments" *Angew. Chem. Int. Ed.* **2015**, 54, 2105–2110

## Design of Efficient Molecular Electrocatalysts for Water and Carbon Dioxide Reduction Using Predictive Models of Thermodynamic Properties

Charlene Tsay, Brooke Livesay, Juliet Khosrowabadi Kotyk, Zachary Thammavongsy, and

Jenny Y. Yang

Department of Chemistry  
University of California, Irvine  
Irvine, CA 92697-2025

Transition metal hydrides are essential intermediates in many reductive fuel forming reactions. Designing energetically efficient (low overpotential) electrocatalysts for these reactions requires an understanding of the overall free energy of hydride transfer,  $\Delta G_{\text{H}^-}$  (eq 1) relative to the substrate,  $\text{H}^+$  to make  $\text{H}_2$ , or  $\text{CO}_2$  to make  $\text{HCO}_2^-$ . To this end, we are measuring the hydride donor ability of different transition metal complexes in solvents of varying polarity. This will lead to a better understanding of how to tune the catalyst to the optimal hydricity value for the desired substrate and solvent conditions. Of particular interest to our program thus far is the development of catalysts that can operate under aqueous conditions at very high or low pH, since most membrane (ion transport) materials used in electrolytic cells operate at limited pH values.

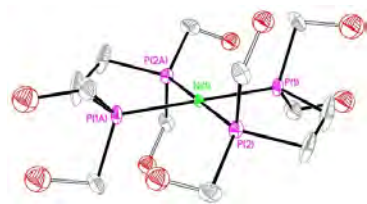


**Figure 1.** Single crystal X-ray structure of Ni(II) bis(diphosphine) aqueous hydrogen production catalyst discussed herein. Protons and the two  $\text{BF}_4^-$  anions are not shown.

Solvent	$\Delta G_{\text{H}^-}$ (kcal/mol)
$\text{H}_2\text{O}$	29.6
$\text{CH}_3\text{CN}$	55
DMSO	54-63

**Table 1.**  $\Delta G_{\text{H}^-}$  of the corresponding Ni-H complex in three different solvents.

We have currently measured the hydride donor ability of a nickel bis(diphosphine) complex in  $\text{H}_2\text{O}$ ,  $\text{CH}_3\text{CN}$ , and DMSO. The values are shown in **Table 1**, and represent the first time to our knowledge the hydricity of a single compound has been measured in three different solvents. The single crystal X-ray structure of the Ni(II) species is shown in **Figure 1**. This complex is stable under aqueous low pH conditions (0-2), showing no signs of degradation after a period of days. This complex is a competent electrocatalyst for aqueous proton reduction at pH 1, producing hydrogen at greater than 98% Faradaic efficiency. Furthermore, we have been able to isolate each intermediate in the catalytic cycle in the non-protic solvent DMSO, including the Ni(0) complex and Ni-H, and can follow the catalytic cycle via  $^1\text{H}$  and  $^{31}\text{P}$  NMR by sequential addition of  $\text{H}^+$  to the Ni(0) complex,

confirming the role of the nickel hydride in the catalytic cycle.

We are currently expanding our efforts in measuring the hydride donor ability and electrocatalytic activity towards proton reduction in other first row metals. Some of our targets are anticipated to have sufficiently low  $\Delta G_{\text{H}^-}$  to reduce  $\text{CO}_2$  to  $\text{HCO}_2^-$ , so electrocatalytic activity towards this reaction will also be explored. Funding through this grant has also supported the development of new ligands with pendant proton donor and accepting groups, in an effort to develop electrocatalysts that control both electronic structure (redox potentials) via the primary coordination sphere, and proton inventory in the secondary coordination sphere.

## A Molecular Cobalt Catalyst Architected and TiO<sub>2</sub> Modified p-GaInP<sub>2</sub> Photoelectrode for Hydrogen Production

Jing Gu, Yong Yan, James Young, Kenneth Steirer, Nathan R. Neale, and John Turner

Chemical and Material Science Center  
National Renewable Energy Laboratory  
Golden, CO, 80215

The use of sunlight to drive the conversion of water into H<sub>2</sub> and O<sub>2</sub> via a photoelectrochemical (PEC) reactor provides a strategy for storing solar energy, providing an energy carrier for transportation and a feedstock for ammonia production. To collect enough sunlight to produce the amounts of hydrogen necessary will require covering large land areas. Utilizing precious metal catalysts over such large areas could prove to be difficult, thus alternative catalyst systems need to be considered. Homogeneous catalysts provide a rich area for both hydrogen and oxygen catalysts with a variety of redox potentials and catalytic activity. Combining the high photoconversion efficiency of a semiconductor electrode with the versatility of homogeneous catalysts could prove to be a winning combination making PEC hydrogen production viable.

Here we demonstrate that by employing a hybrid molecular/semiconductor interface with atomic layer deposited (ALD) TiO<sub>2</sub> as an intermediate layer, a robust and corrosion resistant GaInP<sub>2</sub>-TiO<sub>2</sub>-cobaltoxime-TiO<sub>2</sub> photocathode can be operated in alkaline media (pH = 13).

An earth-abundant first row transition Cobalt catalyst Co(oxm)(pyCOOH) [oxm = bis-glyoxime; pyCOOH = 4-carboxyl pyridine] as shown in figure 1 was attached onto a TiO<sub>2</sub> modified GaInP<sub>2</sub> surface through a carboxylic linkage group. A 35 nm amorphous TiO<sub>2</sub> layer was deposited onto bare GaInP<sub>2</sub> as protection and linkage layer. To further protect the linkage stability, an additional 10 cycle (~0.4 nm) TiO<sub>2</sub> ALD layer was deposited on top of the catalyst layer.

The photoelectrochemical photocurrent density (J) versus potential (V) plots of the cobaltoxime modified electrode showed that its activity and stability were comparable to the similarly modified Pt electrodes.

It should also be pointed out that for the application presented here, that of a photoelectrochemical water splitting system, the stability of the homogeneous catalyst is less important. This is because the system will be inoperative every night allowing for the possibility of rejuvenating the catalyst system by some means.

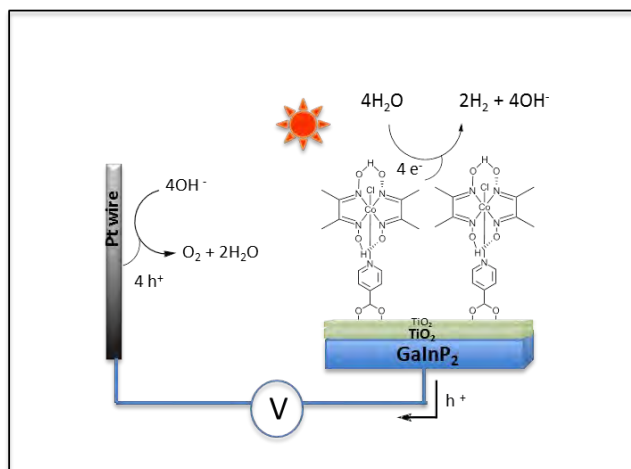


Figure 1. Cobaltoxime and TiO<sub>2</sub> modified GaInP<sub>2</sub> electrode

## Transition Metal Polypyridine Complexes: Studies of Mediation in Dye-Sensitized Solar Cells and Charge Separation

Amy L. Prieto (for C. Michael Elliott)  
Chemistry Department  
Colorado State University

Our group's recent research efforts have primarily focused on improving open-circuit voltage ( $V_{OC}$ ) values in dye-sensitized solar cells (DSSCs). Historically, these values have largely been limited by the redox potential of the mediator. We take advantage of mediators based on cobalt tris-bipyridyl complexes, which can be synthetically tuned, in order to positively shift the mediator's redox potential and thus increase  $V_{OC}$ . Several avenues are being explored pursuant to this goal.

We have successfully synthesized several novel bipyridine ligands employing electron withdrawing groups at the 4,4' positions which, when complexed with cobalt, result in species with highly positive redox potentials. In characterizing our high-potential complexes, multiple pieces of evidence reveal a trend of decreasing complex stability with increasing redox potential. These include the appearance of multiple waves in the cyclic voltammetry, a color change upon addition of 4-*tert*-butylpyridine indicating the formation of a new species, direct NMR evidence of dissociated free ligand in acetonitrile solution, and potential-independent DSSC recombination currents paralleling the stability trends as determined by NMR. We have taken advantage of a simple quantitative NMR experiment to determine approximate ligand-binding equilibrium (stability) constants for each of our complexes in acetonitrile at room temperature.

It has also been shown that cobalt tris-bipyridyl complexes with electron withdrawing substitutions at the 5,5' positions can cause the observed potential to shift significantly positive of the unsubstituted bipyridine complex. For example, the  $E_{1/2}$  for the tris 5,5'-diethyl ester-2,2'-bipyridine cobalt complex was found to be 0.76 V vs. SCE whereas the reported potential for the unsubstituted complex is ca. 0.3 V vs. SCE. However, the assembled complexes are even more unstable than their 4,4' analogues. This is particularly true in the presence of 4-*tert*-butylpyridine and is probably exasperated by the conformational strain introduced with bulky side groups. Methods of combatting that instability are currently being explored. Synthetic progress has been made to link the substituted bipyridines together into a single moiety in order to take advantage of the chelating effect.

We have also made efforts to increase  $J_{SC}$  values in DSSCs mediated by cobalt tris-bipyridyl complexes. One of the chief concerns with these complexes is their relatively large size which typically leads to currents limited by restricted mass transport through the dyed  $TiO_2$  framework. In an effort to combat this issue,  $Ru(bpy)_2(SCN)_2$ -type sensitizers have been developed which incorporate covalently bound electron donors to shuttle the photo-generated hole away from the dye and farther into the mediator solution. The intent is twofold: first, to reduce the distance the cobalt complex must travel in order to regenerate the dye; and second, to encourage mediator reduction away from the  $TiO_2$  surface so the oxidized mediator does not scavenge injected electrons. We borrow from past work in our group on similar donor-chromophore-acceptor triad assemblies towards this end.

### **Transport along conjugated polymer chains**

M. J. Bird, A. R. Cook, L. Zaikowski, G. Mauro, X. Li., G. Rumbles, J. Blackburn, O. G. Reid  
and J. R. Miller

Department of Chemistry  
Brookhaven National Laboratory  
Upton, NY 11973

Through the use of pulse-radiolysis time resolved microwave conductivity (PR-TRMC), the effects of chain length, curvature, defects, “push-pull” copolymerization and ion-pairing on single chain microwave mobility have been studied in solution. Differences have been seen between electron and hole mobility along push-pull polymers where the electron and hole wavefunctions are predicted to be different. Microwave conductivity, as compared to optical absorptions, appears to be a very sensitive tool for detecting the presence of a counter ion near a polymer polaron.

For PR-TRMC measurements of solid polymer samples, knowledge of the ion-yield for a given dose of ionizing radiation is necessary to convert conductivity into mobility, however a technique for doing this had yet to be established. By pressing films into thin discs (~100um thick) and using IR quantum cascade lasers (QCLs) we have been able to observe the IR absorptions from charge carriers and, for the first time, establish yields of ions in these solid samples. Remarkable differences in yields are seen for some polymers attributed to microstructural differences that can cause excited states to dissociate into free charges in the absence of an electron acceptor.

Finally, analysis of steady state fluorescence measurements of a series of different length polyfluorene chains with end traps have shown that, along single chains, singlet excitons can travel large distances (~34nm). Exploiting such long diffusion lengths could lead to new possibilities for OPV device architectures.

## Do TFSA Anions Slither? Pressure Exposes the Role of Anion Conformational Exchange in Self-Diffusion

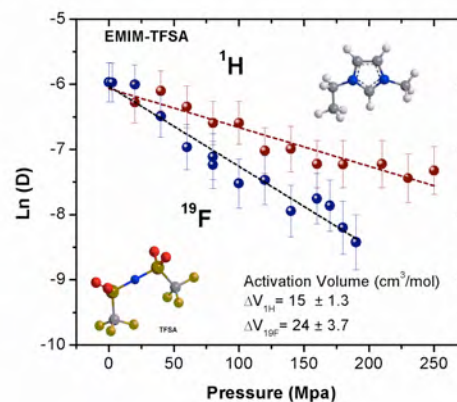
James F. Wishart,<sup>‡</sup> Sophia N. Suarez,<sup>†</sup> David Cuffari,<sup>†</sup> Armando Rua,<sup>§</sup> Kartik Pillar,<sup>§</sup>  
Jasmine L. Hatcher,<sup>‡</sup> Sharon Ramati,<sup>‡</sup> and Steven G. Greenbaum<sup>§</sup>

<sup>‡</sup>Chemistry Department, Brookhaven National Laboratory, Upton, NY 11973, <sup>†</sup>Physics Department, Brooklyn College, Brooklyn, NY 11210 and <sup>§</sup>Department of Physics, Hunter College, New York, NY 10021

The transport properties of ionic liquids (viscosity, conductivity, ionic self-diffusion and solute diffusion) are very distinct from those of conventional solvents. Since these properties are important for the application of ILs to the capture, storage and use of energy, they have been a major focus of the five-institution SISGR team on “Physical Chemistry of Reaction Dynamics in Ionic Liquids”.

Several experimental and theoretical (MD) studies have taught us a great deal about why IL transport properties are so unique. Temperature-dependence measurements have provided information about activation barriers and the glassy, distributed nature of IL dynamics. However, pressure is a valuable (but less well known) variable that can provide complementary and sometimes unique mechanistic insight. At BNL, we have been using high-pressure kinetics measurements to decipher reaction mechanisms for over 23 years. In this study, we use high-pressure NMR methods to investigate the transport properties of selected ILs.

Multi-nuclear (<sup>1</sup>H, <sup>2</sup>H, and <sup>19</sup>F) magnetic resonance spectroscopy techniques were applied as functions of temperature and pressure to the study of selectively deuterated 1-alkyl-3-methylimidazolium (alkyl = ethyl (EMIM) or butyl (BMIM)) bis(trifluoromethylsulfonyl)amide (TFSA) ionic liquids (ILs). Studies of relaxation times gave information about changes in the structure of the ILs with temperature and pressure. Most significantly, the pressure dependences of the ionic self-diffusion coefficients in EMIM TFSA revealed that the displacements of the cations and anions are uncoupled, with the TFSA anions being more affected by increasing pressure as supported by a larger activation volume ( $24 \pm 4$  cm<sup>3</sup>/mol) compared to that of the EMIM cations ( $15 \pm 1$  cm<sup>3</sup>/mol). This dramatic difference is unique among the nine imidazolium ILs for which such data is available. A less pronounced effect is seen in BMIM TFSA, but for all other cases the activation volumes for the anion and cation are similar. Increasing pressure may lower the mobility of the TFSA anion by hindering its interconversion between trans and cis conformers, a process that previous MD simulations suggested would be coupled to diffusion. The effect is visible in EMIM TFSA due to the small cation size. The high-pressure diffusion data provide clear experimental evidence for the MD prediction.



Plot of ionic self-diffusion rates versus pressure for emim cation (<sup>1</sup>H) and TFSA anion (<sup>19</sup>F) measured by high-pressure PGSE NMR.



## *List of Participants*



## Participants List – 37<sup>th</sup> Solar Photochemistry P. I. Meeting

Neal Armstrong  
University of Arizona  
Dept. Chemistry and Biochemistry  
Tucson, AZ 85721  
520-730-7365  
nra@email.arizona.edu

John Asbury  
Pennsylvania State University  
Department of Chemistry  
University Park, PA 16801  
814-863-6309  
jba11@psu.edu

Marc Baldo  
Massachusetts Institute of Technology  
77 Massachusetts Ave.  
Cambridge, MA 02139-4307  
617-452-5132  
baldo@mit.edu

Allen Bard  
University of Texas at Austin  
105 E. 24th St., Stop A5300  
Austin, TX 78712-1224  
512-471-3761  
ajbard@mail.utexas.edu

Robert Bartynski  
Rutgers University  
136 Frelinghuysen Rd.  
Piscataway, NJ 08854  
732-445-5500  
bart@physics.rutgers.edu

Victor Batista  
Yale University  
P.O. Box 208107  
New Haven, CT 06477  
203-432-6672  
victor.batista@yale.edu

Matt Beard  
National Renewable Energy Laboratory  
15013 Denver West Pkwy.  
Golden, CO 80401  
303-384-6781  
matt.beard@nrel.gov

Matthew Bird  
Brookhaven National Laboratory  
Chemistry Department  
Upton, NY 11973  
631-344-4331  
mbird@bnl.gov

David Blank  
University of Minnesota  
207 Pleasant St. SE  
Minneapolis, MN 55455  
612-624-0571  
blank@umn.edu

Andrew Bocarsly  
Princeton University  
Frick Laboratory  
Princeton, NJ 08544  
609-258-3888  
bocarsly@princeton.edu

David Bocian  
University of California, Riverside  
Department of Chemistry  
Riverside, CA 92521  
951-827-3660  
David.Bocian@ucr.edu

Shannon Boettcher  
University of Oregon  
Department of Chemistry  
Eugene, OR 97403  
541-346-2543  
swb@uoregon.edu

Kara Bren  
University of Rochester  
120 Trustee Rd.  
Rochester, NY 14627-0216  
585-275-4335  
bren@chem.rochester.edu

Gary Brudvig  
Yale University  
P.O. Box 208107  
New Haven, CT 06477  
203-432-5202  
gary.brudvig@yale.edu

## Participants List – 37<sup>th</sup> Solar Photochemistry P. I. Meeting

Emilio Bunel  
Argonne National Laboratory  
9700 S. Cass Ave.  
Argonne, IL 60439  
630-252-4309  
ebunel@anl.gov

Ian Carmichael  
University of Notre Dame  
223 Radiation Laboratory  
Notre Dame, IN 46556  
574-631-4502  
carmichael.1@nd.edu

Felix N. Castellano  
North Carolina State University  
2620 Yarbrough Dr.  
Raleigh, NC 27695  
919-515-3021  
fncastel@ncsu.edu

Edward Castner  
Rutgers University  
610 Taylor Rd.  
Piscataway, NJ 08854  
732-445-2564  
ed.castner@rutgers.edu

Lin Chen  
Argonne National Lab/Northwestern Univ.  
9700 S. Cass Ave.  
Argonne, IL 60439  
630-252-3533  
lchen@anl.gov

Kyoung-Shin Choi  
University of Wisconsin, Madison  
1101 University Ave.  
Madison, WI 53706  
608-262-5859  
kschoi@chem.wisc.edu

Javier Concepcion  
Brookhaven National Laboratory  
Chemistry Department  
Upton, NY 11973-5000  
631-344-4369  
jconcepc@bnl.gov

Philip Coppens  
University at Buffalo SUNY Buffalo  
732 NSC Complex  
Buffalo, NY 14260-3000  
716-645-4273  
coppens@buffalo.edu

Robert Crabtree  
Yale University  
225 Prospect St.  
New Haven, CT 06520  
203-432-3925  
robert.crabtree@yale.edu

Nada Dimitrijevic  
U.S. Department of Energy  
1000 Independence Ave., SW  
Washington, DC 20585  
301-903-5805  
Nada.Dimitrijevic@science.doe.gov

Linda Doerrer  
Boston University  
590 Commonwealth Ave.  
Boston, MA 02139  
617-358-4335  
doerrer@bu.edu

Kim Dunbar  
Texas A&M University  
Department of Chemistry  
College Station, TX 77843-3255  
979-845-5235  
dunbar@mail.chem.tamu.edu

Richard Eisenberg  
University of Rochester  
Department of Chemistry  
Rochester, NY 14627-0216  
585-275-5573  
eisenberg@chem.rochester.edu

John Endicott  
Wayne State University  
Chem. 321  
Detroit, MI 48202  
313-5787-2607  
jfe@chem.wayne.edu

## Participants List – 37<sup>th</sup> Solar Photochemistry P. I. Meeting

Christopher Fecko  
U.S. Department of Energy  
1000 Independence Ave., SW  
Washington, DC 20585  
301-903-1303  
Christopher.Fecko@science.doe.gov

Susanne Ferrere  
National Renewable Energy Laboratory  
15013 Denver West Pkwy.  
Golden, CO 80401  
303-384-6502  
Suzanne.Ferrere@nrel.gov

Heinz Frei  
Lawrence Berkeley National Laboratory  
One Cyclotron Rd.  
Berkeley, CA 94720  
510-486-4325  
HMFrei@lbl.gov

Richard A. Friesner  
Columbia University  
3000 Broadway, MC 3110  
New York, NY 10027  
212-854-7606  
rich@chem.columbia.edu

Etsuko Fujita  
Brookhaven National Laboratory  
Chemistry Department  
Upton, NY 11973-5000  
631-344-4356  
fujita@bnl.gov

Elena Galoppini  
Rutgers University  
73 Warren St.  
Newark, NJ 07041  
973-353-5317  
galoppin@rutgers.edu

Theodore Goodson III  
University of Michigan at Ann Arbor  
930 N. University Ave.  
Ann Arbor, MI 48109-1055  
734-647-0274  
tgoodson@umich.edu

David Grills  
Brookhaven National Laboratory  
Chemistry Department  
Upton, NY 11973-5000  
631-344-4332  
dcgrills@bnl.gov

Erik Grumstrup  
Montana State University  
240 Gaines Hall  
Bozeman, MT 59717  
406-994-2988  
erik.grumstrup@montana.edu

Devens Gust  
Arizona State University  
Dept. Chemistry and Biochemistry  
Tempe, AZ 85287  
480-965-4547  
gust@asu.edu

Thomas Hamann  
Michigan State University  
578 S. Shaw Ln., RM 411  
East Lansing, MI 48824  
517-355-9715  
hamann@chemistry.msu.edu

Alexander Harris  
Brookhaven National Laboratory  
Chemistry Department  
Upton, NY 11973-5000  
631-344-4301  
alexh@bnl.gov

Michael Henderson  
Pacific Northwest National Laboratory  
P.O. Box 999, K8-87  
Richland, WA 99352  
509-371-6527  
ma.henderson@pnnl.gov

Craig Hill  
Emory University  
1515 Dickey Dr., NE  
Atlanta, GA 30322  
404-727-6611  
chill@emory.edu

## Participants List – 37<sup>th</sup> Solar Photochemistry P. I. Meeting

Dewey Holten  
Washington University  
Chemistry Department  
One Brookings Dr.  
St. Louis, MO 63130  
314-93 5-6502  
holten@wustl.edu

Joseph Hupp  
Northwestern University  
2145 Sheridan Rd.  
Evanston, IL 60208  
847-441-0136  
j-hupp@northwestern.edu

Justin Johnson  
National Renewable Energy Laboratory  
15013 Denver West Pkwy.  
Golden, CO 80401  
303-384-6190  
justin.johnson@nrel.gov

David Jonas  
University of Colorado  
215 UCB  
Boulder, CO 80309-0215  
303-492-3818  
david.jonas@colorado.edu

Prashant Kamat  
University of Notre Dame  
223 Radiation Laboratory  
Notre Dame, IN 46556  
574-631-5411  
pkamat@nd.edu

David Kelley  
University of California, Merced  
5200 N. Lake Rd.  
Merced, CA 95343  
209-228-4354  
dfkelley@ucmerced.edu

Peter Khalifah  
Stony Brook University  
Department of Chemistry  
Stony Brook, NY 11794-3400  
631-632-7796  
kpete@bnl.gov

Christine Kirmaier  
Washington University  
Dept. of Chemistry, Box 1134  
St. Louis, MO 63130  
314-725-6157  
kirmaier@wustl.edu

Bruce Koel  
Princeton University  
Dept. Chem. & Biol. Eng.  
Princeton, NJ 08544  
609-258-4524  
bkoel@princeton.edu

Todd Krauss  
University of Rochester  
120 Trustee Rd.  
Rochester, NY 14627-0216  
585-275-5093  
krauss@chem.rochester.edu

Frederick Lewis  
Northwestern University  
2145 Sheridan Rd.  
Evanston, IL 60208  
847-491-3441  
fdl@northwestern.edu

Nathan Lewis  
California Institute of Technology  
1200 E. California Blvd.  
Pasadena, CA 91125  
626-395-6335  
nslewis@caltech.edu

Tianquan Lian  
Emory University  
1515 Dickey Dr. NE  
Atlanta, GA 30322  
404-727-6649  
tlian@emory.edu

Jonathan Lindsey  
North Carolina State University  
CB8204, 2620 Yarbrough Dr.  
Raleigh, NC 27695-8204  
919-5 15-6406  
jlindsey@ncsu.edu

## Participants List – 37<sup>th</sup> Solar Photochemistry P. I. Meeting

Mark Lonergan  
University of Oregon  
1253 Department of Chemistry  
Eugene, OR 97403  
541-346-4748  
lonergan@uoregon.edu

Rene Lopez  
University of North Carolina  
343 Chapman Hall, Physics Dept.  
Chapel Hill, NC 27713  
919-962-7216  
rln@physics.unc.edu

Stephen Maldonado  
University of Michigan at Ann Arbor  
930 N. University Ave.  
Ann Arbor, MI 48109-1055  
734-647-4750  
smald@umich.edu

Thomas Mallouk  
Pennsylvania State University  
Department of Chemistry  
University Park, P A 16801  
814-863-9637  
tom@chem.psu.edu

Diane Marceau  
U.S. Department of Energy  
1000 Independence Ave., SW  
Washington, DC 20585  
301-903-0235  
Diane.Marceau@science.doe.gov

Claudio Margulis  
University of Iowa  
118 TATL  
Iowa City, IA 52242  
319-335-0615  
claudio-margulis@uiowa.edu

Mark Maroncelli  
Pennsylvania State University  
408 Chemistry Building  
University Park, PA 16802  
814-865-0898  
maroncelli@psu.edu

James McCusker  
Michigan State University  
578 South Shaw Ln.  
East Lansing, MI 48824-1322  
517-355-9715  
jkm@chemistry.msu.edu

Gail McLean  
U.S. Department of Energy  
1000 Independence Ave., SW  
Washington, DC 20585  
301-903-7807  
Gail.Mclean@science.doe.gov

Gerald Meyer  
University of North Carolina  
Department of Chemistry  
Chapel Hill, NC 27599-3290  
919-962-6320  
gjmeyer@email.unc.edu

Thomas Meyer  
University of North Carolina  
Department of Chemistry  
Chapel Hill, NC 27599-3290  
919-843-8313  
tjmeyer@unc.edu

Josef Michl  
University of Colorado  
Dept. Chem. and Biochem., 215 UCB  
Boulder, CO 80309-0215  
303-492-6519  
michl@eefus.colorado.edu

Eric Miller  
U.S. Department of Energy  
1000 Independence Ave., SW  
Washington, DC 20585  
202-287-5829  
Eric.Miller@ee.doe.gov

John Miller  
Brookhaven National Laboratory  
Chemistry Department  
Upton, NY 11973  
631-344-4354  
jrmiller@bnl.gov

## Participants List – 37<sup>th</sup> Solar Photochemistry P. I. Meeting

Ana Moore  
Arizona State University  
Dept. Chemistry and Biochemistry  
Tempe, AZ 85287-1604  
480-965-2747  
amoore@asu.edu

Robert Moore  
Virginia Polytechnic Institute  
Department of Chemistry  
Blacksburg, VA 24061-0212  
540-231-6015  
rbmoore3@vt.edu

Thomas Moore  
Arizona State University  
Dept. Chemistry and Biochemistry  
Tempe, AZ 85287-1604  
480-965-3308  
tmoore@asu.edu

Amanda Morris  
Virginia Polytechnic Institute  
Department of Chemistry  
Blacksburg, VA 24061-0212  
540-231-5585  
ajmorris@vt.edu

James Muckerman  
Brookhaven National Laboratory  
Chemistry Department  
Upton, NY 11973-5000  
631-344-4368  
muckerma@bnl.gov

Charles Mullins  
University of Texas at Austin  
Dept. of Chemical Eng. C0400  
Austin, TX 78712  
512-471-5817  
mullins@che.utexas.edu

Djamaladdin Musaev  
Emory University  
1515 Dickey Dr.  
Atlanta, GA 30322  
404-727-2382  
dmusaev@emory.edu

Nathan Neale  
National Renewable Energy Laboratory  
15013 Denver West Pkwy.  
Golden, CO 8040 1  
303-384-6165  
nathan.neale@nrel.gov

Marshall Newton  
Brookhaven National Laboratory  
Chemistry Department  
Upton, NY 11973  
631-344-4366  
newton@bnl.gov

Daniel Nocera  
Harvard University  
12 Oxford St.  
Cambridge, MA 02138  
617-495-8904  
dnocera@fas.harvard.edu

Arthur Nozik  
University of Colorado  
215 UCB  
Boulder, CO 80309  
303-384-6603  
arthur.nozik@colorado.edu

Bruce Parkinson  
University of Wyoming  
1000 E. University Ave.  
Laramie, WY 82071  
303-766-9891  
bparkin1@uwyo.edu

Hrvoje Petek  
University of Pittsburgh  
3941 O'Hara St., G01 Allen  
Pittsburgh, P A 15260  
412-624-3599  
petek@pitt.edu

Tanja Pietraß  
U.S. Department of Energy  
1000 Independence Ave., SW  
Washington, DC 20585  
301-903-8165  
Tanja.Pietrass@science.doe.gov

## Participants List – 37<sup>th</sup> Solar Photochemistry P. I. Meeting

Oleg Poluektov  
Argonne National Laboratory  
9700 S. Cass Ave.  
Argonne, IL 60439  
630-252-3546  
Oleg@anl.gov

Dmitry Polyansky  
Brookhaven National Laboratory  
Chemistry Department  
Upton, NY 11973-5000  
631-344-4315  
dmitriyp@bnl.gov

Oleg Prezhdo  
University of Southern California  
Department of Chemistry  
Los Angeles, CA 90089  
213-821-3116  
prezhdo@usc.edu

Amy Prieto  
Colorado State University  
Department of Chemistry  
Campus Delivery 0922  
Fort Collins, CO 80523  
970-491-1592  
alprieto@lamar.colostate.edu

Sylwia Ptasinska  
University of Notre Dame  
223 Radiation Laboratory  
Notre Dame, IN 46556  
574-631-1846  
sptasins@nd.edu

Yulia Pushkar  
Purdue University  
525 Northwestern Ave.  
West Lafayette, IN 97407  
765-496-3279  
ypushkar@purdue.edu

Jeffrey Pyun  
University of Arizona  
1306 E. University Blvd.  
Tucson, AZ 85721  
520-626-1834  
jpyun@email.arizona.edu

Garry Rumbles  
National Renewable Energy Laboratory  
15013 Denver West Pkwy.  
Golden, CO 80401  
303-384-6502  
garry.rumbles@nrel.gov

Scott Saavedra  
University of Arizona  
1306 E. University Blvd.  
Tucson, AZ 85721-0041  
520-621-9761  
saavedra@email.arizona.edu

Richard Schaller  
Argonne National Laboratory  
9700 S. Cass Ave.  
Argonne, IL 60439  
630-252- 1423  
schaller@anl.gov

Bernhard Schlegel  
Wayne State University  
Department of Chemistry  
Detroit, MI 48202  
313-577-2562  
hbs@chem.wayne.edu

Charles Schmuttenmaer  
Yale University  
225 Prospect St.  
New Haven, CT 06520-8107  
203-432-5049  
charles.schmuttenmaer@yale.edu

Mark Spitler  
U.S. Department of Energy  
1000 Independence Ave., SW  
Washington, DC 20585  
301-903-4568  
mark.spitler@science.doe.gov

Michael Therien  
Duke University  
124 Science Dr. 5330 FFSC  
Durham, NC 27708-0346  
919-660-1670  
michael.therien@duke.edu

## Participants List – 37<sup>th</sup> Solar Photochemistry P. I. Meeting

Randolph Thummel  
University of Houston  
Chemistry Department  
Houston, TX 77204-5003  
713-743-2734  
thummel@uh.edu

David Tiede  
Argonne National Laboratory  
9700 S. Cass Ave.  
Argonne, IL 60439  
630-252-3539  
tiede@anl.gov

William Tumas  
National Renewable Energy Laboratory  
15013 Denver West Pkwy.  
Golden, CO 80401  
303-384-7955  
bill.tumas@nrel.gov

John Turner  
National Renewable Energy Laboratory  
15013 Denver West Pkwy.  
Golden, CO 80401-3393  
303-275-4270  
John.Turner@nrel.gov

Claudia Turro  
Ohio State University  
100 W. 18th Ave.  
Columbus, OH 43210  
614-292-6708  
turro@chemistry.ohio-state.edu

Roel van de Krol  
Helmholtz-Zentrum Berlin  
Institute for Solar Fuels  
Berlin, Germany  
+49 8062-43035  
roel.vandekrol@helmholtz-berlin.de

Jao van de Lagemaat  
National Renewable Energy Laboratory  
15013 Denver West Pkwy.  
Golden, CO 80401  
303-384-6143  
jao.vandelagemaat@nrel.gov

Claudio Verani  
Wayne State University  
5101 Cass Ave.  
Detroit, MI 48202  
311-577-1076  
cnverani@chem.wayne.edu

Michael Wasielewski  
Northwestern University  
2145 Sheridan Rd.  
Evanston, IL 60208  
847-467-1423  
m-wasielewski@northwestern.edu

James Wishart  
Brookhaven National Laboratory  
Chemistry Department  
Upton, NY 11973-5000  
631-344-4327  
wishart@bnl.gov

Jenny Yang  
University of California, Irvine  
3038D Frederick Reines Hall  
Irvine, CA 92697  
949-824-1533  
j.yang@uci.edu

## *Author Index*



Abdi, Fatwa F. ....	53	Cha, Hyun Gil .....	142
Abraham, B. ....	152	Chaudhuri, Subhajyoti .....	144
Ackerman, Paul J. ....	71	Chemelewski, William C. ....	169
Ahrenholtz, Spencer R. ....	93	Chen, Jeffrey .....	144
Alibabai, Leila .....	48	Chen, Jinquan .....	68
Antic, Dean .....	16	Chen, Lin X. ....	140,141,179
Antoniuk-Pablant, Antaeres .....	154	Chen, Yong-Siou .....	3
Araque, J. C. ....	134	Chen, Yuan Jang .....	147
Arias, Dylan .....	159	Chen, Zheyuan .....	68
Armstrong, Neal R. ....	65	Choi, Kyoung-Shin .....	142
Asbury, John B. ....	129	Chomas, Andrew J. ....	16
Bachman, Benjamin F. ....	137	Christians, Jeffrey A. ....	3
Baillargeon, Josh .....	156	Cogan, Nicole M. B. ....	161
Bair, Jonathan B. ....	16	Concepcion, Javier J. ....	143
Baker, Gary A. ....	132	Congreve, Dan .....	13
Baldo, Marc .....	13	Conway, Brian .....	136
Baranov, Dmitry .....	80	Cook, A. R. ....	167,186
Bard, Allen J. ....	169	Cook, Jasper .....	145
Bartynski, R. A. ....	152	Coppens, Philip .....	45
Basu, Debashis .....	180,182	Crabtree, Robert H. ....	131,139,144
Batarseh, A. ....	152	Cuffari, David .....	187
Batista, Victor S. ....	131,139,144,177	Culnane, Lance F. ....	16
Batra, A. ....	131	Damrauer, Niels H. ....	145
Bawendi, Mounqi .....	13	Devine, Jessalyn A. ....	132
Baydoun, Habib .....	180,181	Ding, Wendu .....	131,177
Beane, Gary .....	77	Doerrer, L. H. ....	146
Beard, Matthew C. ....	133	Dogutan, Dilek .....	171
Bediako, D. Kwabena .....	89,171	Dron, Paul I. ....	16,159
Benson, Eric .....	148	Dunbar, Kim R. ....	91
Berglund, Sean P. ....	53	Durrell, Alec C. ....	139
Bergren, Matthew R. ....	133	Dyar, Scott M. ....	19
Bird, M. J. ....	167,186	Eaton, Samuel W. ....	19
Blackburn, J. ....	167,186	Eisenberg, Richard .....	138
Blank, David A. ....	97,130	Ekanayake, Danushka .....	182
Bocarsly, Andrew B. ....	135	Emery, Jonathan D. ....	179
Bocian, David F. ....	104	Endicott, John F. ....	147
Boettcher, Shannon W. ....	137	Ertem, Mehmed Z. ....	143
Bradley, Colin .....	163	Fan, H. ....	152
Bren, Kara L. ....	138	Farnum, Byron H. ....	38,48,166
Brennaman, M. Kyle .....	166	Fazi, Diego .....	179
Brennan, Bradley J. ....	139,144	Ferrere, Sue .....	148
Brown, Chelsea .....	155	Frei, Heinz .....	149
Brown, Elizabeth .....	164	Friesner, Richard A. ....	150
Brown, Kristen E. ....	19	Fu, Yulan .....	48
Brudvig, Gary W. ....	131,139,144,177	Fujita, Etsuko .....	151,173
Brus, Louis .....	150	Gadisa, Abay .....	48
Buchanan, Eric A. ....	16	Galoppini, E. ....	152
Bulović, Vladimir .....	13	Gardner, Daniel M. ....	19
Carey, Thomas .....	145	Garvey, Timothy .....	48
Castellano, Felix N. ....	8,141	Gervaldo, Miguel .....	155
Castner Jr., Edward W. ....	97,132,136	Ghosh, Rudresh .....	48

Givelet, Cecile .....	16	Kopecky, Andrew .....	178
Gonawala, Sunalee .....	181	Kraus, Theodore .....	31
Gong, Ke .....	77	Krauss, Todd D. ....	138,161
Goodson III, Theodore .....	25	Kronawitter, Coleman X. ....	59
Greenbaum, Steven G. ....	187	Kwon, Gihan .....	179
Gregg, Brian A. ....	148	Leed, Nicholas .....	91
Grieco, Christopher .....	129	Lemouchi, Cyprien .....	16
Grills, David C. ....	153	Lestrangle, P. J. ....	140
Gu, Jing .....	135,184	Lewis, Frederick D. ....	101
Gundlach, L. ....	152	Lewis, Nathan S. ....	162
Gust, Devens .....	154,155,165	Li, Chuanhao .....	177
Hamann, Thomas W. ....	156	Li, X. ....	140,141
Hammes-Schiffer, Sharon .....	171	Li, X. ....	167,186
Hara, Yukihiro .....	48	Li, Yuguang .....	165
Hartnett, Patrick E. ....	19	Li, Zhanyong .....	91
Hatcher, Jasmine L. ....	187	Lian, Tianquan .....	68,158
Havlas, Zdenek .....	16	Liang, Min .....	136
Healy, Andrew T. ....	130	Lin, Fuding .....	137
Henderson, M. A. ....	157	Lindsey, Jonathan S. ....	104
Hervault, Yves-Marie .....	16	Livesay, Brooke .....	183
Hill, Craig L. ....	158	Llansola-Portoles, Manuel J. ....	155
Holroyd, R. ....	167	Lonergan, Mark .....	163
Holten, Dewey .....	104	Lopez, Rene .....	48
Hu, Ke .....	38	Maggard, Paul .....	155
Hu, Yuan .....	135	Maldonado, Stephen .....	164
Hupp, Joseph T. ....	111	Mallouk, Thomas E. ....	165
Huynh, Michael X. ....	89	Manbeck, Gerald .....	143
Ishitani, Osamu .....	166	Mandal, Dhritabrata .....	156
Jackson, N. E. ....	140	Mani, T. ....	167
Jerome, Steve .....	150	Manser, Joseph S. ....	3
Jiang, Zhong-Jie .....	77	Mara, M. W. ....	140
Johansson, Patrik .....	38	Mardis, Kristy L. ....	119
John, Jimmy .....	162	Margulies, Eric A. ....	19
Johnson, Justin C. ....	159	Margulis, Claudio J. ....	97,134
Jonas, David M. ....	80	Marks, Tobin J. ....	19
Kamat, Prashant V. ....	3	Maroncelli, Mark .....	97,132,134,136
Kankanamalage, Pavithra .....	182	Marsh, Hilary .....	123
Kelley, David F. ....	77	Martinson, Alex B. F. ....	179
Kern, Meghan .....	31	Mauro, G. ....	167,186
Khalifah, Peter .....	160	Maza, William A. ....	93
Khosrowabadi Kotyk, Juliet .....	183	Mazumder, Shivnath .....	147,180,182
Kim, Jaehong .....	177	McCool, Nicholas S. ....	165
Kim, Wooyul .....	149	McCusker, Catherine E. ....	8
King, Laurie .....	31	McCusker, James K. ....	35
Kirmaier, Christine .....	104	McGoorty, Michelle M. ....	8
Kodis, Gerdenis .....	154,155	Meyer, Gerald J. ....	38
Koel, Bruce E. ....	59	Meyer, Thomas J. ....	166
Koenigsmann, Christopher .....	131,177	Michl, Josef .....	16,159
Koepf, Matthieu .....	131,139,144	Miller, J. R. ....	167,186
Kohler, Lars .....	178	Mills, Thomas J. ....	137
Konezny, Steven J. ....	177	Molins i Domenech, Francesc .....	130

Moore, Ana L. ....	154,155,165	Schmittenmaer, Charles A. ....	131,139,144,177
Moore, Thomas A. ....	154,155,165	Schreiber, Matthew R. ....	16
Morris, Amanda J. ....	93	Seideman, T. ....	141
Muckerman, James T. ....	151,168,173	Shadeck, M. ....	134
Mulfort, Karen L. ....	119,141,179	Shaffer, David W. ....	143
Mullins, C. Buddie ....	169	Shelby, M. L. ....	140
Mundoor, Haridas ....	71	Shoer, Leah E. ....	19
Musaev, Djamaladdin G. ....	158	Skoruspka, Katarzyna ....	31
Nakada, Akinobu ....	166	Smalyukh, Ivan I. ....	71
Nayak, Animesh ....	166	Smirnova, Yuliana ....	176
Neale, Nathan R. ....	56,133,184	Smith, Millicent B. ....	16
Negre, C. F. A. ....	131	Snyder, Jamie ....	145
Newton, Marshall D. ....	170	Solis, Brian H. ....	171
Nieto-Pescador, J. ....	152	Spitler, Mark ....	31
Niklas, Jens ....	119	Stamplecoskie, Kevin ....	3
Nocera, Daniel G. ....	89,171	Steele, J. L. ....	146
Nozik, Arthur J. ....	159,172	Steigerwald, Mike ....	150
Olive, Alexandre G. L. ....	16	Steirer, Kenneth ....	184
Park, Jaehong ....	123	Stewart, Robert J. ....	129
Park, Samuel D. ....	80	Stickrath, A. B. ....	140
Parkinson, Bruce ....	31	Strayer, Megan E. ....	165
Petek, Hrvoje ....	83	Suarez, Sophia N. ....	187
Pillar, Kartik ....	187	Sullivan, Ian ....	155
Poluektov, Oleg G. ....	119	Sun, Chen S. ....	146
Polyansky, Dmitry E. ....	173	Svedruzic, Drazenka ....	148
Prezhdo, Oleg ....	174	Swierk, John R. ....	165
Prieto, Amy L. ....	185	Tahsini, L. ....	146
Ptasinska, Sylwia ....	175	Tamadon, Farhad ....	16
Pushkar, Yulia ....	176	Thammavongsy, Zachary ....	183
Pyuan, Jeffrey ....	65	Therien, Michael J. ....	115
Ramati, Sharon ....	187	Thomas, Ryan A. ....	147
Ramirez, Jessica ....	123	Thompson, Nick ....	13
Rangan, S. ....	152	Thummel, Randolph P. ....	178
Ratner, M. A. ....	141	Tiede, David M. ....	119,141,179
Regan, Kevin P. ....	177	Tong, Lianpeng ....	178
Reid, Obadiah G. ....	123,167,186	Tsai, Chia Nung ....	147
Rettie, Alexander J. E. ....	169	Tsay, Charlene ....	183
Rimshaw, Adam.....	129	Turner, John ....	184
Rua, Armando ....	187	Turro, Claudia ....	91
Rudshteyn, Benjamin ....	144,177	Umamoto, Teruo ....	16
Rumbles, Garry ....	123,167,186	Utschig, Lisa M. ....	119
Ryerson, Joseph L. ....	159	van de Krol, Roel ....	53
Ryu, Jisu ....	80	van de Lagemaat, Jao ....	71,133
Saavedra, S. Scott ....	65	Van Voorhis, Troy ....	13
Saladin, Marissa ....	132	Vargas-Barbosa, Nella M. ....	165
Sammakia, Tarek ....	145	Velazquez, Jesus M. ....	162
Sasaki, Kotaro ....	151	Venkataraman, L. ....	131
Schäfer, Sebastian ....	161	Verani, Claudio N. ....	147,180,181,182
Schaller, R. D. ....	141	Walker, Ethan ....	163
Schatz, G. C. ....	141	Ward, William ....	38
Schlegel, H. Bernhard ....	147,180,182	Wasielewski, Michael R. ....	19

Watkins, Kevin .....	31
Weber, Chris .....	163
Weisman, Andrew .....	150
Wen, Jin .....	16
White, Travis .....	91
Wickramasinghe, Lanka .....	178
Wiensch, Joshua D. ....	162
Wishart, James F. ....	97,132,187
Witt, Suzanne .....	91
Wu, Kaifeng .....	68
Wu, Mengfei .....	13
Wu, Yi-Lin .....	19
Wuttig, Anna .....	135
Xie, Yan .....	143
Xie, Yuling .....	156
Xu, C. ....	134
Xu, Pengtao .....	165
Yadav, S. K. ....	134
Yan, Lifen .....	176
Yan, Yong .....	135,184
Yang, Jenny Y. ....	183
Yang, Ke R. ....	177
Yang, Ye .....	68,133
Youmans, M. K. ....	146
Young, James .....	184
Young, L. ....	141
Zachäus, Carolin .....	53
Zaikowski, L. ....	167,186
Zamadar, Matibur .....	16
Zeitler, Elizabeth L. ....	135
Zeng, Youhong .....	77
Zhang, Xin-Xing .....	136
Zhang, Xueqiang .....	175
Zhao, Peng .....	59
Zhou, Rongwei .....	178
Zhu, Guibo .....	176
Zhu, Haiming .....	68
Zhu, Kai .....	133
Zong, Ruifa .....	178